UNIVERSIDAD CARLOS III DE MADRID

TESIS DOCTORAL

STUDY OF KINETIC MODELS FOR NONLINEAR ELECTRON TRANSPORT IN SEMICONDUCTOR SUPERLATTICES

Autor: Mariano Álvaro Ballesteros

Director: Luis Francisco López Bonilla

DEPARTAMENTO DE CIENCIA E INGENIERÍA DE MATERIALES E INGENIERÍA QUÍMICA

Julio de 2011

UNIVERSIDAD CARLOS III DE MADRID

STUDY OF KINETIC MODELS FOR NONLINEAR ELECTRON TRANSPORT IN SEMICONDUCTOR SUPERLATTICES

Memoria que se presenta para optar al título de Doctor por la Universidad Carlos III de Madrid por el Programa en Ingeniería Matemática

Autor: Mariano Álvaro Ballesteros

Director: Luis Francisco López Bonilla

DEPARTAMENTO DE CIENCIA E INGENIERÍA DE MATERIALES
E INGENIERÍA QUÍMICA

Julio de 2011

TESIS DOCTORAL

Study of kinetic models for for nonlinear electron transport in semiconductor superlattices

Autor: Mariano Álvaro Ballesteros
Director: Luis Francisco López Bonilla

Firma del Tribunal Calificador:

	Nombre y apellidos	Firma
Presidente:		
Vocal:		
Vocal:		
Vocal:		
Secretario:		

Calificación:

Leganés, Julio de 2011

A mi familia

Agradecimientos

El primer y el más profundo agradecimiento es para mi director de tesis Luis L. Bonilla, por su confianza al incluirme en su proyecto de investigación, su dedicación y sus sugerencias durante la realización de esta tesis. Agradezco también la ayuda prestada por Manuel Carretero. Doy las gracias también al Grupo de Modelización, Simulación Numérica y Matemática Industrial, así como al Departamento de Ciencia e Ingeniería de Materiales e Ingeniería Química, por los medios materiales y humanos de los que he disfrutado durante el tiempo de elaboración de la tesis. Finalmente, quiero agradecer a los miembros del tribunal que han accedido a formar parte de éste.

Resumen

Las superredes de semiconductores son cristales unidimensionales artificiales formados por muchos períodos, cada uno de ellos compuesto por dos semiconductores diferentes pero con constantes similares, por ejemplo GaAs y AlAs. Estas nanoestructuras fueron inventadas por Esaki y Tsu con el propósito de desarrollar dispositivos en los que pudieran ser observadas las oscilaciones de Bloch. Tienen aplicaciones prácticas como osciladores de alta frecuencia, láseres de cascada cuántica o detectores infrarrojos. Cuando se aplica un voltaje entre los dos extremos de la superred con dopado de tipo n, se pueden observar una serie de fenómenos no lineales en el transporte de electrones tales como oscilaciones autosostenidas de la corriente, formación de patrones, oscilaciones de Bloch, comportamiento caótico, etc.

En esta tesis se presenta un estudio sobre distintos modelos cinéticos que describen diversos fenómenos no lineales de transporte de electrones en superredes semiconductoras fuertemente acopladas, en las que la longitud de onda del electrón es mayor que el período de la superred. Todos estos modelos se basan en ecuaciones cinéticas de transporte de tipo Boltzmann o Wigner con tratamiento de las colisiones mediante términos BGK (Bhatnagar, Gross y Krook). La idea que subyace en todos estos modelos es que la función de distribución tiende hacia la distribución de equilibrio local. El término de colisión se sustituye por un término proporcional a la diferencia entre la función de distribución y la función de equilibrio local con un tiempo de relajación constante. La principal ventaja de esta aproximación es que permite obtener mediante métodos de perturbación, en el límite hiperbólico, ecuaciones de balance hidrodinámicas o de convección-difusión para las densidades de electrones, corriente y energía. Estas ecuaciones de balance pueden ser resueltas numéricamente, con condiciones de contorno apropiadas, mediante métodos basados en diferencias finitas. De esta forma, los resultados numéricos obtenidos muestran fenómenos no lineales de interés.

En concreto se presentan cuatro modelos que describen distintos fenómenos no lineales de las superredes fuertemente acopladas. En el primero, se utiliza el modelo más simple basado en una ecuación de tipo Boltzmann-Poisson

BGK con transporte de electrones en la minibanda inferior y se demuestra un teorema H mediante un funcional que tiene la forma de una energía libre, asumiendo condiciones de contorno ideales. Este funcional se puede aproximar mediante el método de Chapman-Enskog y calcular numéricamente en un régimen en el que existen oscilaciones autosostenidas de la corriente de tipo Gunn en una superred con condiciones de contorno realistas, observándose que en ese caso la función de energía libre deja de ser un funcional de Lyapunov y oscila periódicamente.

Aunque Zener predijo la existencia de las oscilaciones de Bloch en 1934 y Esaki y Tsu idearon las superredes en 1970, no fueron comprobadas experimentalmente hasta 1992, lo que da una idea sobre la dificultad de su modelización. Además de su interés teórico, las aplicaciones prácticas de las oscilaciones de Bloch incluyen su utilización como osciladores de frecuencias en el rango de los THz. En el segundo modelo propuesto, con el fin de encontrar oscilaciones de Bloch en una superred en la que al mismo tiempo exista un perfil no homogéneo del campo eléctrico, se utiliza una función de distribución de equilibrio local que depende, además de la densidad de electrones, de la densidad de corriente y de la energía media, y de esta manera puede oscilar a la frecuencia de Bloch. Mediante una combinación de métodos de escalas múltiples (Chapman-Enskog y expansiones asintóticas) en el límite en que la frecuencia de las oscilaciones de Bloch y la frecuencia de las colisiones son del mismo orden, se obtienen en el régimen hidrodinámico, unas ecuaciones de balance para el campo eléctrico y la envolvente compleja de la amplitud de las oscilaciones de Bloch. La solución numérica de estas ecuaciones muestra que para una superred con tiempos entre colisiones suficientemente altos es posible que coexistan oscilaciones de Bloch estables confinadas en una región de la superred junto con dominios no homogéneos del campo eléctrico. Este descubrimiento contradice la creencia actual sobre la necesidad de un campo eléctrico homogéneo para que existan oscilaciones de Bloch.

En los dos últimos modelos se utiliza el método de Chapman-Enskog para obtener ecuaciones reducidas de balance para superredes con dos minibandas. Partiendo de ecuaciones Wigner-Poisson-BGK se obtiene un sistema de ecuaciones no locales de tipo convección-difusión cuánticas para la densidad de electrones y el campo eléctrico, cuyas soluciones numéricas muestran oscilaciones de la corriente de tipo Gunn con efectos cuánticos. Este resultado se aplica al caso de una superred lateral con interacción spin-órbita de tipo Rashba que se comportaría como un oscilador de spin. Si se añade un término

de acoplamiento entre las minibandas dependiente del campo, el modelo describe el transporte de electrones por túnel resonante entre las minibandas así como oscilaciones autosostenidas de la corriente.

Contents

1 Introduction **19**

2 Electronic properties of superlattices and electron transport **25**
2.1 Superlattices and their electronic spectrum 25
2.1.1 Bloch states for the unbiased superlattice 26
2.1.2 Wannier states for the unbiased superlattice 28
2.1.3 Superlattice biased by a constant electric field 28
2.1.4 Strongly and weakly coupled superlattices 29
2.2 Scattering and transport phenomena 30
2.2.1 Wigner-Poisson equation 32
2.2.2 Scattering treatment 36
2.3 Derivation of balance equations by the Chapman-Enskog method 39
2.3.1 Equivalent form of the Wigner-Poisson-BGK equations 39
2.3.2 Chapman-Enskog method 41

3 Nonequilibrium free energy, H theorem and self-sustained oscillations for Boltzmann-BGK descriptions of semiconductor superlattices **45**
3.1 Introduction 45
3.2 BPBGK kinetic equation and generalized drift-diffusion balance equation 46
3.2.1 Kinetic equation and local equilibrium distribution . . 47
3.2.2 Chapman-Enskog perturbation method and drift-diffusion system 49
3.3 H theorem and entropy for ideal boundary conditions 51
3.3.1 Derivation of a free energy density 51
3.3.2 Boltzmann limit and physical meaning of $\eta(x,t)$ 54
3.3.3 Boundary conditions and free energy as a Lyapunov functional 55
3.4 Numerical results 57

3.5 Conclusions 60

4 Spatially confined Bloch oscillations in semiconductor superlattices 61
4.1 Introduction 61
4.2 Dissipative BGK collision model 63
4.2.1 BGK-Poisson (KSS) model 63
4.2.2 Dissipative BGK collision model 64
4.3 Moment equations and their spatially uniform solutions 67
4.3.1 Space and time independent moments 68
4.3.2 Time evolution of space independent moments 69
4.4 Hydrodynamic regime in the almost elastic limit 70
4.4.1 BGK-Poisson system and moment equations in nondimensional form 70
4.4.2 Hydrodynamic equations 72
4.5 Numerical results 74
4.6 Almost elastic collisions and damped Bloch oscillations 78
4.7 Chapman-Enskog method for almost elastic collisions 82
4.8 Concluding remarks 87

5 Nonlinear electron and spin transport in semiconductor superlattices 89
5.1 Introduction 89
5.2 Single miniband superlattice 91
5.3 Wigner description of a two-miniband superlattice 94
5.4 Derivation of balance equations by the Chapman-Enskog method 98
5.5 Spintronics: Quantum drift-diffusion equations for a lateral superlattice with Rashba spin-orbit interaction 101
5.6 Conclusions 107

6 Two mini-band model for self-sustained oscillations of the current through resonant tunneling semiconductor superlattices 109
6.1 Introduction 109
6.2 Model Hamiltonian 110
6.3 Wigner function description 111
6.4 The Chapman-Enskog method and balance equations 115
6.5 Numerical results 119
6.6 Derivation of the single miniband model equations 123
6.7 Conclusions 128

7 Conclusions and future work **131**

Appendices **133**

A Boltzmann local equilibrium distribution **133**

B Inelastic collisions and the hyperbolic limit **135**

C Balance equations from compatibility conditions **141**

D Complete expressions for $D_{\pm}$ and R **143**

E Numerical method for the hydrodynamic equations describing spatially confined Bloch oscillations **153**
E.1 Nondimensional equations 153
E.2 Numerical scheme 155

F Numerical method for quantum drift diffusion equations for a lateral superlattice with Rashba spin-orbit interaction **161**
F.1 Nondimensional equations 161
F.2 Numerical scheme 168

G Numerical method for quantum drift diffusion equations for a two miniband superlattice **173**
G.1 Nondimensional equations 173
G.2 Numerical scheme 177

Chapter 1

Introduction

Electron transport in semiconductors at high fields explains many nonlinear phenomena observed in these materials. In bulk semiconductors, transport coefficients at low fields such as the electron mobility can be calculated by using simple local equilibrium approximations in the Boltzmann transport equation with appropriate scattering models. At high fields, the distribution function of the Boltzmann equation is no longer close to local equilibrium and a host of new phenomena may arise. For instance, in bulk gallium arsenide (GaAs), for sufficiently large applied electric field, electrons may be transferred by scattering from the global minimum to high energy valleys of the GaAs band structure (see, for example, the review [22]). This electron transfer effect causes the electron drift velocity to become nonlinear at higher fields: in fact it reaches a maximum at a certain field and then it decays monotonically to a saturation value. The negative slope of the drift velocity is called negative differential conductivity (NDC). When the hydrodynamic balance equations containing the drift velocity (with a NDC region) and other transport coefficients are solved for appropriate geometries, the current through the semiconductor may exhibit self-sustained oscillations with frequencies in the microwave regime. In turn, these oscillations are due to the periodic formation of electric field domains (pulses of the electric field) at an injecting contact, and their motion and disappearance at the collecting contact. The resulting phenomenon is the Gunn effect in n-doped GaAs (see the review [51] and, for a mathematical study, [17]) which is the basis of many devices producing microwave radiation.

In recent years, molecular beam epitaxy and other growth techniques allow the construction of heterostructures comprising a number of nano-sized layers of different semiconductors. Due to the different bandgap energies of the component semiconductors, the resulting conduction and valence band

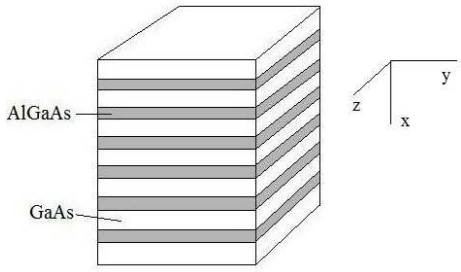

Figure 1.1: Schematic drawing of a superlattice.

edges follow the spatial alignment of the layers. Then almost any kind of potential can be tailored by using the right constituents for the semiconductor heterostructure. Among the simplest structures, Esaki and Tsu proposed in 1970 [33] to build an artificial one dimensional crystal, which they called a semiconductor superlattice (SL), by growing periodic array of two alternating materials (see fig. 1.1). Thus in addition to the three dimensional lattice of the crystal, an additional one dimensional SL is formed on a much larger scale. High field phenomena can be observed at much lower fields than in bulk materials due to the much larger superlattice constant. Furthermore the large potential drop per SL period causes field-induced localization of the carriers and subsequent quantum effects that are more prominent than in bulk semiconductors. Several phenomena known in bulk transport appear also in superlattice: NDC accompanied by quantum mechanical localization of the electron states occurs at moderate fields. Stationary and traveling electric field domains (related to the Gunn oscillations) have been observed in the NDC regime. New phenomena such as Bloch oscillations and sequential tunneling between neighboring SL periods occur in superlattices but not in bulk materials. These reasons and the simplicity inherent to their one-dimensional nature make superlattices a good system to study high field and quantum transport effects, many of which can be tested experimentally. See [14] for a review of theory and experiments on nonlinear transport in superlattices. For formulations of transport in SL based on the nonequilibrium Green function, see the review [76], for photon-assisted transport in SL, see [64], for semiclassical transport and quantum hopping transport, see Rott's PhD Thesis [68]. This thesis contributes to the understanding of nonlinear high-field phenomena in strongly coupled semiconductor superlattices for which the coherence length of the electron wave packet is larger than the SL period. Our approach consists of deriving hydrodynamic or drift-diffusion balance

equations from Boltzmann or Wigner transport kinetic equations. Balance equations are then solved numerically for appropriate initial, boundary and bias conditions and these solutions exhibit nonlinear phenomena of interest.

Our first model describes a superlattice with only one populated miniband by means of a Boltzmann-Poisson system with a Bhatnagar-Gross-Krook (BGK) collision model [8] and a one-dimensional impurity scattering term originally due to Ktitorov, Simin and Sindalovskii (1971) [54]. We prove an H-theorem for this kinetic theory when the superlattice ends at insulating contacts with zero voltage bias between them. For a SL under nonzero voltage bias and conducting contacts, the free energy used to prove the H-theorem is no longer a Lyapunov functional and it may oscillate periodically with time if the SL displays Gunn-type oscillations [2]. To show this, we use the approximate distribution function that Bonilla, Escobedo and Perales (2003) [12] employed in their derivation of a drift-diffusion system by means of the Chapman-Enskog perturbation method. Unlike the typical derivations of hydrodynamic equations from the Boltzmann transport equation for gases in the parabolic limit[1], we consider that the collision and the field-dependent convective terms in the Boltzmann equation are of the same order and that all other terms are small compared to them. This hyperbolic limit captures the strong field dependence of the transport coefficients and it is different from the conventional parabolic limit which is appropriate for small fields. In the hyperbolic limit, the Chapman-Enskog method provides a drift-diffusion equation in which a small nonlinear diffusion term regularizes a first order hyperbolic equation (the 'drift' part of the drift-diffusion equation) [12].

Although Esaki and Tsu invented the superlattice in order to develop a device exhibiting Bloch oscillations, the previous kinetic system cannot describe them. According to the Bloch theorem, the band energies are periodic functions of the wave vector and so are their derivatives, the group velocities. The periodic group velocity enters the convective part of the Boltzmann-BGK equation. Ignoring collisions, the characteristic curves of the resulting hyperbolic equation give a wave vector proportional to the applied electric field and the time and a time-periodic position with a Bloch frequency proportional to the field and the SL period. In the absence of scattering, this gives rise to a periodic oscillation of the current through the SL which is the Bloch oscillation. The existence of damped Bloch oscillations was discovered

[1] collision terms are of order 1, convective terms are of order ϵ and the time derivative of the distribution function is of order ϵ^2 as the dimensionless mean free path $\epsilon \to 0$. See the classical books by Chapman and Cowling [30] and by Cercignani [29] for details. Comparisons of results obtained in the parabolic and the hyperbolic limits can be found in the book [17].

in experiments with undoped superlattices in which the carriers were optically generated [35]. A good reference on Bloch oscillations is the book by K. Leo [60]. Scattering tends to destroy Bloch oscillations and it is also the primary reason for the existence of NDC and the subsequent stable Gunn oscillations due to the dynamics of electric field domains (EFDs) in doped SL. Since the connection between Bloch oscillations and EFDs is not clear, many people believed that it is necessary to suppress EFDs in order to attain Bloch oscillations in doped SLs. Many works assume homogeneity in space and enquire whether it is possible to obtain positive gain when driving harmonically the SL in the Terahertz regime (Bloch gain [60, 74]) [40, 41]. None of these works prove that it is possible to attain the assumed spatially homogeneous state as a solution of the kinetic equations that are often used in their descriptions. We include space dependence in our models right from the start. We show that it is possible to have Bloch oscillation states that are spatially confined to part of a superlattice where there is a high field domain. The catch is that we need sufficiently long scattering times that may not be easy to realize in materials. To obtain this result, we derive hydrodynamic equations for the electron density, the electric field and the complex amplitude of the Bloch oscillations and solve them numerically. Our derivation starts from a dissipative Boltzmann-Poisson-BGK kinetic system in which the local equilibrium distribution depends on the electron, current and energy densities [11]. We consider a double limiting process of almost elastic collisions and high electric fields such that Bloch frequencies and collision frequencies are of the same order and dominate all other terms in the kinetic equation. We use a combination of multiple scales, the Chapman-Enskog method and matched asymptotic expansions to obtain the balance equations. Their numerical solution shows that, starting from an initial state with a nonzero amplitude of the Bloch oscillations, a stable state eventually appears in which there is an inhomogeneous electric field domain coexisting with a Bloch oscillation confined to a region of the superlattice that extends up to the collecting contact. There seems to be a critical value of the damping due to scattering (proportional to inverse scattering times) above which the Bloch oscillation disappears.

Quantum effects in strongly coupled SLs are described by kinetic equations that are nonlocal in space and momentum. Moreover detailed modelling of scattering at the quantum level may lead to quite complicated formulations, particularly if they are space dependent. In fact there are few systematic and consistent derivations of balance equations from quantum kinetic equations in the limit of high fields and small mean free path. For strongly coupled SLs having only one populated miniband, Bonilla and Escobedo

(2005) [13] found a nonlocal drift-diffusion system for the electron density and the electric field that described Gunn type oscillations with some quantum effects. The starting model was quite similar to the Ktitorov et al model with BGK collisions in which the distribution function was replaced by the Wigner transform of the two-point one-time matrix density. Then the convective terms in the kinetic equation become pseudo-differential operators that can be handled using that the Wigner distribution is periodic in the wave vector. The simplicity of the BGK collision term makes it possible to approximate the Wigner equation by means of the Chapman-Enskog method. We have used related methods to analyze the case of strongly coupled SLs with two populated minibands. Firstly we study a single miniband SL with a Rashba spin-orbit interaction that forces as to consider differentiated populations of electrons with spin up or down. We find stable self-sustained oscillations of the current and the spin polarization in a lateral SL that behaves as a spin oscillator [9, 10]. Our second example is a SL with two minibands which may undergo resonant tunneling through a field-dependent inter-miniband coupling similar to that proposed by Morandi and Modugno (2005) for a resonant tunneling diode [63]. Again we find Gunn-type self-sustained oscillations of the current through the SL that exhibit resonant tunneling between minibands during certain parts of each period [3].

Chapter 2

Electronic properties of superlattices and electron transport

In this chapter, we review the basic models of nonlinear charge transport in a semiconductor superlattice with a single populated miniband and the derivation of reduced balance equations for electron density and electric field using the Chapman-Enskog method.

2.1 Superlattices and their electronic spectrum

A superlattice is a periodic structure formed by repeatedly growing layers of different semiconductors with different energy gaps, but similar lattice constants, e.g. GaAs and AlAs (see fig. 1.1). Growth techniques allow to control the thicknesses of the layers with high precision, so that it is possible to tailor artificial periodic structures with features similar to standard crystals. In its simplest form, a SL is a layered structure WB WB ... WB WB containing many identical periods. The period l of a SL is of the order of ten nanometers whereas the SL extends laterally over distances of tens or hundreds of microns. Thus the SL cross section S is much larger than l^2. The different band energies of the two semiconductor materials give rise to a step-like conduction band that follows the underlying SL.

2.1.1 Bloch states for the unbiased superlattice

The effect of the microscopic crystal lattice is incorporated into the effective electron mass in each semiconductor. Thus the electrons have different effective masses m_W^* and m_B^* in the two layers W (well) and B (barrier) of lengths L_W and L_B, respectively. In the absence of external field and scattering, the envelope wave function is [6]

$$\varphi_\nu(\mathbf{x},\mathbf{k}) \equiv \varphi_\nu(x,\mathbf{x}_\perp,k,\mathbf{k}_\perp) = \frac{1}{\sqrt{S}} e^{i\mathbf{k}_\perp\cdot\mathbf{x}_\perp}\varphi_\nu(x,k), \tag{2.1}$$

where x is the growth direction, $\mathbf{x}_\perp = (y,z)$, and $\mathbf{k} = (k,\mathbf{k}_\perp)$, $\mathbf{k}_\perp = (k_y,k_z)$, is the wave vector. The one-dimensional electron energy and wave function solves the eigenvalue problem:

$$\left(-\frac{\hbar^2}{2}\frac{\partial}{\partial x}\frac{1}{m(x)}\frac{\partial}{\partial x} + V_c(x)\right)\varphi_\nu = \mathcal{E}_\nu(k)\varphi_\nu, \tag{2.2}$$

$$E_\nu(\mathbf{k}) = \mathcal{E}_\nu(k) + \frac{\hbar^2\mathbf{k}_\perp^2}{2m_\perp} + E_c, \tag{2.3}$$

where $E_\nu(\mathbf{k})$ is the three-dimensional energy, E_c is the quantum well conduction band edge, $m(x)$ is the effective mass (i.e. m_W^* when x corresponds to a well, and m_B^* for a barrier) and V_c is the conduction band offset between the well and the barrier. Thus $V_c(x)$ is 0 for the well and V_c for the barrier. The effective mass $m_\perp$ for motion in the layers perpendicular to the growth direction is calculated by averaging the AlAs and GaAs masses according to the respective probability density of the wave function in the barrier and well material.

According to the Bloch theorem, $\varphi_\nu = e^{ikx}u(x;k)$, where $u_k(x+l;k) = u_k(x;k)$ has the same period $l = L_W + L_B$ as the SL. The wave function in Equation (2.2) is determined by the conditions that φ_ν and $(1/m(x))\partial\varphi_\nu/\partial x$ be continuous at the interfaces between barriers and wells. With this approach, the energy states in the growth direction, $\mathcal{E}_\nu(k)$ can be calculated by solving the resulting one-dimensional Krönig-Penney model. As in bulk crystals, the periodic SL potential $V_c(x)$ leads to the formation of energy bands, the SL minibands, separated by gaps in which no allowed states exist. Defining $k_W = \sqrt{2m_W^*\mathcal{E}}/\hbar$ and $\kappa_B = \sqrt{2m_B^*(V_c-\mathcal{E})}/\hbar$, the miniband

energies $\mathcal{E}_\nu$ are solutions of the following transcendental equation [6]:

$$\cos(kl) = \cos(k_W L_W)\cosh(\kappa_B L_B) - \frac{1}{2}\left(\xi - \frac{1}{\xi}\right)\sin(k_W L_W)\sinh(\kappa_B L_B), \tag{2.4}$$

$$\xi = \frac{k_W m_B^*}{\kappa_B m_W^*}. \tag{2.5}$$

Due to the large SL spatial period, of the order of nanometers (Ångstrøms in bulk semiconductors), these minibands have small energy widths of the order of 1 to 100 meV (compared to energy widths of the order of eV in bulk semiconductors). The Bloch functions are $2\pi/l$-periodic in k, satisfying the orthogonality condition

$$\int_\infty^\infty \varphi_\mu^*(x;k)\varphi_\nu(x;k')\,dx = \delta_{\mu\nu}\delta(k-k') \tag{2.6}$$

and the closure condition

$$\int_\infty^\infty \varphi_\mu^*(x;k)\varphi_\nu(x';k)\,dk = \delta_{\mu\nu}\delta(x-x'), \tag{2.7}$$

provided the integral of $|\varphi_\nu|^2$ over one SL period is unity.

If the SL barriers are not too small, the tunneling probability from one well to the next one is much larger than that from one well to the second next nearest well. in this case, the miniband formation can be described in a tight-binding approach, including only coupling between adjacent quantum wells. Denoting the right hand side of (2.4) by $f(\mathcal{E})$, this function will display large variations and the band widths, which are energy segments where $|f(\mathcal{E})| < 1$, will be narrow. In the limit of thick barriers, we may expand $f(\mathcal{E})$ in the vicinity of the bound states of isolated wells $\mathcal{E}_\nu$. The resulting dispersion relations are

$$\mathcal{E}_\nu(k) = \mathcal{E}_\nu + s_\nu + 2t_\nu\cos(kl), \tag{2.8}$$

with

$$s_\nu = -\frac{f(\mathcal{E}_\nu)}{f'(\mathcal{E}_\nu)}, \qquad 2t_\nu = \frac{1}{f'(\mathcal{E}_\nu)}. \tag{2.9}$$

The dispersion relation of the lowest miniband may be written as

$$\mathcal{E}(k) = \frac{\Delta}{2}[1-\cos(kl)]. \tag{2.10}$$

Here the miniband width Δ is four times the tunneling matrix element between adjacent wells, t_1.

2.1.2 Wannier states for the unbiased superlattice

Instead of Bloch states, we can choose Wannier wave functions as orthogonal basis functions. The Wannier function *localized in the mth SL period* is $\chi_\nu(x - ml)$, in which

$$\chi_\nu(x) = \frac{l}{2\pi} \int_{-\pi/l}^{\pi/l} \varphi_\nu(x; k)\, dk \tag{2.11}$$

is the zeroth harmonic in the Fourier series of the Bloch function considered as a function of k. The orthogonality property is

$$\int_{\infty}^{\infty} \chi_\mu^*(x - rl)\chi_\nu(x - sl), dx = \delta_{\mu\nu}\delta_{rs}, \tag{2.12}$$

The Wannier basis is used in sequential tunneling theories for weakly coupled SLs, because the Wannier wave functions are close to the subbands of an isolated quantum well in this case [76].

2.1.3 Superlattice biased by a constant electric field

If scattering is ignored and an external electric field $-F$ is present, a term $-eFx$ should be added to the potential $V_c(x)$ in (2.2), where $-e < 0$ is the charge of the electron. Equation (2.2) is no longer invariant to translations by one period l. Instead, the conduction band potential is invariant under the operation $x \to x + l$, $\mathcal{E} \to \mathcal{E} - eFl$. Thus if $\varphi(x)$ is the wave function corresponding to energy $\mathcal{E}$, the same state shifted by one period, $\varphi(x - l)$ is a solution corresponding to the energy $\mathcal{E} - eFl$. By repeating this operation, we obtain an infinite ladder of states for each Wannier wave function which is close to one bound state of a single quantum well. This periodic energy spectrum is the Wannier-Stark (WS) ladder.

The WS wave functions extend over several SL periods if the WS levels of neighboring wells are in resonance. In this case, the electrons can tunnel between adjacent wells and spread coherently over a certain distance Λ. The condition for coherent tunneling between two wells separated by a distance ml is $meFl < \Delta$, in which the miniband width, Δ, gives a measure of the energetic broadening of the basic quantum well state. Then $\Lambda = ml = \Delta/(eF)$, i.e. the spatial extension of the WS states is inversely proportional to the field. Thus, the WS states become extended over the whole SL for vanishing fields (the same as for zero-field Bloch functions), whereas they become localized in one well if $eFl > \Delta$. It is possible to write the WS wave

function in terms of the corresponding Bloch states at zero field. Each Bloch state is multiplied by a phase factor proportional to $1/F$, which gives rise to a singularity as $F \to 0$. Then WS states do not match the Wannier states for vanishing fields. See Rott's PhD Thesis [68] for longer discussions and references.

2.1.4 Strongly and weakly coupled superlattices

To include scattering in theoretical formulations, the starting point is to select a wave function basis for the unperturbed Hamiltonian of the system described previously. Depending on the SL features some bases may be more convenient and it is essential to distinguish between weakly coupled and strongly coupled SLs. Weakly coupled SLs contain rather thick barriers separating the SL quantum wells, i.e. the barrier width is much larger than the typical electron wavelength inside the barrier, $1/\kappa_B$. Therefore, a description of the electronic properties of weakly coupled SLs can be based on the subband structure of the corresponding isolated quantum well together with resonant tunneling across the barrier of two adjacent wells [25]. Alternatively, Wannier wave functions may be a convenient basis [76]. In contrast, the quantum wells of strongly coupled SLs are separated by thin barriers so that the electronic properties of strongly coupled SLs can be described in terms of extended states such as Bloch functions [73].

The simplest mathematical models applied to a SL give rise to balance equations involving mesoscopic quantities such as the electric field, the electron density and the drift velocity. A fundamental difference between weakly and strongly coupled SLs is that the former are governed by spatially discrete balance equations, whereas the latter are governed by spatially continuous equations. Both types of equations may have solutions whose electric field profiles display regions of high electric field coexisting with regions of low electric field. The resulting dynamical behavior is very different for these two types of equations. For strongly coupled SLs, which are described by continuous balance equations, the field profile consists of a charge dipole moving with the flow of electrons, which resembles closely the Gunn effect in bulk semiconductors [51]. Under dc voltage bias, this basic motion results in self-sustained oscillations of the current (SSOC) through the SL due to the periodic movement of dipole domains. In contrast, in weakly coupled SLs, which are described by discrete balance equations, electric field domains (EFDs) are separated by a domain wall, which consists of a charge monopole. See the review [14] for a more elaborate discussion of weakly and strongly coupled SLs.

In this work we will focus on modeling nonlinear electron transport phenomena for strongly coupled SLs, which will be described by continuous kinetic equations.

2.2 Scattering and transport phenomena

We will consider an n-doped SL with cross section, $S \gg l^2$. We shall assume that the SL is under a dc voltage bias, which is equivalent to an external electric field directed along the SL growth direction. Before performing any quantum calculation we have to define a basis set of states to be used. Although the choice of the basis has no influence on the exact solution, that is not true when approximations are made for solving realistic problems. Therefore, the choice of the set of basis states is important due to its effect on the approximations obtained. Typically, the basis set is chosen as the set of eigenstates of the one electron Hamiltonian H_0 considered in the previous section. If the remaining part of the Hamiltonian $H - H_0$ is small, it can be treated as a perturbation and Fermi's golden rule for transition rates can be applied. For n-doped SLs, we can restrict ourselves to studying electronic transport in the conduction band of the SL, and we will assume that it is a single band with spin degeneracy. The corresponding Hamiltonian is

$$H = H_0 + H_{e-e} + H_{sc}. \tag{2.13}$$

Where H_{e-e} represents the electron-electron interaction, and H_{sc} takes into account the other scattering processes (impurity, phonon, etc). Typically, the electron-electron interaction is treated in the Hartree approximation and modeled with the Poisson equation:

$$\varepsilon(x)\frac{\partial W}{\partial x^2} = e(n_0(x) - N_{3D}(x)). \tag{2.14}$$

where $W(x)$ is the electric potential due to the electron-electron interaction, $n_0(x)$ is the $3D$ equilibrium electron density, given by

$$n_0(x) = \frac{1}{Sl}\sum_{\nu,k,\mathbf{k}_\perp} |\varphi_\nu(x,k,\mathbf{k}_\perp)|^2 n_\nu^F(k,\mathbf{k}_\perp), \tag{2.15}$$

where n_ν^F is the Fermi function of the miniband ν. $N_{3D}(x) = N_D/l$ is the three-dimensional doping density (N_D is the two-dimensional doping density) and $\varepsilon(x)$ is the permittivity (i.e., $\varepsilon(x) = \varepsilon_W$ when x corresponds to a quantum

well, or $\varepsilon(x) = \varepsilon_B$ when x corresponds to a barrier). Then we can find the spectrum of the Hamiltonian $H_0 + H_{e-e}$:

$$H_0 + H_{e-e} = -\frac{\hbar^2}{2}\frac{\partial}{\partial x}\frac{1}{m(x)}\frac{\partial}{\partial x} + \frac{\hbar^2 \mathbf{k}_\perp^2}{2m(x)} + E_c + V_c(x) - eW(x), \qquad (2.16)$$

by solving a non-linear stationary Schrödinger-Poisson system of equations. Their solutions yield a basis in which quantum kinetic equations describing the scattering processes out of equilibrium can be written.

According to the previous section, we could select Bloch or Wannier states as a basis. We do not select Wannier-Stark states corresponding to a spatially homogeneous electric field because of their singularity at zero field and because we are interested in describing spatially inhomogeneous systems. A basis whose wave functions could describe continuously the Hamiltonian H_0 for all inhomogeneous fields would be ideally suited to study scattering. Since no such basis is known and we will study strongly coupled SLs, we will select the basis of Bloch states.

After selecting the appropriate basis it is necessary to model scattering processes. Scattering different from electron-electron scattering is usually treated with three different approaches:

1. *Density matrix equations.* [20], [36]
2. *Wigner transform.* [67], [21],
3. *Non-equilibrium Green's function* (NGF) [76], [47].

Within the NGF formulation, closed equations for the one-electron NGFs are found by treating weak scattering processes up to second order in the scattering potential, thereby obtaining the Kadanoff-Baym equations [38, 47]. Additional approximations yield closed equations for Wigner functions, although more work connecting both the NGF and the Wigner function approaches seems desirable [38]. Formulations using density matrices can be found in [20, 36], and comparison between non-equivalent NGF and density matrix descriptions of single-miniband SLs can be found in appendices A and B of [76]. Laikhtman and Miller [55] derived equations for the NGF and subsequently for the density matrix of a single-miniband SL using the Wannier representation.

In the semiclassical limit all these formulations end up in the Boltzmann equation. Whatever the chosen formulation, the equations for the one-electron functions depend on two-electron and higher functions, and we have the usual infinite hierarchy of coupled equations, which is well known in

classical kinetic theory. Typically, the hierarchy is closed by assuming some dependence of the two-electron functions on one-electron functions, which is suggested by perturbation theory in the limit of weak scattering [38]. Assuming weak scattering, the differences between the equations corresponding to the different formulations are small. The trouble is that the kinetic equations are often used in the opposite hydrodynamic limit, in which collisions due to scattering are dominant. Then the results of using different formalisms are not equivalent, which has resulted in some discussion and confusion. Here we shall follow the Wigner formulation by Bonilla and Escobedo [13] who approximated the scattering by using a BGK collision model.

2.2.1 Wigner-Poisson equation

To find a kinetic equation, we start writing equations for the coefficients $a_{\nu,\mathbf{k}}(t)$ in the expansion of the wave function

$$\psi(\mathbf{x},t) = \sum_{\nu,\mathbf{k}} a_{\nu,\mathbf{k}}(t)\varphi_\nu(\mathbf{x},\mathbf{k}) \equiv \psi_\nu(\mathbf{x},t). \tag{2.17}$$

If we ignore the scattering term H_{sc}, the coefficients $a_{\nu,\mathbf{k}}(t)$ become

$$i\hbar\frac{\partial}{\partial t}a_{\nu,\mathbf{k}} = E_\nu(\mathbf{k})a_{\nu,\mathbf{k}} - e\sum_{\nu',\mathbf{k'}} \langle\nu\mathbf{k}|W|\nu'\mathbf{k'}\rangle\, a_{\nu',\mathbf{k'}}. \tag{2.18}$$

The equations for the band wave functions ψ_ν of equation (2.17) can be obtained from this equation after some algebra:

$$i\hbar\frac{\partial}{\partial t}\psi_\nu = -\frac{\hbar^2}{2m^*}\frac{\partial^2}{\mathbf{x}_\perp^2}\psi_\nu + \sum_{m=-\infty}^{\infty} E_\nu(m)\psi_\nu(x+ml,\mathbf{x}_\perp,t) - e\sum_{\nu'}\int \Phi_\nu(\mathbf{x},\mathbf{x'})W(\mathbf{x'})\psi_{\nu'}(\mathbf{x'},t)d\mathbf{x'}, \tag{2.19}$$

$$\Phi_\nu(\mathbf{x},\mathbf{x'}) = \sum_{\mathbf{k}} \varphi_\nu(\mathbf{x},\mathbf{k})\varphi_\nu^*(\mathbf{x'},\mathbf{k}), \tag{2.20}$$

$$\mathcal{E}_\nu(k) = \sum_{m=-\infty}^{\infty} E_\nu(m)e^{imkl}. \tag{2.21}$$

Note that equation (2.1) implies

$$\Phi_\nu(\mathbf{x},\mathbf{x'}) = \delta(\mathbf{x}_\perp - \mathbf{x'}_\perp)\phi_\nu(x,x'), \tag{2.22}$$

$$\phi_\nu(x,x') = \sum_k \varphi_\nu(x,k)\varphi_\nu^*(x',k) \tag{2.23}$$

and the closure condition in equation (2.7) yields

$$\sum_{\nu} \Phi_{\nu}(\mathbf{x}, \mathbf{x'}) = \delta(\mathbf{x} - \mathbf{x'}). \tag{2.24}$$

Thus $\Phi_{\nu}(\mathbf{x}, \mathbf{x'})$ can be considered as the projection of the delta function $\delta(\mathbf{x} - \mathbf{x'})$ onto the band ν. After second quantization, the band density matrix is defined by

$$\rho_{\mu,\nu}(\mathbf{x}, \mathbf{y}, t) = \left\langle \psi_{\mu}^{\dagger}(\mathbf{x}, t)\psi_{\nu}(\mathbf{y}, t) \right\rangle, \tag{2.25}$$

so that the two-dimensional electron density is (the factor 2 is due to spin degeneracy)

$$n(\mathbf{x}, t) = 2l \sum_{\mu,\nu} \left\langle \psi_{\mu}^{\dagger}(\mathbf{x}, t)\psi_{\mu}(\mathbf{x}, t) \right\rangle = 2l \sum_{\mu,\nu} \rho_{\mu,\nu}(\mathbf{x}, \mathbf{x}, t). \tag{2.26}$$

Using equations (2.25) and (2.26), we can derive the following evolution equation for the band density matrix

$$i\hbar \frac{\partial}{\partial t}\rho_{\mu,\nu} + \frac{\hbar^2}{2m^*}\left(\frac{\partial^2}{\partial \mathbf{y}_{\perp}^2} - \frac{\partial^2}{\partial \mathbf{x}_{\perp}^2}\right)\rho_{\mu,\nu} \tag{2.27}$$

$$- \sum_{m=-\infty}^{\infty} [E_{\nu}(m)\rho_{\mu,\nu}(\mathbf{x}, y + ml, \mathbf{y}_{\perp}, t) - E_{\mu}(m)\rho_{\mu,\nu}(x - ml, \mathbf{x}_{\perp}, \mathbf{y}, t)] +$$

$$e \sum_{\nu'} \int W(\mathbf{z})[\Phi_{\nu}(\mathbf{y}, \mathbf{z})\rho_{\mu,\nu'}(\mathbf{x}, \mathbf{z}, t) - \Phi_{\mu}(\mathbf{z}, \mathbf{x})\rho_{\nu',\nu}(\mathbf{z}, \mathbf{y}, t)]\, d\mathbf{z} = Q[\rho], \tag{2.28}$$

with $Q[\rho] \equiv 0$ in the absence of scattering. The Hartree potential satisfies the Poisson equation

$$\varepsilon \frac{\partial^2 W}{\partial x^2} = \frac{e}{l}(n - N_D). \tag{2.29}$$

When considering scattering, the right-hand side of equation (2.27) is equal to a non-zero functional of the band density matrix $Q[\rho]$, whose form depends on the closure assumption we have made to close the density matrix hierarchy. In the semiclassical limit, the kernel of the collision term $Q[\rho]$ is usually found by using leading order perturbation theory in the impurity potential, electron-phonon interaction, etc. We will treat the collision models later, so that in order to obtain the kinetic equations in the semiclassical limit, we shall rewrite equation (2.27) in terms of the band Wigner function

$$w_{\mu,\nu}(\mathbf{x}, \mathbf{k}, t) = \int \rho_{\mu,\nu}\left(\mathbf{x} + \frac{1}{2}\xi, \mathbf{x} - \frac{1}{2}\xi, t\right) e^{i\mathbf{k}\cdot\xi}\, d\xi. \tag{2.30}$$

The symmetry properties of the density matrix imply that the Wigner matrix is Hermitian,

$$w_{\mu,\nu}(\mathbf{x},\mathbf{k},t) = w^*_{\nu,\mu}(\mathbf{x},\mathbf{k},t). \tag{2.31}$$

The evolution equation for the Wigner function is

$$\begin{aligned}
&\frac{\partial}{\partial t}w_{\mu,\nu} + \frac{\hbar\mathbf{k}_\perp}{m^*}\frac{\partial}{\partial \mathbf{x}_\perp}w_{\mu,\nu} + \frac{i}{\hbar}\sum_{m=-\infty}^{\infty} e^{imkl}\left[E_\nu(m)w_{\mu,\nu}\left(x+ml/2,\mathbf{x}_\perp,\mathbf{k},t\right) - \right.\\
&\left. E_\mu(m)w_{\mu,\nu}\left(x-ml/2,\mathbf{x}_\perp,\mathbf{k},t\right)\right] + \frac{ie}{\hbar}\sum_{\nu'}\int\left[W\left(z+\frac{1}{2i}\frac{\partial}{\partial k},x_\perp\right)\right.\\
&\times\phi_\mu(z,x)e^{ik(x-z)}w_{\nu',\nu}\left(\frac{x+z}{2},\mathbf{x}_\perp,\mathbf{k},t\right) - W\left(z-\frac{1}{2i}\frac{\partial}{\partial k},x_\perp\right)\\
&\left.\times\phi_\nu(x,z)e^{-ik(x-z)}w_{\mu,\nu'}\left(\frac{x+z}{2},\mathbf{x}_\perp,\mathbf{k},t\right)\right]\,dz = Q_{\mu,\nu}[w]
\end{aligned} \tag{2.32}$$

in which the collision term is again left unspecified. Note that the two-dimensional electron density is

$$n(\mathbf{x},t) = \frac{2l}{8\pi^3}\sum_{\mu,\nu}\int w_{\mu,\nu}(\mathbf{x},\mathbf{k},t)d\mathbf{k} \tag{2.33}$$

because of equation (2.26) and the definition in equation (2.30). From equations (2.32) and (2.33), we obtain the charge continuity equation,

$$\frac{e}{l}\frac{\partial n}{\partial t} + \frac{\partial}{\partial \mathbf{x}}\cdot\mathbf{J} = 0, \tag{2.34}$$

$$\mathbf{J}_\perp = \frac{2e}{8\pi^3}\int\frac{\hbar\mathbf{k}_\perp}{m^*}\sum_{\mu,\nu}w_{\mu,\nu}(\mathbf{x},\mathbf{k},t)\,d\mathbf{k}, \tag{2.35}$$

$$\begin{aligned}
\frac{\partial\mathbf{J}}{\partial x} = \frac{ie}{4\pi^3\hbar}\sum_{\mu,\nu,m}\int e^{imkl}&\left[E_\nu(m)w_{\mu,\nu}(x+ml/2,\mathbf{x}_\perp,\mathbf{k},t) - \right.\\
&\left. E_\mu(m)w_{\mu,\nu}(x-ml/2,\mathbf{x}_\perp,\mathbf{k},t)\right]\,d\mathbf{k},
\end{aligned} \tag{2.36}$$

provided our collision model satisfies $\int\sum_{\mu,\nu}Q_{\mu,\nu}\,d\mathbf{k} = 0$. A related formulation of the band Wigner functions (without collision terms) is due to Demeio et al [32]. One difficulty with our formulation is that the Wigner function in equation (2.30) is not $2\pi/l$-periodic in k. This can be corrected by using the

following definition:

$$f_{\mu,\nu}(\mathbf{x},\mathbf{k},t) \equiv \sum_{s=-\infty}^{\infty} w_{\mu,\nu}(\mathbf{x},k+2\pi s/l,\mathbf{k}_\perp,t) \tag{2.37}$$

$$= \sum_{j=-\infty}^{\infty} e^{ijkl} l \int \rho_{\mu,\nu}(x+jl/2,\mathbf{x}_\perp+\xi_\perp/2,x-jl/2,\mathbf{x}_\perp-\xi_\perp/2,t) e^{i\mathbf{k}_\perp\cdot\xi_\perp}\, d\xi_\perp.$$

To derive this equation, we have used the identity

$$\sum_{j=-\infty}^{\infty} \delta(\xi - jl) = \frac{1}{l} \sum_{s=-\infty}^{\infty} e^{i2\pi\xi s/l}, \tag{2.38}$$

together with the definition of equation (2.30). From equations (2.33) and (2.38), we obtain the two-dimensional electron density in terms of $f_{\mu,\nu}$:

$$n(x,t) = \frac{2l}{8\pi^3} \sum_{\mu,\nu} \int_{-\pi/l}^{\pi/l} \int f_{\mu,\nu}(\mathbf{x},\mathbf{k},t)\, dk d\mathbf{k}_\perp. \tag{2.39}$$

Similarly, the transversal current density can be obtained from equations (2.35) and (2.38):

$$\mathbf{J}_\perp = \frac{2e}{8\pi^3} \int_{-\pi/l}^{\pi/l} \int \frac{\hbar\mathbf{k}_\perp}{m^*} \sum_{\mu,\nu} f_{\mu,\nu}(\mathbf{x},\mathbf{k},t)\, dk d\mathbf{k}_\perp. \tag{2.40}$$

The current density along the growth direction has the form

$$J = \frac{2e\hbar}{8\pi^3 m^*} \sum_{\mu,\nu,s} \int_{-\pi/l}^{\pi/l} \int w_{\mu,\nu}(x,k+2\pi s/l,\mathbf{k}_\perp,t)\, dk d\mathbf{k}_\perp. \tag{2.41}$$

The definition of the periodic band Wigner function is related to that adopted by Bechouche et al [7]. These authors have rigorously proved that the collisionless Wigner-Poisson equations for a crystal become the crystal Vlasov-Poisson equations in the semiclassical limit, assuming that the initial conditions are concentrated in isolated bands. Scattering other than electron-electron scattering is not considered in these works. Further progress can be made specifying models for the collision terms. It is convenient to distinguish two cases:

1. miniband transport corresponding to field values, for which only the first miniband of the SL is populated, and

2. transport in several minibands.

Strongly coupled SLs at relatively low fields are well described by miniband transport, whereas weakly coupled SLs typically require consideration of transport in several minibands. In both cases, non-linear phenomena are better described by reduced equations for moments of the Wigner functions, such as the electron density, the electric field and the electron average momentum and energy. For miniband transport, we can find these reduced equations using singular perturbation methods if we start from a sufficiently simple quantum kinetic equation. The study of transport in several minibands was less advanced and a new contribution for strongly coupled SLs is presented in chapters 5 and 6 [10] [2].

We now sum all the Wigner equations (2.32) over the band indices and use the closure condition in equation (2.24), so as to find an equation for $w(\mathbf{x},\mathbf{k},t)=\sum_{\mu,\nu} w_{\mu,\nu}(\mathbf{x},\mathbf{k},t)$, assume that only the first miniband is populated and that there are no transitions between minibands, i.e. $w(\mathbf{x},\mathbf{k},t)\approx w_{1,1}(\mathbf{x},\mathbf{k},t)$. Then we obtain the following equation for the periodic Wigner function in equation (2.38):

$$\frac{\partial}{\partial t}f+\frac{\hbar\mathbf{k}_\perp}{m^*}\frac{\partial}{\partial \mathbf{x}_\perp}f+\frac{i}{\hbar}\sum_{m=-\infty}^{\infty}e^{imkl}E_1(m)\left[f(x+ml/2,\mathbf{x}_\perp,\mathbf{k},t)-f(x-ml/2,\mathbf{x}_\perp,\mathbf{k},t)\right]+$$
$$\frac{ie}{\hbar}\left[W\left(x+\frac{1}{2i}\frac{\partial}{\partial k},\mathbf{x}_\perp\right)-W\left(x-\frac{1}{2i}\frac{\partial}{\partial k},\mathbf{x}_\perp\right)\right]f=Q[f]. \tag{2.42}$$

If we use the tight-binding approximation, the dispersion relation $\mathcal{E}_1(k)$ is (2.10), $\mathcal{E}_1(k)=\Delta_1[1-\cos(kl)]/2$ plus a constant (Δ_1 denotes the width of the first miniband). Moreover, the field $F=\partial W/\partial x$ satisfies the Poisson equation:

$$\varepsilon\left(\frac{\partial F}{\partial x}+\frac{\partial}{\partial \mathbf{x}_\perp}\mathbf{F}_\perp\right)=\frac{e}{l}(n-N_D), \tag{2.43}$$

and the electron density is:

$$n(x,\mathbf{x}_\perp,t)=\frac{l}{4\pi^3}\int_{-\pi/l}^{\pi/l}\int_{-\infty}^{\infty}\int_{-\infty}^{\infty}f(x,\mathbf{x}_\perp,k,\mathbf{k}_\perp.t)\,dkd\mathbf{k}_\perp. \tag{2.44}$$

2.2.2 Scattering treatment

Scattering processes such as phonon scattering change the energy and momentum of the electrons, leading the distribution function towards thermal equilibrium. A simple way to describe these processes is the following

Bhatnagar-Gross-Krook (BGK) collision model [10, 13]:

$$Q_{en}[f] \equiv -\nu_{en}\,\left(f - f^{FD}\right). \tag{2.45}$$

Here $1/\nu_{en}$ represents the inelastic collisions relaxation time, and f^{FD} is the Fermi-Dirac local equilibrium distribution function:

$$f^{FD}(k;n) = \frac{m^* k_B T}{\pi\hbar^2}\int_{-\infty}^{\infty} \ln\left[1+\exp\left(\frac{\mu - E}{k_B T}\right)\right] \frac{\sqrt{2}\,\Gamma^3/\pi}{[E-\mathcal{E}_1(k)]^4+\Gamma^4}\,dE. \tag{2.46}$$

where Γ measures the finite width of the spectral function in thermal equilibrium (energy broadening) due to scattering [76]. As $\Gamma \to 0$, the first factor in equation (2.46) becomes a delta function, and we recover the usual Fermi-Dirac distribution function with a chemical potential μ. The chemical potential $\mu = \mu(x, \mathbf{x}_\perp, t)$ is a function of the exact electron density, n, of equation (2.44) that is calculated by solving the equation:

$$n(x,t) = \frac{l}{4\pi^3}\int_{-\pi/l}^{\pi/l}\int_{-\infty}^{\infty}\int_{-\infty}^{\infty} f^{FD}(k, \mathbf{k}_\perp; n(x,t))dk d\mathbf{k}_\perp. \tag{2.47}$$

$$\tag{2.48}$$

With these definitions, the integral

$$\int_{-\pi/l}^{\pi/l} Q_{en}\,dk = 0 \tag{2.49}$$

indicates charge conservation. Other scattering processes, such as impurity scattering, conserve the energy of the electron, change only its momentum and also preserve charge continuity. Gerhardts [37] used the following model:

$$Q_{imp}[f] = -\frac{\tilde{\nu}_{imp}}{4\pi^3}\int_{-\pi/l}^{\pi/l}\int_{-\infty}^{\infty}\int_{-\infty}^{\infty} \delta[E(k,\mathbf{k}_\perp) - E(k',\mathbf{k'}_\perp)][f(k,\mathbf{k}_\perp) - f(k',\mathbf{k'}_\perp)]\,dk' d\mathbf{k'}_\perp, \tag{2.50}$$

This collision term couples the vertical motion of the electron to the lateral degrees of freedom. Assuming that the variation of the energy in the lateral direction is negligible, i.e. $E(k,\mathbf{k}_\perp) - E(k',\mathbf{k'}_\perp) \approx \mathcal{E}(k) - \mathcal{E}(k')$, and therefore:

$$Q_{imp}[f] \approx -\frac{\tilde{\nu}_{imp}}{2\pi}\int_{-\pi/l}^{\pi/l} delta[\mathcal{E}(k) - \mathcal{E}(k')][f(k) - f(k')]\,dk' d\mathbf{k'} dk. \tag{2.51}$$

Let us now suppose that the initial Wigner function does not depend on $\mathbf{x}_\perp$. Then (2.42)-(2.52) imply that the reduced Wigner function

$$f(x,k,t) = \frac{1}{2\pi^2 S}\int\int f(x,\mathbf{x}_\perp,k,\mathbf{k'}_\perp,t)\,d\mathbf{k'}_\perp d\mathbf{x}_\perp \tag{2.52}$$

(independent of $\mathbf{x}_\perp$) solves the following Wigner-Poisson-BGK system of equations:

$$\begin{aligned}
&\frac{\partial f}{\partial t} + \frac{i}{\hbar}\sum_{j=-\infty}^{\infty} e^{ijkl}E_1(j)\left[f\left(x+jl/2,k,t\right) - f\left(x-jl/2,k,t\right)\right] \\
&\quad + \frac{ie}{\hbar}\left[W\left(x+\frac{1}{2i}\frac{\partial}{\partial k},t\right) - W\left(x-\frac{1}{2i}\frac{\partial}{\partial k},t\right)\right] f \\
&\quad = Q[f] \equiv -\nu_{en}\left(f - f^{FD}\right) - \nu_{\rm imp}\,\frac{f(x,k,t) - f(x,-k,t)}{2},
\end{aligned} \tag{2.53}$$

$$\varepsilon\,\frac{\partial^2 W}{\partial x^2} = \frac{e}{l}\,(n - N_D), \tag{2.54}$$

$$n = \frac{l}{2\pi}\int_{-\pi/l}^{\pi/l} f(x,k,t)dk = \frac{l}{2\pi}\int_{-\pi/l}^{\pi/l} f^{FD}(k;n(x,t))dk, \tag{2.55}$$

$$f^{FD}(k;n) = \frac{m^* k_B T}{\pi\hbar^2}\int_{-\infty}^{\infty} \ln\left[1+\exp\left(\frac{\mu - E}{k_B T}\right)\right]\frac{\sqrt{2}\,\Gamma^3/\pi}{[E-\mathcal{E}_1(k)]^4 + \Gamma^4}\,dE. \tag{2.56}$$

In the semiclassical limit, the pseudo-differential operators in the left hand side of (2.53) become the usual convective terms:

$$\frac{\partial f}{\partial t} + v(k)\,\frac{\partial f}{\partial x} + \frac{eF}{\hbar}\,\frac{\partial f}{\partial k} = -\nu_{en}\left(f - f^{FD}\right) - \nu_{\rm imp}\,\mathcal{A}f, \tag{2.57}$$

$$F = \frac{\partial W}{\partial x}, \quad \mathcal{A}f = \frac{f(k) - f(-k)}{2}, \quad v(k) = \frac{1}{\hbar}\,\frac{d\mathcal{E}}{dk} = \frac{\Delta l}{2\hbar}\,\sin(kl), \tag{2.58}$$

for the tight binding dispersion relation (2.10). For an external spatially homogeneous field, when f^{FD} is the global thermal equilibrium distribution, (2.57) becomes the equation proposed by Ktitorov, Simin and Sindalovskii (KSS) in 1971 [54]. When f^{FD} in (2.57) is replaced by the Boltzmann local equilibrium, this equation becomes the Boltzmann-BGK equation used by Ignatov and Shashkin [43].

2.3 Derivation of balance equations by the Chapman-Enskog method

In this section, we shall derive reduced balance equations for the electric field and the electron density starting from the miniband Wigner-Poisson-BGK system following [13]. In the context of single-miniband SLs, Büttiker and Thomas [23] and later Lei and collaborators (see for example [56,57,59]) have exploited the use of balance equations based on hydrodynamic variables. These models are not derived from kinetic equations using a systematic and consistent perturbation analysis. Lei [56] writes moment equations for the electron density, its average velocity and its average energy directly from a quantum theory. These equations are part of an infinite hierarchy, which is closed by assuming that the distribution function is a three-parameter Fermi-Dirac distribution depending on the electron density, an electron temperature and a moving wave vector within the lowest miniband described in the tight-binding approximation [58]. Cao and Lei [24] have described current self-oscillations in doped, strongly coupled SLs by means of hydrodynamic balance equations.

2.3.1 Equivalent form of the Wigner-Poisson-BGK equations

We rewrite the Wigner equation (2.53) in a more convenient form by using the Fourier series of the Wigner function (which is periodic in k):

$$f(x,k,t) = \sum_{j=-\infty}^{\infty} f_j(x,t)\, e^{ijkl}. \tag{2.59}$$

The third term of the LHS of equation (2.53) becomes:

$$\begin{aligned} &\frac{ie}{\hbar}\left[W\left(x+\frac{1}{2i}\frac{\partial}{\partial k},t\right)-W\left(x-\frac{1}{2i}\frac{\partial}{\partial k},t\right)\right] f = \\ &\quad \sum_{j=-\infty}^{\infty}\left[W\left(x+jl/2,t\right)-W\left(x-jl/2,t\right)\right] f_j e^{ijkl} = \\ &\quad \sum_{j=-\infty}^{\infty} jl\langle F\rangle_j f_j e^{ijkl}. \end{aligned} \tag{2.60}$$

Here $\langle F\rangle_j$ is the spatial average:

$$\langle F\rangle_j(x,t) = \frac{1}{jl}\int_{-jl/2}^{jl/2} F(x+s,t)\,ds, \tag{2.61}$$

whose first spatial derivative can be expressed in terms of a finite difference:

$$\frac{\partial}{\partial x}\langle F\rangle_j(x,t) = \frac{1}{jl}(F(x+jl/2,t) - F(x-jl/2,t)). \tag{2.62}$$

Then the second term in LHS of equation (2.53) is:

$$\frac{i}{\hbar}\sum_{j=-\infty}^{\infty}\left[f\left(x+jl/2,t\right) - f\left(x-jl/2,t\right)\right]E_1(j)e^{ijkl} = \sum_{j=-\infty}^{\infty}\frac{ijl}{\hbar}e^{ijkl}E_1(j)\frac{\partial}{\partial x}\langle f\rangle_j, \tag{2.63}$$

which in the case of the tight-binding dispersion relation (2.10), $\mathcal{E}_1(k) = \Delta_1(1-\cos kl)/2$, becomes $v(k)\,\partial\langle f\rangle_j/\partial x$. Inserting equations (2.60) and (2.63) into equation (2.53), we obtain the following equivalent form of the Wigner equation, which is particularly suitable for treating SL problems:

$$\begin{aligned}\frac{\partial f}{\partial t} + \sum_{j=-\infty}^{\infty}\frac{ijl}{\hbar}e^{ijkl}\left(E_1(j)\frac{\partial}{\partial x}\langle f\rangle_j + e\langle F\rangle_j f_j\right)\\ = -\nu_{en}\left(f - f^{FD}\right) - \nu_{\text{imp}}\frac{f(x,k,t) - f(x,-k,t)}{2},\end{aligned} \tag{2.64}$$

By integrating this equation over k, we get the charge continuity equation:

$$\frac{\partial n}{\partial t} + \frac{\partial}{\partial x}\sum_{j=1}^{\infty}\frac{2jl}{\hbar}\left\langle Im(E_1(-j)f_j)\right\rangle_j = 0. \tag{2.65}$$

We can eliminate the electron density from equation (2.64) by using the Poisson equation (2.54) and integrating the result over x, thereby obtaining the non-local Ampère's law:

$$\varepsilon\frac{\partial F}{\partial t} + \frac{2e}{\hbar}\sum_{j=1}^{\infty} j\left\langle Im(E_1(-j)f_j)\right\rangle_j = J(t), \tag{2.66}$$

wher $J(t)$ is the total current density. Equations (2.64)-(2.66) are spatially non-local versions of the corresponding semiclassical equations. The charge continuity and Ampère's equations have their traditional form as derived from semiclassical Boltzmann equations, except that the electron current is averaged over the SL periods. This non-locality will be transmitted to the QDDE obtained by means of the Chapman-Enskog method [13].

2.3.2 Chapman-Enskog method

To apply the Chapman-Enskog method, we first define two different scales in equation (2.53). Let v_M and F_M denote the electron velocity and field scales, respectively, typical of the macroscopic phenomena described by the sought-after balance equation; for example, let them be the positive values at which the (zeroth order) drift velocity reaches its maximum. In the hyperbolic limit, the time t_0 it takes an electron with speed v_M to traverse a distance $x_0 = \varepsilon F_M l/(eN_D)$ (given by the Poisson equation), over which the field variation is of order F_M, is much longer than the mean time between collisions, $\nu_{en}^{-1} = \hbar/(eF_M l) = t_1$. Note that $1/t_1$ is of the order of the Bloch frequency. We therefore define the small parameter $\lambda = t_1/t_0 = \hbar v_M N_D/(\varepsilon F_M^2 l^2) \ll 1$ and formally multiply the first two terms on the left-hand side of equation (2.53) by λ. After obtaining the number of desired terms, we set $\lambda = 1$.

The Chapman-Enskog ansatz consists of writing the distribution function as an expansion in powers of the small parameter λ:

$$f(x,k,t;\lambda) = \sum_{m=0}^{\infty} f^{(m)}(k;F,n)\lambda^m, \tag{2.67}$$

$$\frac{\partial F}{\partial t} + \sum_{m=0}^{\infty} \mathcal{J}^{(m)}(F,n)\,\lambda^m = J(t), \tag{2.68}$$

The coefficients $f^{(m)}(k;F,n)$ depend on x and t only through their dependence on the electric field and the electron density (which are related through the Poisson equation). Moreover, if we integrate (2.67) over k, we find that

$$\int_{-\pi/l}^{\pi/l} f^{(m)}(k;n)\,dk = \frac{2\pi}{l}\, f_0^{(m)} = 0, \quad m \geq 1, \tag{2.69}$$

in other words, $f^{(m)}$ do not contain contributions proportional to the zero-order term $f^{(0)}$.
If we write (2.53) in terms of the small parameter λ, the result is

$$\lambda\left(\frac{\partial f}{\partial t} + \sum_{j=-\infty}^{\infty} \frac{ijl}{\hbar}\, e^{ijkl}\mathcal{E}_j\, \frac{\partial}{\partial x}\langle f\rangle_j\right) = Q[f] - \sum_{j=-\infty}^{\infty} \frac{iejl}{\hbar}\, e^{ijkl}\langle F\rangle_j\, f_j. \tag{2.70}$$

The solution of Eq. (2.70) for $\lambda = 0$ is calculated in terms of its Fourier coefficients as

$$f^{(0)}(k;F) = \sum_{j=-\infty}^{\infty} \frac{(1 - ij\mathcal{F}_j/\tau_e)\, f_j^{FD}}{1 + j^2\mathcal{F}_j^2}\, e^{ijkl}, \tag{2.71}$$

where $\mathcal{F}_j = \langle F \rangle_j / F_M$, $F_M = \frac{\hbar}{el}\sqrt{\nu_{en}(\nu_{en}+\nu_{imp})}$ and $\tau_e = \sqrt{(\nu_{en}+\nu_{imp})/\nu_{en}}$. Coefficients f_j^{FD} are the Fourier coefficients of f^{FD}, which are real because f^{FD} is even in k. Note that (2.56) implies that $f_0 = f_0^{FD} = n$.

The rest of the Chapman-Enskog expansion terms ($f^{(m)}$, $m \geq 1$) can be obtained by inserting equations (2.67) and (2.68) into equation (2.70) and equating all coefficients of λ^m in the resulting series to zero. We find the hierarchy:

$$\mathcal{L}f^{(1)} = -\left(\frac{\partial}{\partial t} + \sum_{j=-\infty}^{\infty} \frac{ijl}{\hbar}\, e^{ijkl} E_1(j)\, \frac{\partial}{\partial x}\langle f^{(0)}\rangle_j\right)\Bigg|_0, \tag{2.72}$$

$$\mathcal{L}f^{(2)} = -\left(\frac{\partial f^{(1)}}{\partial t} + \sum_{j=-\infty}^{\infty} \frac{ijl}{\hbar}\, e^{ijkl} E_1(j)\, \frac{\partial}{\partial x}\langle f^{(1)}\rangle_j\right)\Bigg|_0 - \frac{\partial}{\partial t} f^{(0)}\Bigg|_1, \tag{2.73}$$

and so on. Here

$$\mathcal{L}u(k) \equiv \frac{ie}{\hbar} \sum_{j=-\infty}^{\infty} jl\langle F\rangle_j u_j e^{ijkl} + \left(\nu_{en} + \frac{\nu_{\text{imp}}}{2}\right) u(k) - \frac{\nu_{\text{imp}} u(-k)}{2}, \tag{2.74}$$

and the subscripts 0 and 1 in the RHS of these equations mean that $\varepsilon\, \partial F/\partial t$ is replaced by $J - J^{(0)}(F)$ and by $-J^{(1)}(F)$, respectively. The linear equation $\mathcal{L}u = S$ has a bounded $2\pi/l$-periodic solution, provided that the integral of S over k is null. Using this, the solvability conditions for the linear hierarchy of equations yield

$$J^{(m)} = \frac{2e}{\hbar} \sum_{j=1}^{\infty} j\langle \text{Im}(\mathcal{E}_{-j} f_j^{(m)})\rangle_j, \tag{2.75}$$

which can also be obtained by insertion of Eq. (2.67) in (2.66). Equation (2.72) yields the first order correction of f:

$$f_j^{(1)}(F) = \frac{Re S_j^{(1)} + i\tau_e^{-2} Im S_j^{(1)} - ij\mathcal{F} S_j^{(1)}/\tau_e}{(1 + j^2\mathcal{F}^2)\nu_{en}} \tag{2.76}$$

where the subscript j means the jth Fourier coefficient, and S is the RHS of (2.72). Now we can insert $f^{(0)}$ and $f^{(1)}$ from (2.71) and (2.76) into the Ampère's law (2.66) obtaining the QDDE for the field. This QDDE can be numerically solved together with the Poisson equation (2.54), obtaining self sustained oscillations of the current (SSOC) for a strongly coupled SL

under dc voltage bias due to the periodic recycling and motion of charge dipoles [13]. Note that the local *generalized* DDE (GDDE) [12], semiclassical limit of the QDDE, can be obtained by ignoring all the local spatial averages (i.e. $\langle u(x,t)\rangle_j \approx u(x,t)$) in the QDDE.

Using equation (2.76), we can now explicitly write two terms in equation (2.68), thereby obtaining a balance equation for the field and the electron density. For the tight-binding dispersion relation (2.10), this equation is

$$\begin{aligned}
&\varepsilon\frac{\partial F}{\partial t} + \frac{eN_D v_M}{l}\,\mathcal{N}\left(F, \frac{\partial F}{\partial x}\right) \\
&\quad = \varepsilon\left\langle D\left(F, \frac{\partial F}{\partial x}, \frac{\partial^2 F}{\partial x^2}\right)\right\rangle_1 + \left\langle A\left(F, \frac{\partial F}{\partial x}\right)\right\rangle_1 J(t), && (2.77)\\
&A = 1 + \frac{2ev_M}{\varepsilon F_M l(\nu_{en}+\nu_{\rm imp})}\,\frac{1-(1+2\tau_e^2)\,\mathcal{F}^2}{(1+\mathcal{F}^2)^3}\,n\mathcal{M}, && (2.78)\\
&\mathcal{N} = \langle nV\mathcal{M}\rangle_1 + \langle (A-1)\langle\langle nV\mathcal{M}\rangle_1\rangle_1\rangle_1 \\
&\quad -\frac{l\tau_e\Delta_1}{F_M\hbar(\nu_{en}+\nu_{\rm imp})}\left\langle\frac{B}{1+\mathcal{F}^2}\right\rangle_1, && (2.79)\\
&V(\mathcal{F}) = \frac{2\mathcal{F}}{1+\mathcal{F}^2}, \quad v_M = \frac{l\,\mathcal{I}_1(M)\Delta_1}{4\hbar\tau_e\mathcal{I}_0(M)}, && (2.80)\\
&D = \frac{l^2\Delta_1^2}{8\hbar^2(\nu_{en}+\nu_{\rm imp})(1+\mathcal{F}^2)}\left(\frac{\partial^2\langle F\rangle_1}{\partial x^2} - \frac{4\hbar v_M\tau_e C}{l\Delta_1}\right), && (2.81)\\
&B = \left\langle\frac{4\mathcal{F}_2 n\mathcal{M}_2}{(1+4\mathcal{F}_2^2)^2}\frac{\partial\langle F\rangle_2}{\partial x}\right\rangle_1 \\
&\quad +\mathcal{F}\left\langle\frac{n\mathcal{M}_2(1-4\mathcal{F}_2^2)}{(1+4\mathcal{F}_2^2)^2}\frac{\partial\langle F\rangle_2}{\partial x}\right\rangle_1 \\
&-\frac{4\hbar v_M(1+\tau_e^2)\mathcal{F}(n\mathcal{M})'}{l\tau_e(1+\mathcal{F}^2)\,\Delta_1}\left\langle n\mathcal{M}\frac{1-\mathcal{F}^2}{(1+\mathcal{F}^2)^2}\frac{\partial\langle F\rangle_1}{\partial x}\right\rangle_1 && (2.82)\\
&C = \left\langle\frac{(n\mathcal{M}_2)'}{1+4\mathcal{F}_2^2}\,\frac{\partial^2 F}{\partial x^2}\right\rangle_1 - 2\mathcal{F}\left\langle\frac{(n\mathcal{M}_2)'\mathcal{F}_2}{1+4\mathcal{F}_2^2}\,\frac{\partial^2 F}{\partial x^2}\right\rangle_1 \\
&\quad +\frac{8\hbar v_M(1+\tau_e^2)(n\mathcal{M})'\,\mathcal{F}}{l\tau_e\,(1+\mathcal{F}^2)\,\Delta_1}\left\langle\frac{(n\mathcal{M})'\mathcal{F}}{1+\mathcal{F}^2}\,\frac{\partial^2 F}{\partial x^2}\right\rangle_1. && (2.83)\\
& && (2.84)
\end{aligned}$$

$$\mathcal{M}(n/N_D) = \frac{\mathcal{I}_1(\tilde{\mu})\,\mathcal{I}_0(M)}{\mathcal{I}_0(\tilde{\mu})\,\mathcal{I}_1(M)}, \quad \mathcal{M}_2(n/N_D) = \frac{\mathcal{I}_2(\tilde{\mu})\,\mathcal{I}_0(M)}{\mathcal{I}_0(\tilde{\mu})\,\mathcal{I}_1(M)}, \quad (2.85)$$

$$\mathcal{I}_m(\tilde{\mu}) = \frac{1}{\pi}\int_0^{\pi} \cos(mk) \times \left[\int_{-\infty}^{\infty} \frac{\sqrt{2}\,\tilde{\Gamma}^3}{(\tilde{E}-\delta+\delta\cos k)^4+\tilde{\Gamma}^4}\,\ln\left(1+e^{\tilde{\mu}-\tilde{E}}\right)d\tilde{E}\right] dk. \quad (2.86)$$

The electric field and the electron density are related by the Poisson equation (2.29). Here g' denotes dg/dn, $\delta = \Delta_1/(2k_BT)$, $\tilde{\mu} = \mu/(k_BT)$, $\tilde{\Gamma} = \Gamma/(k_BT)$, $\mathcal{F} = \mathcal{F}_1$, and $n = N_D$ at the particular value of the dimensionless chemical potential $\tilde{\mu} = M$. If the electric field and the electron density do not change appreciably over two SL periods, $\langle F\rangle_j \approx F$, the spatial averages can be ignored, and the *non-local* QDDE (2.77) becomes the *local* generalized DDE (GDDE) obtained from the semiclassical theory [12].

Chapter 3

Nonequilibrium free energy, H theorem and self-sustained oscillations for Boltzmann-BGK descriptions of semiconductor superlattices

3.1 Introduction

In this chapter, we find the Lyapunov functional for a BGK-Poisson kinetic equation describing a SL for idealized boundary conditions (infinite SL, periodic boundary conditions or finite SL with insulated contacts at zero voltage bias). This functional has the form of a free energy and the corresponding entropy production contains a generalized force which is proportional to the difference between distribution and local equilibrium distribution functions. It is remarkable that formulas of irreversible thermodynamics hold in a regime that is very far from equilibrium. We approximate the free energy functional using the leading order approximation of the Chapman-Enskog method and calculate it numerically in two cases: insulated contacts at zero voltage bias (*closed system*) and contacts having finite conductivity at nonzero voltage bias (*open system*) in a regime where there are self-sustained oscillations of the current through the SL. In the first case, we have checked that the free energy indeed decreases monotonically towards its equilibrium value, whereas for the case of the *open system* (nonzero voltage bias and nonzero contact conductivity) the free energy oscillates in time following the evolution of the

current and the electric field inside the SL.

The rest of this chapter is as follows. Section 3.2 presents the model kinetic equation and a generalized drift-diffusion system that can be derived from it by means of the Chapman-Enskog method [12]. In Section 3.3, we derive an entropy density functional from a given form of the local equilibrium distribution, and then find a free energy density from which we prove the H theorem provided the contacts at the SL ends are insulating and there is a zero voltage bias between them. In such conditions, any initial condition evolves towards the globally stable equilibrium and the free energy decreases monotonically until it reaches its equilibrium value. Of course under realistic boundary conditions of charge injecting and collecting contacts and nonzero voltage bias, the SL is far from equilibrium and, in fact, self-sustained oscillations of the current due to periodic recycling and motion of charge dipole domains are possible stable solutions [14, 27]. In this case, the free energy is no longer a Lyapunov functional and it oscillates periodically in time in the regime of current self-oscillations. In Section 3.4, these different regimes and behaviors of the free energy are confirmed by solving numerically the generalized drift-diffusion system, reconstructing the approximate distribution function provided by the Chapman-Enskog method and finding the free energy as a function of time. The last section contains our conclusions.

3.2 BPBGK kinetic equation and generalized drift-diffusion balance equation

In this Section, we present the Boltzmann-Poisson kinetic description of a one-miniband SL and recall the drift-diffusion balance equation that can be derived therefrom by means of the Chapman-Enskog method [12].

3.2.1 Kinetic equation and local equilibrium distribution

The Boltzmann-Poisson-Bhatnagar-Gross-Krook (BPBGK) system for 1D electron transport in the lowest miniband of a strongly coupled SL is [12]:

$$\frac{\partial f}{\partial t} + \frac{1}{\hbar}\frac{d\mathcal{E}}{dk}\frac{\partial f}{\partial x} + \frac{e}{\hbar}\frac{\partial W}{\partial x}\frac{\partial f}{\partial k} = Q[f] \equiv -\nu_{en}\left(f - f^{FD}\right) - \nu_{imp}\mathcal{A}f, \tag{3.1}$$

$$\varepsilon\frac{\partial^2 W}{\partial x^2} = \frac{e}{l}(n - N_D), \tag{3.2}$$

$$n(x,t) = \frac{l}{2\pi}\int_{-\pi/l}^{\pi/l} f(x,k,t)dk = \frac{l}{2\pi}\int_{-\pi/l}^{\pi/l} f^{FD}(k; n(x,t))dk, \tag{3.3}$$

$$f^{FD}(k;n) = \frac{m^* k_B T}{\pi\hbar^2}\int_{-\infty}^{\infty} \ln\left[1 + \exp\left(\frac{\mu - E}{k_B T}\right)\right] \frac{\sqrt{2}\,\Gamma^3/\pi}{[E - \mathcal{E}(k)]^4 + \Gamma^4}\,dE. \tag{3.4}$$

Here f, $\mathcal{A}f = [f(x,k,t - f(x,-k,t)]/2$, $f^{FD}(k;n)$, n, N_D, $\mathcal{E}(k)$, d_B, d_W, $l = d_B + d_W$, W, ε, m^*, k_B, T, Γ, ν_{en}, ν_{imp} and $-e < 0$ are the one-particle distribution function, its odd part (in k), the 1D local equilibrium distribution function, the 2D electron density, the 2D doping density, the miniband dispersion relation ($\mathcal{E}(k)$ is even: $\mathcal{E}(-k) = \mathcal{E}(k)$), the barrier width, the well width, the SL period, the electric potential, the SL permittivity, the effective mass of the electron in the lateral directions, the Boltzmann constant, the lattice temperature, the energy broadening of the equilibrium distribution due to collisions [46] (page 28), the constant frequency of the inelastic collisions responsible for energy relaxation, the constant frequency of the elastic impurity collisions and the electron charge, respectively. The chemical potential μ is a function of the electron density n that can be obtained by inserting (3.4) into (3.3) and solving for $\mu = \mu(n)$. Thus μ is a functional of f which we may write as $\mu[f]$.

Integrating (3.1) over k and using $\mu[f]$ given by (3.3), we find the charge continuity equation:

$$\frac{e}{l}\frac{\partial n}{\partial t} + \frac{\partial J_n}{\partial x} = 0, \tag{3.5}$$

where $J_n(x,t)$ is the electron current density:

$$J_n(x,t) = \frac{e}{2\pi}\int_{-\pi/l}^{\pi/l} v(k)\, f(x,k,t)dk, \quad v(k) = \frac{1}{\hbar}\frac{d\mathcal{E}}{dk}, \tag{3.6}$$

and $v(k)$ is the electron group velocity. From (3.2) and (3.5), we obtain

$$\varepsilon \frac{\partial F}{\partial t} + J_n = J(t), \quad F = \frac{\partial W}{\partial x}, \tag{3.7}$$

where $-F$ is the electric field, $J(t)$ is the total current density and (3.7) is a form of Ampère's law. The main idea behind the BGK collision model is to substitute the linear, quadratic or quartic Boltzmann collision terms, which are *nonlocal* in k, by a nonlinear collision term, $Q[f]$, that is *local* and preserves charge continuity, as in (3.5). It is convenient to use the following tight binding dispersion relation for the miniband with lowest energy:

$$\mathcal{E}(k) = \frac{\Delta}{2}(1 - \cos kl), \quad v(k) = \frac{\Delta l}{2\hbar} \sin kl. \tag{3.8}$$

Eq. (3.8) contains the first two harmonics in a Fourier series of the periodic function $\mathcal{E}(k)$. (3.8) approximates the band dispersion relation of any crystal provided the band width Δ is small compared to the energy difference between bands (band gaps) [5]. Besides being a reasonable approximation for a SL with well-separated minibands, (3.8) produces simple analytic expressions for the balance equations and is often used in comparisons between theory and experiments [14].

The system (3.1)-(3.4) is the semiclassical limit of the Wigner system of equations considered in Section 2 of Ref. [10]. Note that the 1D Fermi-Dirac local equilibrium distribution (3.4) can be written as

$$f^{FD}(k;n) = \gamma(E[f]), \quad E[f] = \frac{\mathcal{E}(k) - \mu[f]}{k_B T}, \tag{3.9}$$

$$\gamma(E) = \frac{m^* k_B T}{\pi\hbar^2} \int_{-\infty}^{\infty} \ln(1 + e^{-s}) \frac{\frac{\sqrt{2}}{\pi}\left(\frac{\Gamma}{k_B T}\right)^3}{(s-E)^4 + \left(\frac{\Gamma}{k_B T}\right)^4} ds. \tag{3.10}$$

$\gamma(E)$ is a decreasing function that takes on positive values for real values of E. If broadening due to scattering is negligible, $\Gamma \to 0$, and (3.10) becomes

$$\gamma(E) = \frac{m^* k_B T}{\pi\hbar^2} \ln(1 + e^{-E}). \tag{3.11}$$

In the Boltzmann limit, $E \to \infty$, and we have

$$\gamma(E) = \frac{m^* k_B T}{\pi\hbar^2} e^{-E}. \tag{3.12}$$

This local equilibrium distribution was used by Ignatov and Shashkin [43] to analyze particular solutions of the BPBGK system for constant electric field.

3.2.2 Chapman-Enskog perturbation method and drift-diffusion system

In the hyperbolic limit where collisions and field-dependent terms in the BPBGK system dominate all other terms, it is possible to derive a generalized drift-diffusion equation for the electric field, $-F = -\partial W/\partial x$. Collision and field-dependent terms in (3.1) are of the same order provided $e[F]l/(\hbar) = \nu_{en}$, where $[F]$ gives the order of magnitude of the field. Then $[F] = \hbar\nu_{en}/(el)$. The Poisson equation implies that the distance $[x]$ over which field varies an amount $[F]$ is proportional to $\varepsilon[F]$ divided by eN_D/l, so that $[x] = \varepsilon[F]l/(eN_D) = \varepsilon\hbar\nu_{en}/(e^2N_D)$. Let v_M be the order of magnitude of the electron velocity (see below). The reciprocal of the electron residence time is $v_M/[x]$ and the condition that the field-dependent and collision terms dominate all others in (3.1) is:

$$\frac{v_M}{[x]} \ll \nu_{en} \Longrightarrow \delta = \frac{e^2N_Dv_M}{\varepsilon\hbar\nu_{en}^2} \ll 1. \tag{3.13}$$

Provided this condition holds, the terms $\partial f/\partial t$ and $v(k)\,\partial f/\partial x$, with $\hbar v(k) = \mathcal{E}'(k) \equiv d\mathcal{E}/dk$, are both of order $\delta \ll 1$ compared to $e\hbar^{-1}\partial W/\partial x\,\partial f/\partial k$ and $Q[f]$ in (3.1). Ignoring these small terms, (3.1) can be approximated by

$$\mathcal{L}f^{(0)}(k;F) \equiv \left(\frac{eF}{\hbar}\frac{\partial}{\partial k} + \nu_{en} + \nu_{imp}\mathcal{A}\right) f^{(0)}(k;F) = \nu_{en}f^{FD}. \tag{3.14}$$

The solution of this equation,

$$f^{(0)}(k;F) = \sum_{j=-\infty}^{\infty} \frac{(1 - ij\mathcal{F}/\tau_e)\, f_j^{FD}}{1 + j^2\mathcal{F}^2}\, e^{ijkl}, \quad \mathcal{F} = \frac{F}{F_M}, \tag{3.15}$$

$$f_j^{FD} = \frac{l}{2\pi}\int_{-\pi/l}^{\pi/l} e^{-ijkl} f^{FD}(k;n)dk, \quad F_M = \frac{\hbar\nu_{en}\tau_e}{el},\ \tau_e = \sqrt{1 + \frac{\nu_{imp}}{\nu_{en}}}, \tag{3.16}$$

is the Fermi-Dirac local equilibrium modified by a high electric field. The field-dependent local equilibrium $f^{(0)}$ is the leading order term of a Chapman-Enskog expansion

$$f \sim f^{(0)}(k;F) + f^{(1)}(k;F) + f^{(2)}(k;F), \tag{3.17}$$

$$\varepsilon\frac{\partial F}{\partial t} + \mathcal{J}^{(0)}[F] + \mathcal{J}^{(1)}[F] \sim J(t). \tag{3.18}$$

(3.17) becomes a power series in the small dimensionless parameter δ of (3.13) if we nondimensionalize the BPBGK system using the scales $\mathcal{F}$, $\tilde{x} = x/[x]$,

$\tilde{k} = kl$, $\tilde{t} = v_M t/[x]$, etc. The corrections $f^{(m)}$, $m = 1, 2$, solve the equations

$$\mathcal{L}f^{(1)} = -\frac{\partial f^{(0)}}{\partial t}\bigg|_0 - v(k)\frac{\partial f^{(0)}}{\partial x}, \tag{3.19}$$

$$\mathcal{L}f^{(2)} = -\frac{\partial f^{(1)}}{\partial t}\bigg|_0 - v(k)\frac{\partial f^{(1)}}{\partial x} - \frac{\partial}{\partial t}f^{(0)}\bigg|_1, \tag{3.20}$$

in which the subscripts 0 and 1 in their right hand side (RHS) mean that $\varepsilon\,\partial F/\partial t$ is replaced by $J - \mathcal{J}^{(0)}[F]$ and by $-\mathcal{J}^{(1)}[F]$, respectively. The conditions that $f^{(1)}$ and $f^{(2)}$ be bounded and $2\pi/l$ periodic in k determine the functionals $\mathcal{J}^{(m)}[F]$ [10]. When these functionals are inserted in (3.18) and (3.8) is used, we obtain the following generalized drift-diffusion system for the field [10, 12]

$$\varepsilon\frac{\partial F}{\partial t} + \frac{ev_M}{l}\mathcal{N}\left(F, \frac{\partial F}{\partial x}\right) = \varepsilon\, D\left(F, \frac{\partial F}{\partial x}\right)\frac{\partial^2 F}{\partial x^2} + A\left(F, \frac{\partial F}{\partial x}\right)J(t), \tag{3.21}$$

$$n = N_D + \frac{\varepsilon l}{e}\frac{\partial F}{\partial x}, \quad \mathcal{N} = nV\mathcal{M}_1 A - \frac{e\Delta l^2}{\hbar^2\nu_{en}^2\tau_e^2}\frac{B}{1+\mathcal{F}^2}\frac{\partial F}{\partial x}, \tag{3.22}$$

$$V(\mathcal{F}) = \frac{2\mathcal{F}}{1+\mathcal{F}^2}, \quad v_M = \frac{\Delta l\,\mathcal{I}_1(M)}{4\hbar\tau_e\mathcal{I}_0(M)}, \quad \tilde{\mu} = \frac{\mu}{k_B T}, \tag{3.23}$$

$$A = 1 + \frac{2e^2 v_M[1-(1+2\tau_e^2)\mathcal{F}^2]}{\varepsilon\hbar\nu_{en}^2\tau_e^3(1+\mathcal{F}^2)^3}\,n\mathcal{M}_1,\ \mathcal{M}_m(n/N_D) = \frac{\mathcal{I}_m(\tilde{\mu})\mathcal{I}_0(M)}{\mathcal{I}_1(M)\mathcal{I}_0(\tilde{\mu})}, \tag{3.24}$$

$$\mathcal{I}_m(\tilde{\mu}) = \frac{l}{2\pi}\int_{-\pi}^{\pi}\gamma\left(\frac{\mathcal{E}(k)}{k_B T} - \tilde{\mu}\right)\cos(mkl)\,dk, \tag{3.25}$$

$$B = \frac{n\mathcal{M}_2\mathcal{F}(5-4\mathcal{F}^2)}{(1+4\mathcal{F}^2)^2} - \frac{4\hbar v_M(1+\tau_e^2)}{\Delta l\tau_e}n\mathcal{M}_1(n\mathcal{M}_1)'\mathcal{F}\frac{1-\mathcal{F}^2}{(1+\mathcal{F}^2)^3}, \tag{3.26}$$

$$D = \frac{\Delta^2 l^2}{8\hbar^2\nu_{en}\tau_e^2(1+\mathcal{F}^2)}\left(1 - \frac{4\hbar v_M\tau_e C}{\Delta l}\right), \tag{3.27}$$

$$C = (n\mathcal{M}_2)'\frac{1-2\mathcal{F}^2}{1+4\mathcal{F}^2} + \frac{8(1+\tau_e^2)\hbar v_M}{\Delta l\tau_e}\left(\frac{(n\mathcal{M}_1)'\mathcal{F}}{1+\mathcal{F}^2}\right)^2. \tag{3.28}$$

In these equations, $\tilde{\mu} = M$ provided $n = N_D$. Equation (3.21) is a form of Ampère's law establishing that the sum of the electron current density and Maxwell's displacement current equals the total current density. Numerical solution of both the kinetic system (3.1)-(3.4) and of the drift-diffusion system (3.21)-(3.28) show that the later is a very good approximation to the

former for realistic parameter ranges [27]. Note that equations (3.21)-(3.28) are the semiclassical limit of equations (2.77)-(2.86) derived in section 2.3.2 if the spatial averages are ignored.

3.3 H theorem and entropy for ideal boundary conditions

In this section, we find a Lyapunov function for the BPBGK kinetic system assuming that the SL is infinite or that it is finite but it has ideal boundary conditions at the contact regions (zero voltage bias and either periodic boundary conditions or insulating contacts with zero conductivity). The Lyapunov functional has the form of a free energy and, for a local equilibrium of Boltzmann type, it produces formulas that are very close to those of equilibrium thermodynamics.

3.3.1 Derivation of a free energy density

As in the case of the usual BGK equation in the kinetic theory of gases, let us start by finding an entropy functional [79]. Suppose we have a local equilibrium $\gamma(E)$, with $E = E[f]$, which is a non-negative decreasing function for real values of E. $\gamma(E)$ can be found by maximizing the entropy functional

$$\mathcal{S}(x,t) = \frac{1}{2\pi}\int_{-\pi/l}^{\pi/l} dk \int_0^{f(x,k,t)} ds\, \gamma^{-1}(s) \tag{3.29}$$

(where $\gamma^{-1}(s)$ is the inverse function of $\gamma(E)$; $\mathcal{S}$ has units of 3D density), subject to the conditions

$$\frac{l}{2\pi}\int_{-\pi/l}^{\pi/l} dk f(x,k,t) = n(x,t), \tag{3.30}$$

$$\frac{l}{2\pi}\int_{-\pi/l}^{\pi/l} dk\, \mathcal{E}(k)\, f(x,k,t) = \mathcal{E}(x,t). \tag{3.31}$$

In fact, taking the extremal of

$$\mathcal{S}(x,t) + \frac{\tilde{\mu}(x,t)}{2\pi}\int_{-\pi/l}^{\pi/l} dk f(x,k,t) - \frac{\tilde{\beta}(x,t)}{2\pi}\int_{-\pi/l}^{\pi/l} dk\, \mathcal{E}(k)\, f(x,k,t), \tag{3.32}$$

we obtain $\gamma^{-1}(f^{FD}) = \tilde{\beta}\mathcal{E}(k) - \tilde{\mu}$. Then

$$f^{FD} = \gamma(\tilde{\beta}\mathcal{E}(k) - \tilde{\mu}). \tag{3.33}$$

The Lagrange multipliers $\tilde{\beta}$ and $\tilde{\mu}$ have to be calculated by inserting (3.33) in (3.30)-(3.31) and solving these equations for $\tilde{\beta}(x,t)$ and $\tilde{\mu}(x,t)$ in terms of $n(x,t)$ and $\mathcal{E}(x,t)$. The entropy density $-\mathcal{S}$ was introduced by Aoki et al [4] for a BGK kinetic equation with charge and energy conserving collision terms representing infinitely extended materials with parabolic bands. If we set $\tilde{\beta} = 1/(k_B T)$, $\tilde{\mu} = \mu/(k_B T)$, and, by an appropriate choice of $\mu(x,t)$ with constant T, we impose that (3.30) be still satisfied but not (3.31), f^{FD} given by (3.33) becomes the same function of (3.9)-(3.10).

To find the Lyapunov functional, we define a free energy density

$$\eta(x,t) = \upsilon(x,t) - \mathcal{S}(x,t)l = \upsilon(x,t) - \frac{l}{2\pi}\int_{-\pi/l}^{\pi/l} dk \int_0^{f(x,k,t)} ds\, \gamma^{-1}(s), \quad (3.34)$$

where $\upsilon(x,t)$ is a functional of the distribution function to be specified later. Using periodicity in k, (3.29) and (3.34) yield

$$\begin{aligned}
\frac{\partial}{\partial t}(\eta - \upsilon) &= -\frac{l}{2\pi}\int_{-\pi/l}^{\pi/l} dk\, \gamma^{-1}(f)\, \frac{\partial f}{\partial t} \\
&= \frac{l}{2\pi}\int_{-\pi/l}^{\pi/l} dk \left[\nu_{en}[f - \gamma(E[f])] + \nu_{imp}\mathcal{A}f + v(k)\frac{\partial f}{\partial x} + \frac{eF}{\hbar}\frac{\partial f}{\partial k}\right]\gamma^{-1}(f) \\
&= \frac{l\nu_{en}}{2\pi}\int_{-\pi/l}^{\pi/l} dk \frac{\gamma^{-1}(f) - \gamma^{-1}(\gamma(E[f]))}{f - \gamma(E[f])}\,[f - \gamma(E[f])]^2 \\
&+ \frac{l\nu_{en}}{2\pi}\int_{-\pi/l}^{\pi/l} dk [f - \gamma(E[f])]E[f] \\
&+ \frac{l\nu_{imp}}{8\pi}\int_{-\pi/l}^{\pi/l} dk \frac{\gamma^{-1}(f(k)) - \gamma^{-1}(f(-k))}{f(k) - f(-k)}\,[f(k) - f(-k)]^2 \\
&+ \frac{l}{2\pi}\frac{\partial}{\partial x}\int_{-\pi/l}^{\pi/l} dk\, v(k) \int_0^{f(x,k,t)} ds\, \gamma^{-1}(s). \qquad (3.35)
\end{aligned}$$

The first term in the RHS of this expression is nonpositive because the integrand is proportional to the derivative of the decreasing function γ^{-1} at some intermediate point (mean value theorem). The same argument shows that the third term in the RHS is also nonpositive. This term has been written as indicated using that $\int_{-\pi/l}^{\pi/l} g(k)\mathcal{A}f\, dk = \int_{-\pi/l}^{\pi/l} \mathcal{A}g\, \mathcal{A}f\, dk$ for any function $g(k)$. The fourth term is the x derivative of some function. The second term in the RHS of (3.35) is zero for energy conserving collision terms [4] but this is

not the case for the BPBGK system. Let us rewrite this term by using

$$\frac{l}{2\pi}\frac{\partial}{\partial t}\int_{-\pi/l}^{\pi/l} dk\,\frac{\mathcal{E}(k)}{k_BT}\,f = -\frac{l\nu_{en}}{2\pi}\int_{-\pi/l}^{\pi/l} dk\,[f-\gamma(E[f])]E[f]$$
$$-\frac{l}{2\pi}\int_{-\pi/l}^{\pi/l} dk\,v(k)\frac{\mathcal{E}(k)}{k_BT}\frac{\partial f}{\partial x} + \frac{J_nFl}{k_BT}, \tag{3.36}$$

after integration by parts. The last term in the RHS of (3.36) is

$$\frac{l}{k_BT}\,FJ_n = \frac{lF}{k_BT}\left(J(t)-\varepsilon\frac{\partial F}{\partial t}\right) = \frac{l}{k_BT}\,\frac{\partial(JW)}{\partial x} - \frac{\varepsilon l}{2k_BT}\frac{\partial F^2}{\partial t}. \tag{3.37}$$

Then (3.36) and (3.37) yield

$$\frac{l\nu_{en}}{2\pi}\int_{-\pi/l}^{\pi/l} dk\,[f-\gamma(E[f])]E[f] = -\frac{\partial}{\partial t}\left(\frac{l}{2\pi}\int_{-\pi/l}^{\pi/l} dk\,\frac{\mathcal{E}(k)}{k_BT}\,f + \frac{\varepsilon lF^2}{2k_BT}\right)$$
$$+\frac{l}{2\pi k_BT}\,\frac{\partial}{\partial x}\left(2\pi J(t)W - \int_{-\pi/l}^{\pi/l} dk\,v(k)\mathcal{E}(k)f\right). \tag{3.38}$$

Inserting this expression in (3.35), we obtain

$$\begin{aligned}\frac{\partial}{\partial t}(\eta-\upsilon) &= \frac{l\nu_{en}}{2\pi}\int_{-\pi/l}^{\pi/l} dk\frac{\gamma^{-1}(f)-\gamma^{-1}(\gamma(E[f]))}{f-\gamma(E[f])}\,[f-\gamma(E[f])]^2\\ &+ \frac{l\nu_{imp}}{8\pi}\int_{-\pi/l}^{\pi/l} dk\frac{\gamma^{-1}(f(k))-\gamma^{-1}(f(-k))}{f(k)-f(-k)}\,[f(k)-f(-k)]^2\\ &+ l\,\frac{\partial}{\partial x}\left[\frac{1}{2\pi}\int_{-\pi/l}^{\pi/l} dk\,v(k)\left(\int_0^{f(x,k,t)} ds\,\gamma^{-1}(s) - \frac{\mathcal{E}(k)}{k_BT}f\right) + \frac{JW}{k_BT}\right]\\ &- \frac{\partial}{\partial t}\left(\frac{l}{2\pi}\int_{-\pi/l}^{\pi/l} dk\,\frac{\mathcal{E}(k)\,f}{k_BT} + \frac{\varepsilon lF^2}{2k_BT}\right).\end{aligned} \tag{3.39}$$

We have omitted the dependance on x, t in the second term of the RHS of (3.39) to simplify this formula. Selecting now

$$\upsilon = \frac{l}{2\pi k_BT}\left(\pi\varepsilon F^2 + \int_{-\pi/l}^{\pi/l} dk\,\mathcal{E}(k)f\right) + C \tag{3.40}$$

(C is a constant to be determined), so that

$$\begin{aligned}\eta &= \frac{l}{2\pi k_BT}\left(\pi\varepsilon F^2 + \int_{-\pi/l}^{\pi/l} dk\,\mathcal{E}(k)f\right)\\ &- \frac{l}{2\pi}\int_{-\pi/l}^{\pi/l} dk\int_0^{f(x,k,t)} ds\,\gamma^{-1}(s) + C,\end{aligned} \tag{3.41}$$

we find

$$\frac{\partial \eta}{\partial t} + \frac{\partial J_\eta}{\partial x} = \sigma_\eta, \tag{3.42}$$

$$J_\eta = -\frac{l}{2\pi}\int_{-\pi/l}^{\pi/l} dk\, v(k)\left(\int_0^f ds\, \gamma^{-1}(s) - \frac{\mathcal{E}(k)}{k_B T} f\right) - \frac{JlW}{k_B T}$$

$$= -\frac{l}{2\pi}\int_{-\pi/l}^{\pi/l} dk\, v(k)\int_0^f ds\, [\gamma^{-1}(s) - \gamma^{-1}(f^{FD})] + \frac{\mu J_n l}{e k_B T} - \frac{JlW}{k_B T}, \tag{3.43}$$

$$\sigma_\eta = \frac{l\nu_{en}}{2\pi}\int_{-\pi/l}^{\pi/l} dk \frac{\gamma^{-1}(f) - \gamma^{-1}(\gamma(E[f]))}{f - \gamma(E[f])}\,[f - \gamma(E[f])]^2$$

$$+ \frac{l\nu_{imp}}{8\pi}\int_{-\pi/l}^{\pi/l} dk \frac{\gamma^{-1}(f(k)) - \gamma^{-1}(f(-k))}{f(k) - f(-k)}\,[f(k) - f(-k)]^2 \leq 0. \tag{3.44}$$

The free energy production σ_η in (3.44) is zero only if $f = \gamma(E[f]) = f^{FD}$ (which is even in k). Moreover $\gamma^{-1}(s)$ is decreasing from infinity at $s = 0$ and therefore it vanishes at a unique value $s = s_0 > 0$. This value yields the maximum of the integral $\int_0^f \gamma^{-1}(s)ds$. Let us select

$$C \;=\; \int_0^{s_0} ds\, \gamma^{-1}(s), \tag{3.45}$$

then the free energy density becomes

$$\eta \;=\; \frac{l}{2\pi k_B T}\left(\pi\varepsilon F^2 + \int_{-\pi/l}^{\pi/l} dk\, \mathcal{E}(k) f\right)$$

$$-\; \frac{l}{2\pi}\int_{-\pi/l}^{\pi/l} dk \int_{s_0}^{f(x,k,t)} ds\, \gamma^{-1}(s) \geq 0. \tag{3.46}$$

3.3.2 Boltzmann limit and physical meaning of $\eta(x,t)$

In the Boltzmann limit, (3.12) yields $\gamma^{-1}(s) = -\ln(s/Q)$, with $Q = m^* k_B T/(\pi\hbar^2)$. Then $-\int_0^f \gamma^{-1}(s)\, ds = f\ln(f/Q) - f$, $s_0 = C = Q$ because of (3.45), and (3.46) gives

$$\frac{k_B T}{l}\,\eta \;=\; \frac{1}{2\pi}\int_{-\pi/l}^{\pi/l} dk\, \mathcal{E}(k) f + \frac{\varepsilon F^2}{2} - \frac{k_B T}{l}\left(n - \frac{m^* k_B T}{\pi\hbar^2}\right)$$

$$-\; T\left[-\frac{k_B}{2\pi}\int_{-\pi/l}^{\pi/l} f\ln\left(\frac{\pi\hbar^2 f}{m^* k_B T}\right) dk\right]. \tag{3.47}$$

The first two terms in the RHS of (3.47) are the internal energy density (including the contribution from the electric field) and, except for an additive constant, the two last terms can be written as $-T\,s(x,t)$, the temperature times the entropy density if we define

$$s(x,t) \;=\; -\frac{k_B}{2\pi}\int_{-\pi/l}^{\pi/l} f\,\ln\left(\frac{\pi\hbar^2 f}{m^* k_B T\exp(1)}\right)dk. \tag{3.48}$$

Thus $k_BT\eta/l$ is the free energy density. It is remarkable that the classical expression for the free energy holds exactly for out of equilibrium states described by the BPBGK equation in the Boltzmann limit. For other local equilibrium distributions, the entropy functional (3.29) does not yield the recognizable extensive form of entropy. In the Boltzmann limit, (3.3) gives

$$\mu \quad = k_BT\ln\left(\frac{n}{n_0}\right), \tag{3.49}$$

$$n_0 \quad = \frac{m^*k_BT}{\pi\hbar^2}\frac{l}{2\pi}\int_{-\pi/l}^{\pi/l} e^{-\mathcal{E}(k)/(k_BT)}dk = \frac{m^*k_BT}{\pi\hbar^2}e^{-\Delta/(2k_BT)}I_0\left(\frac{\Delta}{2k_BT}\right), \tag{3.50}$$

which is the usual logarithmic dependence of the chemical potential on the electron density. The explicit formula in (3.50), where $I_0(x)$ is a modified Bessel function, is found for the tight binding dispersion relation (3.8). If the distribution function is the local equilibrium (3.12), the free energy density (3.47) becomes

$$\begin{aligned}\frac{k_BT}{l}\,\eta^B \;&=\; \left(\frac{\Delta}{2}-k_BT\right)\frac{n}{l}+\frac{m^*k_B^2T^2}{\pi\hbar^2 l}+\frac{\varepsilon F^2}{2}\\ &+\; \frac{k_BT}{l}n\ln\left[\frac{\pi\hbar^2 n}{m^*k_BT\,I_0\left(\frac{\Delta}{2k_BT}\right)}\right].\end{aligned} \tag{3.51}$$

3.3.3 Boundary conditions and free energy as a Lyapunov functional

For an infinitely long SL under zero voltage bias conditions or for a finite SL with periodic boundary conditions, the free energy flux (3.43) obeys $J_\eta(L,t) = J_\eta(0,t)$, and (3.42)-(3.44) and (3.46) imply that the total free energy,

$$\Phi(t) = \frac{k_BTA}{l}\int_0^L \eta(x,t)\,dx, \tag{3.52}$$

is a Lyapunov functional of the BPBGK system ($\Phi(t) \geq 0$, $d\Phi/dt \leq 0$; A is the area of the SL cross section). Then the local equilibrium with $n = N_D$ and $F = 0$ is the globally stable stationary solution. These idealized boundary conditions do not hold for a finite SL under voltage bias and with realistic boundary conditions [27]. We have

$$\frac{d\Phi}{dt} = \frac{k_B T A}{l} \left[\int_0^L \sigma_\eta(x,t)\, dx - J_\eta(L,t) + J_\eta(0,t) \right], \tag{3.53}$$

which no longer has a definite sign.

What are the boundary conditions used to solve the BPBGK system? For a finite SL of length $L = Nl$ (N is the number of SL periods) and a tight binding dispersion relation, appropriate boundary conditions are [27]

$$\text{At } x = 0\text{: } W = 0, \quad f^+ = \frac{2\pi\hbar\sigma_0 F}{e\Delta} - \frac{f^{(0)}}{\int_0^{\frac{\pi}{l}} v(k) f^{(0)}\, dk} \int_{-\frac{\pi}{l}}^0 v(k) f^-\, dk. \tag{3.54}$$

$$\text{At } x = L\text{: } W = V,\ f^- = \frac{2\pi\hbar\sigma_L n F}{e\Delta N_D} - \frac{f^{(0)}}{\int_{-\frac{\pi}{l}}^0 v(k) f^{(0)}\, dk} \int_0^{\frac{\pi}{l}} v(k) f^+\, dk, \tag{3.55}$$

where $f^\pm$ means $f(x,k,t)$ for $\text{sign}(k) = \pm 1$ and $f^{(0)}(k;F)$ is given by (3.15). Integrating the second relations in (3.54) and (3.55) over k, we get

$$J_n(0,t) = \sigma_0 F(0,t), \quad J_n(L,t) = \sigma_L F(L,t)\, \frac{n(L,t)}{N_D}, \tag{3.56}$$

These relations are of the forms: $J_n(0,t) = j_0(F(0,t))$ and $J_n(L,t) = j_L(F(L,t))$ $n(L,t)/N_D$ in which the contact currents $j_0(F)$ and $j_L(F)$ have been linearized according to Ohm's law (with contact conductivities σ_0 and σ_L, respectively). A derivation of these relations from quantum theory can be found in [16]. They are often used in the literature; cf the review [14]. We prove below that $J_\eta(L,t) - J_\eta(0,t) \geq 0$ provided $\sigma_0 = \sigma_L = 0$ (insulated contacts) and $V = 0$ (zero voltage bias). Then the total free energy, $\Phi(t)$, is a Lyapunov functional of the BPBGK system and the distribution function tends to equilibrium which is the unique globally stable stationary solution of the system.

Proof that $J_\eta(L,t) - J_\eta(0,t) \geq 0$ for zero contact conductivity and zero voltage bias. (Adapted from Chapter 8 of [29]). In (3.43), the function

$$C(f) = -\int_0^f ds\, [\gamma^{-1}(s) - \gamma^{-1}(f^{FD})], \tag{3.57}$$

is convex for non-negative f and it reaches a minimum at $f = f^{FD}$. Then Jensen's inequality implies that

$$C\left(\int_0^{\pi/l} \Omega(k',k) f(k') dk'\right) \leq \int_0^{\pi/l} \Omega(k',k) C(f(k'))\, dk', \quad (3.58)$$

at $x = L$, where

$$\Omega(k',k) = \frac{|v(k')|\, f^{(0)}(k)}{\int_{-\pi/l}^0 |v(\kappa)|\, f^{(0)}(\kappa) d\kappa} = -\frac{v(k')\, f^{(0)}(k)}{\int_{-\pi/l}^0 v(\kappa)\, f^{(0)}(\kappa) d\kappa}, \quad (3.59)$$

with $k' > 0$ and $k < 0$. We have omitted the dependence on $x = L$ and t in the distribution functions. In the left hand side of (3.58),

$$\int_0^{\pi/l} \Omega(k',k) f(k') dk' = f(k), \quad (3.60)$$

according to (3.55) with $\sigma_L = 0$. We now substitute (3.60) in (3.58), multiply the result by $|v(k)| = -v(k)$, integrate over k in $-\pi/l \leq k \leq 0$, and use that $-\int_{-\pi/l}^0 v(k)\Omega(k',k) dk = v(k')$ due to (3.59). The result is

$$-\int_{-\pi/l}^0 v(k)\, C(f(k))\, dk \leq \int_0^{\pi/l} v(k)\, C(f(k))\, dk, \quad \text{therefore}$$
$$\int_{-\pi/l}^{\pi/l} v(k)\, C(f(k))\, dk \geq 0. \quad (3.61)$$

Similarly, we can prove that $\int_{-\pi/l}^{\pi/l} v(k)\, C(f(k))\, dk \leq 0$ at $x = 0$ if $\sigma_0 = 0$. Since $J_n = 0$ for insulating contacts, (3.43) implies $J_\eta(L,t) - J_\eta(0,t) \geq -JlV/(k_B T) = 0$ for $V = 0$ (zero voltage bias). Then (3.53) and (3.44) yield $d\Phi/dt \leq 0$.

3.4 Numerical results

In order to calculate numerically the Lyapunov functional $\Phi(t)$, we have first obtained $F(x,t)$, $n(x,t)$ and $J(t)$ by solving (3.21)-(3.28) under appropriate dc voltage bias and the boundary conditions (3.56). From equation (3.15) we have calculated the leading order approximation of $f \sim f^{(0)}$ using the Boltzmann local equilibrium distribution (3.12) (in this case $f_j^B = n\, I_j(\frac{\Delta}{2K_B T})/I_0(\frac{\Delta}{2K_B T})$, where $I_j(x)$ is a modified Bessel function). Then we

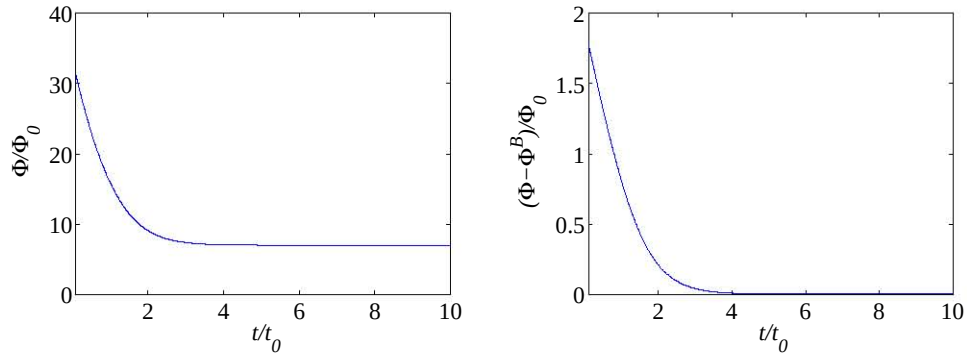

Figure 3.1: Time evolution of the Lyapunov functional $\Phi(t)$ for zero contact conductivity and zero voltage bias. Here $\Phi_0 = 190.27$ eV, $t_0 = 0.82$ ps.

have obtained the free energy density η from (3.47). Finally, we have calculated the Lyapunov functional $\Phi(t)$ from equation (3.52).

In our numerical simulations, we have used the following typical parameters [14]: $d_B = 1.5$ nm, $d_W = 9$ nm, $l = d_B + d_W = 10.5$ nm, $N_D = 2.5 \times 10^{10}$ cm^{-2}, $\nu_{en} = 9 \times 10^{12}$ Hz, $\nu_{imp} = 0$, $N = 80$, $T = 5$ K, $\Delta = 2.6$ meV, $\varepsilon = 12.85\,\varepsilon_0$, $A = 100\,\mu$m^2. We have selected the following units to present our results graphically: $F_M = \hbar\nu_{en}/(el) = 5.64$ kV/cm, $x_0 = \varepsilon F_M l/(eN_D) = 16.83$ nm, $v_M = \Delta l/(2\hbar) = 20.46$ km/s, $J_0 = eN_D v_M/l = 7.8$ kA/cm^2, $t_0 = x_0/v_M = 0.82$ ps, $\eta_0 = \frac{\varepsilon\nu_{en}^2\hbar^2}{2k_BTe^2l} = 2.76 \times 10^{11}$ cm^{-2}, $\Phi_0 = k_BTA\,\eta_0\,x_0/l = 190.27$ eV. The chosen unit η_0 reflects the fact that the most important contribution to the free energy density is the electrostatic one.

We have studied the following cases:

- Zero contact conductivity and zero voltage bias: We see in figure 3.1 that the Lyapunov functional $\Phi(t)$ tends asymptotically to the local equilibrium $\Phi^B(t) = \frac{k_BTA}{l}\int_0^L \eta^B(x,t)\,dx$, as expected.

- Realistic contact conditions: For an applied voltage bias $V = 1.7$ V and contact conductivities $\sigma_0 = 1.38\,\Omega^{-1}$m^{-1} and $\sigma_L = 0.69\,\Omega^{-1}$m^{-1}, the total current exhibits self sustained oscillations due to the repeated nucleation of dipole waves at the injecting contact and their motion towards the collector [14], as shown in Figure 3.2. Figure 3.3 shows that free energy $\Phi(t)$ oscillates at the same frequency and, obviously,

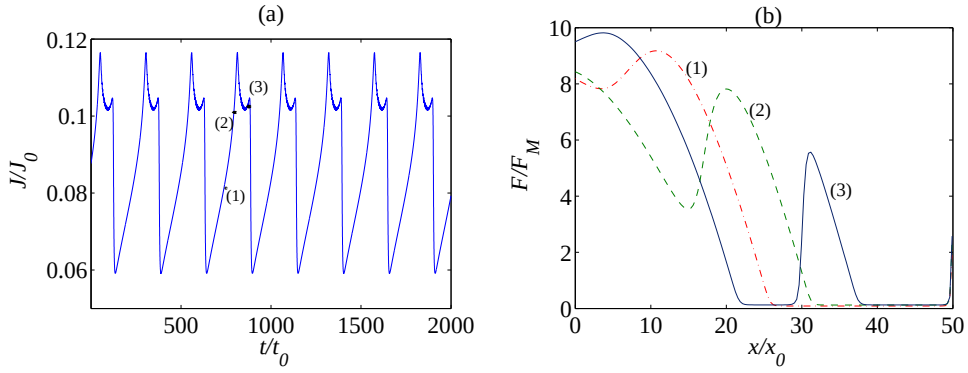

Figure 3.2: (a) Total current density vs time. (b) Electric field profiles at several times during one oscillation period. Here $J_0 = 7.8$ kA/cm^2, $t_0 = 0.82$ ps, $F_M = 5.64$ kV/cm, $x_0 = 16.83$ nm.

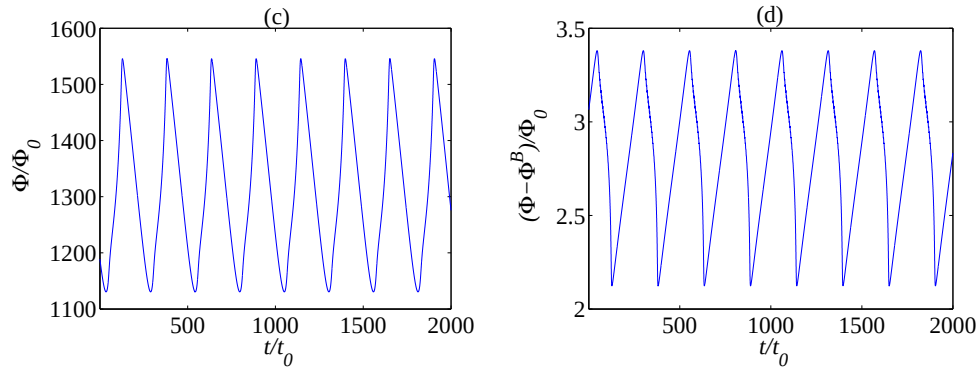

Figure 3.3: (a) Time evolution of the free energy $\Phi(t)$ during self sustained current oscillations in a SL with nonzero contact conductivity biased at 1.7 V. (b) Same for $\Phi(t) - \Phi^B(t)$.

it is no longer a Lyapunov functional. Global equilibrium is precluded by injection and depletion of carriers at the contacts and the nonzero voltage bias. Figure 3.3(b) shows that the free energy differs from that of local equilibrium whereas a comparison to Figure 3.3(a) indicates that Φ^B has the same order of magnitude as Φ.

3.5 Conclusions

Electron transport in strongly coupled miniband superlattices is described by a BPBGK kinetic system of equations. For this system, we have found a free energy density $\eta(x,t)$ and its corresponding free energy $\Phi(t)$. We have proved that the free energy is a Lyapunov functional ($\Phi \geq 0$, $d\Phi/dt \leq 0$) for idealized boundary conditions in the SL (zero voltage bias and either zero contact conductivity or periodic boundary conditions). Thus for a *closed* SL with insulating contacts and zero voltage bias, the distribution function tends to equilibrium which is the unique globally stable stationary solution of the BPBGK system. In the Boltzmann limit, it is remarkable that the expression of the free energy density $\eta(x,t)$ is similar to that of equilibrium thermodynamics, including the internal energy density minus a $T\,s(x,t)$ term (temperature times the entropy density). However, an *open* SL (nonzero voltage and nonzero conductivity at contacts) may be very far from equilibrium and display self-sustained current oscillations due to repeated nucleation and motion of charge dipole waves as in Figure 3.2. In this case, $d\Phi/dt$ has no definite sign. Numerical solutions of the BPBGK system of equations illustrate the monotonic decay of the free energy of a closed SL towards its equilibrium value and show that, during self-oscillations in an open SL, $\Phi(t)$ oscillates stably and periodically in time at the same frequency as the total current.

Our results are based on selecting an entropy density based on the local equilibrium distribution $\gamma(E[f])$ by using the maximum entropy principle and therefore they can be applied to other forms of $\gamma(E)$ (decreasing with E, compact support [4]) or to higher dimensional models of similar type (collision operator preserving charge but not energy or momentum).

Chapter 4

Spatially confined Bloch oscillations in semiconductor superlattices

4.1 Introduction

In this chapter we derive hydrodynamic equations containing BO and EFD among their solutions for a dc voltage biased SL. Bloch gain for a dc+ac driven SL will be studied elsewhere. Hydrodynamic equations are derived in a double limit: (i) the field-dependent term and the collision term are of the same order and dominate all others in the kinetic equation, and (ii) the collisions are almost elastic so that energy and momentum dissipation are of the same order as the spatial gradients in the balance equations. Extensions of classical kinetic theory methods based on assumption (i), such as the Chapman-Enskog technique, yield transport coefficients which become singular if the electric field becomes zero. Fixing this shortcoming requires matching to a multiple time scales expansion based on assumption (ii). Our techniques might be useful in other problems in kinetic theory having a similar structure.

Once these difficulties are overcome, we can show that, in the appropriate limit, the electron current density and mean energy oscillate at the Bloch frequency, whereas the electron density, the electric field and the envelope of the BO vary on a slower scale and are described by balance equations (hydrodynamic regime). Numerical solutions in the appropriate parameter range show that initial profiles for the field and the BO amplitude evolve to a stable stationary spatially inhomogeneous solution with nonzero amplitude of

the BO near the collecting contact. This solution disappears as the collisions in the kinetic equation become more inelastic because the BO amplitude becomes zero everywhere. If the amplitude of the BO is set to zero, the electric field satisfy drift-diffusion equations similar to those obtained with a local equilibrium distribution that depends only on the electron density [12]. It is well known that these drift-diffusion models describe very well the Gunn-type self-oscillations due to pulse dynamics.

The rest of the chapter is as follows. The dissipative BGK collision model is presented in Section 4.2. In Section 4.3, we derive the moment equations for the electron density, current density and mean energy (these magnitudes are moments of the distribution function, more precisely, they are its zero and first harmonics in a complex Fourier series in the wave vector), which are closed if we restrict ourselves to space independent solutions. For inelastic collisions, their constant solutions yield an electron drift velocity of Esaki-Tsu form whereas for elastic collisions their solutions are undamped oscillations at the Bloch frequency which is proportional to the electric field. These oscillations become damped for inelastic collisions and decay to the constant solutions mentioned before. Section 4.4 lists the system of the Boltzmann-BGK-Poisson equations and the equations obtained in the hydrodynamic regime by our perturbation methods. The results of numerical simulations of the hydrodynamic equations with appropriate boundary and initial conditions are presented in section 4.5. Our perturbation procedure is presented in two separate sections. In section 4.6, we use the method of multiple scales to find equations for the electric field, the electron density and the complex amplitude of the BO *assuming that we know a closure expression for the second harmonic of the distribution function in terms of the zero and first harmonics*. The precise form of the closure expression is found in Appendix B by matching the resulting hydrodynamic equations for electric field, electron density and amplitude of the BO to the result of using the Chapman-Enskog method on a modified kinetic equation for a distribution function that depends on the phase of the BO. This method yields equations with transport coefficients which are singular in the limit of vanishing electric field but they are compatible with the hydrodynamic equations of section 4.6 in an intermediate limit of sufficiently small fields. This compatibility yields the sought closure expression. Section 4.8 contains our conclusions. Appendix A gives some technical details on the local Boltzmann equilibrium. In Appendix B, we derive a drift-diffusion system for the electric field in superlattices with strongly inelastic collisions by using a Chapman-Enskog method similar to that described in Refs. [12, 17].

4.2 Dissipative BGK collision model

4.2.1 BGK-Poisson (KSS) model

We shall present our ideas in the very simple case of a n-doped semiconductor SL having only one populated miniband with the tight-binding dispersion relation:

$$\mathcal{E}(k) = \frac{\Delta}{2}\,(1 - \cos kl), \quad v(k) = \frac{1}{\hbar}\,\frac{d\mathcal{E}}{dk} = \frac{\Delta l}{2\hbar}\,\sin kl. \tag{4.1}$$

Here Δ is the miniband width, l the SL period, $\hbar$ is the Planck constant and $v(k)$ is the electron group velocity. Electron motion and the electric field are directed along the SL growth direction which we take as the x axis. In this case, the following modified KSS model describes electron motion including impurity collisions (which conserve energy but not momentum) and inelastic electron-phonon collisions [12]:

$$\frac{\partial f}{\partial t} + v(k)\,\frac{\partial f}{\partial x} + \frac{eF}{\hbar}\,\frac{\partial f}{\partial k} = Q_e(f) + Q_p(f), \tag{4.2}$$

$$\varepsilon\,\frac{\partial F}{\partial x} = \frac{e}{l}\,(n - N_D), \tag{4.3}$$

$$n = \frac{l}{2\pi}\int_{-\pi/l}^{\pi/l} f(x,k,t)\,dk, \tag{4.4}$$

$$Q_e(f) = -\nu_e\,(f - f^{1D}), \tag{4.5}$$

$$f^{1D}(k;n) = \frac{m^* k_B T_0}{\pi\hbar^2}\,\ln\left[1 + \exp\left(\frac{\mu - \mathcal{E}(k)}{k_B T_0}\right)\right], \tag{4.6}$$

$$\frac{l}{2\pi}\int_{-\pi/l}^{\pi/l} f^{1D}(k;n)\,dk = n, \tag{4.7}$$

$$Q_p(f) = -\nu_p\,\mathcal{A}f \equiv -\frac{\nu_p}{2}\,[f(x,k,t) - f(x,-k,t)]. \tag{4.8}$$

Here f, n, N_D, ε, k_B, $-e < 0$, m^*, μ and $-F = -\partial W/\partial x$ are the one-particle distribution function, the 2D electron density, the 2D doping density, the dielectric constant, the Boltzmann constant, the electron charge, the effective mass of the electron, the electro-chemical potential and the electric field, respectively. W is the electric potential. Note that the 1D distribution functions have the same units as the 2D electron density n and that the electrochemical potential μ is a function of n obtained by solving (4.6)-(4.7). The 1D Fermi-Dirac local equilibrium (4.6) is obtained by integrating the 3D Fermi-Dirac distribution $1/(1 + e^{[\mu - \mathcal{E}(\mathbf{k})]/(k_B T_0)})$ with $\mathcal{E}(\mathbf{k}) = \mathcal{E}(k) + \hbar^2\mathbf{k}_\perp^2/(2m^*)$

over the transversal wave vector $\mathbf{k}_\perp$. T_0 is the lattice temperature, ν_e and ν_p are collision frequencies which we take as given constants. The distribution function is periodic in k with period $2\pi/l$. For the BGK-Poisson system (4.2)-(4.8) there is a free energy functional and an associated H theorem provided the SL has insulating contacts and zero voltage bias, whereas for Ohmic contacts with appropriate conductivity Gunn-type current oscillations are possible in a dc voltage biased SL [2]. A quantum version of these semiclassical equations was studied in [13].

Since $\mathcal{E}(k)$ and f^{1D} are even in k and $v(k)$ and $\mathcal{A}f$ are odd in k, the collision operators $Q_e(f)$ and $Q_p(f)$ satisfy the conditions:

$$\int_{-\pi/l}^{\pi/l} Q_{e,p}(f)\,dk = 0, \quad \int_{-\pi/l}^{\pi/l} \mathcal{E}(k)\,Q_p(f)\,dk = 0,$$
$$\frac{e}{2\pi}\int_{-\pi/l}^{\pi/l} v(k)\,Q_{e,p}(f)\,dk = -\nu_{e,p}J_n, \quad \int_{-\pi/l}^{\pi/l} \mathcal{E}(k)\,Q_e(f)\,dk \neq 0,$$

where

$$J_n(x,t) = \frac{e}{2\pi}\int_{-\pi/l}^{\pi/l} v(k)\,f(x,k,t)\,dk, \tag{4.9}$$

is the electronic current density. Thus $Q_e(f)$ dissipates energy and momentum whereas $Q_p(f)$ dissipates momentum but not energy. For a finite SL with insulating contacts and zero voltage bias, the collision terms dissipate the electron energy and momentum until the electrons reach equilibrium at the lattice temperature T_0 and zero current [2].

4.2.2 Dissipative BGK collision model

To account for thermal effects, we replace the following more general Fermi-Dirac distribution instead of f^{1D} [11]:

$$f^{1D\alpha}(k;\tilde{\beta},\tilde{u},\tilde{\mu}) = \frac{m^* k_B T_\alpha}{\pi\hbar^2}\,\ln\left[1+\exp\left(\frac{\mu_\alpha+\hbar k u_\alpha-\mathcal{E}(k)}{k_B T_\alpha}\right)\right]. \tag{4.10}$$

Here $\hbar u_\alpha k$ should be considered a periodic function of k with period $2\pi/l$. Then $f^{1D\alpha}$ is $2\pi/l$-periodic in k, same as the electron distribution function f. The multipliers μ_α, u_α and T_α should be selected so that the electron density (4.4), the electronic current density (4.9) and the mean energy,

$$E(x,t) = \frac{l}{2\pi\,n(x,t)}\int_{-\pi/l}^{\pi/l}\left[\frac{\Delta}{2}-\mathcal{E}(k)\right]f(x,k,t)\,dk, \tag{4.11}$$

satisfy the equations:

$$\frac{l}{2\pi}\int_{-\pi/l}^{\pi/l} f^{1D\alpha}\,dk = n, \tag{4.12}$$

$$\frac{e}{2\pi}\int_{-\pi/l}^{\pi/l} v(k)\,f^{1D\alpha}\,dk = (1-\alpha_j)J_n, \tag{4.13}$$

$$\frac{l}{2\pi n}\int_{-\pi/l}^{\pi/l}\left[\frac{\Delta}{2}-\mathcal{E}(k)\right] f^{1D\alpha}\,dk = \alpha_e E_0 + (1-\alpha_e)E. \tag{4.14}$$

Here α_j and α_e are restitution coefficients taking values on the interval $[0,1]$ (see below). E_0 is the mean energy at the lattice temperature of the global equilibrium reached by a finite SL with insulating contacts and zero voltage bias. Equivalent results are obtained if we define the mean energy as the average of $\mathcal{E}(k)$, which is equal to $(\Delta/2-E)$, but Eq. (4.11) leads to a simpler relation between energy density and lattice temperature. The dimensionless multipliers

$$\tilde{\mu} = \frac{\mu_\alpha}{k_B T_\alpha}, \quad \tilde{u} = \frac{\hbar u_\alpha}{k_B T_\alpha l}, \quad \tilde{\beta} = \frac{\Delta}{2k_B T_\alpha}, \tag{4.15}$$

in the local equilibrium distribution

$$f^{1D\alpha} = \frac{m^*\Delta}{2\pi\tilde{\beta}\hbar^2}\,\ln\left(1+e^{\tilde{\mu}+\tilde{u}\,kl-\tilde{\beta}+\tilde{\beta}\cos kl}\right), \tag{4.16}$$

are functions of n, J_n and E determined by solving (4.12), (4.13) and (4.14). With these definitions, the inelastic part of the collision operator describing momentum and energy dissipation satisfies

$$\int_{-\pi/l}^{\pi/l} Q_e(f)\,dk = 0, \tag{4.17}$$

$$\frac{e}{2\pi}\int_{-\pi/l}^{\pi/l} v(k)\,Q_e(f)\,dk = -\nu_e\alpha_j J_n, \tag{4.18}$$

$$\frac{l}{2\pi n}\int_{-\pi/l}^{\pi/l}\left[\frac{\Delta}{2}-\mathcal{E}(k)\right] Q_e(f)\,dk = -\nu_e\alpha_e(E-E_0). \tag{4.19}$$

The coefficients α_j and α_e, $0 \le \alpha_{j,e} \le 1$, measure the fraction of momentum and of energy lost in inelastic collisions, and correspond to the restitution coefficient used in granular gases [19]. Obviously for $\alpha_{e,j} = 0$ the collisions are elastic. Note that we do not use the temperature $T_\alpha = \alpha T$ as in granular gases because the relation between energy density and temperature is

not linear in the present case. To simplify matters, we shall assume that the restitution coefficients are constant. For space independent solutions of the kinetic equation, this leads to exponentially fast decay of the average energy and momentum in contrast with the algebraic decay of energy found in granular gases [19].

4.2.2.1 Equations of the model

Since (4.18) and (4.19) show that our collision model dissipates both momentum and energy, we propose a simpler equation for the distribution function with $\nu_p = 0$ and (4.16) as the local distribution function instead of (4.6). Recapitulating, the equations governing our inelastic BGK model are (4.2) and (4.3) with $Q_p = 0$ and $Q_e = -\nu_e(f - f^{1D\alpha})$ given by (4.16) - (4.19). n, J_n and E are the moments of the distribution function given by (4.4), (4.9) and (4.11), respectively. When modeling a finite SL, we need boundary conditions for f and F at the contacts attached to the SL boundaries and an initial condition for f. See References [14] and [27] for a discussion.

4.2.2.2 Boltzmann distribution

Explicit formulas can be obtained in the low temperature limit in which $\tilde{\beta} \to \infty$, $\tilde{u} = O(\tilde{\beta})$, $\tilde{\mu} \to -\infty$ in (4.16), which becomes the Boltzmann distribution

$$f^B = \frac{m^* \Delta}{2\pi\hbar^2\tilde{\beta}}\, e^{\tilde{\mu}+\tilde{u}kl-\tilde{\beta}\,(1-\cos kl)}, \tag{4.20}$$

and integrals over k are calculated using Laplace's method. For sufficiently high temperature, the Boltzmann distribution (4.20) is again a good approximation and it yields simpler formulas. The parameter $\tilde{\mu}$ can be explicitly calculated using (4.12) and the resulting distribution is

$$f^B = n\,\frac{\pi\, e^{\tilde{u}kl+\tilde{\beta}\cos kl}}{\int_0^\pi e^{\tilde{\beta}\cos K}\cosh(\tilde{u}K)\,dK}, \tag{4.21}$$

in which $\tilde{u}$ and $\tilde{\beta}$ are obtained in terms of J_n/n and E by solving (4.13) and (4.14). As shown in Appendix A, the latter equations yield

$$\frac{(1-\alpha_j)\,J_n}{n} = \frac{e\Delta}{2\hbar\tilde{\beta}}\left[\tilde{u} - \frac{e^{-\tilde{\beta}}\sinh(\tilde{u}\pi)}{\int_0^\pi e^{\tilde{\beta}\cos K}\cosh(\tilde{u}K)\,dK}\right], \tag{4.22}$$

$$\alpha_e E_0 + (1-\alpha_e)E = \frac{\Delta}{2}\,\frac{\int_0^\pi e^{\tilde{\beta}\cos K}\cos K\cosh(\tilde{u}K)\,dK}{\int_0^\pi e^{\tilde{\beta}\cos K}\cosh(\tilde{u}K)\,dK}. \tag{4.23}$$

At the lattice temperature, $\tilde{\beta}_0 = \Delta/(2k_BT_0)$, and for zero current, $\tilde{u} = 0$, $E = E_0$, and (4.23) yields

$$\frac{2E_0}{\Delta} = \frac{I_1(\tilde{\beta}_0)}{I_0(\tilde{\beta}_0)}, \tag{4.24}$$

where $I_s(x)$, $s = 0, 1$, are modified Bessel functions. Further simplification follows if we impose $\alpha_j = 1$ in (4.13) (which implies $\tilde{u} = 0$) so that the BGK collision term dissipates momentum and energy according to (4.18) and (4.19). Then (4.21) becomes

$$f^B = \frac{n\, e^{\tilde{\beta}\cos kl}}{I_0(\tilde{\beta})}, \tag{4.25}$$

and $\tilde{\beta}$ is obtained in terms of E by solving (4.23) with $\tilde{u} = 0$, i.e.

$$\alpha_e E_0 + (1 - \alpha_e)E = \frac{\Delta}{2}\,\frac{I_1(\tilde{\beta})}{I_0(\tilde{\beta})}. \tag{4.26}$$

The Fourier coefficients of the Boltzmann distribution (4.25) are simply

$$f_j^B = \frac{l}{2\pi}\int_{-\pi/l}^{\pi/l} e^{-ijkl} f^B(k;n)\, dk = n\,\frac{I_j(\tilde{\beta})}{I_0(\tilde{\beta})}. \tag{4.27}$$

4.3 Moment equations and their spatially uniform solutions

Integrating the kinetic equation (4.2) times 1, $v(k)$ and $\Delta/2 - \mathcal{E}(k)$ over the wave vector and using (4.12)-(4.14), we obtain the following moment equations:

$$\frac{e}{l}\frac{\partial n}{\partial t} + \frac{\partial J_n}{\partial x} = 0, \tag{4.28}$$

$$\frac{\partial J_n}{\partial t} + \frac{e\Delta^2 l}{8\hbar^2}\frac{\partial}{\partial x}(n - \mathrm{Re}\, f_2) - \frac{e^2 l\, nEF}{\hbar^2} = -\nu_e\alpha_j J_n, \tag{4.29}$$

$$\frac{\partial E}{\partial t} - \frac{lE}{en}\frac{\partial J_n}{\partial x} - \frac{\Delta^2 l}{8\hbar n}\frac{\partial}{\partial x}\mathrm{Im} f_2 + \frac{F\, J_n l}{n} = -\nu_e\alpha_e\,(E - E_0). \tag{4.30}$$

Here we have used (4.1) and the Fourier coefficients f_j of the distribution function:

$$f(x,k,t) = \sum_{j=-\infty}^{\infty} f_j(x,t)\, e^{ijkl}. \tag{4.31}$$

Note that $J_n = -e\Delta\ \mathrm{Im} f_1/(2\hbar)$ and $E = \Delta\,\mathrm{Re} f_1/(2n)$. We can eliminate the electron density from (4.28) by using the Poisson equation (4.3) and integrating the result over x, thereby obtaining the following form of Ampère's law

$$\varepsilon \frac{\partial F}{\partial t} + J_n = J(t). \tag{4.32}$$

Here $J(t)$ is the total current density. Note that (4.28) - (4.30) are a closed system of equations in the case of space independent moments. The dissipation terms in the right hand side of (4.29) and (4.30) ensure that a global equilibrium with no current density and mean energy $E = E_0$ is reached.

4.3.1 Space and time independent moments

A time-independent spatially uniform solution of (4.29) and (4.30) provides the following relations between n, J_n and E:

$$J_n = \frac{enE}{\hbar\tilde{\tau}_e}\mathcal{F}, \quad \tilde{\tau}_e = \sqrt{\frac{\alpha_j}{\alpha_e}}, \tag{4.33}$$

$$E = \frac{E_0}{1+\mathcal{F}^2}, \tag{4.34}$$

$$\mathcal{F} = \frac{F}{\tilde{F}_M},\ \tilde{F}_M = \frac{\hbar\nu_e}{el}\sqrt{\alpha_j\alpha_e} = \frac{\hbar\nu_e\alpha_e\tilde{\tau}_e}{el}, \tag{4.35}$$

in which we have assumed $\alpha_e < 1$. Inserting (4.34) and (4.24) in (4.33), we obtain $J_n = env_d(F)/l$, where $v_d(F)$ is the following drift velocity

$$v_d(F) = \frac{2v_M\mathcal{F}}{1+\mathcal{F}^2}, \quad v_M = \frac{\Delta l}{4\hbar\tilde{\tau}_e}\frac{I_1(\tilde{\beta}_0)}{I_0(\tilde{\beta}_0)}. \tag{4.36}$$

This formula is similar to that obtained by Ignatov and Shashkin for the KSS model with a BGK collision term and a Boltzmann local distribution [43]. It reduces to the Esaki-Tsu drift velocity in the limit $\tilde{\beta}_0 \to \infty$ (zero lattice temperature), in which the Bessel functions are absent. According to (4.34), the mean energy E decreases as the field F increases, whereas the average energy $\langle\mathcal{E}\rangle$ obtained by averaging (4.1),

$$\langle\mathcal{E}\rangle = \frac{l}{2\pi n}\int_{-\pi/l}^{\pi/l}\mathcal{E}\, f dk = \frac{\Delta}{2} - E, \tag{4.37}$$

increases with the electric field, as one would have expected. Note that the stationary solution (4.33) - (4.35) is asymptotically stable if we ignore the spatial dependence of n, J_n and E provided $\alpha_e < 1$.

4.3.2 Time evolution of space independent moments

Space independent moments solve the evolution equations:

$$\frac{\partial J_n}{\partial t} - \frac{e^2 l\, nEF}{\hbar^2} = -\nu_e \alpha_j J_n, \tag{4.38}$$

$$\frac{\partial E}{\partial t} + \frac{F\, J_n l}{n} = -\nu_e \alpha_e (E - E_0), \tag{4.39}$$

where n and F are constants. The solutions of these linear equations are:

$$J_n = J_{n,s} + na\, e^{-\Gamma t} \left[\frac{\nu_e(\alpha_j - \alpha_e)}{2} \cos(\Omega_B t + \varphi) + \Omega_B \sin(\Omega_B t + \varphi) \right], \tag{4.40}$$

$$E = E_s + Fla\, e^{-\Gamma t} \cos(\Omega_B t + \varphi), \tag{4.41}$$

$$\omega_B = \frac{eFl}{\hbar}, \tag{4.42}$$

$$\Omega_B = \sqrt{\omega_B^2 - \left(\frac{\nu_e(\alpha_e - \alpha_j)}{2} \right)^2}, \tag{4.43}$$

$$\Gamma = \frac{\alpha_e + \alpha_j}{2}\, \nu_e, \tag{4.44}$$

where $J_{n,s}$ and E_s are the stationary current and energy densities given by (4.33) and (4.34), respectively, and a and φ are real constants. Eqs. (4.40) and (4.41) hold provided $\omega_B > \nu_e|\alpha_e - \alpha_j|/2$, and a similar formula describes overdamped decay to (4.33) and (4.34) otherwise.

For the special case of elastic collisions, $\alpha_e = \alpha_j = 0$, we have $\Gamma = J_{n,s} = E_s = 0$ and the stable solutions are undamped oscillations at the Bloch frequency ω_B given by Eq. (4.42):

$$J_n = \frac{en}{\hbar}\, \tilde{a}\, \sin(\omega_B t + \varphi), \tag{4.45}$$

$$E = \tilde{a}\, \cos(\omega_B t + \varphi), \tag{4.46}$$

in which $\tilde{a} = aFl$ is another real constant. Eqs. (4.40) and (4.41) imply that inelastic collisions dissipate energy and momentum and damp oscillations (at a frequency $\Omega_B < \omega_B$) with a relaxation time $1/\Gamma$ until the stationary current and energy densities (4.33) - (4.35) are reached.

The stable solutions (4.33) - (4.35) ($\alpha_e > 0$) or (4.45) - (4.46) (in the case of elastic collisions) indicate which balance equations are appropriate in the hyperbolic limit. In the inelastic case with nonzero restitution coefficients, (4.33) - (4.35) provide the leading order approximation to the electronic current density and energy in terms of n and F which vary slowly when the

convective term $v(k)\,\partial f/\partial x$ of the kinetic equation is taken into account. The resulting balance equations will be drift-diffusion ones. In the case of elastic collisions, n, F, $\tilde{a}$ and φ in (4.45) - (4.46) vary slowly when the term $v(k)\,\partial f/\partial x$ of the kinetic equation is considered. The resulting balance equations will be of hydrodynamic type. There is an interesting case of *almost elastic collisions*, $\alpha_{e,j} \ll 1$, in which the Bloch oscillations are slowly damped. In this case, n, F, $\tilde{a}$, φ and the non-oscillatory part of the current and the energy densities vary slowly when the convective term $v(k)\,\partial f/\partial x$ of the kinetic equation is considered. The equations for these slowly-varying magnitudes will describe the damping of the Bloch oscillations.

4.4 Hydrodynamic regime in the almost elastic limit

f, n	F	$\mathcal{E}$, E	$v(k)$	J_n	x	k	t	δ
N_D	$\frac{\hbar\nu_e}{el}$	$\frac{\Delta}{2}$	$\frac{l\Delta}{2\hbar}$	$\frac{eN_D\Delta}{2\hbar}$	$\frac{\varepsilon\hbar\nu_e}{e^2N_D}$	$\frac{1}{l}$	$\frac{2\varepsilon\hbar^2\nu_e}{e^2N_Dl\Delta}$	$\frac{e^2N_Dl\Delta}{2\varepsilon\hbar^2\nu_e^2}$
$10^{10}\mathrm{cm}^{-2}$	kV/cm	meV	10^4m/s	$10^4\mathrm{A/cm}^2$	nm	1/nm	ps	–
4.048	130	8	6.15	7.88	116	0.2	1.88	0.0053

Table 4.1: Hyperbolic scaling and nondimensionalization with $\nu_e = 10^{14}$ Hz.

4.4.1 BGK-Poisson system and moment equations in nondimensional form

It is convenient to nondimensionalize the BGK-Poisson system using the units indicated in Table 4.1. They are appropriate for the hyperbolic limit $\delta \to 0$, in which the collision and Bloch frequencies are comparable and the corresponding terms dominate all others in (4.2). Defining $\hat{f} = f/N_D$, $\hat{n} = n/N_D$, $\hat{E} = 2E/\Delta$, $\hat{J}_n = J/[J_n]$, $\hat{x} = x/[x]$, ... (where $[y]$ are the units in Table 4.1), we can rewrite all equations so far shown in nondimensional form. Omitting the hats over the variables, we find the following nondimensional kinetic equations

$$F\,\frac{\partial f}{\partial k}+f-f^{1D\alpha}=-\delta\left(\frac{\partial f}{\partial t}+\sin k\,\frac{\partial f}{\partial x}\right), \tag{4.47}$$

$$\frac{\partial F}{\partial x}=n-1, \tag{4.48}$$

$$f^{1D\alpha}=\rho_0\,\ln\left(1+e^{\tilde{\mu}-\tilde{\beta}+\tilde{\beta}\cos k+\tilde{u}k}\right),\quad \rho_0=\frac{m^*\Delta}{2\pi\tilde{\beta}\hbar^2N_D}, \tag{4.49}$$

$$n=\frac{1}{2\pi}\int_{-\pi}^{\pi}f(x,k,t)dk, \tag{4.50}$$

$$J_n=\frac{1}{2\pi}\int_{-\pi}^{\pi}\sin k\,f(x,k,t)dk,\quad E=\frac{1}{2\pi n}\int_{-\pi}^{\pi}\cos k\,f(x,k,t)dk, \tag{4.51}$$

$$\frac{1}{2\pi}\int_{-\pi}^{\pi}f^{1D\alpha}(k;\tilde{\beta},\tilde{u},\tilde{\mu})dk=n, \tag{4.52}$$

$$\frac{1}{2\pi}\int_{-\pi}^{\pi}\sin k\,f^{1D\alpha}(k;\tilde{\beta},\tilde{u},\tilde{\mu})\,dk=(1-\delta\gamma_j)\,J_n, \tag{4.53}$$

$$\frac{1}{2\pi n}\int_{-\pi}^{\pi}\cos k\,f^{1D\alpha}(k;\tilde{\beta},\tilde{u},\tilde{\mu})dk=E-\delta\gamma_e(E-E_0), \tag{4.54}$$

$$\delta=\frac{e^2N_Dl\Delta}{2\varepsilon\hbar^2\nu_e^2}. \tag{4.55}$$

Here we have assumed that the restitution coefficients are of order $\delta\ll 1$: $\alpha_{e,j}=\delta\gamma_{e,j}$. The moment equations (4.28)-(4.30) for n, J_n and E become

$$\frac{\partial n}{\partial t}+\frac{\partial J_n}{\partial x}=0, \tag{4.56}$$

$$nEF=\delta\left[\frac{\partial J_n}{\partial t}+\frac{1}{2}\,\frac{\partial}{\partial x}(n-\mathrm{Re}\,f_2)+\gamma_jJ_n\right], \tag{4.57}$$

$$\frac{F\,J_n}{n}=-\delta\left[\frac{\partial E}{\partial t}-\frac{E}{n}\,\frac{\partial J_n}{\partial x}-\frac{1}{2n}\,\frac{\partial}{\partial x}\mathrm{Im}f_2+\gamma_e(E-E_0)\right]. \tag{4.58}$$

We can rewrite (4.57) and (4.58) in terms of $f_1=nE-iJ_n$:

$$\left(\delta\,\frac{\partial}{\partial t}+iF+\delta\,\frac{\gamma_e+\gamma_j}{2}\right)f_1+\delta\,\frac{\gamma_e-\gamma_j}{2}f_1^*=\delta\gamma_enE_0-\frac{\delta}{2i}\frac{\partial}{\partial x}(n-f_2). \tag{4.59}$$

The Ampère law is simply

$$\frac{\partial F}{\partial t}+J_n=J. \tag{4.60}$$

In terms of a fast time scale, $\tau = t/\delta$, (4.56), (4.59) and (4.60) become

$$\frac{\partial n}{\partial \tau} = -\delta \frac{\partial J_n}{\partial x}, \tag{4.61}$$

$$\frac{\partial F}{\partial \tau} = \delta\,(J - J_n), \tag{4.62}$$

$$\left(\frac{\partial}{\partial \tau} + iF\right) f_1 = \delta \left[\gamma_e n E_0 - \frac{\gamma_e + \gamma_j}{2} f_1 - \frac{\gamma_e - \gamma_j}{2} f_1^* - \frac{1}{2i}\frac{\partial}{\partial x}(n - f_2)\right]. \tag{4.63}$$

Remark 1. The moment equations (4.56) and (4.59) for $n = f_0$ and f_1 are not closed because the higher moment f_2 appears in them. In general, equations for moments $f_0, \ldots, f_n$ will contain terms depending on f_{n+1}.

Remark 2. For a dc voltage biased SL, setting $\delta = 0$ in (4.61)-(4.63) yields a BO as a leading order approximation:

$$n = n(x,t), \quad F = F(x,t), \quad f_1 = A(x,t)\, e^{-iF\tau}, \tag{4.64}$$

in which $n(x,t)$, $F(x,t)$ and the envelope function $A(x,t)$ do not depend on the fast time scale. For an ac voltage biased SL driven at a frequency of order $1/\delta$, the total current will also be of order $1/\delta$ and (4.62) has to be rewritten accordingly.

4.4.2 Hydrodynamic equations

In the hyperbolic limit as $\delta \to 0$, we can close the moment equations by using the singular perturbation theory described later in section 4.6. We find

$$n = n(x,t), \quad F = F(x,t), \quad f_1 = A(x,t)e^{-i\theta} + f_{1,S}(x,t), \quad \theta = \frac{1}{\delta}\int_0^t F(x,s)\, ds, \tag{4.65}$$

where $n(x,t)$, $F(x,t)$ and the complex envelope function $A(x,t)$ are solutions of the equations

$$\frac{\partial F}{\partial t} + \frac{\delta}{F^2+\delta^2\gamma_j\gamma_e}\left[\gamma_e E_0 n F + \frac{F}{2}\frac{\partial}{\partial x}\mathrm{Im}\,\frac{f_{2,0}^{1D\alpha(0)}}{1+2iF}\right.$$
$$\left. -\frac{\delta\gamma_e}{2}\frac{\partial}{\partial x}\left(n - \mathrm{Re}\,\frac{f_{2,0}^{1D\alpha(0)}}{1+2iF}\right) - F\mathrm{Re}\,h_S + \delta\gamma_e\mathrm{Im}\,h_S\right] = J(t), \quad (4.66)$$

$$\frac{\partial F}{\partial x} = n - 1, \quad (4.67)$$

$$\frac{\partial A}{\partial t} = -\frac{\gamma_e+\gamma_j}{2}A + \frac{1}{2i}\frac{\partial}{\partial x}\left(\frac{f_{2,-1}^{1D\alpha(0)} + \delta\, r_{2,-1}^{(1)}}{1+iF}\right), \quad (4.68)$$

$$r_{2,-1}^{(1)} = f_{2,-1}^{1D\alpha(1)} - \left(\mathcal{A}^{(0)}\frac{\partial}{\partial A} + J\frac{\partial}{\partial F}\right)\frac{f_{2,-1}^{1D\alpha(0)}}{1+iF} - \frac{1}{2i}\frac{\partial}{\partial x}\left(A - \frac{f_{3,-1}^{1D\alpha(0)}}{1+2iF}\right), \quad (4.69)$$

$$\mathcal{A}^{(0)} = -\frac{\gamma_e+\gamma_j}{2}A + \frac{1}{2i}\frac{\partial}{\partial x}\left(\frac{f_{2,-1}^{1D\alpha(0)}}{1+iF}\right), \quad (4.70)$$

$$h_S = -\frac{\delta\gamma_e n E_0 J(t)}{(\delta^2\gamma_e\gamma_j + F^2)^2}\,[2\delta\gamma_j F + i(\delta^2\gamma_e\gamma_j - F^2)]. \quad (4.71)$$

Here $f^{1D\alpha(0)}$ is a 2π-periodic function of θ and k obtained by solving (4.49), (4.52), (4.53) and (4.54) for $\tilde{\mu}$, $\tilde{u}$ and $\tilde{\beta}$ in terms of n and $f_1 = nE - iJ_n = A\,e^{-i\theta}$. Then we have the Fourier coefficients

$$f_{j,l}^{1D\alpha(0)} = \frac{1}{(2\pi)^2}\int_{-\pi}^{\pi}\int_{-\pi}^{\pi} f^{1D\alpha(0)}(k; n, f_1 = A\,e^{-i\theta})\,e^{-ijk-il\theta}dkd\theta. \quad (4.72)$$

The quasi-stationary part of f_1 is of order δ:

$$\begin{aligned} f_{1,S} &= nE_S - iJ_{n,S} \\ &= \frac{\delta}{F^2+\delta^2\gamma_j\gamma_e}\,[\gamma_e n E_0(\delta\gamma_j - iF) \\ &+ \frac{F+i\delta\gamma_e}{2}\frac{\partial}{\partial x}\left(n - \mathrm{Re}\,\frac{f_{2,0}^{1D\alpha(0)}}{1+i2F}\right) - (\delta\gamma_j - iF)\mathrm{Re}h_S \\ &+ \frac{\delta\gamma_j - iF}{2}\,\mathrm{Im}\frac{\partial}{\partial x}\left(\frac{f_{2,0}^{1D\alpha(0)}}{1+i2F}\right) - (F+i\delta\gamma_e)\mathrm{Im}h_S\Bigg], \end{aligned} \quad (4.73)$$

To calculate $f_{2,-1}^{1D\alpha(1)}$ in (4.69), we need to use

$$f^{1D\alpha(1)} = \left(\tilde{\mu}^{(1)} \frac{\partial}{\partial \tilde{\mu}^{(0)}} + \tilde{u}^{(1)} \frac{\partial}{\partial \tilde{u}^{(0)}} + \tilde{\beta}^{(1)} \frac{\partial}{\partial \tilde{\beta}^{(0)}} \right) f^{1D\alpha(0)}, \tag{4.74}$$

where $f^{1D\alpha}$ is given by (4.49). In the resulting expression, we should substitute $\tilde{\mu}^{(0)}$, $\tilde{u}^{(0)}$ and $\tilde{\beta}^{(0)}$ given by simultaneously solving

$$f_0^{1D\alpha(0)} = n, \quad f_1^{1D\alpha(0)} = A\, e^{-i\theta}, \tag{4.75}$$

and also the solutions $\tilde{\mu}^{(1)}$, $\tilde{u}^{(1)}$, $\tilde{\beta}^{(1)}$ of

$$f_0^{1D\alpha(1)} = 0, \tag{4.76}$$

$$f_1^{1D\alpha(1)} = \gamma_e n E_0 + f_{1,S} - \frac{\gamma_e + \gamma_j}{2} A\, e^{-i\theta} - \frac{\gamma_e - \gamma_j}{2} A^* e^{i\theta}. \tag{4.77}$$

4.5 Numerical results

We now solve numerically the hydrodynamic equations (see Appendix E for details of the numerical method) with the boundary conditions [14]

$$\left. \frac{\partial F}{\partial t} + \sigma_0 F \right|_{x=0} = J, \quad \left. \frac{\partial F}{\partial t} + \sigma_1 n F \right|_{x=L} = J, \tag{4.78}$$

$$\frac{1}{L} \int_0^L F(x,t)\, dx = \phi, \tag{4.79}$$

$$\frac{\partial A}{\partial x} = 0, \quad \text{at } x = 0. \tag{4.80}$$

We obtain similar numerical results with $A = 0$ at $x = 0$. Here $L = Nl/[x]$ and $\phi = eV/(\hbar\nu N))$ are dimensionless SL length and average field (proportional to the applied voltage V), respectively. We have used contact conductivities $\sigma_{0,1} = 12.1\ (\Omega\,\mathrm{m})^{-1}$ which yield dimensionless conductivities $\sigma_{0,1} = 0.2$ (conductivity units are $[\sigma] = e^2 N_D \Delta l/(2\hbar^2\nu)$). Initially, $F(x,0) = \phi$ and $A(x,0) = A_0$ (constant). The latter condition means that we have prepared the SL in an initial state having a coherent BO with complex amplitude A_0.

We solve (4.66)-(4.68) with the parameter values indicated in Table 4.1 (which are similar to those in Ref. [71]), without considering, as a first approximation, the first order correction of (4.68). We start with $\alpha_e = \alpha_j = 0.01$ so

that $\nu\alpha_e = \nu\alpha_j = 10^{12}$ Hz.[1] The 3D doping density $N_{3D} = 8 \times 10^{16}$ cm^{-3} gives $N_D = N_{3D}l = 4.048 \times 10^{10}$ cm^{-2} as in Table 4.1, and $\varepsilon = 12.85\,\varepsilon_0$. We find $\delta \approx 0.0053$ and $\gamma_{e,j} = \alpha_{e,j}/\delta = 1.8781$. We consider a 50-period ($N = 50$) dc voltage biased SL with lattice temperature 300 K. For $V = 0.2$ V (therefore $\phi = 0.06$ [3] we observe that $|A(x,t)|$ first diminishes uniformly from $A_0 = 0.153$ to almost zero after a relaxation time $2/(\gamma_e + \gamma_j) \approx 0.53$ (about 1 ps). Later a small pulse is formed at about $x = L/4$ which subsequently extends to the remaining part of the sample and it grows more near its end. The BOs are confined to the second half of the sample that is closer to $x = L$ and are zero in the first half of the sample closer to $x = 0$. Thus the profile of $|A|$ has a compact support with a maximum near $x = L$. $|A(x,t)|$ is close to a periodic oscillation in time: small pulses are formed at the left of its support, climb up towards the maximum of the pulse which then diminishes and the same behavior repeats itself. Figure 4.1(a) shows four snapshots of $|A(x,t)|$ illustrating this behavior which can also be observed in two movies [3]. The field profile depicted in Fig. 4.1(b) is almost stationary. The mean energy and electron current densities during one BO can be reconstructed by means of (4.65). We show them for $\theta = 0$ in Fig. 4.1(c). At the two different SL locations marked in Fig. 4.1(b), the graphs of J_n versus time are shown in Fig. 4.1(d). This figure and two additional movies showing the evolution of the J_n and $1 - E$ profiles illustrate that the Bloch frequencies depend strongly on space and are higher near the collector where the field is larger.

For the scattering times reported in Ref. [71], the restitution coefficients are $\alpha_e = 0.09$ and $\alpha_j = 0.29$, but the BO amplitude becomes zero everywhere after a short relaxation time. BOs also disappear for $\alpha_e = 0.01$ and $\alpha_j = 0.29/9 \approx 0.032$, and there is a smaller critical value of α_j (for fixed α_e) below which BOs can be sustained. They also persist for $\alpha_j = 0.01$ and

[1] Schomburg et al. calculated in Ref. [71] the scattering frequencies ν_e (inelastic, energy dissipating, scattering) and ν_p (elastic, momentum dissipating, scattering) of the KSS collision terms by fitting (in the appropriate units) the current-voltage characteristics of the SL to the same drift velocity as in [2]. In particular, they fitted the peak velocity and field, v_M and F_M. Acting similarly, we can calculate $\alpha_e = \nu_e/\nu$ and $\alpha_j = \alpha_e + \nu_p/\nu$. From the values of ν_e and ν_p in Ref. [71], we get $\alpha_e = 0.09$ and $\alpha_j = 0.29$, which yields $\tilde{\tau}_e = \sqrt{29/9}$. $\alpha_e = \alpha_j = 0.01$ means that the elastic scattering frequency is $\nu_p = 0$ and the inelastic scattering frequency is $\nu\alpha_e = 10^{12}$Hz.

[2] In dimensional units, the drift velocity is $v_d(F) = 2v_M\mathcal{F}/(1 + \mathcal{F}^2)$, where $v_M = \Delta l I_1(\tilde{\beta}_0)/(4\hbar I_0(\tilde{\beta}_0)\tilde{\tau}_e)$, $\tilde{\tau}_e = \sqrt{\alpha_j/\alpha_e}$ and $\mathcal{F} = eFl/(\hbar\nu\alpha_e\tilde{\tau}_e) = F/F_M$. v_M and F_M are the velocity and field at the peak of $v_d(F)$.

[3] This is about 6 times the peak field in the drift velocity, $F_M = \hbar\nu\sqrt{\alpha_e\alpha_j}/(el)$.

[3] See supplementary material for movies of $|A|$, J_n and $1 - E$.

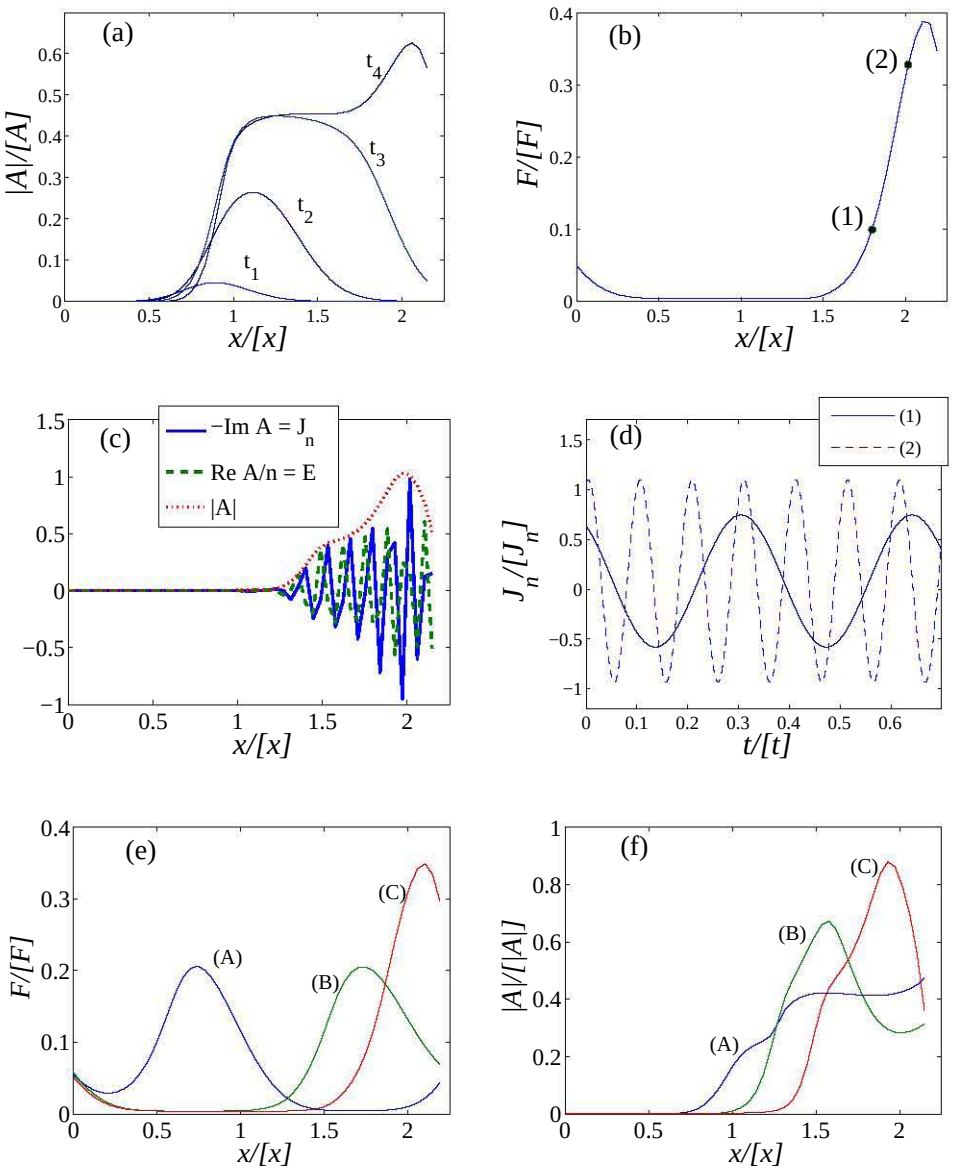

Figure 4.1: (a) Modulus of the BO complex amplitude vs space, during the initial transient, at times $t_1 = 7$, $t_2 = 9$, $t_3 = 11$, $t_4 = 13$. (b) Stationary field profile. (c) Profiles of the nondimensional mean energy density E and nondimensional electron current density J_n for $\theta = 0$ when the field has reached the stationary state. (d) Current density at the two different points marked by (1) and (2) in (b) during BOs. Clearly, the frequency at point (2) is larger than at (1). (e) and (f) Evolution of the field and BO complex amplitude profiles. At time (C) the field reaches its stationary state. To transform the magnitudes in this figure to dimensional units, use Table 4.1. $[A] = \Delta N_D/2$.

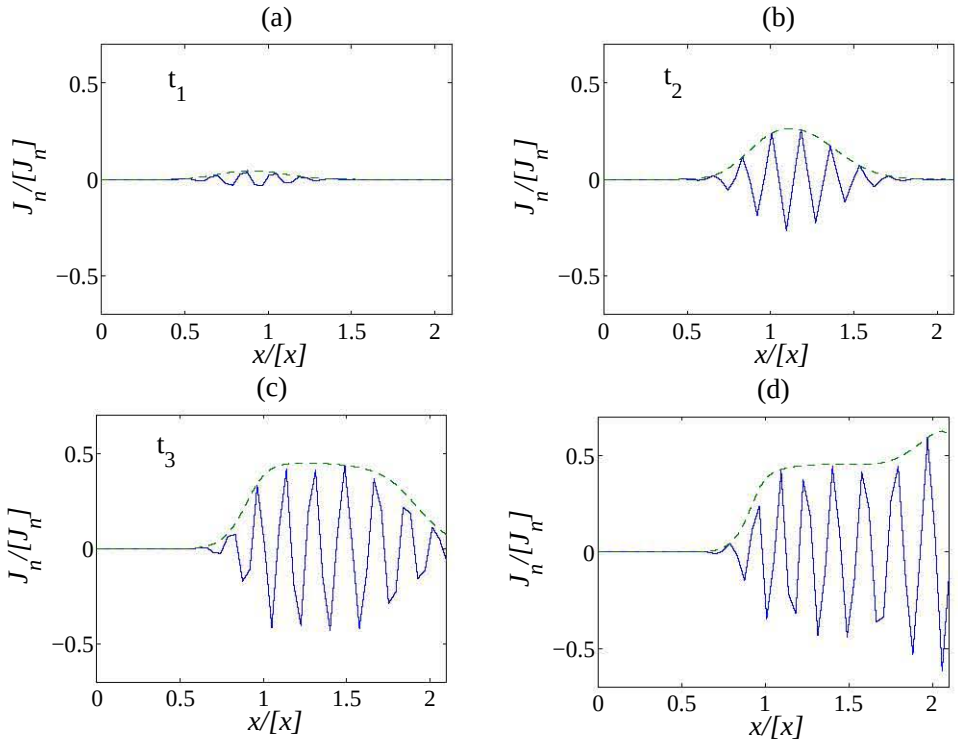

Figure 4.2: Profiles of the nondimensional electron current density J_n for BOs at $\theta = 0$ corresponding to the initial instants $t_1 - t_4$ of fig. 4.1 (a). The dash lines indicate the modulus of the BO complex amplitude.

$\alpha_e = 0.09/29$ which keep the same ratio $\alpha_j/\alpha_e = 29/9 \approx 3.22$ as in Ref. [71]. There is a critical curve in the plane of restitution coefficients such that, for $(\gamma_e + \gamma_j)/2 > \gamma_{\rm crit}$ ($\gamma_{\rm crit} \approx 2.5$ for $\delta = 0.0053$), BOs disappear after a relaxation time but they persist for smaller values of $(\gamma_e + \gamma_j)$.

In summary, we have analyzed the Boltzmann-BGK-Poisson equations with local equilibrium depending on the electron density, current density and energy density in the hyperbolic limit in which the BO period is much shorter than the dielectric relaxation time and collisions are almost elastic. In the long-time scale, there is a hydrodynamic regime described by coupled equations for the electric field, the electron density and the BO complex amplitude. When the restitution coefficients (equivalently the inverse of the scattering times) are sufficiently small, there are stable spatially inhomogeneous profiles of current and energy densities displaying BOs confined to a fraction of the SL extent.

4.6 Almost elastic collisions and damped Bloch oscillations

Singular perturbation methods such as the method of multiple scales or the Chapman-Enskog expansion produce a closure of the moment equations (4.56) - (4.58) by yielding a constitutive relation between the moment f_2 and n, F, $f_1 = nE - iJ_n$ and their derivatives with respect to x (see [17] and section 4.7). Let this constitutive relation be the functional

$$f_2 = g(n, F, f_1), \tag{4.81}$$

and let us assume that collisions are almost elastic, so that $\alpha_{e,j} = \delta\,\gamma_{e,j}$. Then the moment equations (4.61)-(4.63), (4.81) and the Poisson equation (4.3) provide a closed system of equations. If we assume (as it is usually done in the method of multiple scales) that the moments and the field are functions of both the fast time scale τ and the slow time scale $t = \delta\tau$, these equations

become

$$\frac{\partial n}{\partial \tau} = -\delta \left(\frac{\partial n}{\partial t} + \frac{\partial J_n}{\partial x} \right), \tag{4.82}$$

$$\frac{\partial F}{\partial \tau} = \delta \left(J - J_n - \frac{\partial F}{\partial t} \right), \tag{4.83}$$

$$\left(\frac{\partial}{\partial \tau} + iF \right) f_1 = \delta \left[\gamma_e n E_0 - \frac{\gamma_e + \gamma_j}{2} f_1 - \frac{\gamma_e - \gamma_j}{2} f_1^* - \frac{1}{2i} \frac{\partial}{\partial x}(n - g) - \frac{\partial f_1}{\partial t} \right], \tag{4.84}$$

$$\frac{\partial F}{\partial x} = n - 1. \tag{4.85}$$

Setting now $\delta = 0$, (4.82) indicates that n varies slowly on the time scale t. Similarly and according to (4.83), F is independent of τ provided the total current density $J(t)$ is of order 1. In practice, the size of J is set by J_n and by the bias condition. Imposing a voltage bias condition between contacts at the ends of a SL with finitely many periods, $J = O(1)$ if we assume that this voltage is constant or it varies on the slow scale t. We shall not consider in this work the case of voltage bias varying on the fast time scale τ, for which $J = O(1/\delta)$, and we have to modify the present analysis.

The solution of (4.82) - (4.84) for $\delta = 0$ exhibits BO with frequency F: $f_1 = nE - iJ_n = K\, e^{-iF\tau}$. Here we will derive modulation equations for the slow damping of these BO. For this purpose, it is useful to first obtain a τ-independent solution of (4.84):

$$f_{1,S} = \frac{\delta}{F^2 + \delta^2 \gamma_j \gamma_e} \left[\gamma_e n E_0 (\delta \gamma_j - iF) + \frac{F + i\delta\gamma_e}{2} \frac{\partial}{\partial x}(n - \mathrm{Re}\, g_S) \right.$$
$$\left. + \frac{\delta\gamma_j - iF}{2} \frac{\partial}{\partial x} \mathrm{Im}\, g_S - (\delta\gamma_j + iF) \mathrm{Re}\ h_S - (F + i\delta\gamma_e) \mathrm{Im}\ h_S \right], \tag{4.86}$$

provided we have replaced $h(x,t) = \partial f_1 / \partial t$. We introduce the function $h(x,t)$ because extra terms having this form appear in the moment equations when we use the Chapman-Enskog method. The specific expressions for g_S and h_S will be obtained by matching our results in this Section with those obtained by the Chapman-Enskog method. See Sections 4.7 and Appendix B. Eq.

(4.86) is equivalent to

$$\begin{aligned} J_{n,S} &= \frac{\delta}{F^2+\delta^2\gamma_j\gamma_e}\left[\gamma_e E_0 nF + \frac{F}{2}\frac{\partial}{\partial x}\mathrm{Im}\, g_S\right. \\ &- \left.\frac{\delta\gamma_e}{2}\frac{\partial}{\partial x}(n-\mathrm{Re}\, g_S) - F\,\mathrm{Re}\, h_S + \delta\gamma_e \mathrm{Im}\, h_S\right], \qquad (4.87) \\ E_S &= \frac{\delta}{F^2+\delta^2\gamma_j\gamma_e}\left[\delta\gamma_j\left(\gamma_e E_0 + \frac{1}{2n}\frac{\partial}{\partial x}\mathrm{Im}\, g_S\right)\right. \\ &\left. +\frac{F}{2n}\frac{\partial}{\partial x}(n-\mathrm{Re}\, g_S) - \frac{\delta\gamma_j}{n}\,\mathrm{Re}\, h_S - \frac{F}{n}\,\mathrm{Im}\, h_S\right]. \qquad (4.88) \end{aligned}$$

Without the x-derivatives and the function h, the right hand sides of (4.87) and (4.88) correspond to the uniform stationary state (4.33) - (4.34). The other terms are the nonuniform parts of the space-dependent stationary state. The subscript S in g_S and in h_S stresses that these functions are calculated with τ-independent n, F, $J_{n,S}$ and E_S. Note that for $F = O(1)$, $f_{1,S} = O(\delta/F)$, whereas $f_{1,S} = O(1)$ if $F \ll \delta$. Thus the order of $f_{1,S}$ depends on the order of magnitude of F and it is better to treat the compact expression (4.86) as an $O(\delta)$ quantity.

If we insert $f_1 = f_{1,S} + \Phi(x,t,\tau)$ in (4.84), we obtain the equation:

$$\left(\frac{\partial}{\partial\tau} + iF\right)\Phi = -\delta\left[\frac{\gamma_e+\gamma_j}{2}\Phi + \frac{\gamma_e-\gamma_j}{2}\Phi^* + \frac{\partial\Phi}{\partial t} - \frac{1}{2i}\frac{\partial}{\partial x}(g-g_S)\right]. \qquad (4.89)$$

Given that F and n are still varying on the slow time scale t, it is appropriate to introduce the following nonlinear fast time scale instead of τ:

$$\theta = \frac{1}{\delta}\int_0^t F(x,s)\,ds, \qquad (4.90)$$

which yields $\partial\theta/\partial t = F/\delta$, $\partial\theta/\partial\tau = F$. Note that, in dimensional units, the phase θ equals the integral of the Bloch frequency $eFl/\hbar$ over dimensional time, and therefore the partial derivative of θ over dimensional time equals the Bloch frequency. Thus θ is the phase of the Bloch oscillations.

The fast and slow time scales θ and t will be used to set up a method of nonlinear multiple scales below in order to find out the modulation equations on the slow time scale t. If we consider n, F and Φ to be functions of θ and

t, Eqs. (4.82) and (4.89) become

$$F\frac{\partial n}{\partial \theta} = -\delta\left[\frac{\partial n}{\partial t} - \frac{\partial}{\partial x}\mathrm{Im}\,(f_{1,S}+\Phi)\right], \tag{4.91}$$

$$\begin{aligned} F\left(\frac{\partial}{\partial\theta}+i\right)\Phi &= -\delta\left[\frac{\partial\Phi}{\partial t}+\frac{\gamma_e+\gamma_j}{2}\Phi\right. \\ &+ \left.\frac{\gamma_e-\gamma_j}{2}\Phi^* - \frac{1}{2i}\frac{\partial}{\partial x}(g-g_S)\right]. \end{aligned} \tag{4.92}$$

The method of multiple scales is based on the expansions:

$$n(x,t;\delta) = \sum_{m=0}^{1}\delta^m n^{(m)}(\theta,x,t) + O(\delta^2), \tag{4.93}$$

$$F(x,t;\delta) = \sum_{m=0}^{1}\delta^m F^{(m)}(\theta,x,t) + O(\delta^2), \tag{4.94}$$

$$\Phi(x,t;\delta) = \sum_{m=0}^{1}\delta^m \Phi^{(m)}(\theta,x,t) + O(\delta^2), \tag{4.95}$$

and on assuming that $n^{(m)}$, $F^{(m)}$ and $\Phi^{(m)}$ are 2π-periodic functions of θ. Inserting (4.93) - (4.95) in (4.91) - (4.92) and (4.85), we obtain the following hierarchy of equations:

$$\frac{\partial n^{(0)}}{\partial\theta} = 0, \tag{4.96}$$

$$\frac{\partial F^{(0)}}{\partial x} = n^{(0)} - 1, \tag{4.97}$$

$$F^{(0)}\left(\frac{\partial}{\partial\theta}+i\right)\Phi^{(0)} = 0, \tag{4.98}$$

$$F^{(0)}\frac{\partial n^{(1)}}{\partial\theta} = -\frac{\partial n^{(0)}}{\partial t} + \frac{\partial}{\partial x}\mathrm{Im}\,(f_{1,S}+\Phi^{(0)}), \tag{4.99}$$

$$\frac{\partial F^{(1)}}{\partial x} = n^{(1)}, \tag{4.100}$$

$$\begin{aligned} F^{(0)}\left(\frac{\partial}{\partial\theta}+i\right)\Phi^{(1)} &= -\frac{\partial\Phi^{(0)}}{\partial t} - \frac{\gamma_e+\gamma_j}{2}\Phi^{(0)} \\ &+ \frac{\gamma_e-\gamma_j}{2}\Phi^{(0)\,*} + \frac{1}{2i}\frac{\partial}{\partial x}(g^{(0)}-g_S^{(0)}), \end{aligned} \tag{4.101}$$

and so on.

The solution of (4.98) is

$$\Phi^{(0)} = A(x,t)\, e^{-i\theta}, \tag{4.102}$$

whereas (4.96) and (4.97) indicate that $n^{(0)}$ and $F^{(0)}$ do not depend on θ [4]. The solutions of (4.99) and (4.101) are 2π-periodic functions of θ only if the right hand sides of these equations do not contain secular terms proportional to 1 and $e^{-i\theta}$, respectively. This is the case if the integral of the right hand side of (4.99) and the integral of $e^{i\theta}$ times the right hand side of (4.101) over $[-\pi, \pi]$ are both zero. These solvability conditions give:

$$\frac{\partial n^{(0)}}{\partial t} - \frac{\partial}{\partial x}\mathrm{Im}\ f_{1,S} = 0, \tag{4.103}$$

$$\frac{\partial A}{\partial t} = -\frac{\gamma_e + \gamma_j}{2}\, A + \frac{1}{2i}\,\frac{\partial}{\partial x}\int_{-\pi}^{\pi} e^{i\theta} g(n^{(0)}, F^{(0)}, f_{1,S} + Ae^{-i\theta})\,\frac{d\theta}{2\pi}. \tag{4.104}$$

Instead of (4.103), we can use the Ampère's law (4.60) with (4.87) replacing $\mathrm{Im} f_{1,S}$:

$$\frac{\partial F^{(0)}}{\partial t} + \frac{\delta}{F^{(0)\,2} + \delta^2\gamma_j\gamma_e}\left[\gamma_e E_0 n^{(0)} F^{(0)} + \frac{F^{(0)}}{2}\,\frac{\partial}{\partial x}\mathrm{Im}\, g_S \right.$$
$$\left. -\frac{\delta\gamma_e}{2}\,\frac{\partial}{\partial x}(n^{(0)} - \mathrm{Re}\, g_S) - F^{(0)}\mathrm{Re}\, h_S + \delta\gamma_e \mathrm{Im}\, h_S\right] = J(t), \tag{4.105}$$

where $J(t)$ is the total current density. Equations (4.104), (4.105) and (4.97) (the Poisson equation) describe the damping of the Bloch oscillations. In the next section, we will find g and h.

4.7 Chapman-Enskog method for almost elastic collisions

In this Section, we shall derive (4.66)-(4.77) in the case of almost elastic collisions with $0 < \alpha_{e,j} \ll 1$. To show this, we shall use the Chapman-Enskog method (CEM) [17] to obtain equations for the electric field, the electron density and the envelope of the BO, A. Then we will compare these equations with (4.104) and (4.105) and identify g and h.

[4] $F^{(0)}$ could include as an additional term an arbitrary function of θ and t but this would correspond to the case of a rapidly varying voltage bias which we do not consider in this work.

To implement the CEM, we assume that the distribution function f is a function of θ, k, x and t, which is 2π-periodic in θ and in k and that F is of order 1. Eq. (4.47) becomes

$$\mathbb{M}f - f^{1D\alpha} = -\delta\left(\frac{\partial f}{\partial t} + \sin k\,\frac{\partial f}{\partial x}\right), \tag{4.106}$$

$$\mathbb{M}u(k,\theta) = F\left(\frac{\partial}{\partial\theta} + \frac{\partial}{\partial k}\right)u(k,\theta) + u(k,\theta), \tag{4.107}$$

Equations (4.106) - (4.107) with $F = O(1)$ display a dominant balance between the collisions, the force due to the electric field and the change of f over the fast time scale θ. We are ignoring a possible fast relaxation from an initial distribution function to the BO represented by the fast time scale θ and the condition that f be periodic in θ, but we are considering the possibility of slow modulations of the BO in the time scale t.

As explained in the previous section, the moment $f_1 = f_{1S} + \Phi$, $\Phi = Ae^{-i\theta} + O(\delta)$, has a dominant part of order one, $Ae^{-i\theta}$, and a remainder. The remainder is 2π-periodic in θ, it vanishes as $\delta \to 0$ and it can be chosen not to contain a term proportional to $e^{-i\theta}$. Thus we assume:

$$f_1 = Ae^{-i\theta} + \delta B + \delta^2 C + O(\delta^3). \tag{4.108}$$

The local equilibrium $f^{1D\alpha}$ is a function of k, n and f_1 through (4.12) - (4.14). Due to (4.108), $f^{1D\alpha}$ is a 2π-periodic function of k and of θ, which also depends on the slowly-varying functions $n(x,t)$, $F(x,t)$, $A(x,t)$, $B(x,t)$ and $C(x,t)$.

Using the notation

$$f^{1D\alpha}(k,\theta;\delta) = \sum_{j,l} f^{1D\alpha}_{j,l} e^{i(jk+l\theta)}, \tag{4.109}$$

$$f(k,\theta;x,t,\delta) = \sum_{j,l} f_{j,l}(x,t;\delta)\, e^{i(jk+l\theta)}, \tag{4.110}$$

we see that the solution of (4.106) with $\delta = 0$ satisfies

$$f^{(0)}_{j,l} = \frac{f^{1D\alpha(0)}_{j,l}}{1 + iF(j+l)}, \tag{4.111}$$

where the superscripts (0) refer to having set $\delta = 0$ in (4.106) (see below).

In the CEM, we start from a leading order expression for the distribution function, (4.111), which does not depend explicitly on x and t. Instead,

it depends on k and θ, and it is a function of quantitites that vary slowly with x and t (the moments: n, F, A, B, C, ...). These moments are not expanded in powers of δ. Instead, their equations are expanded. Thus the Chapman-Enskog Ansatz is

$$f(x,k,t;\delta) = \sum_{m=0}^{\infty} f^{(m)}(k,\theta;F,n,A,B,C)\,\delta^m, \tag{4.112}$$

$$\frac{\partial F}{\partial t} + \sum_{m=0}^{\infty} \mathcal{J}^{(m)}(F,n,A,B,C)\,\delta^m = J(t), \tag{4.113}$$

$$\frac{\partial n}{\partial t} = -\sum_{m=0}^{\infty} \frac{\partial}{\partial x}\mathcal{J}^{(m)}(F,n,A,B,C)\,\delta^m, \tag{4.114}$$

$$\frac{\partial A}{\partial t} = \sum_{m=0}^{\infty} \mathcal{A}^{(m)}(F,n,A,B,C)\,\delta^m. \tag{4.115}$$

We have used the Poisson equation (4.85) to obtain (4.114). The local distribution function $f^{1D\alpha}$ can be expanded in powers of δ,

$$f^{1D\alpha} = \sum_{m=0}^{\infty} f^{1D\alpha(m)}\delta^m, \tag{4.116}$$

and then (4.12) - (4.14) and (4.108) yield the following compatibility conditions:

$$f_{0,0}^{(m)} = f_{0,0}^{1D\alpha(m)} = n\,\delta_{0m}, \tag{4.117}$$

$$f_{1,-1}^{(m)} = f_{1,-1}^{1D\alpha(m)} = A\,\delta_{0m}, \tag{4.118}$$

$$f_{1,0}^{(1)} = B_0, \quad f_{1,0}^{1D\alpha(1)} = B_0 + \gamma_e n\,E_0, \tag{4.119}$$

$$f_{1,0}^{(2)} = C_0, \quad f_1^{1D\alpha(2)} = C_0 - \gamma_e n\,\mathrm{Re}B_0 - i\gamma_j \mathrm{Im}B_0, \tag{4.120}$$

and so on. Inserting (4.112) - (4.116) into (4.106), we obtain a hierarchy of linear equations for the $f^{(m)}$ whose right hand sides contain the functionals $\mathcal{I}^{(m)}$ and $\mathcal{A}^{(m)}$. The latter are calculated in such a way that the compatibility conditions (4.117) - (4.120) hold.

The equations for $f^{(1)}$ and $f^{(2)}$ are:

$$\mathbb{M}f^{(1)} = f^{1D\alpha(1)} - \left(\left.\frac{\partial f^{(0)}}{\partial t}\right|_0 + \sin k\,\frac{\partial f^{(0)}}{\partial x}\right), \tag{4.121}$$

$$\mathbb{M}f^{(2)} = f^{1D\alpha(2)} - \left(\left.\frac{\partial f^{(1)}}{\partial t}\right|_0 + \sin k\,\frac{\partial f^{(1)}}{\partial x}\right) - \left.\frac{\partial f^{(0)}}{\partial t}\right|_1. \tag{4.122}$$

The subscript m in the right hand side of these equations means that $\partial F/\partial t$, $\partial n/\partial t$ and $\partial A/\partial t$ are replaced by $(J\delta_{m0} - \mathcal{J}^{(m)})$, $-\partial\mathcal{J}^{(m)}/\partial x$ and $-\mathcal{A}^{(m)}$, respectively.

Upon insertion of (4.111) in (4.121), the compatibility conditions (4.117) - (4.119) yield

$$\mathcal{J}^{(0)} = 0, \tag{4.123}$$

$$\mathcal{A}^{(0)} = -\frac{1}{2}(\gamma_e + \gamma_j)\, A + \frac{1}{2i}\,\frac{\partial f_{2,-1}^{(0)}}{\partial x}, \tag{4.124}$$

$$B = \frac{\gamma_e n E_0}{iF} + \frac{1}{2F}\,\frac{\partial}{\partial x}\left(n - \frac{f_{2,0}^{1D\alpha(0)}}{1 + i2F}\right). \tag{4.125}$$

Note that B becomes singular in the limit as $F \to 0$. This is not surprising: we have assumed in this Section that $F = O(1)$ as $\delta \to 0$ so that $\theta \neq 0$ and the first harmonic in (4.108) is different from all other ones contained in B, C, etc. If F tends to 0, then the first two terms in (4.107) are smaller than the third one and the assumption (4.108) does not make sense. Even though the CEM has such evident shortcomings, we shall use it to identify g and h of the previous Section. The coefficients in the resulting modulation equations, (4.103) - (4.105), are no longer singular.

The compatibility conditions (4.117) and (4.118) for $f^{(2)}$ provide the following functionals

$$\mathcal{J}^{(1)} = -\mathrm{Im}\ B, \tag{4.126}$$

$$\mathcal{A}^{(1)} = \frac{1}{2i}\,\frac{\partial f_{2,-1}^{(1)}}{\partial x}. \tag{4.127}$$

Then the Ampère's law and the equation for A including up to $O(\delta)$ terms are

$$\frac{\partial F}{\partial t} - \delta\,\mathrm{Im}\,B = J(t), \tag{4.128}$$

$$\frac{\partial A}{\partial t} = -\frac{1}{2}(\gamma_e + \gamma_j)\, A + \frac{1}{2i}\,\frac{\partial}{\partial x}(f_{2,-1}^{(0)} + \delta\, f_{2,-1}^{(1)}), \tag{4.129}$$

in which B is given by (4.125). We now impose that these equations match (4.105) and (4.104), respectively. The result is that these equations match term by term in the overlap region

$$\delta \ll F \ll 1,$$

(with $B\delta \sim f_{1,S}$) provided

$$g_S = f^{(0)}_{2,0}, \tag{4.130}$$

$$g_{-1} = f^{(0)}_{2,-1} + \delta\, f^{(1)}_{2,-1}. \tag{4.131}$$

Both equations hold if

$$g = f^{(0)}_2 + \delta\, f^{(1)}_2. \tag{4.132}$$

We have not yet calculated h in (4.105). We shall determine h in such a way that the resulting equation for the field coincides with the drift-diffusion equation (B.38) that we derive in Appendix B for the case of inelastic collisions. The result is that we should replace h in (4.105) by the uniform part of $f_{1,S}$ in (4.86), i.e.,

$$h \;=\; \frac{\partial}{\partial t}\left(\frac{\delta\gamma_e n E_0(\delta\gamma_j - iF)}{\delta^2\gamma_e\gamma_j + F^2}\right)\bigg|_0 = J\,\frac{\partial}{\partial F}\left(\frac{\delta\gamma_e n E_0(\delta\gamma_j - iF)}{\delta^2\gamma_e\gamma_j + F^2}\right) \tag{4.133}$$

As we shall see in the next Section, (4.105) with h given by (4.133) matches the drift-diffusion equation (B.38) obtained in the case of inelastic collisions when $A = 0$ and the Bloch oscillations are absent.

The Fourier coefficients of the solution of (4.121) are

$$f^{(1)}_{j,l} = \frac{r^{(1)}_{j,l}}{1 + iF(j+l)}, \tag{4.134}$$

$$r^{(1)} = f^{1D\alpha(1)} - \left(\frac{\partial}{\partial t}\bigg|_0 + \sin k\,\frac{\partial}{\partial x}\right) f^{(0)}. \tag{4.135}$$

After straightforward calculations, we obtain the following reduced equations:

$$\frac{\partial F}{\partial t} + \frac{\delta}{F^2 + \delta^2\gamma_j\gamma_e}\left[\gamma_e E_0 n F + \frac{F}{2}\,\frac{\partial}{\partial x}\mathrm{Im}\,\frac{f^{1D\alpha(0)}_{2,0}}{1+2iF}\right. \tag{4.136}$$

$$\left. -\frac{\delta\gamma_e}{2}\,\frac{\partial}{\partial x}\left(n - \mathrm{Re}\,\frac{f^{1D\alpha(0)}_{2,0}}{1+2iF}\right) - F\mathrm{Re}\,h_S + \delta\gamma_e\mathrm{Im}\,h_S\right] = J(t),$$

$$\frac{\partial A}{\partial t} = -\frac{\gamma_e + \gamma_j}{2}\,A + \frac{1}{2i}\frac{\partial}{\partial x}\left(\frac{f^{1D\alpha(0)}_{2,-1} + \delta\, r^{(1)}_{2,-1}}{1+iF}\right), \tag{4.137}$$

$$r^{(1)}_{2,-1} = f^{1D\alpha(1)}_{2,-1} - \left(\mathcal{A}^{(0)}\frac{\partial}{\partial A} + J\frac{\partial}{\partial F}\right)\frac{f^{1D\alpha(0)}_{2,-1}}{1+iF} - \frac{1}{2i}\frac{\partial}{\partial x}\left(A - \frac{f^{1D\alpha(0)}_{3,-1}}{1+2iF}\right), \tag{4.138}$$

in addition to (4.133) and to the Poisson equation (4.85). To calculate $f_{2,-1}^{1D\alpha(1)}$ in (4.138), we need to use

$$f^{1D\alpha(1)} = \left(\tilde{\mu}^{(1)} \frac{\partial}{\partial \tilde{\mu}^{(0)}} + \tilde{u}^{(1)} \frac{\partial}{\partial \tilde{u}^{(0)}} + \tilde{\beta}^{(1)} \frac{\partial}{\partial \tilde{\beta}^{(0)}} \right) f^{1D\alpha(0)}. \tag{4.139}$$

In this expression, we should substitute $\tilde{\mu}^{(0)}$, $\tilde{u}^{(0)}$ and $\tilde{\beta}^{(0)}$ given by simultaneously solving

$$f_0^{1D\alpha(0)} = n, \quad f_1^{1D\alpha(0)} = A\, e^{-i\theta}, \tag{4.140}$$

and also the solutions $\tilde{\mu}^{(1)}$, $\tilde{u}^{(1)}$, $\tilde{\beta}^{(1)}$ of

$$f_0^{1D\alpha(1)} = 0, \tag{4.141}$$

$$f_1^{1D\alpha(1)} = \gamma_e n E_0 + f_{1,S} - \frac{\gamma_e + \gamma_j}{2} A\, e^{-i\theta} - \frac{\gamma_e - \gamma_j}{2} A^* e^{i\theta}. \tag{4.142}$$

When we substitute these solutions, (4.139) becomes a function of k, θ, n, A and $f_{1,S} \sim B\delta$ which is 2π-periodic in k and θ. Its Fourier coefficient $f_{2,-1}^{1D\alpha(1)}$ is then inserted in (4.138).

4.8 Concluding remarks

We have proposed a Boltzmann-BGK kinetic equation for electron transport in miniband semiconductor superlattices. Its local equilibrium depends on electron density, mean energy and current density and therefore it oscillates periodically in time with the Bloch frequency when the mean energy and the current density do the same. This model is richer than the usual BGK models traditionally used in this field and its corresponding hydrodynamic equations may exhibit Bloch oscillations which are absent in the hydrodynamic regime of the KSS and related models. We have introduced novel singular perturbation methods to derive hydrodynamic equations describing Bloch oscillations in the limit in which collision and Bloch frequencies dominate all other terms in the kinetic equation and the collisions are almost elastic. By numerically solving the hydrodynamic equations with appropriate initial and boundary conditions, we find that nonlinearities may stabilize Bloch oscillations if the restitution coefficients are small enough. We have found that Bloch oscillations have nonzero amplitudes only in a portion of the superlattice and are therefore confined there. The corresponding current density and mean energy profiles are spatially inhomogeneous. As the collisions become more inelastic, the parameter range for which BO appear

shrinks and these oscillations disappear for the standard superlattices used in experiments [71]. In the absence of Bloch oscillations, the hydrodynamic equations become the known drift-diffusion system valid for inelastic collisions that may exhibit Gunn-type self-sustained oscillations due to periodic recycling of charge dipole domains [14].

Chapter 5

Nonlinear electron and spin transport in semiconductor superlattices

5.1 Introduction

In this chapter we present systematic derivations of quantum balance equations for SLs with two populated minibands, and it shows that their numerical solutions may predict space and time-dependent nonlinear phenomena occurring in these materials. Our methods can be used in 3D crystals, but their application to 1D structures such as SLs and LSLs leads to simpler equations that are less costly to solve. Although nonlinear charge transport in SLs has been widely studied in the last decade (see the reviews [14, 64, 76]), systematic derivations of tractable balance equations for miniband populations and electric field are scarce. One reason is that quantum kinetic equations are nonlocal in space and their collision terms may be nonlocal in space and time [38, 76]. Using them to analyze space and time-dependent phenomena such as wave propagation or self-sustained oscillations is problematic. In fact, only extremely simple solutions of general quantum kinetic equations (such as thermal equilibrium, disturbances thereof due to weak external fields and so on) are known, theoretical analysis of these equations is lacking and numerical solutions describing spatio-temporal phenomena are not available. One way to proceed is to adopt simple collision models similar to the Bhatnagar-Gross-Krook (BGK) collision model for classical kinetic theory [8]. We discuss in this chapter how to implement a BGK collision model for a quantum kinetic equation that is simple to handle yet keeps

an important quantum feature such as the broadening of energy levels [13]. Once we have a quantum kinetic equation for a sufficiently general SL having two minibands, we implement a Chapman-Enskog perturbation procedure to derive the sought balance equations and solve them numerically for realistic SL configurations.

Previous to this work, Lei and coworkers derived quantum hydrodynamic equations describing SL having only one miniband [57,59]. They use a closure assumption to close a hierarchy of moment equations. For the case of quantum particles in an arbitrary external three-dimensional potential, Degond and Ringhofer [31] have used a similar procedure to derive balance equations. They close the system of moment equations by means of a local equilibrium density obtained by maximizing entropy. The Chapman-Enskog method has been used to derive drift-diffusion equations for single-miniband SLs described by semiclassical [12] and quantum kinetic equations [13]. Earlier, Cercignani, Gamba and Levermore used the Chapman-Enskog method to derive balance equations for a semiclassical BGK-Poisson kinetic description of a semiconductor with one parabolic band under strong external bias [28].

The rest of this chapter is as follows. In Section 5.2, we review the simpler case of nonlinear electron transport in a strongly coupled n-doped SL having only one populated miniband [13]. Starting with a kinetic equation for the Wigner function, we use the Chapman-Enskog perturbation method to derive balance equations for the electron density and the electric field. When these equations are solved numerically for a dc voltage biased SL with finitely many QWs and realistic parameter values, stable self-sustained oscillations of the current through the SL are found among their solutions, in agreement with experimental observations [13]. Sections 5.3 to 5.5 contain the main results of the present work. In Section 5.3, we describe a SL having two populated minibands by proposing a kinetic equation for the Wigner matrix. In Section 5.4, we derive balance equations for the miniband electron populations and the electric field, using an appropriate Chapman-Enskog method and a tight-binding approximation to obtain explicit formulas. The case of a LSL having strong Rashba spin-orbit interaction [66] is important for spintronic applications and has been considered in Section 5.5. We derive and solve numerically the resulting balance equations. Novel self-sustained oscillations of the spin current and polarization are obtained for appropriate values of the parameters. Finally Section 5.6 contains our conclusions and some technical matters are relegated to the Appendix C.

5.2 Single miniband superlattice

The Wigner-Poisson-Bhatnagar-Gross-Krook (WPBGK) system of equations (2.53)-(2.56) for 1D electron transport in the lowest miniband of a strongly coupled SL was already derived in section 2.2. The left-hand side of Eq. (2.53) can be straightforwardly derived from the Schrödinger-Poisson equation for the wave function in the miniband using the definition of the 1D Wigner function [13]:

$$f(x,k,t) = \frac{2l}{S}\sum_{j=-\infty}^{\infty}\int_{\mathbb{R}^2}\langle\psi^{\dagger}(x+jl/2,y,z,t)\psi(x-jl/2,y,z,t)\rangle e^{ijkl}d\mathbf{x}_{\perp} \quad (5.1)$$

(the second quantized wave function $\psi(x,\mathbf{x}_{\perp},t) = \sum_{q,\mathbf{q}_{\perp}} a(q,q_{\perp},t)\phi_q(x)e^{i\mathbf{q}_{\perp}\cdot\mathbf{x}_{\perp}}$, $\mathbf{x}_{\perp} = (y,z)$, is a superposition of the Bloch states corresponding to the miniband and S is the SL cross section [13]). The right hand side in Eq. (2.53) is the sum of $-\nu_{en}\left(f - f^{FD}\right)$, which represents energy relaxation towards a 1D effective Fermi-Dirac (FD) distribution $f^{FD}(k;n)$ (local equilibrium), and $-\nu_{imp}[f(x,k,t) - f(x,-k,t)]/2$, which accounts for impurity elastic collisions [12]. For simplicity, the collision frequencies ν_{en} and ν_{imp} are fixed constants. Exact and FD distribution functions have the same electron density, thereby preserving charge continuity as in the classical BGK collision models [8]. The chemical potential μ is a function of n resulting from solving equation (2.55) with the integral of the collision-broadened 3D Fermi-Dirac distribution over the lateral components of the wave vector $(k,\mathbf{k}_{\perp}) = (k,k_y,k_z)$:

$$f^{FD}(k;n) = \int_{-\infty}^{\infty}\frac{D_{\Gamma}\left(E-\mathcal{E}_1(k)\right)}{1+\exp\left(\frac{E-\mu}{k_BT}\right)}\,dE, \quad (5.2)$$

$$D_{\Gamma}(E) = \frac{2}{(2\pi)^2}\int_{\mathbb{R}^2}\delta_{\Gamma}\left(\frac{\hbar^2\mathbf{k}_{\perp}^2}{2m^*} - E\right)d\mathbf{k}_{\perp} = \frac{m^*}{\pi\hbar^2}\int_0^{\infty}\delta_{\Gamma}(E_{\perp}-E)\,dE_{\perp}. \quad (5.3)$$

Using the residue theorem for a line-width:

$$\delta_{\Gamma}(E) \;=\; \frac{\sqrt{2}\,\Gamma^3/\pi}{\Gamma^4+E^4}, \quad (5.4)$$

(5.3) yields

$$
\begin{aligned}
D_\Gamma(E) &= \frac{m^*}{\pi\hbar^2}\left\{1+\frac{1}{4\pi}\ln\left[\frac{E^2+\sqrt{2}\Gamma E+\Gamma^2}{E^2-\sqrt{2}\Gamma E+\Gamma^2}\right]\right. \\
&- \frac{\theta(\sqrt{2}|E|-\Gamma)}{2\pi}\left[2\pi-\arctan\left(\frac{\Gamma}{\sqrt{2}|E|+\Gamma}\right)-\arctan\left(\frac{\Gamma}{\sqrt{2}|E|-\Gamma}\right)\right] \\
&- \frac{\theta(\Gamma-\sqrt{2}|E|)}{2\pi}\left[\pi+\arctan\left(\frac{\Gamma}{\sqrt{2}E+\Gamma}\right)-\arctan\left(\frac{\Gamma}{\Gamma-\sqrt{2}E}\right)\right] \\
&- \left.\frac{\theta(\sqrt{2}E-\Gamma)}{2\pi}\left[\arctan\left(\frac{\Gamma}{\sqrt{2}E+\Gamma}\right)+\arctan\left(\frac{\Gamma}{\sqrt{2}E-\Gamma}\right)\right]\right\},
\end{aligned}
\tag{5.5}
$$

which is equivalent to Eq. (2.56)[1]. Here $\theta(E)$ is the Heaviside unit step function. As $\Gamma \to 0+$, the line-width (5.4) tends to the delta function $\delta(E)$, $D_\Gamma(E)$ tends to the 2D density of states, $D(E) = m^*\theta(E)/(\pi\hbar^2)$, and f^{FD} tends to the 3D Fermi-Dirac distribution function integrated over the lateral wave vector $\mathbf{k}_\perp$. In Ref. [13], a Lorentzian line-width was used instead of (5.4) and the integral over E in (5.2) extended from 0 to ∞. The integral with the Lorentzian function is not convergent in $E = -\infty$, which is why we prefer using convolution with the "super-Lorentzian" function (5.4) in this work. The integration in (5.3) cannot be carried out explicitly for other standard line-widths such as a Gaussian or a hyperbolic secant. This unnecessarily complicates the numerical integration of the balance equations we will obtain later. Note that, following Ignatov and Shashkin [43], we have not included the effects of the electric potential in our Fermi-Dirac distribution. These model equations can be improved by including scattering processes with change of lateral momentum and an electric field-dependent local equilibrium. However the resulting model could only be treated numerically and the qualitative features of our derivation and of the nonlocal drift-diffusion equation would be lost in longer formulas.

A different way to introduce a quantum BGK collision model is to define a local equilibrium density matrix operator by minimizing quantum entropy (defined with the opposite sign of the convention that is usual in physics) under constraints giving the electron density and energy density in terms of the density matrix. The resulting expression involves an inverse Wigner transform and another transform is needed to deduce the local equilibrium Wigner function f^{FD} entering the BGK formula [31]. This f^{FD} is nonlocal

[1]Integrate (5.2) by parts using (5.5).

in space and can only be found by solving some partial differential equation [31]. As a model for quantum collisions [38, 76], the resulting quantum BGK model is not realistic, in the same way as the original BGK model is not a realistic model for classical collisions. Moreover, the implicit manner in which the model is defined defeats the main asset of the classical BGK collision model: its simplicity, that makes it possible to obtain results analytically. Thus we prefer to introduce a BGK model that can be handled more easily and incorporates quantum effects realistically. The most important quantum effect affecting the collision term is the broadening of energy levels due to scattering, $\Gamma \approx \hbar/\tau$ (where τ is the lifetime of the level), and this is taken phenomenologically into account by the convolution with the line-width function (5.4) in (5.2). In the semiclassical limit "$\hbar \to 0$", $\Gamma \to 0$ and we recover the semiclassical FD distribution.

From the WPBGK system (2.53) to (2.56) we can derive the QDDE (2.77)-(2.86) by means of the Chapman-Enskog method as described in section 2.3.2, assuming that the electric field contribution in Eq. (2.70) is comparable to the collision terms and that they dominate the other terms (*the hyperbolic limit*) [12]. Note that the semiclassical equations (3.21)-(3.28) derived in section 3.2.2 coincide with the QDDE (2.53)-(2.56) if the spatial averages are ignored.

The boundary conditions for the QDDE (2.53), which contains triple spatial averages, need to be specified for the intervals $[-2l, 0]$ and $[Nl, Nl + 2l]$, and not just at the points $x = 0$ and $x = Nl$ (N denotes the number of SL periods spanning the device), as in the case of the parabolic semiclassical GDDE. Similarly, the initial condition has to be defined on the extended interval $[-2l, Nl + 2l]$. Note that the spatial averages in the nonlocal QDDE give rise to finite differences of partial derivatives in the diffusion terms, and therefore lead to a type of equations for which little seems to be known.

For realistic values of the parameters representing a strongly coupled SL under dc voltage bias, the numerical solution of the QDDE yields a stable self-sustained oscillation of the current [13] in quantitative agreement with experiments [71]. Fig. 5.1 shows the evolution of the current during the self-sustained oscillations that appear when the QDDE (2.53)-(2.56) are numerically solved for boundary condition $\varepsilon \partial F/\partial t + \sigma_0 F = J$ at each point of the injector contact ($-2l \leq x \leq 0$) and boundary condition $\varepsilon \partial F/\partial t + \sigma_L F n/N_D = J$ at each point of the colector contact ($Nl \leq x \leq Nl + 2l$) and appropriate dc voltage bias. The contact conductivity σ_0 is selected so that $\sigma_0 F$ intersects $eN_D v_M V(F/F_M)/l$ on its decreasing branch,

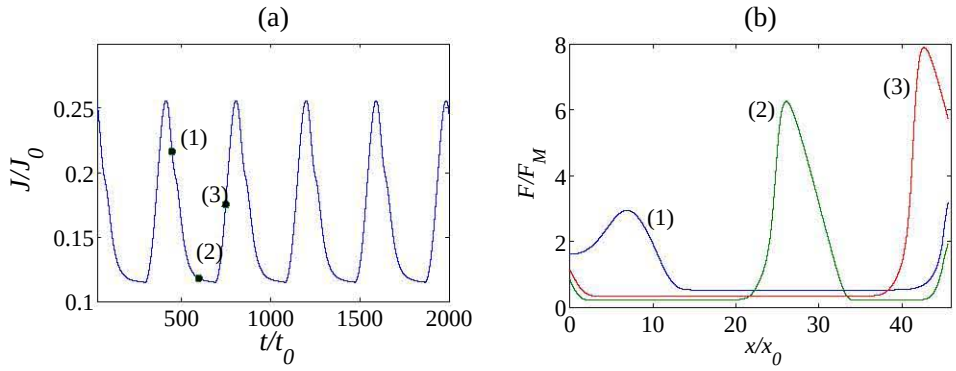

Figure 5.1: (a) Current ($J_0 = ev_M N_D/l$) vs. time during self-oscillations, and (b) field profile at different times during one oscillation cycle. Parameter values: $x_0 = 16$ nm, $t_0 = 0.064$ ps, $J_0 = 4 \times 10^5$ A/cm^2.

as in the theory of the Gunn effect [14]. Parameter values correspond to a 157-period 3.64 nm GaAs/0.93 nm AlAs SL at 14 K, with $N_D = 4.57 \times 10^{10}$ cm^{-2}, $\nu_{imp} = 2\nu_{en} = 18 \times 10^{12}$ Hz [71], under a dc voltage bias of 1.62 V and collision broadening $\Gamma = 1$ meV. Cathode and anode contact conductivities are 2.5 and 0.62 Ω^{-1}cm^{-1}, respectively.

5.3 Wigner description of a two-miniband superlattice

We shall consider a 2×2 Hamiltonian $\mathbf{H}(x, -i\partial/\partial x)$, in which [48]

$$\begin{aligned}\mathbf{H}(x,k) &= [h_0(k) - eW(x)]\boldsymbol{\sigma}_0 + \vec{h}(k)\cdot\vec{\boldsymbol{\sigma}}] \\ &\equiv \begin{pmatrix} (\alpha+\gamma)(1-\cos kl) - eW(x) + g & -i\beta\sin kl \\ i\beta\sin kl & (\alpha-\gamma)(1-\cos kl) - eW(x) - g \end{pmatrix}.\end{aligned} \tag{5.6}$$

Here

$$\begin{aligned} h_0(k) &= \alpha\,(1-\cos kl), & h_1(k) &= 0, \\ h_2(k) &= \beta\sin kl, & h_3(k) &= \gamma\,(1-\cos kl) + g, \end{aligned} \tag{5.7}$$

and

$$\boldsymbol{\sigma}_0 = \begin{pmatrix} 1 & 0 \\ 0 & 1 \end{pmatrix}, \boldsymbol{\sigma}_1 = \begin{pmatrix} 0 & 1 \\ 1 & 0 \end{pmatrix}, \boldsymbol{\sigma}_2 = \begin{pmatrix} 0 & -i \\ i & 0 \end{pmatrix}, \boldsymbol{\sigma}_3 = \begin{pmatrix} 1 & 0 \\ 0 & -1 \end{pmatrix} \tag{5.8}$$

are the Pauli matrices.

The Hamiltonian (5.6) corresponds to the simplest 2×2 Kane model in which the quadratic and linear terms $(kl)^2/2$ and kl are replaced by $(1 - \cos kl)$ and $\sin kl$, respectively. For a SL with two minibands, $2g$ is the miniband gap and $\alpha = (\Delta_1 + \Delta_2)/4$ and $\gamma = (\Delta_1 - \Delta_2)/4$, provided Δ_1 and Δ_2 are the miniband widths. In the case of a LSL, $g = \gamma = 0$, and $h_2\boldsymbol{\sigma}_2$ corresponds to the precession term in the Rashba spin-orbit interaction [50]. The other term, the intersubband coupling, depends on the momentum in the y direction and we have not included it here. Small modifications of (5.6) represent a single miniband SL with dilute magnetic impurities in the presence of a magnetic field B: $g = \gamma = h_2 = 0$, and $h_1 = \beta(B)$ [69]. As in the case of a single miniband SL, $W(x)$ is the electric potential.

The energy minibands $\mathcal{E}^{\pm}(k)$ are the eigenvalues of the free Hamiltonian $\mathbf{H}_0(k) = h_0(k)\boldsymbol{\sigma}_0 + \vec{h}(k) \cdot \vec{\boldsymbol{\sigma}}$ and are given by

$$\mathcal{E}^{\pm}(k) = h_0(k) \pm |\vec{h}(k)|. \tag{5.9}$$

The corresponding spectral projections are

$$\mathbf{P}^{\pm}(k) = \frac{\boldsymbol{\sigma}_0 \pm \vec{\nu}(k) \cdot \vec{\boldsymbol{\sigma}}}{2}, \quad \text{where} \quad \vec{\nu}(k) = \vec{h}(k)/|\vec{h}(k)|, \tag{5.10}$$

so that we can write

$$\mathbf{H}_0(k) = \mathcal{E}^{+}(k)\mathbf{P}^{+}(k) + \mathcal{E}^{-}(k)\mathbf{P}^{-}(k). \tag{5.11}$$

We shall now write the WPBGK equations for the Wigner matrix written in terms of the Pauli matrices:

$$\mathbf{f}(x,k,t) = \sum_{i=1}^{3} f^i(x,k,t)\boldsymbol{\sigma}_i = f^0(x,k,t)\boldsymbol{\sigma}_0 + \vec{f}(x,k,t) \cdot \vec{\boldsymbol{\sigma}}. \tag{5.12}$$

The Wigner components are real and can be related to the coefficients of the Hermitian Wigner matrix by

$$\begin{array}{ll} f_{11} = f^0 + f^3, & f_{12} = f^1 - if^2, \\ f_{21} = f^1 + if^2, & f_{22} = f^0 - f^3. \end{array} \tag{5.13}$$

Hereinafter we shall use the equivalent notations

$$f = \begin{pmatrix} f^0 \\ \vec{f} \end{pmatrix} = \begin{pmatrix} f^0 \\ f^1 \\ f^2 \\ f^3 \end{pmatrix}. \tag{5.14}$$

The populations of the minibands with energies $\mathcal{E}^{\pm}$ are given by the moments:

$$n^{\pm}(x,t) = \frac{l}{2\pi} \int_{-\pi/l}^{\pi/l} \left[f^0(x,k,t) \pm \vec{\nu}(k) \cdot \vec{f}(x,k,t) \right] dk, \tag{5.15}$$

and the total electron density is $n^+ + n^-$. After some algebra, we can obtain the following WPBGK equations for the Wigner components

$$\frac{\partial f^0}{\partial t} + \frac{\alpha}{\hbar} \sin kl \, \Delta^- f^0 + \vec{b} \cdot \Delta^- \vec{f} - \Theta f^0 = Q^0[f], \tag{5.16}$$

$$\frac{\partial \vec{f}}{\partial t} + \frac{\alpha}{\hbar} \sin kl \, \Delta^- \vec{f} + \vec{b} \, \Delta^- f^0 + \vec{\omega} \times \vec{f} - \Theta \vec{f} = \vec{Q}[f], \tag{5.17}$$

$$\varepsilon \frac{\partial^2 W}{\partial x^2} = \frac{e}{l} (n^+ + n^- - N_D), \tag{5.18}$$

whose right hand sides contain collision terms to be described later. Here

$$(\Delta^{\pm} u)(x,k) = u(x + l/2, k) \pm u(x - l/2, k), \tag{5.19}$$

$$\vec{\omega} = \vec{\omega}_0 + \vec{\omega}_1, \tag{5.20}$$

$$\vec{\omega}_0 = \frac{2g}{\hbar} (0, 0, 1), \tag{5.21}$$

$$\vec{\omega}_1 = \frac{1}{\hbar} (0, \beta \sin kl \, \Delta^+, 2\gamma - \gamma \cos kl \, \Delta^+), \tag{5.22}$$

$$\vec{b} = \frac{1}{\hbar} (0, \beta \cos kl, \gamma \sin kl), \tag{5.23}$$

$$\Theta f^i(x,k,t) = \sum_{j=-\infty}^{\infty} \frac{ejl}{i\hbar} \langle F(x,t) \rangle_j e^{ijkl} f_j^i(x,t). \tag{5.24}$$

Our collision model contains two terms: a BGK term which tries to send the miniband Wigner function to its local equilibrium and a scattering term

from the miniband with higher energy to the lowest miniband:

$$Q^0[f] = -\frac{f^0 - \Omega^0}{\tau}, \tag{5.25}$$

$$\vec{Q}[f] = -\frac{\vec{f} - \vec{\Omega}}{\tau} - \frac{\vec{\nu} f^0 + \vec{f}}{\tau_{\rm sc}}, \tag{5.26}$$

$$\Omega^0 = \frac{\phi^+ + \phi^-}{2}, \quad \vec{\Omega} = \frac{\phi^+ - \phi^-}{2}\,\vec{\nu}, \tag{5.27}$$

$$\phi^{\pm}(k; n^{\pm}) = \frac{m^* k_B T}{\pi\hbar^2} \int_{-\infty}^{\infty} \frac{\sqrt{2}\,\Gamma^3/\pi}{\Gamma^4 + [E - \mathcal{E}^{\pm}(k)]^4} \ln\left(1 + e^{\frac{\mu^{\pm} - E}{k_B T}}\right) dE, \tag{5.28}$$

$$n^{\pm} = \frac{l}{2\pi} \int_{-\pi/l}^{\pi/l} \phi^{\pm}(k; n^{\pm})\, dk. \tag{5.29}$$

Note that the single miniband Wigner equations correspond to the particular case $\beta = \gamma = g = 1/\tau_{\rm sc} = 0$. In this case, $E^+ = E^-$, $n^+ = n^-$, $\phi^+ = \phi^- = f^{FD}$, $f_{11} = f_{22} = f^0 = f$, $f_{12} = f_{21} = f^1 = f^2 = 0$, equations (5.26) and (5.17) disappear and equation (5.16) coincide with the previously derived single miniband Wigner equations (2.64) if the impurity collisions are ignored ($\nu_{imp} = 0$). In other words, the two miniband Wigner equations derived in this section are consistent with the previous single miniband equations except for the impurity collisions term, which is ignored in the two miniband case.

The chemical potentials of the minibands, μ^+ and μ^- are calculated in terms of n^+ and n^- respectively, by inserting (5.28) in (5.29) and solving the resulting equations. Our collision model should enforce charge continuity. To check this, we first calculate the time derivative of $n^{\pm}$ using (5.15) to (5.17):

$$\frac{\partial n^{\pm}}{\partial t} + \frac{\alpha l \Delta^-}{2\pi\hbar} \int_{-\pi/l}^{\pi/l} \sin kl\, (f^0 \pm \vec{\nu}\cdot\vec{f})\, dk + \frac{l\Delta^-}{2\pi} \int_{-\pi/l}^{\pi/l} (\vec{b}\cdot\vec{f} \pm \vec{\nu}\cdot\vec{b} f^0)\, dk \tag{5.30}$$

$$\pm \frac{l\Delta^-}{2\pi} \int_{-\pi/l}^{\pi/l} \vec{\nu}\cdot\vec{\omega}\times\vec{f}\, dk \mp \frac{l\Delta^-}{2\pi} \int_{-\pi/l}^{\pi/l} \vec{\nu}\cdot\Theta\vec{f}\, dk$$

$$= \frac{l\Delta^-}{2\pi} \int_{-\pi/l}^{\pi/l} (Q^0[f] \pm \vec{\nu}\cdot\vec{Q}[f])\, dk = \mp\frac{n^+}{\tau_{\rm sc}},$$

where we have employed $\int \Theta f^0 dk = 0$. Then we obtain:

$$\frac{\partial}{\partial t}(n^+ + n^-) + \Delta^- \left[\frac{l}{\pi} \int_{-\pi/l}^{\pi/l} \left(\frac{\alpha}{\hbar} \sin kl\, f^0 + \vec{b}\cdot\vec{f}\right) dk\right] = 0. \tag{5.31}$$

Noting that $\Delta^- u(x) = l\,\partial\langle u(x)\rangle_1/\partial x$, we see that this equation corresponds to charge continuity. Differentiating in time the Poisson equation (5.18), using (5.31) in the result and integrating with respect to x, we get the following nonlocal Ampère's law for the balance of current:

$$\varepsilon\frac{\partial F}{\partial t} + \left\langle \frac{el}{\pi}\int_{-\pi/l}^{\pi/l}\left(\frac{\alpha}{\hbar}\sin kl\, f^0 + \vec{b}\cdot\vec{f}\right)dk\right\rangle_1 = J(t). \tag{5.32}$$

Here the space independent function $J(t)$ is the total current density. Since the Wigner components are real, we can rewrite (5.32) in the following equivalent form:

$$\varepsilon\frac{\partial F}{\partial t} - \frac{2e}{\hbar}\left\langle \alpha\,\mathrm{Im} f_1^0 - \beta\,\mathrm{Re} f_1^2 + \gamma\,\mathrm{Im} f_1^3\right\rangle_1 = J(t). \tag{5.33}$$

5.4 Derivation of balance equations by the Chapman-Enskog method

In this Section, we shall derive the reduced balance equations for our two-miniband SL using the Chapman-Enskog method. First of all, we should decide the order of magnitude of the terms in the WPBGK equations (5.16) and (5.17) in the hyperbolic limit. Recall that in this limit, the collision frequency $1/\tau$ and the Bloch frequency $eF_M l/\hbar$ are of the same order, about 10 THz for the SL of Section 5.2. Typically, $2g/\hbar$ is of the same order, so that the term containing $\vec{\omega}_0$ should also balance the BGK collision term. What about the other terms?

The scattering time τ_{sc} is much longer than the collision time τ, and we shall consider $\tau/\tau_{\mathrm{sc}} = O(\lambda) \ll 1$. Moreover, the gap energy is typically much larger than the miniband widths or the spin-orbit coefficient and a rich dominant balance is obtained by assuming that β/g and γ/g are of order λ. Then we can expand the unit vector $\vec{\nu}$ as follows:

$$\vec{\nu} = (0,0,1) + \frac{\lambda\beta}{g}\sin kl\,(0,1,0) - \lambda^2\left[\frac{\beta\gamma}{g^2}\sin kl(1-\cos kl)\,(0,1,0) + \frac{\beta^2\sin^2 kl}{2g^2}\,(0,0,1)\right] + O(\lambda^3). \tag{5.34}$$

In this expansion, we have inserted the book-keeping parameter λ which is set equal to 1 at the end of our calculations (cf. Section 5.2). From (5.16)

and (5.17), we can write the scaled WPBGK equations as follows:

$$\mathbb{L}f - \Omega = -\lambda \left(\tau \frac{\partial f}{\partial t} + \Lambda f \right). \tag{5.35}$$

Here the operators $\mathbb{L}$ and Λ are defined by

$$\mathbb{L}f = f - \tau\, \Theta f + \delta_1 \begin{pmatrix} 0 \\ -f^2 \\ f^1 \\ 0 \end{pmatrix}, \tag{5.36}$$

$$\Lambda f = \delta_2 \begin{pmatrix} 0 \\ \vec{f} + \vec{\nu} f^0 \end{pmatrix} + \frac{\alpha\tau}{\hbar} \sin kl\, \Delta^- f + \Delta^- \begin{pmatrix} \tau \vec{b} \cdot \vec{f} \\ \tau\, \vec{b}\, f^0 \end{pmatrix} + \begin{pmatrix} 0 \\ \tau\, \vec{\omega}_1 \times \vec{f} \end{pmatrix}, \tag{5.37}$$

where

$$\delta_1 = \frac{2g\tau}{\hbar}, \quad \delta_2 = \frac{\tau}{\tau_{\rm sc}}. \tag{5.38}$$

The expansion of $\vec{\nu}$ in powers of λ gives rise to a similar expansion of Ω and Λ.

To derive the reduced balance equations, we use the following Chapman-Enskog ansatz:

$$f(x,k,t;\epsilon) = f^{(0)}(k; n^+, n^-, F) + \sum_{m=1}^{\infty} f^{(m)}(k; n^+, n^-, F)\, \lambda^m, \tag{5.39}$$

$$\varepsilon \frac{\partial F}{\partial t} + \sum_{m=0}^{\infty} J_m(n^+, n^-, F)\, \lambda^m = J(t), \tag{5.40}$$

$$\frac{\partial n^\pm}{\partial t} = \sum_{m=0}^{\infty} A_m^\pm(n^+, n^-, F)\, \lambda^m. \tag{5.41}$$

The functions $A_m^\pm$ and J_m are related through the Poisson equation (5.18), so that

$$A_m^+ + A_m^- = -\frac{l}{e} \frac{\partial J_m}{\partial x}. \tag{5.42}$$

Inserting (5.39) to (5.41) into (5.35), we get

$$\mathbb{L}f^{(0)} = \Omega_0, \tag{5.43}$$

$$\mathbb{L}f^{(1)} = \Omega_1 - \tau \left. \frac{\partial f^{(0)}}{\partial t} \right|_0 - \Lambda_0 f^{(0)}, \tag{5.44}$$

$$\mathbb{L}f^{(2)} = \Omega_2 - \tau \left. \frac{\partial f^{(1)}}{\partial t} \right|_0 - \Lambda_0 f^{(1)} - \tau \left. \frac{\partial f^{(0)}}{\partial t} \right|_1 - \Lambda_1 f^{(0)}, \tag{5.45}$$

and so on. The subscripts 0 and 1 in the right hand side of these equations mean that we replace $\varepsilon\,\partial F/\partial t|_m = J\delta_{0m} - J_m$, $\partial n^{\pm}/\partial t|_m = A_m^{\pm}$. Moreover, inserting (5.34) and (5.39) into (5.15) yields the following compatibility conditions:

$$f_0^{(1)\,0} = 0, \quad f_0^{(1)\,3} = \frac{\beta}{g}\,\mathrm{Im} f_1^{(0)\,2}, \tag{5.46}$$

$$f_0^{(2)\,0} = 0, \tag{5.47}$$

$$f_0^{(2)\,3} = \frac{\beta}{g}\,\mathrm{Im} f_1^{(1)\,2} + \frac{\beta^2}{4g^2}\,(f_0^{(0)\,3} - \mathrm{Re} f_2^{(0)\,3}) - \frac{\beta\gamma}{g^2}\,\mathrm{Im}\left(f_1^{(0)\,2} - \frac{f_2^{(0)\,2}}{2}\right),$$

etc.

To solve (5.43) for $f^{(0)} \equiv \varphi$, we first note that

$$-\tau\,\Theta\varphi = \sum_{j=-\infty}^{\infty} i\vartheta_j \varphi_j e^{ijkl}, \tag{5.48}$$

$$\vartheta_j \equiv \frac{\tau e j l}{\hbar}\,\langle F\rangle_j. \tag{5.49}$$

Then (5.43), (5.27) and (5.34) yield

$$\varphi_j^0 = \frac{\phi_j^+ + \phi_j^-}{2}\,\frac{1 - i\vartheta_j}{1 + \vartheta_j^2}, \quad \varphi_j^1 = \varphi_j^2 = 0, \quad \varphi_j^3 = \frac{\phi_j^+ - \phi_j^-}{2}\,\frac{1 - i\vartheta_j}{1 + \vartheta_j^2}, \tag{5.50}$$

where we have used that the Fourier coefficients

$$\phi_j^{\pm} = \frac{l}{\pi}\int_0^{\pi/l} \cos(jkl)\,\phi^{\pm}\,dk, \tag{5.51}$$

are real because $\phi^{\pm}$ are even functions of k. Similarly, the solution of (5.44) is $f^{(1)} \equiv \psi$ with

$$\begin{aligned}
\psi_j^m &= r_j^m\,\frac{1 - i\vartheta_j}{1 + \vartheta_j^2} \quad (m = 0, 3),\\
\psi_j^1 &= \frac{(1 + i\vartheta_j)\,r_j^1 + \delta_1\,r_j^2}{(1 + i\vartheta_j)^2 + \delta_1^2},\\
\psi_j^2 &= \frac{(1 + i\vartheta_j)\,r_j^2 - \delta_1\,r_j^1}{(1 + i\vartheta_j)^2 + \delta_1^2}.
\end{aligned} \tag{5.52}$$

Here r is the right hand side of (5.44). The balance equations can be found in two ways. We can calculate $A_m^{\pm}$ for $m = 0, 1$ by using the compatibility

conditions (5.46) and (5.47) in Equations (5.44) and (5.45), respectively. More simply, we can insert the solutions (5.50) and (5.52) in the balance equations (5.30) and in the Ampère's law (5.32). The result is:

$$\frac{\partial n^{\pm}}{\partial t} + \Delta^{-} D_{\pm}(n^{+}, n^{-}, F) = \pm R(n^{+}, n^{-}, F), \tag{5.53}$$

$$\varepsilon \frac{\partial F}{\partial t} + \frac{e}{\hbar} \left\langle \left[\alpha \left(\phi_1^{+} + \phi_1^{-}\right) + \gamma \left(\phi_1^{+} - \phi_1^{-}\right)\right] \frac{\vartheta_1}{1+\vartheta_1^2} \right\rangle_1 \tag{5.54}$$
$$+ \frac{2e}{\hbar} \left[\beta \mathrm{Re}\langle\psi_1^2\rangle_1 - \alpha\, \mathrm{Im}\langle\psi_1^0\rangle_1 - \gamma\, \mathrm{Im}\langle\psi_1^3\rangle_1\right] = J,$$

$$D_{\pm} = \frac{\alpha \pm \gamma}{\hbar} \left[\frac{\phi_1^{\pm}\vartheta_1}{1+\vartheta_1^2} - \mathrm{Im}(\psi_1^0 \pm \psi_1^3)\right] + \frac{\beta}{\hbar}\, \mathrm{Re}\psi_1^2 \pm \frac{\beta^2 \vartheta_2}{4g\hbar} \frac{\phi_2^{+} + \phi_2^{-}}{1+\vartheta_2^2}, \tag{5.55}$$

$$R = -\frac{\delta_2 n^{+}}{\tau} - \frac{\beta^2 \vartheta_2^2 (\phi_2^{+} - \phi_2^{-})}{8g^2\tau(1+\vartheta_2^2)} + \frac{\beta}{g\tau}\, \vartheta_1 \mathrm{Re}\psi_1^2 + \frac{\beta}{\hbar}\,(2 - \Delta^{+})\mathrm{Im}\psi_1^1. \tag{5.56}$$

Appendix C justifies this second and more direct method by showing that equivalent expressions are obtained from the compatibility conditions. Note that Eq. (5.54) can be obtained from (5.53) and the Poisson equation.

5.5 Spintronics: Quantum drift-diffusion equations for a lateral superlattice with Rashba spin-orbit interaction

In the simpler case of a LSL with the precession term of Rashba spin-orbit interaction (but no intersubband coupling), we can obtain explicit rate equations for $n^{\pm}$ by means of the Chapman-Enskog method. In the Hamiltonian (5.6), we have $\gamma = g = 0$, so that $h_3 = 0$ and $\vec{\nu} = (0, 1, 0)$. However, the Fermi-Dirac distribution is different from (5.2) for a LSL. We have to replace E_n instead of $\hbar^2 k_z^2/(2m^*)$, sum over n for all populated QW energy levels and integrate over k_y only. Provided only E_1 is populated, we obtain the following expression instead of (5.28):

$$\phi^{\pm}(k; n^{\pm}) = \int_{-\infty}^{\infty} \frac{D_\Gamma\left(E - \mathcal{E}^{\pm}(k) - E_1\right)}{1 + \exp\left(\frac{E-\mu^{\pm}}{k_B T}\right)}\, dE, \tag{5.57}$$

where the broadened density of states is

$$D_\Gamma(E) = \frac{1}{2\pi L_z} \int_{-\infty}^{\infty} dk_y \delta_\Gamma\left(\frac{\hbar^2 k_y^2}{2m^*} - E\right) = \frac{\sqrt{2m^*}}{2\pi\hbar L_z} \int_0^{\infty} dE_y\, \frac{\delta_\Gamma(E_y - E)}{\sqrt{E_y}}. \tag{5.58}$$

Note that (5.58) becomes the 1D density of states $D(E) = \sqrt{2m^*}\theta(E)/(2\pi\hbar L_z\sqrt{E})$ as $\Gamma \to 0+$. We have not included a factor 2 in (5.58) because all the electrons in each of the minibands (with energies $\mathcal{E}^{\pm}(k)$) have the same spin. Inserting (5.4) in (5.58) and using the residue theorem to evaluate the integral, we obtain

$$\begin{aligned} D_\Gamma(E) &= \frac{\sqrt{m^*}}{4\pi\hbar L_z} \qquad (5.59)\\ &\times \left[\frac{\sqrt{\sqrt{E^2+\sqrt{2}\Gamma E+\Gamma^2}+E+\frac{\Gamma}{\sqrt{2}}} - \sqrt{\sqrt{E^2+\sqrt{2}\Gamma E+\Gamma^2}-E-\frac{\Gamma}{\sqrt{2}}}}{\sqrt{E^2+\sqrt{2}\Gamma E+\Gamma^2}} \right.\\ &+ \left. \frac{\sqrt{\sqrt{E^2-\sqrt{2}\Gamma E+\Gamma^2}+E-\frac{\Gamma}{\sqrt{2}}} + \sqrt{\sqrt{E^2-\sqrt{2}\Gamma E+\Gamma^2}-E+\frac{\Gamma}{\sqrt{2}}}}{\sqrt{E^2-\sqrt{2}\Gamma E+\Gamma^2}} \right]. \end{aligned}$$

As $E \to +\infty$, $D_\Gamma(E) \sim \sqrt{2m^*}/(2\pi\hbar L_z\sqrt{E})$, whereas $D_\Gamma(E) = O(|E|^{-5/2})$ as $E \to -\infty$. Then the convolution integral (5.57) is convergent.

In the present case, minibands correspond to electrons with spin up or down which have different energy. Scattering between minibands is the same as in (5.26), $-(\vec{\nu}f^0 + \vec{f})/\tau_{\rm sc}$ which yields $\partial n^{\pm}/\partial t + \ldots = \mp n^{\pm}/\tau_{\rm sc}$ in (5.30), only if the chemical potential of the miniband with lowest energy, μ^-, is less than the minimum energy of the other miniband, $\mathcal{E}^+_{\rm min} = \min_k \mathcal{E}^+(k)$. Otherwise ($\mu^- > \mathcal{E}^+_{\rm min}$), the scattering term should be $-2\vec{f}/\tau_{\rm sc}$, which yields $\partial n^{\pm}/\partial t + \ldots = \mp(n^+ - n^-)/\tau_{\rm sc}$ in (5.30), thereby trying to equalize n^+ and n^-; cf. Ref. [69].

Now we shall derive the balance equations in the hyperbolic limit using the Chapman-Enskog method as in Section 5.4. In the scaled WPBGK equations (5.35), the operators $\mathbb{L}$ and Λ are

$$\begin{aligned} \mathbb{L}f &= f - \tau\,\Theta f, \qquad (5.60)\\ \Lambda f &= \delta_2 \begin{pmatrix} 0 \\ 2\vec{f} + (\vec{\nu}f^0 - \vec{f})\,\theta(\mathcal{E}^+_{\rm min} - \mu^-) \end{pmatrix} + \frac{\alpha\tau}{\hbar}\sin kl\,\Delta^- f \qquad (5.61)\\ &+ \frac{\beta\tau}{\hbar}\cos kl\,\Delta^- \begin{pmatrix} f^2 \\ 0 \\ f^0 \\ 0 \end{pmatrix} + \frac{\beta\tau}{\hbar}\sin kl\,\Delta^+ \begin{pmatrix} 0 \\ f^3 \\ 0 \\ -f^1 \end{pmatrix}, \end{aligned}$$

where δ_2 is given by (5.38), $\theta(x)$ is the Heaviside unit step function and $\Omega^0 = (\phi^+ + \phi^-)/2$, $\vec{\Omega} = (0,1,0)\,(\phi^+ - \phi^-)/2$. The hierarchy of equations

(5.43) - (5.45) is simply

$$\mathbb{L}f^{(0)} = \Omega, \tag{5.62}$$

$$\mathbb{L}f^{(1)} = -\,\tau\,\frac{\partial f^{(0)}}{\partial t}\bigg|_0 - \Lambda f^{(0)}, \tag{5.63}$$

$$\mathbb{L}f^{(2)} = -\,\tau\,\frac{\partial f^{(1)}}{\partial t}\bigg|_0 - \Lambda f^{(1)} - \tau\,\frac{\partial f^{(0)}}{\partial t}\bigg|_1, \tag{5.64}$$

and so on. The compatibility and solvability conditions are:

$$f_0^{(m)\,0} = f_0^{(m)\,2} = 0 \quad \Longrightarrow (\mathbb{L}f^{(m)\,0})_0 = (\mathbb{L}f^{(m)\,2})_0 = 0, \quad m \geq 1. \tag{5.65}$$

The solution $f^{(0)} \equiv \varphi$ of (5.62) is

$$\varphi_j^0 = \frac{\phi_j^+ + \phi_j^-}{2}\,\frac{1 - i\vartheta_j}{1 + \vartheta_j^2}, \quad \varphi_j^1 = \varphi_j^3 = 0, \quad \varphi_j^2 = \frac{\phi_j^+ - \phi_j^-}{2}\,\frac{1 - i\vartheta_j}{1 + \vartheta_j^2}, \tag{5.66}$$

where we have used that the Fourier coefficients $\phi_j^\pm$ are real because $\phi^\pm$ are even functions of k. Similarly, the solution of (5.63) is $f^{(1)} \equiv \psi$ with

$$\psi_j^m = r_j^m\,\frac{1 - i\vartheta_j}{1 + \vartheta_j^2} \quad (m = 0, 2), \quad \psi_j^1 = \psi_j^3 = 0. \tag{5.67}$$

Here r is the right hand side of (5.63). The balance equations can be found in two ways. We can calculate $A_m^\pm$ for $m = 0, 1$ by using the solvability conditions (5.65) in Equations (5.63) and (5.64), respectively. More simply, we can insert the solutions (5.66) and (5.67) in the balance equations (5.30) and in the Ampère's law (5.32). In both cases, the result is:

$$\frac{\partial n^\pm}{\partial t} + \Delta^- D_\pm(n^+, n^-, F) = \mp R(n^+, n^-, F), \tag{5.68}$$

$$\varepsilon\,\frac{\partial F}{\partial t} + e\,\langle D_+ + D_- \rangle_1 = J, \tag{5.69}$$

$$D_\pm = -\frac{\alpha}{\hbar}\,\Delta^- \mathrm{Im}(\varphi_1^0 \pm \varphi_1^2 + \psi_1^0 \pm \psi_1^2) \pm \frac{\beta}{\hbar}\,\Delta^- \mathrm{Re}(\varphi_1^0 \pm \varphi_1^2 + \psi_1^0 \pm \psi_1^2), \tag{5.70}$$

$$R = \frac{n^+ - n^-\,\theta(\mu^- - \mathcal{E}_{\min}^+)}{\tau_{sc}}. \tag{5.71}$$

A straightforward calculation of (5.70) yields

$$
\begin{aligned}
D_{\pm} = & \frac{(\alpha\vartheta_1 \pm \beta)\phi_1^{\pm}}{\hbar\,(1+\vartheta_1^2)} \mp \frac{\tau\,(\phi_1^{+}-\phi_1^{-})\,[2\alpha\vartheta_1 \pm \beta(1-\vartheta_1^2)]}{2\hbar\tau_{\rm sc}(1+\vartheta_1^2)^2} \\
& + \frac{[2\alpha\vartheta_1 \pm \beta(1-\vartheta_1^2)]\tau}{\hbar(1+\vartheta_1^2)^2}\frac{\partial\phi_1^{\pm}}{\partial n^{\pm}}\left[\Delta^{-}\left(\frac{\alpha\vartheta_1 \pm \beta}{\hbar\,(1+\vartheta_1^2)}\phi_1^{\pm}\right) \pm \frac{(n^{+}-n^{-})}{\tau_{sc}}\right] \\
& + \frac{\alpha\,(3\vartheta_1^2-1) \pm \beta\vartheta_1(3-\vartheta_1^2)}{(1+\vartheta_1^2)^3}\,\frac{el\tau^2\phi_1^{\pm}}{\hbar^2\varepsilon}\left(J - \left\langle\left\langle\frac{e\alpha\,(\phi_1^{+}+\phi_1^{-})\vartheta_1}{\hbar(1+\vartheta_1^2)}\right\rangle_1\right\rangle_1\right. \\
& \left. - \left\langle\left\langle\frac{e\beta\,(\phi_1^{+}-\phi_1^{-})}{\hbar(1+\vartheta_1^2)}\right\rangle_1\right\rangle_1\right) - \frac{(\alpha^2+\beta^2)\tau}{2\hbar^2(1+\vartheta_1^2)}\,\Delta^{-}n^{\pm} \\
& + \frac{\tau}{2\hbar^2(1+\vartheta_1^2)}\left[(\alpha^2-\beta^2 \mp 2\alpha\beta\vartheta_1)\,\Delta^{-}\left(\frac{\phi_2^{\pm}}{1+\vartheta_2^2}\right)\right. \\
& \left. + [(\beta^2-\alpha^2)\vartheta_1 \mp 2\alpha\beta]\,\Delta^{-}\left(\frac{\vartheta_2\phi_2^{\pm}}{1+\vartheta_2^2}\right)\right].
\end{aligned}
\tag{5.72}
$$

We have numerically solved (see Appendix F for details of the numerical method) the system of equations (5.68) - (5.72), with the following boundary conditions in the interval $-2l \le x \le 0$:

$$
\varepsilon\frac{\partial F}{\partial t} + \sigma F = J, \tag{5.73}
$$

$$
n^{+} = n^{-} = \frac{N_D}{2}, \tag{5.74}
$$

whereas in the collector $Nl \le x \le Nl + 2l$:

$$
\frac{\partial F}{\partial x} = \frac{\partial n^{\pm}}{\partial x} = 0 \tag{5.75}
$$

hold. We have used the following values of the parameters: $\alpha = \Delta_1/2 = 8$ meV, $\beta = 2.63$ meV, $d_W = 3.1$ nm, $d_B = 1.96$ nm, $l = d_W + d_B = 5.06$ nm, $L_z = 3.1$ nm, $T = 5$ K, $\tau = 5.56 \times 10^{-14}$ s, $\tau_{\rm sc} = 5.56 \times 10^{-13}$ s, $N_D = 4.048 \times 10^{10}$ cm^{-2}, $m^* = (0.067 d_W + 0.15 d_B)m_0/l$, $V = 3$ V, $N = 110$. We have used a large conductivity of the injecting contact $\sigma = 11.78\,\Omega^{-1}\mathrm{m}^{-1}$. With these values, we select the following units to present our results graphically: $F_M = \hbar/(el\tau) = 23.417$ kV/cm, $x_0 = \varepsilon F_M l/(eN_D) = 19.4$ nm, $t_0 = \hbar/\alpha = 0.082$ ps, $J_0 = \alpha e N_D/(2\hbar) = 3.94 \times 10^4$ A/cm^2. Figure 5.2(b)-(d) illustrates the resulting stable self-sustained current oscillations. They are due to the periodic formation of a pulse of the electric field at the cathode $x = 0$ and its motion through the LSL. Figure 5.2(b) depicts the pulse when it is far from the contacts, and the corresponding spin polarization is shown

in Figure 5.2(d). It is interesting to consider the influence of the broadening Γ and the Boltzmann statistics on the oscillations. At high temperatures, Boltzmann statistics and a semiclassical approximation should provide a good description. The semiclassical approximation is equivalent to dropping all spatial averages in our previous formulas. Since $x_0 \gg l$, the effect of dropping spatial averages should be rather small. Using Boltzmann statistics yields explicit formulas for $\mu^{\pm}$ in terms of $n^{\pm}$. In fact, we only have to replace $e^{(\mu^{\pm}-E)/(k_BT)}$ instead of the 3D Fermi distribution $[1+e^{(E-\mu^{\pm})/(k_BT)}]^{-1}$ in Eq. (5.57). Using the relation (5.29) between $n^{\pm}$ and $\phi^{\pm}$, we obtain

$$\phi^{\pm} = n^{\pm} \frac{\pi \, \exp\left(\frac{\alpha \, \cos kl \mp \beta \, |\sin kl|}{k_BT}\right)}{\int_0^{\pi} dK \, \exp\left(\frac{\alpha \, \cos K \mp \beta \, \sin K}{k_BT}\right)}, \tag{5.76}$$

and therefore,

$$\phi_j^{\pm} = n^{\pm} \frac{\int_0^{\pi} dK \, \cos(jK) \, \exp\left(\frac{\alpha \cos K \mp \beta \, \sin K}{k_BT}\right)}{\int_0^{\pi} dK \, \exp\left(\frac{\alpha \cos K \mp \beta \, \sin K}{k_BT}\right)}, \tag{5.77}$$

for $j = 0, 1, \ldots$ Similar relations hold for the case of a SL with Boltzmann statistics in the tight-binding approximation.

The results are shown in Fig. 5.2. Fig. 5.2(a) depicts the relation between electron current and field for a spatially uniform stationary solution with $n^{\pm} = N_D/2$. We observe that all curves are similar. However the curves for $\Gamma = 0$ and $\Gamma = 1$ meV are close while the curve for $\Gamma = 5$ meV has dropped noticeably. The shapes of $J(t)$ for $\Gamma = 0$ and $\Gamma = 1$ meV are close and quite different from that for $\Gamma = 5$ meV. If we look at the corresponding field profiles, to $\Gamma = 0$ and $\Gamma = 1$ meV the oscillations of the current are caused by the periodic nucleation of a pulse of the electric field at x = 0 and its motion towards the end of the LSL. The pulse far from the contacts shown in Figure 5.2(c) is larger in the case of $\Gamma = 0$ than for $\Gamma = 1$ meV. In the case of $\Gamma = 5$ meV (not shown), the pulse created at $x = 0$ becomes attenuated and disappears before arriving at $x = Nl$. This seems to indicate that the lowest voltage at which there exist stable self-sustained current oscillations is an increasing function of Γ: If we fix the voltage at 3 V and increase Γ, the critical voltage threshold to have stable oscillations approaches our fixed voltage of 3 V. Then the observed oscillations are smaller and the field profiles correspond to waves that vanish before reaching the end of the device, as it also occurs in models of the Gunn effect in bulk semiconductors [15].

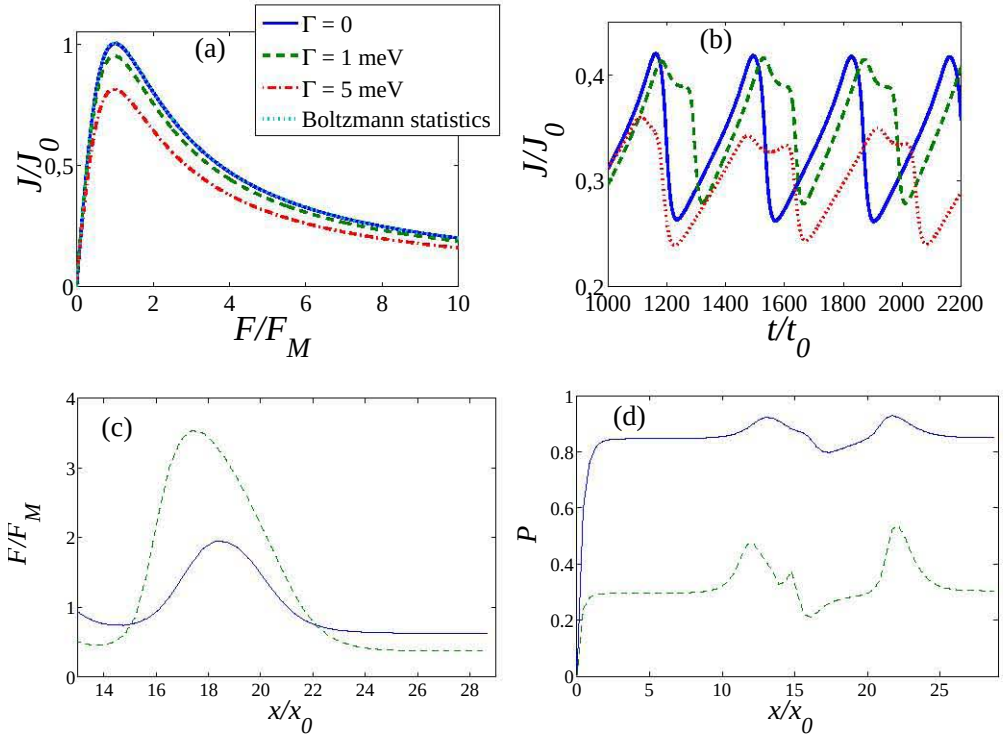

Figure 5.2: (a) Electron current ($J_0 = \alpha e N_D/2\hbar$) vs field in a spatially uniform stationary state for different values of the broadening Γ using the Fermi-Dirac distribution and for the Boltzmann distribution without broadening. The case of the Boltzmann distribution is very similar to the case with no energy broadening ($\Gamma = 0$). (b) Total current density vs time ($t_0 = \hbar/\alpha$), and the (c) electric field and (d) spin polarization profiles during current self-oscillations for $\Gamma = 0$ (solid line) and 1 meV (dashed line). Parameter values are $N = 110$, $N_D = 4.048 \times 10^{10}$ cm^{-2}, $d_B = 1.96$ nm, $L_z = d_W = 3.1$ nm, $l = 5.06$ nm, $\tau = 0.0556$ ps, $\tau_{\rm sc} = 0.556$ ps, $V = 3$ V, $\sigma = 11.78\ \Omega^{-1}$m^{-1}, $T = 5$ K, $\alpha = 8$ meV, $\beta = 2.63$ meV. With these values, $\Delta_1 = 16$ meV, $x_0 = 19.4$ nm, $t_0 = 0.082$ ps, $J_0 = 3.94 \times 10^4$ A/cm^2.

5.6 Conclusions

We have presented a Wigner-Poisson-BGK system of equations with a collision broadened local Fermi-Dirac distribution for strongly coupled SLs having only one populated miniband. In the hyperbolic limit in which the collision and Bloch frequencies are of the same order and dominate all other frequencies, the Chapman-Enskog perturbation method yields a quantum drift-diffusion equation for the field. Numerical solutions of this equation exhibit self-sustained oscillations of the current due to recycling and motion of charge dipole domains [13].

For strongly coupled SLs having two populated minibands, we have introduced a periodic version of the Kane Hamiltonian and derived the corresponding Wigner-Poisson-BGK system of equations. The collision model comprises two terms, a BGK term trying to bring the Wigner matrix closer to a broadened Fermi-Dirac local equilibrium at each miniband, and a scattering term that brings down electrons from the upper to the lower miniband. By using the Chapman-Enskog method, we have derived quantum drift-diffusion equations for the miniband populations which contain generation-recombination terms. As it should be, the recombination terms vanish if there is no inter-miniband scattering and the off-diagonal terms in the Hamiltonian are zero. These terms may represent a Rashba spin-orbit interaction for a lateral superlattice. For a lateral superlattice under dc voltage bias in the growth direction, numerical solutions of the corresponding quantum drift-diffusion equations show self-sustained current oscillations due to periodic recycling and motion of electric field pulses. The periodic changes of the spin polarization and spin polarized current indicate that this system acts as a spin oscillator.

Chapter 6

Two mini-band model for self-sustained oscillations of the current through resonant tunneling semiconductor superlattices

6.1 Introduction

In this chapter, we present a simplified model of a two-miniband SL using a field dependent coupling between minibands similar to that introduced for resonant tunneling diodes [63]. We consider the corresponding WP system with BGK collision terms that include collision broadening and decay between minibands due to scattering. Electron-electron scattering is treated in the Hartree approximation through the Poisson equation. We are interested in the *hyperbolic* limit in which electric field effects, including field-dependent inter-miniband transitions, are as strong as the BGK collision terms and dominate electron transport. By using the Chapman-Enskog perturbation method, we derive nonlocal balance equations for the electron population of the minibands and the electric field that inherit the nonlocality of the quantum Wigner equation. Numerical solutions of these nonlocal equations allow us to reconstruct the time-resolved Wigner matrix and they exhibit resonant tunneling between minibands and SSOC. During SSCO, we show that the miniband with higher-energy is practically empty except when the local electric field is sufficiently large to allow resonant tunneling from the miniband

with lowest energy. Our calculations provide a first-principles description of SSCO in a resonant tunneling SL under dc voltage bias.

The rest of the chapter is organized as follows. Section 6.2 contains the Hamiltonian we use as the basis of our kinetic theory. The governing WP-BGK equations for the Wigner functions are introduced in Section 6.3. The derivation of nonlocal balance equations by the Chapman-Enskog method is given in Section 6.4. Section 6.5 presents numerical results obtained by solving the nonlocal balance equations with appropriate boundary conditions for the contact regions and dc voltage bias. In particular, these solutions include SSCO. Finally Section 6.7 contains our conclusions.

6.2 Model Hamiltonian

Let us assume that the total Hamiltonian describing our system is

$$\mathbf{H}_{\text{total}} = \mathbf{H} + \mathbf{H}_{\text{sc}}, \tag{6.1}$$

where $\mathbf{H}_{\text{sc}}$ represents scattering and $\mathbf{H}(x, -i\partial/\partial x)$ is a 2×2 Hamiltonian $\mathbf{H}$ corresponding to a SL with two minibands of widths Δ_1 and Δ_2, gap energy $2g$ and SL period l,

$$\begin{aligned}\mathbf{H}(x,k) &= \begin{pmatrix} -\frac{\Delta_2}{2}(1-\cos kl) - eW(x) + g & eFl\delta \\ eFl\delta & \frac{\Delta_1}{2}(1-\cos kl) - eW(x) - g \end{pmatrix}, \\ &\equiv [h_0(k) - eW(x)]\boldsymbol{\sigma}_0 + \vec{h}(k)\cdot\vec{\boldsymbol{\sigma}} + eFl\delta\,\boldsymbol{\sigma}_{\mathbf{1}}, \end{aligned} \tag{6.2}$$

Here we have considered tight-binding dispersion relations for the minibands and $-e < 0$, W and $-F = -\partial W/\partial x$ are the electron charge, the electric potential, and the electric field, respectively. The electric potential W in $\mathbf{H}$ describes electron-electron interaction in a self-consistent Hartree approximation.

The matrix Hamiltonian $\mathbf{H}$ can be written as a linear combination of the Pauli matrices

$$\boldsymbol{\sigma}_0 = \begin{pmatrix} 1 & 0 \\ 0 & 1 \end{pmatrix}, \boldsymbol{\sigma}_1 = \begin{pmatrix} 0 & 1 \\ 1 & 0 \end{pmatrix}, \boldsymbol{\sigma}_2 = \begin{pmatrix} 0 & -i \\ i & 0 \end{pmatrix}, \boldsymbol{\sigma}_3 = \begin{pmatrix} 1 & 0 \\ 0 & -1 \end{pmatrix},$$

with coefficients:

$$\begin{aligned} h_0(k) &= -\alpha\,(1-\cos kl), & h_1(k) &= 0, \\ h_2(k) &= 0, & h_3(k) &= -\gamma\,(1-\cos kl) + g, \\ \alpha &= \tfrac{\Delta_2 - \Delta_1}{4}, & \gamma &= \tfrac{\Delta_2 + \Delta_1}{4}. \end{aligned} \tag{6.3}$$

The term $eFl\delta\,\boldsymbol{\sigma}_1$ in (6.2) is a field-dependent tunneling term derived by means of the k-p theory for the evolution of the Wannier envelope functions [cf. Equations (33) of Ref. [63] without second order terms, i.e. with $M_{nn'} = 0$]. The dimensionless parameter δ is a phenomenological parameter proportional to the interminiband momentum matrix element:

$$\delta = \frac{\hbar P}{2m^* gl}, \quad P = \frac{\hbar}{l}\int_{-l/2}^{l/2} u_2^* \frac{\partial u_1}{\partial x} dx, \tag{6.4}$$

where $u_{1,2}$ are the periodic parts of the miniband Bloch functions. A related model has been used to describe coherent transport in a resonant interband tunnelling diode [61–63].

The miniband energies $\mathcal{E}^{\pm}(k)$ are the eigenvalues of the free Hamiltonian $\mathbf{H}_0(k) = h_0(k)\boldsymbol{\sigma}_0 + \vec{h}(k)\cdot\vec{\boldsymbol{\sigma}}$ (zero electric potential), given by

$$\mathcal{E}^{\pm}(k) = h_0(k) \pm h_3(k). \tag{6.5}$$

The corresponding spectral projections are

$$\mathbf{P}^{\pm} = \frac{\boldsymbol{\sigma}_0 \pm \boldsymbol{\sigma}_3}{2}, \tag{6.6}$$

so that we can write

$$\mathbf{H}_0(k) = \mathcal{E}^{+}(k)\mathbf{P}^{+} + \mathcal{E}^{-}(k)\mathbf{P}^{-}. \tag{6.7}$$

6.3 Wigner function description

If $\psi_a(x, y, z, t)$, $a = 1, 2$, are the second quantized wave function amplitudes expressed in the Bloch basis, the Wigner matrix is [10]

$$f_{ab}(x, k, t) = \frac{2l}{S}\sum_{j=-\infty}^{\infty}\int_{\mathbb{R}^2}\langle\psi_a^{\dagger}(x + jl/2, y, z, t)\psi_b(x - jl/2, y, z, t)\rangle e^{ijkl} d\mathbf{x}_{\perp}, \tag{6.8}$$

where S is the SL cross section. Note that the Wigner matrix is periodic in k with period $2\pi/l$. It is convenient to write the Wigner matrix $\mathbf{f}(x, k, t)$ in terms of the Pauli matrices:

$$\mathbf{f}(x, k, t) = \sum_{i=0}^{3} f^i(x, k, t)\boldsymbol{\sigma}_i = f^0(x, k, t)\boldsymbol{\sigma}_0 + \vec{f}(x, k, t)\cdot\vec{\boldsymbol{\sigma}}. \tag{6.9}$$

The Wigner components $f^i(x,k,t)$ are real and can be related to the coefficients of the Hermitian Wigner matrix by

$$\begin{array}{ll} f_{11} = f^0 + f^3, & f_{12} = f^1 - if^2, \\ f_{21} = f^1 + if^2, & f_{22} = f^0 - f^3. \end{array} \tag{6.10}$$

Hereinafter we shall use the equivalent notations

$$f = \begin{pmatrix} f^0 \\ \vec{f} \end{pmatrix} = \begin{pmatrix} f^0 \\ f^1 \\ f^2 \\ f^3 \end{pmatrix}. \tag{6.11}$$

The populations of the minibands with energies $\mathcal{E}^{\pm}$ are given by the moments:

$$n^{\pm}(x,t) = \frac{l}{2\pi} \int_{-\pi/l}^{\pi/l} \left[f^0(x,k,t) \pm f^3(x,k,t) \right] \, dk, \tag{6.12}$$

and the total electron density is $n^+ + n^-$.

After some algebra, from the time-dependent Schrödinger equations for wave functions ψ_a with the Hamiltonian $\mathbf{H}_{\rm tot}$ in (6.1), we can obtain the following Wigner-Poisson-Bhatnagar-Gross-Krook (WPBGK) equations for the Wigner components

$$\frac{\partial f^0}{\partial t} - \frac{\alpha}{\hbar} \sin kl \, \Delta^- f^0 - \frac{\gamma}{\hbar} \sin kl \, \Delta^- f^3 - \Theta_1 f^0 - \Theta_2 f^1 = Q^0[f], \tag{6.13}$$

$$\frac{\partial \vec{f}}{\partial t} - \frac{\alpha}{\hbar} \sin kl \, \Delta^- \vec{f} - \frac{\gamma}{\hbar} \sin kl \, \Delta^- f^0 \, \vec{\nu} + \vec{\omega} \times \vec{f} - \vec{\Theta}[f] = \vec{Q}[f], \tag{6.14}$$

whose right hand sides contain collision terms $Q[f]$ arising from $\mathbf{H}_{\rm sc}$. These terms will be modeled phenomenologically and described later. Electron-electron collisions are treated in the Hartree approximation and described by the Poisson equation for the electrostatic potential:

$$\varepsilon \frac{\partial^2 W}{\partial x^2} = \frac{e}{l} (n^+ + n^- - N_D), \tag{6.15}$$

where ε and N_D are the SL permittivity and the 2D doping density, respec-

tively. In (6.13) - (6.14),

$$\vec{\omega} = \frac{2(g-\gamma) + \gamma \cos kl\, \Delta^+}{\hbar}\, \vec{\nu}, \quad \vec{\nu} = (0,0,1), \tag{6.16}$$

$$\Theta_1 f^m(x,k,t) = \frac{el}{i\hbar} \sum_{j=-\infty}^{\infty} j \langle F(x,t) \rangle_j e^{ijkl} f_j^m(x,t), \tag{6.17}$$

$$\Theta_2 f^m(x,k,t) = -\frac{el\delta}{i\hbar} \sum_{j=-\infty}^{\infty} e^{ijkl} f_j^m(x,t)\, \Delta_j^- F(x,t), \tag{6.18}$$

$$\Theta_3 f^m(x,k,t) = \frac{el\delta}{i\hbar} \sum_{j=-\infty}^{\infty} e^{ijkl} f_j^m(x,t)\, \Delta_j^+ F(x,t), \tag{6.19}$$

$$\vec{\Theta}[f] = \Theta_1\, \vec{f} + \begin{pmatrix} \Theta_2\, f^0 \\ \Theta_3\, f^3 \\ -\Theta_3\, f^2 \end{pmatrix}. \tag{6.20}$$

We have defined the operators

$$(\Delta_j^{\pm} u)(x,k) = u\left(x + \frac{jl}{2}, k\right) \pm u\left(x - \frac{jl}{2}, k\right) \tag{6.21}$$

(the subscript is omitted for $j = 1$) and the spatial averages:

$$\langle F(x,t) \rangle_j \equiv \frac{1}{jl} \int_{-jl/2}^{jl/2} F(x+s,t)\, ds \tag{6.22}$$

$$= \left\langle \frac{\partial W}{\partial x}(x,t) \right\rangle_j = \frac{\partial}{\partial x} \langle W(x,t) \rangle_j = \frac{\Delta_j^- W(x,t)}{jl}. \tag{6.23}$$

Our collision model is similar to that used in Ref. [10] and it contains two terms: a BGK term which tries to send the miniband Wigner function to its local equilibrium and a scattering term that sends electrons from the miniband with higher energy (whose electron density is n^+) to the miniband

with lower energy (whose electron density is n^-):

$$Q^0[f] = -\frac{f^0 - \Omega^0}{\tau}, \tag{6.24}$$

$$\vec{Q}[f] = -\frac{\vec{f} - \vec{\Omega}}{\tau} - \frac{\vec{\nu} f^0 + \vec{f}}{\tau_{\rm sc}}, \tag{6.25}$$

$$\Omega^0 = \frac{\phi^+ + \phi^-}{2}, \quad \vec{\Omega} = \frac{\phi^+ - \phi^-}{2}\,\vec{\nu}, \tag{6.26}$$

$$\phi^{\pm}(k; n^{\pm}) = \frac{m^* k_B T}{\pi\hbar^2} \int_{-\infty}^{\infty} \frac{\sqrt{2}\,\Gamma^3/\pi}{\Gamma^4 + [E - \mathcal{E}^{\pm}(k)]^4} \ln\left(1 + e^{\frac{\mu^{\pm} - E}{k_B T}}\right) dE, \tag{6.27}$$

$$n^{\pm} = \frac{l}{2\pi} \int_{-\pi/l}^{\pi/l} \phi^{\pm}(k; n^{\pm})\, dk. \tag{6.28}$$

The chemical potentials of the minibands, μ^+ and μ^- are calculated in terms of n^+ and n^- respectively, by inserting (6.27) in (6.28) and solving the resulting equations. The local equilibria $\phi^{\pm}$ are the integrals of collision-broadened 3D Fermi-Dirac distributions over the lateral components of the wave vector on the plane perpendicular to the growth direction x. [10] As the broadening energy $\Gamma \to 0$, the line-width function in the integrand of (6.27) becomes $\delta(E - \mathcal{E}^{\pm}(k))$.

Our collision model should enforce charge continuity. To check this, we first calculate the time derivative of $n^{\pm}$ using (6.12) to (6.14):

$$\frac{\partial n^{\pm}}{\partial t} - \frac{\alpha l \Delta^-}{2\pi\hbar} \int_{-\pi/l}^{\pi/l} \sin kl\,(f^0 \pm f^3)\, dk - \frac{\gamma l \Delta^-}{2\pi\hbar} \int_{-\pi/l}^{\pi/l} \sin kl (f^3 \pm f^0)\, dk$$
$$\pm \frac{l}{2\pi} \int_{-\pi/l}^{\pi/l} \Theta_3 f^2\, dk = \frac{l}{2\pi} \int_{-\pi/l}^{\pi/l} (Q^0[f] \pm Q^3[f])\, dk = \mp \frac{n^+}{\tau_{\rm sc}}, \tag{6.29}$$

where we have employed $\int \Theta_1 f^0 dk = \int \Theta_2 f^1 dk = 0$. Then we obtain:

$$\frac{\partial}{\partial t}(n^+ + n^-) - \Delta^- \left[\frac{l}{\pi\hbar} \int_{-\pi/l}^{\pi/l} \sin kl \left(\alpha f^0 + \gamma f^3\right) dk\right] = 0. \tag{6.30}$$

Noting that $\Delta^- u(x) = l\,\partial\langle u(x)\rangle_1/\partial x$, we see that (6.30) *is the charge continuity equation.* Differentiating in time the Poisson equation (6.15), using (6.30) in the result and integrating with respect to x, we get the following nonlocal Ampère's law for the balance of current:

$$\varepsilon \frac{\partial F}{\partial t} - \left\langle \frac{el}{\pi\hbar} \int_{-\pi/l}^{\pi/l} \sin kl \left(\alpha f^0 + \gamma f^3\right) dk \right\rangle_1 = J(t). \tag{6.31}$$

Here the space independent function $J(t)$ is the total current density. Since the Wigner components are real, we can rewrite (6.31) in the following equivalent form:

$$\varepsilon\frac{\partial F}{\partial t}+\frac{2e}{\hbar}\left\langle\alpha\,\mathrm{Im}f_1^0+\gamma\,\mathrm{Im}f_1^3\right\rangle_1=J(t). \tag{6.32}$$

We are using the notation f_j^m for the Fourier coefficients of f^m:

$$f^m(x,k,t)=\sum_{j=-\infty}^{\infty}f_j^m(x,t)\,e^{ijkl}. \tag{6.33}$$

6.4 The Chapman-Enskog method and balance equations

In this Section, we shall derive the reduced balance equations for our two-miniband SL using the Chapman-Enskog method. Note that if we were to know the Wigner matrix as a function of $n^{\pm}$ and the electric field, Equations (6.29) and the Poisson equation (6.15) would be the sought balance equations and could be solved directly. As they are now, Equations (6.29) are not closed. However, in a limit in which collisions and electric potential terms dominate all others in the Wigner equations, it is possible to use perturbation theory to close (6.29). The idea is that in this so-called *hyperbolic limit*, the Wigner matrix is very close to a local equilibrium (modified by the electric field) which depends on $n^{\pm}$ and F. Using two terms in a Chapman-Enskog expansion, we show below that Equations (6.29) can be closed.

First of all, we should decide the order of magnitude of the terms in the WPBGK equations (6.13) and (6.14) in the hyperbolic limit. In this limit, the collision frequency $1/\tau$ and the Bloch frequency $eF_Ml/\hbar$ are of the same order, say about 10 THz. Then $F_M=O(\hbar/(el\tau))$. Typically, $2g/\hbar$ is of the same order, so that the term containing $2g/\hbar$ in (6.14) should also balance the BGK collision term. The other terms are of order $\gamma l/(\hbar x_0)$, where x_0 is the characteristic length over which the field varies, and they are much smaller, so that $\lambda=\gamma\tau l/(\hbar x_0)\ll 1$. From the Poisson equation, we obtain $x_0/l=\varepsilon F_M/(eN_D)=\varepsilon\hbar/(e^2\tau l N_D)$, and therefore the small dimensionless parameter is

$$\lambda=\frac{e^2\tau^2\gamma l N_D}{\varepsilon\hbar^2}. \tag{6.34}$$

The scattering time τ_{sc} is much longer than the collision time τ, and we shall consider $\tau/\tau_{\mathrm{sc}}=O(\lambda)\ll 1$. Equations (6.13) and (6.14) can be written as

the scaled WPBGK equations as follows:

$$\mathbb{L}f - \Omega = -\lambda \left(\tau \frac{\partial f}{\partial t} + \Lambda f \right). \tag{6.35}$$

where we have inserted the book-keeping parameter λ which is set equal to 1 at the end of our calculations. [10, 12] This trick saves us from rewriting our equations in nondimensional units. Here the operators $\mathbb{L}$ and Λ are defined by

$$\mathbb{L}f = f - \tau\,\Theta_1 f - \tau\,\Theta_2 \begin{pmatrix} f^1 \\ f^0 \\ 0 \\ 0 \end{pmatrix} - \tau\,\Theta_3 \begin{pmatrix} 0 \\ 0 \\ f^3 \\ -f^2 \end{pmatrix} + \eta_1 \begin{pmatrix} 0 \\ -f^2 \\ f^1 \\ 0 \end{pmatrix}, \tag{6.36}$$

$$\Lambda f = \eta_2 \begin{pmatrix} 0 \\ \vec{f} + \vec{\nu} f^0 \end{pmatrix} - \frac{\tau}{\hbar} \sin kl\,\Delta^- \left[\alpha f + \gamma \begin{pmatrix} f^3 \\ \vec{\nu} f^0 \end{pmatrix} \right] + \frac{\gamma\tau}{\hbar} (\cos kl\,\Delta^+ - 2) \begin{pmatrix} 0 \\ \vec{\nu} \times \vec{f} \end{pmatrix},$$

where

$$\eta_1 = \frac{2g\tau}{\hbar}, \quad \eta_2 = \frac{\tau}{\tau_{\rm sc}}. \tag{6.37}$$

To derive the reduced balance equations, we use the following Chapman-Enskog ansatz:

$$f(x, k, t; \epsilon) = f^{(0)}(k; n^+, n^-, F) + \sum_{m=1}^{\infty} f^{(m)}(k; n^+, n^-, F)\,\lambda^m, \tag{6.38}$$

$$\varepsilon \frac{\partial F}{\partial t} + \sum_{m=0}^{\infty} J_m(n^+, n^-, F)\,\lambda^m = J(t), \tag{6.39}$$

$$\frac{\partial n^\pm}{\partial t} = \sum_{m=0}^{\infty} A_m^\pm(n^+, n^-, F)\,\lambda^m. \tag{6.40}$$

The functions $A_m^\pm$ and J_m are related through the Poisson equation (6.15), so that

$$A_m^+ + A_m^- = -\frac{l}{e} \frac{\partial J_m}{\partial x}. \tag{6.41}$$

Inserting (6.38) to (6.40) into (6.35), we get

$$\mathbb{L}f^{(0)} = \Omega, \tag{6.42}$$

$$\mathbb{L}f^{(1)} = -\tau \left. \frac{\partial f^{(0)}}{\partial t} \right|_0 - \Lambda f^{(0)}, \tag{6.43}$$

$$\mathbb{L}f^{(2)} = -\tau \left. \frac{\partial f^{(1)}}{\partial t} \right|_0 - \Lambda f^{(1)} - \tau \left. \frac{\partial f^{(0)}}{\partial t} \right|_1, \tag{6.44}$$

and so on. The subscripts 0 and 1 in the right hand side of these equations mean that we replace $\varepsilon\,\partial F/\partial t|_m = J\delta_{0m} - J_m$, $\partial n^{\pm}/\partial t|_m = A_m^{\pm}$, provided $\delta_{00} = 1$ and $\delta_{0m} = 0$ if $m \neq 0$. Moreover, inserting (6.38) into (6.12) yields the following compatibility conditions:

$$f_0^{(1)\,0} = f_0^{(1)\,3} = 0, \tag{6.45}$$

$$f_0^{(2)\,0} = f_0^{(2)\,3} = 0, \tag{6.46}$$

etc.

To solve (6.42) for $f^{(0)} \equiv \varphi$, we first note that

$$-\tau\,\Theta_1\varphi = i\sum_{j=-\infty}^{\infty} \vartheta_j \varphi_j e^{ijkl}, \tag{6.47}$$

$$-\tau\,\Theta_2\varphi = -i\delta\sum_{j=-\infty}^{\infty} \varphi_j e^{ijkl}\Delta_j^-\mathcal{F}, \tag{6.48}$$

$$-\tau\,\Theta_3\varphi = -\delta\sum_{j=-\infty}^{\infty} \varphi_j e^{ijkl}\Delta_j^+\mathcal{F}, \tag{6.49}$$

$$\mathcal{F} \equiv \frac{\tau el}{\hbar}\,F, \quad \vartheta_j \equiv j\,\langle\mathcal{F}\rangle_j. \tag{6.50}$$

Then (6.42) and (6.26) yield

$$\varphi_j^0 = \frac{\phi_j^+ + \phi_j^-}{2}\,\left[\frac{1}{1+i\vartheta_j} - \eta_1\delta^2 Z_j\,M_j^+(\Delta_j^-\mathcal{F})^2\right] \tag{6.51}$$
$$+\; i\frac{\phi_j^+ - \phi_j^-}{2}\eta_1\delta^2 Z_j\,(\Delta_j^-\mathcal{F})\,(\Delta_j^+\mathcal{F}),$$

$$\varphi_j^1 = \frac{1}{2}\eta_1\delta(1+i\vartheta_j)\,Z_j\,\left[(\phi_j^+ + \phi_j^-)\,iM_j^+\Delta_j^-\mathcal{F} + (\phi_j^+ - \phi_j^-)\,\Delta_j^+\mathcal{F}\right], \tag{6.52}$$

$$\varphi_j^2 = -\frac{1}{2}\eta_1\delta(1+i\vartheta_j)\,Z_j\,\left[(\phi_j^+ + \phi_j^-)\,i\Delta_j^-\mathcal{F} - (\phi_j^+ - \phi_j^-)\,M_j^-\,\Delta_j^+\mathcal{F}\right], \tag{6.53}$$

$$\varphi_j^3 = \frac{\phi_j^+ - \phi_j^-}{2}\,\left[\frac{1}{1+i\vartheta_j} - \eta_1\delta^2 Z_j\,M_j^-(\Delta_j^+\mathcal{F})^2\right] \tag{6.54}$$
$$+\; i\frac{\phi_j^+ + \phi_j^-}{2}\eta_1\delta^2 Z_j\,(\Delta_j^-\mathcal{F})\,(\Delta_j^+\mathcal{F}).$$

Here we have used that the Fourier coefficients

$$\phi_j^{\pm} = \frac{l}{\pi}\int_0^{\pi/l} \cos(jkl)\,\phi^{\pm}\,dk, \tag{6.55}$$

are real because $\phi^{\pm}$ are even functions of k. The coefficients Z_j and $M_j^{\pm}$ are defined as

$$M_j^{\pm} \equiv \frac{1}{\eta_1}\left[1 + i\vartheta_j + \frac{\delta^2(\Delta_j^{\pm}\mathcal{F})^2}{1+i\vartheta_j}\right], \tag{6.56}$$

$$Z_j \equiv \frac{1}{\eta_1^2\,(1+i\vartheta_j)^2\,(1+M_j^+\,M_j^-)}. \tag{6.57}$$

The solution $f^{(0)} = \varphi$ given by (6.51)-(6.54) is essentially the local equilibrium Ω given by (6.26)-(6.28) modified by the field-dependent terms Θ_i that appear in the Wigner equations (6.13) and (6.14). This solution yields convective terms in the balance equations which contain first order differences. In the semiclassical limit, these equations become a hyperbolic system which may have discontinuous solutions (shock waves). Then it is convenient to regularize such solutions by keeping diffusion-like terms (second order differences) arising from the next-order Wigner functions $f^{(1)}$.

The solution of (6.43) is $f^{(1)} \equiv \psi$ with

$$\psi_j^0 = \frac{r_j^0}{1+i\vartheta_j}\left[1 - \frac{\delta^2 M_j^+(\Delta_j^-\mathcal{F})^2}{\eta_1(1+i\vartheta_j)(1+M_j^+M_j^-)}\right] \tag{6.58}$$
$$+\frac{i\delta\Delta_j^-\mathcal{F}}{\eta_1(1+i\vartheta_j)(1+M_j^+M_j^-)}\left[M_j^+ r_j^1 + r_j^2 + \frac{\delta\Delta_j^+\mathcal{F}}{1+i\vartheta_j}\,r_j^3\right],$$

$$\psi_j^1 = \frac{1}{\eta_1(1+M_j^+M_j^-)}\left[M_j^+ r_j^1 + \frac{i\delta M_j^+\,\Delta_j^-\mathcal{F}}{1+i\vartheta_j}\,r_j^0 + r_j^2 + \frac{\delta\,\Delta_j^+\mathcal{F}}{1+i\vartheta_j}\,r_j^3\right], \tag{6.59}$$

$$\psi_j^2 = \frac{1}{\eta_1(1+M_j^+M_j^-)}\left[M_j^-\,r_j^2 + \frac{\delta\,M_j^-\,\Delta_j^+\mathcal{F}}{1+i\vartheta_j}\,r_j^3 - r_j^1 - \frac{i\delta\,\Delta_j^-\mathcal{F}}{1+i\vartheta_j}\,r_j^0\right], \tag{6.60}$$

$$\psi_j^3 = \frac{r_j^3}{1+i\vartheta_j}\left[1 - \frac{\delta^2 M_j^-(\Delta_j^+\mathcal{F})^2}{\eta_1(1+i\vartheta_j)(1+M_j^+M_j^-)}\right] \tag{6.61}$$
$$-\frac{\delta\Delta_j^+\mathcal{F}}{\eta_1(1+i\vartheta_j)(1+M_j^+M_j^-)}\left[M_j^-\,r_j^2 - r_j^1 - \frac{i\delta\Delta_j^-\mathcal{F}}{1+i\vartheta_j}\,r_j^0\right].$$

Here r is the right hand side of (6.43).

The balance equations can be found in two ways. We can calculate $A_m^{\pm}$ for $m = 0, 1$ in (6.40) by using the solvability conditions (6.45) and (6.46) in (6.43) and (6.44), respectively. More simply, we can obtain the balance equations by inserting the solutions (6.51) to (6.54) and (6.58) to (6.61) in

the balance equations (6.29) and in the Ampère's law (6.31). The result is:

$$\frac{\partial n^{\pm}}{\partial t} + \Delta^{-} D_{\pm}(n^{+}, n^{-}, F) = \mp R(n^{+}, n^{-}, F), \tag{6.62}$$

$$\varepsilon \frac{\partial F}{\partial t} + e \left\langle D_{+}(n^{+}, n^{-}, F) + D_{-}(n^{+}, n^{-}, F) \right\rangle_{1} = J(t) \tag{6.63}$$

$$D_{\pm} = \frac{\alpha \pm \gamma}{\hbar} \operatorname{Im}(\varphi_1^0 \pm \varphi_1^3 + \psi_1^0 \pm \psi_1^3), \tag{6.64}$$

$$R = \frac{1}{\tau} \left[\eta_2 n^{+} + 2\delta \mathcal{F}(\varphi_0^2 + \psi_0^2) \right]. \tag{6.65}$$

Note that Eq. (6.63) can be obtained from (6.62) and the Poisson equation. Equations (6.62) to (6.65) must be solved together with the Poisson equation (6.15), the expression for the local equilibrium Wigner densities (6.27) and expressions (6.28) for $n^{\pm}$. The zeroth and first order Wigner functions φ_j and ψ_j in (6.64) and (6.65) can be obtained from Equations (6.51)-(6.54) and (6.58)- 6.61), respectively. The complete expressions for $D_{\pm}$ and R can be found in appendix D.

6.5 Numerical results

To solve numerically the system of equations (6.62) - (6.65), we have to add the voltage bias conditions for the electric potential and appropriate boundary conditions at the contact regions. The details of the numerical method used can be found in Appendix F. Note that our equations involve finite differences and several one-period integral averages. This means that we need to give boundary conditions over intervals of size $2l$ before $x = 0$ and after $x = Nl$, not just boundary conditions at $x = 0, Nl$ as we would give for semiclassical drift-diffusion equations. At the injecting region (cathode), the usual boundary condition is that the electron current density satisfies Ohm's law and therefore it is proportional to the electric field there. We use this condition for each point of the interval $-2l \leq x \leq 0$. Similarly, we also need the electron densities $n^{\pm}$ at the cathode. To avoid inconvenient boundary layer effects, we choose their values for a spatially uniform stationary state with a given value of the field. The resulting boundary conditions in $-2l \leq x \leq 0$ are: $W = 0$ and

$$\varepsilon \frac{\partial F}{\partial t} + \sigma_{cathode} F = J, \tag{6.66}$$

$$n^{\pm} = n^{\pm}_{st}, \tag{6.67}$$

where $n_{st}^{\pm}$ are the miniband electron densities corresponding to a spatially uniform stationary state. The latter can be obtained by equating to zero the right hand sides of the rate equation (6.62) and the Poisson equation (6.15): $R(n^+, n^-, F) = 0$ and $n^+ + n^- = N_D$, respectively. The result is

$$n_{st}^{\pm} = N_D \left(\frac{1}{2} \mp \frac{\eta_2(1 + \eta_1^2 + 4\delta^2 \mathcal{F}^2)}{8\delta^2 \mathcal{F}^2 + 2\eta_2(1 + \eta_1^2 + 4\delta^2 \mathcal{F}^2)} \right). \tag{6.68}$$

The boundary conditions in the anode region ($Nl \leq x \leq Nl + 2l$) are: $W = V$ and

$$\varepsilon \frac{\partial F}{\partial t} + \sigma_{anode} \left(\frac{n^+ + n^-}{N_D} \right) F = J, \tag{6.69}$$

$$n^+ = 0. \tag{6.70}$$

The lower miniband electron density n^- in the anode region is obtained from the Poisson equation (6.15).

To present numerical results, we have used the parameter values corresponding to a GaAs/AlAs SL from Table I of [49] which has narrow minibands so that resonant tunneling plays an important role in electron transport. Our parameter values are: $d_B = 1.5$ nm, $d_W = 9$ nm, $l = d_B + d_W = 10.5$ nm, $N_D = 2.5 \times 10^{10}$ cm^{-2}, $\tau = 0.0556$ ps, $\tau_{\rm sc} = 0.556$ ps, [72] $V = 9$ V, $N = 200$, $\sigma_{cathode} = 1.4\,\Omega^{-1}\mathrm{m}^{-1}$, $\sigma_{anode} = 0.7\,\Omega^{-1}\mathrm{m}^{-1}$, $T = 5$ K, $\Delta_1 = 2.6$ meV, $\Delta_2 = 13.2$ meV, [1] $P/\hbar = 0.2238$/nm, $\Gamma = 1$ meV. [10] With these values, $\alpha = 2.6$ meV, $\gamma = 3.9$ meV, $\delta = 0.12$. We have selected the following units to present our results graphically: $F_M = \hbar/(el\tau) = 11.28$ kV/cm, $x_0 = \varepsilon F_M l/(eN_D) = 31.4$ nm, $t_0 = \hbar/\alpha = 0.25$ ps, $J_0 = \alpha e N_D/\hbar = 1.58 \times 10^4$ A/cm^2.

Figure 6.1 (b) illustrates the resulting stable self-sustained current oscillations. They are due to the periodic formation of a pulse of the electric field at the cathode $x = 0$ and its motion through the SL. Figure 6.1 (a) depicts the electron current vs field in a spatially uniform stationary state, with a local maximum at the field resonant value $2g/(el)$. Figure 6.1 (c) depicts the electric field profile at different times during one self-sustained current cycle. Figure 6.1 (d) shows the tunneling transport between minibands when the electric field is above the resonant value (time (1)) calculated at the middle point of the SL ($x = Nl/2$).

Figure 6.2 shows the Wigner matrix elements f^i, from equations (6.51)-(6.54), (6.58)-(6.61) and (6.33), for the middle SL point ($x = Nl/2$) vs k

[1] For numerical estimates of $P/\hbar$, see also [77]

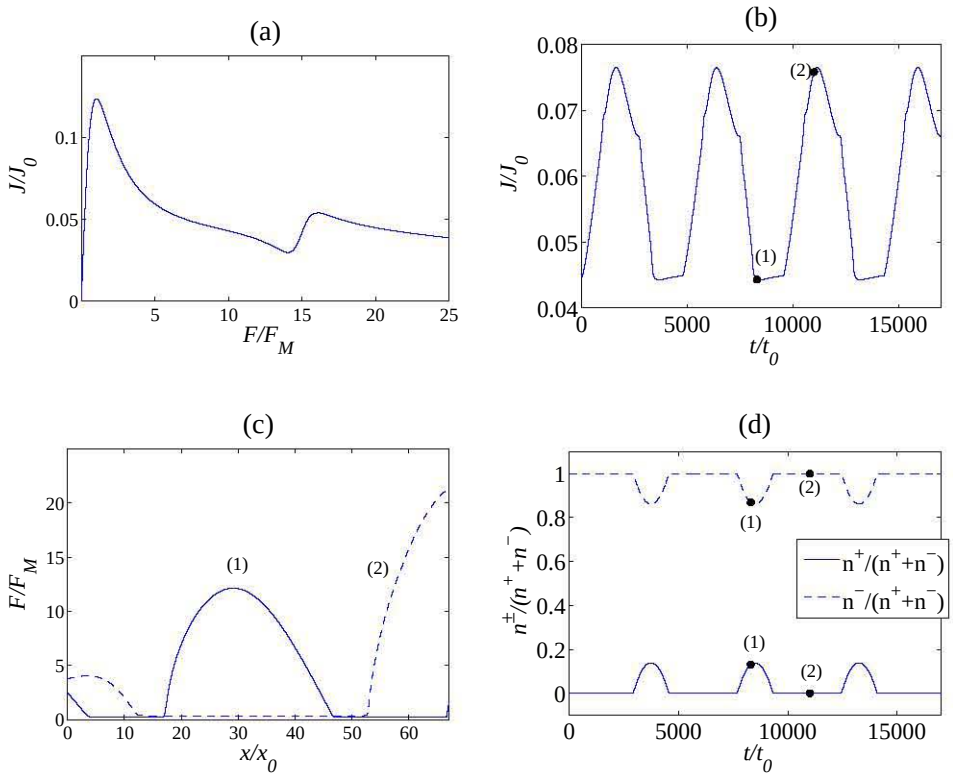

Figure 6.1: (a) Electron current vs field in a spatially uniform stationary state. (b) Total current density vs time. (c) Electric field profile at different times of one current self-oscillations cycle. At time (1) the field is above the resonant value for the middle SL point $x = Nl/2$. (d) Electron densities $n^{\pm}/(n^{+}+n^{-})$ vs time for point $x = Nl/2$. When the electric field is above the resonant value (time (1)), the electron transport between minibands occurs.

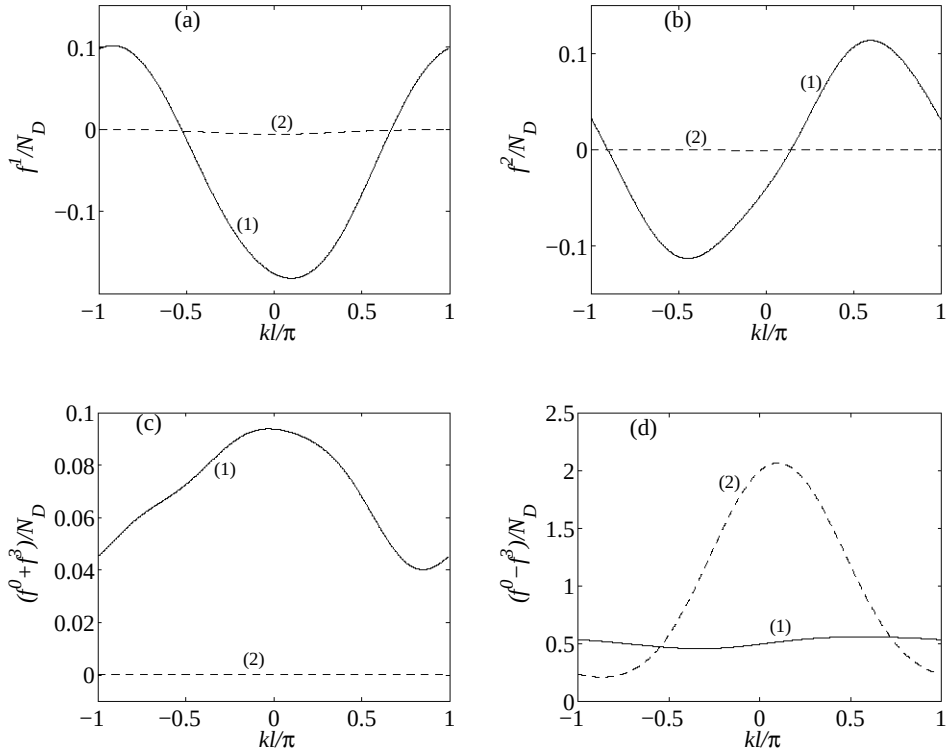

Figure 6.2: (a)-(b) Wigner matrix off-diagonal terms f^1 and f^2 vs k, at time (1) (tunneling transport), and time (2) (no tunneling). (c)-(d) Wigner matrix diagonal terms $f^0 \pm f^3$ vs k

at times (1) (with tunneling transport between minibands) and (2) (with no tunneling). Figure 6.2(a)-(b) illustrates the Wigner matrix off-diagonal terms f^1 and f^2, which are responsible for the tunneling transport between minibands. Figure 6.2(c)-(d) shows $f^0 \pm f^3$, which are related with the electron densities $n^{\pm}$. Figure 6.3 illustrates the effect of varying the voltage bias on the total current for a $N = 60$ period SL. Figure 6.3 (a) depicts the total current density average, maximum and minimum values for different voltages. It can be seen that when the bias is above a critical voltage, the current self sustained oscillations appear and their amplitude increases from zero at the bifurcation point. This circumstance does not depend on whether the voltage is increasing or decreasing, therefore the critical voltage corresponds to a supercritical Hopf bifurcation. Figure 6.3 (b) shows that the oscillation frequencies decrease as the voltage increases above its critical value. Immediately above the critical voltage, self-oscillations are due to repeated triggering of small pulses of the electric field that die near the cathode and before they can reach the end of the SL. As the voltage increases, the pulses are able to grow and reach the anode region. Since their average velocity does not vary that much, the oscillation frequency is correspondingly smaller. In a transition region between 1.5 and 3V, the current oscillation is somewhat irregular. The region of self-oscillations ends at a larger voltage of about 5.3V. Similar phenomena are observed in models of the Gunn effect in bulk GaAs. See Chapter 6 in Ref. [17].

If we use parameters corresponding to a weakly coupled SL with miniband widths below 1 meV (that come from using wider quantum barriers), we run into problems of numerical convergence and, possibly, breakdown of the Chapman-Enskog perturbation scheme. To explore the limit of weakly coupled SL, a different perturbation scheme based on miniband smallness seems necessary. This is outside the scope of the present work.

6.6 Derivation of the single miniband model equations

If we consider only the first miniband in the previous two miniband model, we can obtain the corresponding Wigner function equation. In this particular case we have: $\Delta_1 = \Delta$, $\Delta_2 = 0$, $g = 0$, $\alpha = -\Delta/4$, $\gamma = \Delta/4$, $\mathcal{E}^+(k) = 0$, $\mathcal{E}^-(k) = \Delta/2(1 - \cos kl) = \mathcal{E}(k)$ and $\tau_{sc} \to \infty$ since there is no scattering

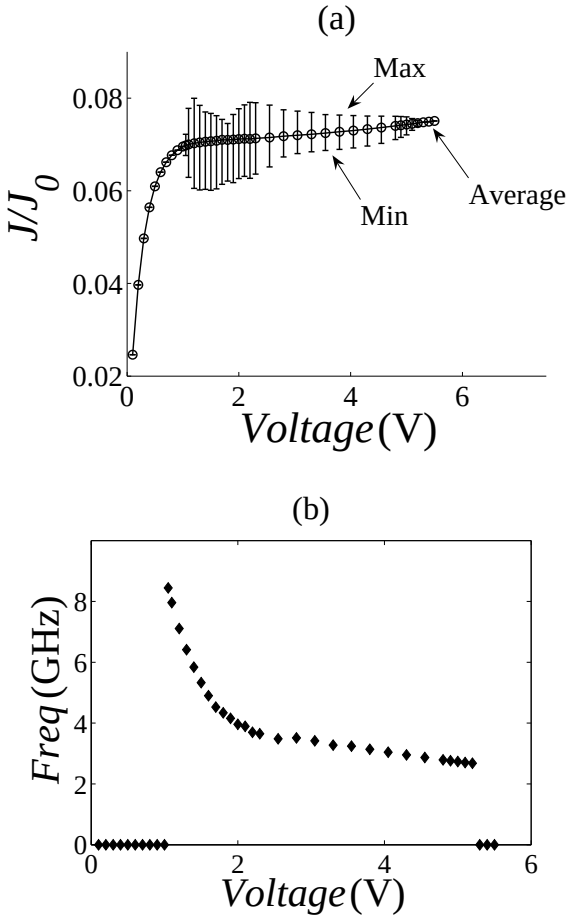

Figure 6.3: (a) Total current density (average, maximum and minimum values) vs voltage bias. (b) Current oscillation frequencies vs voltage bias.

between minibands. The four Wigner functions will be as follows:

$$\begin{aligned} f_{11} &= f^0 + f^3 = 0, \\ f_{12} &= f^1 - if^2 = 0, \\ f_{21} &= f^1 + if^2 = 0, \\ f_{22} &= f^0 - f^3 = f, \end{aligned}$$

and the corresponding Wigner function balance equation becomes:

$$\frac{\partial f}{\partial t} + \frac{\Delta l}{2\hbar} sin(kl) \frac{\partial}{\partial x} \langle f \rangle_1 + \frac{iel}{\hbar} \sum_{j=-\infty}^{\infty} j \langle F \rangle_j e^{ijkl} f_j = \frac{-1}{\tau}(f - f^{FD}), \quad (6.71)$$

where f^{FD} is the local equilibrium Fermi-Dirac distribution function for the first miniband:

$$f^{FD}(k;n) = \frac{m^* k_B T}{\pi\hbar^2} \int_{-\infty}^{\infty} \frac{\sqrt{2}\,\Gamma^3/\pi}{\Gamma^4 + [E - \mathcal{E}(k)]^4} \ln\left(1 + e^{\frac{\mu - E}{k_B T}}\right) dE, \quad (6.72)$$

with broadening energy Γ. Note that equation (6.71) coincides with the Wigner equation (2.64) derived in section 2.3 if the impurity collisions are ignored, i.e. $\nu_{imp} = 0$.

The electron density $n(x,t)$ can be obtained in the following way:

$$n(x,t) = \frac{l}{2\pi} \int_{-\pi/l}^{\pi/l} f(x,t;k) dk = \frac{l}{2\pi} \int_{-\pi/l}^{\pi/l} f^{FD}(k;n)\, dk \quad (6.73)$$

Equations (6.71)-(6.73) can be solved together with the Poisson equation:

$$\varepsilon \frac{\partial F}{\partial x} = \frac{e}{l}(n - N_D), \quad (6.74)$$

where N_D is the doping density.

If we integrate the Wigner function balance equation (6.71) over k, we obtain:

$$\frac{\partial n}{\partial t} - \frac{\Delta l}{2\hbar} \frac{\partial}{\partial x} \langle Im f_1 \rangle_1 = 0, \quad (6.75)$$

By derivating the Poisson equation (6.74) with respect to time and inserting $\partial n/\partial t$ in (6.75), and then integrating it over x we can obtain the Ampere's law:

$$\varepsilon \frac{\partial F}{\partial t} - \frac{e\Delta}{2\hbar} \langle Im f_1 \rangle_1 = J(t), \quad (6.76)$$

where the subscript means the Fourier coefficient:

$$f(x,t,k) = \sum_{j=-\infty}^{\infty} f_j(x,t) e^{ijkl}. \tag{6.77}$$

Assuming that the Bloch frequency $eFl/\hbar$ and the collision frequency $1/\tau$ are of the same order of magnitude, we obtain the electric field dimensionless parameter $F_M = \hbar/(el\tau)$. Considering that the characteristic length (x_0) for the variation of the electric field is given by the Poisson equation, i.e. $\varepsilon \partial F/\partial x \sim eN_D/l$, we have: $x_0 = \varepsilon F_M l/(eN_D)$. The group velocity V_M will be $1/\hbar\, \partial\mathcal{E}/\partial k = \Delta l/(2\hbar)$. The characteristic time for the variation of the field is therefore $t_0 = x_0/v_M$. Equations (6.71)-(6.76) become, in dimensionless form, as follows:

$$\lambda \left(\frac{\partial f}{\partial t} + sin(k) \frac{\partial}{\partial x} \langle f \rangle_1 \right) + i \sum_{j=-\infty}^{\infty} j \langle F \rangle_j e^{ijk} f_j = -(f - f^{FD}), \tag{6.78}$$

$$n(x,t) = \frac{1}{2\pi} \int_{-\pi}^{\pi} f(x,t;k) dk = \frac{1}{2\pi} \int_{-\pi}^{\pi} f^{FD}(k;n) dk, \tag{6.79}$$

$$\frac{\partial F}{\partial x} = n - 1, \tag{6.80}$$

$$f^{FD}(k;n) = \frac{m^* k_B T}{\pi N_D \hbar^2} \int_{-\infty}^{\infty} \frac{\sqrt{2}\,\Gamma^3/\pi}{\Gamma^4 + [E - \mathcal{E}(k)]^4} \ln\left(1 + e^{\frac{\mu - E}{k_B T}}\right) dE, \tag{6.81}$$

$$\frac{\partial F}{\partial t} - \langle Im f_1 \rangle_1 = J(t), \tag{6.82}$$

where $\lambda = \tau/t_0$. We will use dimensionless equations from now on.

We can eliminate k in equation (6.78) by using the Fourier coefficients:

$$\lambda \left(\frac{\partial f_j}{\partial t} + \frac{1}{2i} \frac{\partial}{\partial x} \langle f_{j-1} - f_{j+1} \rangle_1 \right) + ij \langle F \rangle_j f_j = -(f_j - f_j^{FD}). \tag{6.83}$$

The Chapman-Enskog method allows us to obtain f in the hyperbolic limit ($\lambda \ll 1$):

$$f(k,x,t;\lambda) = \sum_{m=0}^{\infty} \lambda^m f^{(m)}(k,n,F), \tag{6.84}$$

$$\frac{\partial F}{\partial t} + \sum_{m=0}^{\infty} J_m(n,F)\, \lambda^m = J(t), \tag{6.85}$$

$$\frac{\partial n}{\partial t} = \sum_{m=0}^{\infty} A_m(n,F)\, \lambda^m. \tag{6.86}$$

By inserting (6.84) in (6.83), we get:

$$f_j^{(0)} = \frac{f_j^{FD}}{1+ij\left\langle F\right\rangle_j}, \tag{6.87}$$

$$f_j^{(1)} = \frac{-1}{1+ij\left\langle F\right\rangle_j}\left(\left.\frac{\partial f_j^{(0)}}{\partial t}\right|_0 + \frac{\partial}{\partial x}\left\langle \frac{f_{j-1}^{(0)}-f_{j+1}^{(0)}}{2i}\right\rangle_1\right|_0\Bigg), \tag{6.88}$$

and so on. The subscripts 0 and 1 in the right hand side of these equations mean that we replace $\partial F/\partial t|_m = J\delta_{0m} - J_m$, $\partial n/\partial t|_m = A_m$, provided $\delta_{00} = 1$ and $\delta_{0m} = 0$ if $m \neq 0$. Moreover, inserting (6.84) into (6.79) yields the following compatibility conditions:

$$f_0^{(0)} = n, \tag{6.89}$$

$$f_0^{(1)} = 0, \tag{6.90}$$

$$f_0^{(2)} = 0, \tag{6.91}$$

etc.

By substituting Imf_1 from (6.87) and (6.88) in (6.82) we can get the following quantum drift diffusion equation:

$$\frac{\partial F}{\partial t} + \left\langle \mathcal{D}(n,F)\right\rangle_1 = J(t), \tag{6.92}$$

where the functional $\mathcal{D}(n,F)$ is the following:

$$\begin{aligned}\mathcal{D}(n,F) = -Imf_1^{(0)} - \lambda Imf_1^{(1)} = \\ &\frac{\vartheta_1}{1+\vartheta_1^2}f_1^{FD} + \\ &2\lambda\frac{\vartheta_1}{1+\vartheta_1^2}\frac{\partial f_1^{FD}}{\partial n}\frac{\partial}{\partial x}\left\langle\frac{\vartheta_1}{1+\vartheta_1^2}f_1^{FD}\right\rangle_1 + \\ &\lambda\frac{1-3\vartheta_1^2}{(1+\vartheta_1^2)^3}f_1^{FD}\left(\left\langle\left\langle\frac{\vartheta_1}{1+\vartheta_1^2}f_1^{FD}\right\rangle_1\right\rangle_1 - J\right) + \\ &\frac{\lambda}{2(1+\vartheta_1^2)}\left(\frac{\partial}{\partial x}\left\langle\frac{f_2^{FD}}{1+\vartheta_2^2}\right\rangle_1 - \vartheta_1\frac{\partial}{\partial x}\left\langle\frac{\vartheta_2 f_2^{FD}}{1+\vartheta_2^2}\right\rangle_1 - \left\langle\frac{\partial^2 F}{\partial x^2}\right\rangle_1\right),\end{aligned} \tag{6.93}$$

where we have used $\vartheta_j = j\left\langle F\right\rangle_j$. Note that equation (6.92) coincides with the QDDE (2.77) derived in section 2.3.2 if $\nu_{en} = 1/\tau$ and the impurity collisions are ignored $\nu_{imp} = 0$.

Equation (6.93) can be numerically solved together with the Poisson equation (6.80) and with the following boundary conditions:

- Voltage bias:

$$\int_0^{Nl} F\,dx = V. \tag{6.94}$$

- Injecting contact (cathod) $-2l \leq x \leq 0$:

$$\varepsilon \frac{\partial F}{\partial t} + \sigma_{cathode}\, F = J, \tag{6.95}$$

$$n = N_D \tag{6.96}$$

- Anode region ($Nl \leq x \leq Nl + 2l$):

$$\varepsilon \frac{\partial F}{\partial t} + \sigma_{anode} \frac{n}{N_D} F = J, \tag{6.97}$$

$$n = N_D + \varepsilon \frac{l}{e} \frac{\partial F}{\partial x} \tag{6.98}$$

For the numerical solution we have used the same numerical values used for the two miniband model, with a $N = 60$ period SL. Fig. 6.4(a) shows the oscillations of the total current density for an external voltage bias $V = 1.2$ V, and 6.4(b) exhibits the evolution of the field profiles at different times during une cycle of the oscillation of the current. We have also calculated the stationary total current density for different applied voltages and compared it with the corresponding values obtained with the two miniband model. When the total current exhibits self sustained oscillations we have calculated the average value of the total current in fig. 6.5. The results (see figure 6.5) show that the total current density obtained with the two miniband model is slightly larger than the current obtained with the single miniband model.

6.7 Conclusions

For strongly coupled SLs having two populated minibands, we have introduced a kp Hamiltonian that contains a field-dependent tunneling term and derived the corresponding Wigner-Poisson-BGK system of equations. The collision model comprises two terms, a BGK term trying to bring the Wigner matrix closer to a broadened Fermi-Dirac local equilibrium at each miniband,

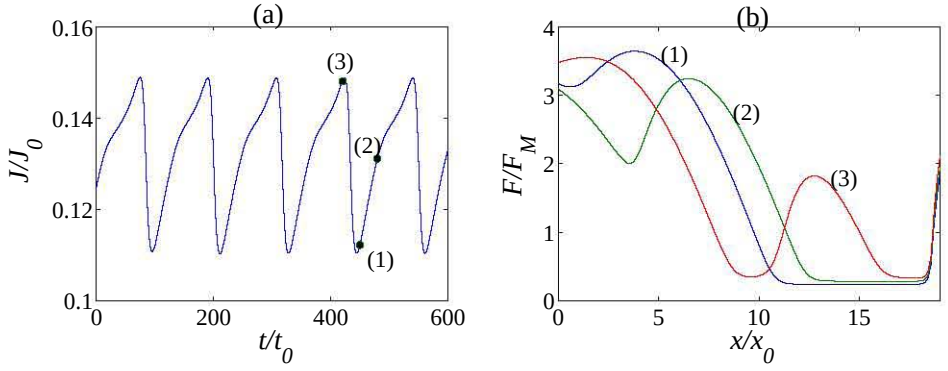

Figure 6.4: (a) Total current density vs time. (b) Field profiles at different times during one cycle of the oscillation of the total current.

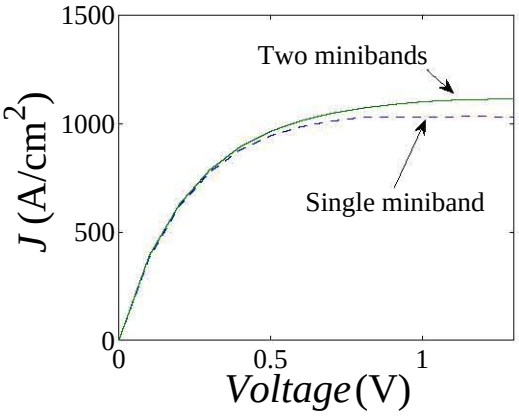

Figure 6.5: Average value of the total current density vs applied voltage for both one and two miniband models.

and a scattering term that brings down electrons from the upper to the lower miniband. By using the Chapman-Enskog method, we have derived quantum drift-diffusion equations for the miniband populations which contain generation-recombination terms. As it should be, the recombination terms vanish if there is no inter-miniband scattering and the off-diagonal terms in the Hamiltonian are zero. These terms represent miniband coupling due to the electric field and originate the resonant tunneling transport. For a superlattice under dc voltage bias in the growth direction, numerical solutions of the corresponding quantum drift-diffusion equations show self-sustained current oscillations due to periodic recycling and motion of electric field pulses, and resonant tunneling between minibands when the electric field is above the resonant value. Numerical reconstruction of the Wigner functions during self-oscillations confirms this picture. Finally, we have derived the single miniband equations from the two miniband model, and calculated the total current density with both models, obtaining slightly larger values from the two miniband model.

Chapter 7

Conclusions and future work

We have presented different kinetic models for strongly coupled semiconductor superlattices that describe nonlinear electron transport phenomena such as Bloch oscillations, Gunn type self sustained current oscillations, spin transport and resonant tunneling between minibands. To analyze these models we have extended the approach used by Bonilla, Escobedo and Perales (2003) [12]: derive reduced balance equations by means of the Chapman-Enskog perturbation method and solve them numerically with appropriate initial and boundary conditions. All the models presented in this thesis are based on Boltzmann or Wigner transport kinetic equations and the collisions are treated by means of Bhatnagar-Gross-Krook (BGK) type terms with constant relaxation times, which try to restore the local thermal equilibrium. Starting with a Boltzmann-Poisson-BGK kinetic model for a single miniband SL, we proved an H-theorem assuming ideal boundary conditions (insulating contacts with zero voltage bias between them) by means of a free energy functional. However, for a SL under realistic boundary conditions (nonzero voltage bias and conducting contacts) displaying Gunn-type oscillations of the current, we showed in our numerical results that the free energy is no longer a Lyapunov functional and it may oscillate periodically with time [2].

In the second model we start also with a Boltzmann-Poisson-BGK equation, but in this case the local equilibrium distribution depends on the electron, current and energy densities, which allows it to oscillate at the Bloch frequency. We use a combination of multiple scales, the Chapman-Enskog method and matched asymptotic expansions to derive the balance equations in the limit of almost elastic collisions and high electric fields. In this limit Bloch frequencies and collision frequencies are of the same order and dominate the rest of the terms in the kinetic equation. The numerical solution

of the balance equations for the electric field and the complex envelope of the Bloch oscillations shows that inhomogeneous electric field domains can coexist together with stable spatially confined Bloch oscillations. Our results show that stable fast Bloch oscillations of the current and energy densities may exist confined to a part of the superlattice close to the receiving contact provided the damping produced by scattering is below a critical value. These spatially inhomogeneous Bloch oscillations are a novel finding that runs contrary to the widespread belief that Bloch oscillations are necessarily spatially homogeneous and incompatible with the existence of electric field domains.

In the last two models we extend the Chapman-Enskog method to find reduced balance equations for superlattices with two minibands. Starting from appropriate Wigner-Poisson-BGK systems of equations, we derive nonlocal quantum drift-diffusion systems for the electron density and the electric field whose numerical solutions display Gunn type oscillations with quantum effects. Results include the description of a lateral superlattice with Rashba spin-orbit interaction that can act as a spin oscillator [10]. After adding a field dependent inter-miniband coupling term, this model describes electron transport in a strongly coupled superlattice having two minibands. Numerical solution of the resulting reduced balance equations shows self sustained current oscillations with resonant tunneling between the minibands when the electric field surpasses an appropriate value [3].

We believe that our work opens promising research venues for the future. Possible ones are the following:

- Find a regime at which Bloch oscillations may coexist together with Gunn type self sustained current oscillations.
- Analyze the onset of Bloch oscillations for sufficiently small amplitude by deriving approximate amplitude equations.
- Use our reduced hydrodynamic equations for Bloch oscillations to study Bloch gain, i.e., whether it is possible to amplify the response of the current to THz driven voltage oscillations taking into account the space dependence of the electric field and the current and energy densities.
- Improve the two miniband model in order to obtain multibranched current-voltage characteristic curves. This also requires new perturbation methods to tackle the limit of vanishingly small miniband widths.
- Use a Weighted Particle Method similar to that in [27] for solving numerically two-miniband kinetic equations.

Appendix A

Boltzmann local equilibrium distribution

In nondimensional units, the Boltzmann distribution (4.21) satisfying $f_0^B = n$ is

$$f^B = n\,\frac{\pi\, e^{\tilde{u}k+\tilde{\beta}\cos k}}{\int_0^\pi e^{\tilde{\beta}\cos K}\cosh(\tilde{u}K)\,dK}. \tag{A.1}$$

The first moments of this distribution can be used to calculate $\tilde{\beta}$ and $\tilde{u}$ in terms of E and J_n by solving

$$\frac{\int_0^\pi e^{\tilde{\beta}\cos K}\cosh(\tilde{u}K)\,\cos K\,dK}{\int_0^\pi e^{\tilde{\beta}\cos K}\cosh(\tilde{u}K)\,dK} = \alpha_e E_0 + (1-\alpha_e)E, \tag{A.2}$$

$$\frac{\int_0^\pi e^{\tilde{\beta}\cos K}\sinh(\tilde{u}K)\,\sin K\,dK}{\int_0^\pi e^{\tilde{\beta}\cos K}\cosh(\tilde{u}K)\,dK} = (1-\alpha_j)\,\frac{J_n}{n}. \tag{A.3}$$

The left hand side of (A.3) can be simplified by integrating the numerator by parts:

$$\frac{\tilde{u}}{\tilde{\beta}} - \frac{e^{-\tilde{\beta}}\sinh(\tilde{u}\pi)}{\tilde{\beta}\int_0^\pi e^{\tilde{\beta}\cos K}\cosh(\tilde{u}K)\,dK} = (1-\alpha_j)\,\frac{J_n}{n}. \tag{A.4}$$

Appendix B

Inelastic collisions and the hyperbolic limit

Here we shall use the CEM to obtain equations for the electric field and the electron density in the case of inelastic collisions with $0 < \alpha_{e,j} \leq 1$. In the method of multiple scales, we expand the distribution function and all its moments in powers of δ and consider slow and fast time scales. The condition that the terms in the distribution function be periodic (or, more generally, bounded as the fast time tends to infinity) in the fast time determines the modulation equations in the slow time scale. In the inelastic case, Γ in (4.40) and (4.41) is of order one. Thus the distribution function relaxes exponentially fast to a quasi-stationary function whose current and energy densities are (to leading order) (4.33) and (4.34). This distribution is the starting point of the CEM which, in the inelastic case, is similar to that described in [12] and [17].

The leading order expression for the distribution function depends on time only through the moments n and F which vary on the slow time scale t. These moments are not expanded in powers of δ. Instead, their evolution equations are expanded (as we show below), and the corresponding terms in the expansion are determined so as to keep compatibility conditions issuing from the assumptions for the distribution function. The CEM can be used to obtain reduced equations for the moments containing terms of different order in δ, and this is something that the method of multiple scales cannot deliver.

The leading-order distribution function is the solution of Eq. (4.47) for

$\delta = 0$. Its Fourier coefficients are

$$\mathrm{Re} f_j^{(0)} = \frac{\mathrm{Re} f_j^{1D\alpha} + jF\,\mathrm{Im} f_j^{1D\alpha}}{1 + j^2F^2}, \tag{B.1}$$

$$\mathrm{Im} f_j^{(0)} = \frac{\mathrm{Im} f_j^{1D\alpha} - jF\,\mathrm{Re} f_j^{1D\alpha}}{1 + j^2F^2}. \tag{B.2}$$

We assume that J_n and E have already acquired their quasi-stationary values after a fast decay on the time scale τ. These quasi-stationary values are functions of n, F and δ to be determined now. Eqs. (4.50), (4.51) and (4.52)-(4.54) are

$$f_0^{(0)} = f_0^{1D\alpha(0)} = n, \tag{B.3}$$

$$\mathrm{Re} f_1^{(0)} = nE^{(0)}, \quad \mathrm{Re} f_1^{1D\alpha(0)} = n\left[\alpha_e E_0 + (1-\alpha_e)E^{(0)}\right], \tag{B.4}$$

$$\mathrm{Im} f_1^{(0)} = -J_n^{(0)}, \quad \mathrm{Im} f_1^{1D\alpha(0)} = -(1-\alpha_j)\, J_n^{(0)}. \tag{B.5}$$

Inserting (B.4) and (B.5) in (B.1) and (B.2), we obtain a system of two algebraic equations for the unknowns $nE^{(0)}$ and $J_n^{(0)}$ whose solution is

$$E^{(0)} = \frac{\alpha_e \alpha_j E_0}{\alpha_j \alpha_e + F^2}, \tag{B.6}$$

$$J_n^{(0)} = \frac{\alpha_e E_0 n F}{\alpha_j \alpha_e + F^2}, \tag{B.7}$$

$$f_1^{(0)} = nE^{(0)} - iJ_n^{(0)} = n\,\frac{\alpha_e E_0(\alpha_j - iF)}{\alpha_j \alpha_e + F^2}. \tag{B.8}$$

The approximate electron current density (B.7) provides an approximate electron drift velocity vs. field, $v_d(F) = J_n^{(0)}/n$, whose maximum value is reached at

$$v_{\max} = \frac{E_0}{2}\sqrt{\frac{\alpha_e}{\alpha_j}} = \frac{I_1(\tilde{\beta}_0)}{2I_0(\tilde{\beta}_0)}\sqrt{\frac{\alpha_e}{\alpha_j}}, \quad F_{\max} = \sqrt{\alpha_e \alpha_j}, \tag{B.9}$$

in which we have used (4.24) to relate E_0 (equal to the dimensional mean energy E_0 divided by $\Delta/2$) to the lattice temperature $1/\tilde{\beta}_0 = 2k_B T_0/\Delta$ for a Boltzmann local equilibrium. In dimensional units, (B.6) - (B.9) become Equations (4.33) - (4.36). For $\alpha_e = \alpha_j = 1$, these are well known values corresponding to the simple BGK-Poisson problem (4.2) - (4.8) with Boltzmann local equilibrium [43]. It is interesting to note that we have derived (B.7) and (B.9) for an unspecified general local equilibrium $f^{1D\alpha}$, not just

for the Boltzmann distribution. This means that this expression for the electron drift velocity is also valid at low temperatures, when the Fermi-Dirac distribution (4.10) is a better description, and it justifies a posteriori the use of (B.7) to fit experimental results [71].

Remark. To leading order, E and J_n in the right hand sides of (A.2) and (A.4) can be eliminated by using (B.6) and (B.7), thereby obtaining

$$\frac{\int_0^\pi e^{\tilde{\beta}\cos K}\cosh(\tilde{u}K)\,\cos K\,dK}{\int_0^\pi e^{\tilde{\beta}\cos K}\cosh(\tilde{u}K)\,dK} = \alpha_e E_0 \frac{\alpha_j + F^2}{\alpha_j\alpha_e + F^2}, \tag{B.10}$$

$$\frac{\tilde{u}}{\tilde{\beta}} - \frac{e^{-\tilde{\beta}}\sinh(\tilde{u}\pi)}{\tilde{\beta}\int_0^\pi e^{\tilde{\beta}\cos K}\cosh(\tilde{u}K)\,dK} = \frac{\alpha_e(1-\alpha_j)E_0 F}{\alpha_j\alpha_e + F^2}. \tag{B.11}$$

Solving these two equations yield the functions $\tilde{\beta}(F)$ and $\tilde{u}(F)$. In the case $\alpha_j = 1$, (B.11) yields $\tilde{u} = 0$ and (B.10) becomes

$$\frac{I_1(\tilde{\beta})}{I_0(\tilde{\beta})} = \frac{\alpha_e(1+F^2)E_0}{\alpha_e + F^2}. \tag{B.12}$$

The CEM consists of expanding f and the equations for the slowly varying n and F in power series in δ:

$$f(x,k,t;\delta) = f^{(0)}(k;F,n) + \sum_{m=1}^{\infty} f^{(m)}(k;F,n)\,\delta^m, \tag{B.13}$$

$$\frac{\partial F}{\partial x} = n - 1, \tag{B.14}$$

$$\frac{\partial F}{\partial t} + \sum_{m=0}^{\infty} \mathcal{J}^{(m)}(F,n)\,\delta^m = J(t), \tag{B.15}$$

$$\frac{\partial n}{\partial t} = -\sum_{m=0}^{\infty} \frac{\partial}{\partial x}\mathcal{J}^{(m)}(F,n)\,\delta^m. \tag{B.16}$$

We have used the Poisson equation (B.14) to obtain (B.16). The Fourier coefficients of $f^{(0)}$ are (B.1) and (B.2). $f^{(m)}$ are 2π-periodic functions of k, and depend on time only through their dependence of n and F (which are linked by the Poisson equation). Note that E and J_n depend on δ unlike the slowly varying variables n and F. This implies that $f^{1D\alpha}$ also depends on δ

and can be expanded in a series similar to Eq. (B.13):

$$
\begin{aligned}
f^{1D\alpha} &= \sum_{m=1}^{\infty} f^{1D\alpha(m)}\,\delta^m, && \text{(B.17)}\\
f_0^{1D\alpha(0)} &= n, \quad f_0^{1D\alpha(m)} = 0, && \text{(B.18)}\\
f_1^{1D\alpha(0)} &= n\left[\alpha_e E_0 + (1-\alpha_e)E^{(0)}\right] - i(1-\alpha_j)J_n^{(0)}, && \text{(B.19)}\\
f_1^{1D\alpha(m)} &= (1-\alpha_e)nE^{(m)} - i(1-\alpha_j)J_n^{(m)},
\end{aligned}
$$

for m=1,2,.... Equations (B.18) and (B.19) are found by insertion of (B.13) in (B.3) - (B.5). Inserting (B.13) - (B.16) in (4.47), a hierarchy of equations for $f^{(m)}$ is found. The functionals of n and F, $\mathcal{J}^{(m)}$, will be calculated in such a way that the compatibility conditions

$$
\begin{aligned}
&f_0^{(0)} = n = f_0^{1D\alpha(0)}, \quad f_0^{(m)} = 0, \text{ for } m = 1, 2, \ldots, && \text{(B.20)}\\
&\mathrm{Re} f_1^{(m)} = nE^{(m)}, \quad \mathrm{Im} f_1^{(m)} = -J_n^{(m)}. && \text{(B.21)}
\end{aligned}
$$

hold. Eqs. (B.20) follow from the definition $n = f_0$ and (B.13). Similarly, (B.21) follow from $f_1 = nE - iJ_n$ and (B.13). Once sufficiently many $\mathcal{J}^{(m)}$ are known, Eq. (B.15) is the sought Ampère's law yielding the drift-diffusion equation for F.

The equations for $f^{(1)}$ and $f^{(2)}$ are

$$
\begin{aligned}
\mathbb{L}f^{(1)} - f^{1D\alpha(1)} &= -\left(\left.\frac{\partial f^{(0)}}{\partial t}\right|_0 + \sin k\,\frac{\partial f^{(0)}}{\partial x}\right), && \text{(B.22)}\\
\mathbb{L}f^{(2)} - f^{1D\alpha(2)} &= -\left(\left.\frac{\partial f^{(1)}}{\partial t}\right|_0 + \sin k\,\frac{\partial f^{(1)}}{\partial x}\right) - \left.\frac{\partial f^{(0)}}{\partial t}\right|_1, && \text{(B.23)}
\end{aligned}
$$

and so on. The subscript $m = 0, 1$ in the right hand side of these equations means that $\partial F/\partial t$ and $\partial n/\partial t$ are replaced by $(J\delta_{m0} - \mathcal{J}^{(m)})$ and $-\partial\mathcal{J}^{(m)}/\partial x$, respectively. In these equations, the operator is defined by

$$
\mathbb{L}u(k) \equiv F\,\frac{\partial u}{\partial k}(k) + u(k). \tag{B.24}
$$

The compatibility conditions (B.20) imply the following solvability conditions for the hierarchy (B.22) and (B.23):

$$
(\mathbb{L}f^{(m)})_j = 0, \quad j = 0, 1. \tag{B.25}
$$

Using the solvability conditions (B.25) for the linear hierarchy of equations, we can show that the reduced balance equations for n and F are

obtained by inserting (B.13) in Equation(4.51) for J_n:

$$J_n = -\sum_{m=0}^{\infty} \delta^m \, \mathrm{Im} f_1^{(m)}, \quad \mathcal{J}^{(m)} = -\mathrm{Im} f_1^{(m)}. \tag{B.26}$$

We have already calculated $\mathcal{J}^{(0)} = J_n^{(0)}$ to be given by Eq. (B.7). To get a diffusive correction to this electron current density, we need to calculate $\mathrm{Im} f_1^{(1)}$. From (B.22), (B.19) and (B.21), we obtain

$$\mathrm{Re} f_1^{(1)} = \frac{\alpha_j \mathrm{Re} r_1 + F \, \mathrm{Im} r_1}{\alpha_e \alpha_j + F^2}, \tag{B.27}$$

$$\mathrm{Im} f_1^{(1)} = \frac{\alpha_e \mathrm{Im} r_1 - F \, \mathrm{Re} r_1}{\alpha_e \alpha_j + F^2}, \tag{B.28}$$

in which

$$r = -\frac{\partial f^{(0)}}{\partial t}\bigg|_0 - \sin k \, \frac{\partial f^{(0)}}{\partial x}. \tag{B.29}$$

Thus we need to find

$$r_1 = -\frac{\partial}{\partial x} \frac{n - f_2^{(0)}}{2i} - \frac{\partial f_1^{(0)}}{\partial t}\bigg|_0, \tag{B.30}$$

in order to calculate (B.28), i.e.,

$$\mathcal{J}^{(1)} = \frac{\alpha_e \left[\mathrm{Im} \, \frac{\partial f_1^{(0)}}{\partial t}\Big|_0 - \frac{\partial}{\partial x} \frac{n - \mathrm{Re} f_2^{(0)}}{2} \right] - F \left[\mathrm{Re} \, \frac{\partial f_1^{(0)}}{\partial t}\Big|_0 - \frac{1}{2} \frac{\partial}{\partial x} \mathrm{Im} f_2^{(0)} \right]}{\alpha_e \alpha_j + F^2}. \tag{B.31}$$

Equation (B.8) yields

$$\begin{aligned} \frac{\partial f_1^{(0)}}{\partial t}\bigg|_0 &= \frac{-\alpha_e E_0}{\alpha_e \alpha_j + F^2} \left[(\alpha_j - iF) \frac{\partial J_n^{(0)}}{\partial x} \right. \\ &+ \left. n(J - J_n^{(0)}) \frac{2\alpha_j F + i(\alpha_e \alpha_j - F^2)}{\alpha_e \alpha_j + F^2} \right]. \end{aligned} \tag{B.32}$$

The calculation of $f_2^{(0)}$ involves that of $f_2^{1D\alpha(0)}$. Using $\cos 2k = 1 - 2\sin^2 k$, $\sin 2k = 2 \sin k \cos k$, integrating by parts and using (A.2), (A.4) from Appendix A, and (B.10) and (B.11), we get

$$\frac{n - \mathrm{Re} \, f_2^B}{2} = \frac{\alpha_e n E_0}{\tilde{\beta}} \, \frac{1 - (1 - \alpha_j)(1 - \tilde{u}F) + F^2}{\alpha_j \alpha_e + F^2}, \tag{B.33}$$

$$\frac{1}{2} \, \mathrm{Im} \, f_2^B = -\frac{n\tilde{u}}{\tilde{\beta}} - \frac{\alpha_e n E_0}{\tilde{\beta}} \, \frac{(1 + F^2)\tilde{u} - (1 - \alpha_j)[\tilde{u} + (1 + \tilde{\beta})F]}{\alpha_j \alpha_e + F^2} \tag{B.34}$$

For $1-\alpha_j=\tilde{u}=0$, we get $\mathrm{Im}f_2^B=0$ and

$$\frac{n-\mathrm{Re}\, f_2^B}{2}=\frac{\alpha_e n E_0}{\tilde{\beta}}\,\frac{1+F^2}{\alpha_e+F^2}. \tag{B.35}$$

In this case, we obtain

$$\frac{n-\mathrm{Re}f_2^{(0)}}{2}=\frac{n}{1+4F^2}\left[2F^2+\frac{\alpha_e E_0(1+F^2)}{\tilde{\beta}\,(\alpha_e+F^2)}\right], \tag{B.36}$$

$$-\frac{1}{2}\mathrm{Im}f_2^{(0)}=\frac{nF}{1+4F^2}\left[1-\frac{2\alpha_e E_0(1+F^2)}{\tilde{\beta}\,(\alpha_e+F^2)}\right], \tag{B.37}$$

where $\tilde{\beta}$ is a function of F found by solving the equation (B.12).

Recapitulating, we have obtained the drift-diffusion equation (B.15) (Ampère's law) for F in which $\mathcal{J}^{(0)}=J_n^{(0)}$ is given by (B.7) and $\mathcal{J}^{(1)}$ is given by (B.31) - (B.32) and, in the particular case of a Boltzmann local equilibrium with $\alpha_j=1$, by (B.36) - (B.37) and (B.12). We have

$$\frac{\partial F}{\partial t}+\frac{1}{\alpha_j\alpha_e+F^2}\left\{\alpha_e\left[E_0 nF-\frac{\delta}{2}\frac{\partial}{\partial x}(n-\mathrm{Re}\, f_2^{(0)})\right.\right. \tag{B.38}$$
$$\left.\left.+\,\delta\,\mathrm{Im}\,\frac{\partial f_1^{(0)}}{\partial t}\right|_0\right]+\delta F\left[\frac{1}{2}\frac{\partial}{\partial x}\mathrm{Im}\, f_2^{(0)}-\mathrm{Re}\,\left.\frac{\partial f_1^{(0)}}{\partial t}\right|_0\right]\Bigg\}=J(t),$$

where $n=1+\partial F/\partial x$ according to the Poisson equation (B.14). Note that the drift-diffusion equation (B.38) coincides with the drift-diffusion equation (4.136) when we substitute $h_S=\partial f_1/\partial t|_0$ given by (B.32) and $g_S=f_2^{(0)}$ in (4.136) (with $\alpha_{e,j}=\delta\gamma_{e,j}$). Eq. (B.38) for almost elastic collisions becomes

$$\frac{\partial F}{\partial t}+\frac{\delta}{F^2+\delta^2\gamma_j\gamma_e}\left[\gamma_e E_0 nF+\frac{F}{2}\,\frac{\partial}{\partial x}\mathrm{Im}\, f_{2,S}^{(0)}+\delta\gamma_e\mathrm{Im}\,\left.\frac{\partial f_1^{(0)}}{\partial t}\right|_{0,S}\right. \tag{B.39}$$
$$\left.-\frac{\delta\gamma_e}{2}\,\frac{\partial}{\partial x}(n-\mathrm{Re}\, f_{2,S}^{(0)})-F\,\mathrm{Re}\,\left.\frac{\partial f_1^{(0)}}{\partial t}\right|_{0,S}\right]=J(t),$$

where (B.32) should be inserted and $f_2^{(0)}$ is given by (B.1) and (B.2). In (4.137), which describes the damping of the oscillation amplitude A, $g=f_2^{(0)}$ with $f_1=f_{1,S}+Ae^{-i\theta}$ and $f_{1,S}$ is given by (B.6) and (B.7). Therefore in the case of almost elastic collisions, if the amplitude of the Bloch oscillations decays to zero, we are left with the drift-diffusion problem derived in this Section.

Appendix C

Balance equations from compatibility conditions

We know that $\varphi^1 = \varphi^2 = 0$ from (5.44). Then the compatibility conditions (5.46) and (5.47) become

$$\psi_0^0 = 0, \quad \psi_0^3 = 0, \tag{C.1}$$

$$f_0^{(2)\,0} = 0, \quad f_0^{(2)\,3} = \frac{\beta}{g}\,\mathrm{Im}\psi_1^2 + \frac{\beta^2}{4g^2}\,(\varphi_0^3 - \mathrm{Re}\varphi_2^3), \tag{C.2}$$

Equations (C.1) imply that $(\mathbb{L}\psi)_0^m = 0$ for $m = 0, 3$ in (5.44). Since $\varphi_0^0 = (n^+ + n^-)/2$ and $\varphi_0^3 = (n^+ - n^-)/2$, these conditions yield

$$\frac{\tau}{2}\,\frac{\partial(n^+ + n^-)}{\partial t}\bigg|_0 - \frac{\alpha\tau}{\hbar}\,\Delta^-\mathrm{Im}\varphi_1^0 - \frac{\gamma\tau}{\hbar}\,\Delta^-\mathrm{Im}\varphi_1^3 = 0,$$

$$\frac{\tau}{2}\,\frac{\partial(n^+ - n^-)}{\partial t}\bigg|_0 + \delta_2 n^+ - \frac{\alpha\tau}{\hbar}\,\Delta^-\mathrm{Im}\varphi_1^3 - \frac{\gamma\tau}{\hbar}\,\Delta^-\mathrm{Im}\varphi_1^0 = 0,$$

wherefrom we obtain

$$A_0^\pm = \mp\frac{n^+}{\tau_{\mathrm{sc}}} + \frac{\alpha \pm \gamma}{\hbar}\,\Delta^-\mathrm{Im}(\varphi_1^0 \pm \varphi_1^3). \tag{C.3}$$

Let us now calculate $A_1^\pm$. Equations (C.2) imply $(\mathbb{L}f^{(2)})_0^0 = 0$ and $(\mathbb{L}f^{(2)})_0^3 = f_0^{(2)\,3}$ given by (C.2) in (5.45). After a little algebra, we find

$$A_1^\pm = \frac{\alpha \pm \gamma}{\hbar}\,\Delta^-\mathrm{Im}(\psi_1^0 \pm \psi_1^3) - \frac{\beta}{\hbar}\,(\Delta^-\mathrm{Re}\psi_1^2 \pm \Delta^+\mathrm{Im}\psi_1^1) \tag{C.4}$$

$$\mp\frac{\beta}{g\tau}\,\mathrm{Im}\psi_1^2 \pm \frac{\beta^2}{8g^2\tau}\,[2\mathrm{Re}\varphi_2^3 + \phi_2^+ - \phi_2^- - 2(n^+ - n^-)].$$

We will now transform (C.4) in an equivalent form by eliminating $\mathrm{Re}\varphi_2^3$ and $\mathrm{Im}\psi_1^2$ in favor of $\mathrm{Re}\varphi_2^3$ and $\mathrm{Im}\psi_1^2$, respectively. Eq. (5.43) implies that $(1+i\vartheta_2)\varphi_2^3 = (\phi_2^+ - \phi_2^-)/2$, and therefore,

$$\mathrm{Re}\varphi_2^3 = \vartheta_2\,\mathrm{Im}\varphi_2^3 + \frac{\phi_2^+ - \phi_2^-}{2}. \tag{C.5}$$

Similarly, Eq. (5.44) implies that $(1+i\vartheta_1)\,\psi_1^2 + \delta_1\,\psi_1^1 = r_1^2$, and therefore,

$$\mathrm{Im}\psi_1^2 = -\vartheta_1\,\mathrm{Re}\psi_1^2 - \delta_1\,\mathrm{Im}\psi_1^1 + \mathrm{Im}r_1^2. \tag{C.6}$$

The right hand side of (5.44) yields

$$r_1^2 = \frac{\beta}{2g}\left(\frac{1-e^{-i2kl}}{2i}\,(\phi^+ - \phi^-)\right)_0 - \frac{\beta\tau}{\hbar}\,\Delta^-\left(\frac{1+e^{-i2kl}}{2}\,\varphi^0\right)_0,$$

wherefrom

$$\mathrm{Im}r_1^2 = \frac{\beta}{4g}\,(\phi_2^+ - \phi_2^- - n^+ + n^-) - \frac{\beta\tau}{2\hbar}\,\Delta^-\mathrm{Im}\varphi_2^0. \tag{C.7}$$

Inserting (C.5), (C.6) and (C.7) in (C.4), we obtain the equivalent form:

$$\begin{aligned} A_1^\pm = {} & \frac{\alpha \pm \gamma}{\hbar}\,\Delta^-\mathrm{Im}(\psi_1^0 \pm \psi_1^3) - \frac{\beta}{\hbar}\,(\Delta^-\mathrm{Re}\psi_1^2 \pm \Delta^+\mathrm{Im}\psi_1^1) \\ & \pm\frac{2\beta}{\hbar}\,\mathrm{Im}\psi_1^1 \pm \frac{\beta}{g\tau}\,\vartheta_1\mathrm{Re}\psi_1^2 \pm \frac{\beta^2}{4g^2\tau}\,\vartheta_2\,\mathrm{Im}\varphi_2^3 \pm \frac{\beta^2}{2\hbar g}\,\Delta^-\mathrm{Im}\varphi_2^0. \end{aligned} \tag{C.8}$$

Inserting (C.3) and this expression in (5.41) and using (5.50), yield (5.53), (5.55) and (5.56). Up to order λ^2, we have thus proven the following statement:

By using the compatibility conditions in the hierarchy of equations (5.44), (5.45), we obtain the same balance equations for $n^\pm$ as by direct substitution of the solutions of the hierarchy into equations (5.30) (which arise from integration of the kinetic equation over k).

Appendix D

Complete expressions for $D_{\pm}$ and R

The recombination term $R(n^+, n^-, F)$ (6.65) depends on φ_0^2 and ψ_0^2 which can be obtained from (6.53) and (6.60) for $j = 0$, taking into account that $\Delta_0^- \mathcal{F} = 0$, $\Delta_0^+ \mathcal{F} = 2\mathcal{F}$ and $\phi_0^{\pm} = n^{\pm}$:

$$
\begin{aligned}
\varphi_0^2 &= \frac{\delta\mathcal{F}\,(n^+ - n^-)}{1 + \eta_1^2 + 4\delta^2\mathcal{F}^2} \\
\psi_0^2 &= \frac{1}{1 + \eta_1^2 + 4\delta^2\mathcal{F}^2}\left[\frac{\alpha\tau}{\hbar}\left[\frac{\delta(1 + \eta_1^2 - 4\delta^2\mathcal{F}^2)(1 - \eta_1^2 - 4\delta^2\mathcal{F}^2(n^+ - n^-))}{1 + \eta_1^2 + 4\delta^2\mathcal{F}^2}\,\frac{\partial\mathcal{F}}{\partial t}\bigg|_0 - \right.\right. \\
&\quad \frac{4\delta^3\mathcal{F}^2}{1 + \eta_1^2 + 4\delta^2\mathcal{F}^2}\left(2(n^+ - n^-)\,\frac{\partial\mathcal{F}}{\partial t}\bigg|_0 + \mathcal{F}\left(\frac{\partial n^+}{\partial t}\bigg|_0 - \frac{\partial n^-}{\partial t}\bigg|_0\right)\right) + \\
&\quad \left.\delta\left((n^+ - n^-)\,\frac{\partial\mathcal{F}}{\partial t}\bigg|_0 + \mathcal{F}\left(\frac{\partial n^+}{\partial t}\bigg|_0 - \frac{\partial n^-}{\partial t}\bigg|_0\right)\right)\right] - \\
&\quad \eta_2\delta\mathcal{F}\left(\frac{1 - \eta_1^2 - 4\delta^2\mathcal{F}^2(n^+ - n^-)}{1 + \eta_1^2 + 4\delta^2\mathcal{F}^2} + 2n^+\right) - \\
&\quad \frac{\alpha\tau}{\hbar}\Delta^-\left[\mathrm{Im}\varphi_1^2 - \eta_1\mathrm{Im}\varphi_1^1 + 2\delta\mathcal{F}\mathrm{Im}\varphi_1^3\right] - \frac{\gamma\tau}{\hbar}\left(-\frac{4\eta_1\delta\mathcal{F}(n^+ - n^-)}{1 + \eta_1^2 + 4\delta^2\mathcal{F}^2} + \right. \\
&\quad \left.2\delta\mathcal{F}\Delta^-\mathrm{Im}\varphi_1^0 + \Delta^+(\mathrm{Re}\varphi_1^1 + \eta_1\mathrm{Re}\varphi_1^2)\right)
\end{aligned}
$$

The time derivatives $\left.\frac{\partial n^{\pm}}{\partial t}\right|_0$ and $\left.\frac{\partial F}{\partial t}\right|_0$, are obtained from the first two

terms of the Chapman-Enskog expansion of (6.62) and (6.63) respectively:

$$\begin{aligned}
\left.\frac{\partial n^{\pm}}{\partial t}\right|_0 &= \mp Q^{(0)} - \Delta^- D_{\pm}^{(0)} = \mp\frac{n^+}{\tau_{sc}} \mp \frac{2\delta^2\mathcal{F}^2(n^+ - n^-)}{\tau(1+\eta_1^2+4\delta^2\mathcal{F}^2)} + \\
&\quad \frac{\alpha \pm \gamma}{\hbar}\Delta^- \left[\phi_1^{\pm}\left(\frac{\vartheta_1}{1+\vartheta_1^2} + \eta_1\delta^2\left(\mp\Delta^-\mathcal{F}\Delta^+\mathcal{F}\mathrm{Re}Z_1 + \right.\right.\right. \\
&\quad \mathrm{Re}Z_1((\Delta^-\mathcal{F})^2\mathrm{Im}M_1^+ + (\Delta^+\mathcal{F})^2\mathrm{Im}M_1^-) + \\
&\quad \left.\left.\left. \mathrm{Im}Z_1((\Delta^-\mathcal{F})^2\mathrm{Re}M_1^+ + (\Delta^+\mathcal{F})^2\mathrm{Re}M_1^-)\right)\right) + \\
&\quad \phi_1^{\mp}\eta_1\delta^2[\mathrm{Re}Z_1((\Delta^-\mathcal{F})^2\mathrm{Im}M_1^+ - (\Delta^+\mathcal{F})^2\mathrm{Im}M_1^-) + \\
&\quad \mathrm{Im}Z_1((\Delta^-\mathcal{F})^2\mathrm{Re}M_1^+ - (\Delta^+\mathcal{F})^2\mathrm{Re}M_1^-)]\Big] \\
\varepsilon\left.\frac{\partial F}{\partial t}\right|_0 &= J - e\left\langle D_+^{(0)} + D_-^{(0)}\right\rangle = J - \frac{e\alpha}{\hbar}\left[(\phi_1^+ + \phi_1^-)\left(\frac{-\vartheta_1}{1+\vartheta_1^2} - \right.\right. \\
&\quad \eta_1\delta^2(\Delta^-\mathcal{F})^2(\mathrm{Re}M_1^+\mathrm{Im}Z_1 + \mathrm{Im}M_1^+\mathrm{Re}Z_1) + \\
&\quad \left.\frac{\gamma}{\alpha}\eta_1\delta^2\Delta^+\mathcal{F}\Delta^-\mathcal{F}\mathrm{Re}Z_1\right) + (\phi_1^+ - \phi_1^-)\left(\eta_1\delta^2\Delta^+\mathcal{F}\Delta^-\mathcal{F}\mathrm{Re}Z_1 - \right. \\
&\quad \left.\left.\frac{\gamma}{\alpha}\left(\frac{\vartheta_1}{1+\vartheta_1^2} + \eta_1\delta^2(\Delta^+\mathcal{F})^2(\mathrm{Re}M_1^-\mathrm{Im}Z_1 + \mathrm{Im}M_1^-\mathrm{Re}Z_1)\right)\right)\right]
\end{aligned}$$

The expression of $D_{\pm}(n^+, n^-, F)$ is based on the first two terms of the Chapman-Enskog expansion $D_{\pm}^{(0)}$ and $D_{\pm}^{(1)}$:

$$D_{\pm}(n^+, n^-, F) = D_{\pm}^{(0)}(n^+, n^-, F) + D_{\pm}^{(1)}(n^+, n^-, F)$$

Where $D_{\pm}^{(0)}$ and $D_{\pm}^{(1)}$ are as follows:

$$\begin{aligned}
D_{\pm}^{(0)}(n^+, n^-, F) &= \frac{\alpha \pm \gamma}{\hbar}\mathrm{Im}(\varphi_1^0 \pm \varphi_1^3) = \\
&\quad -\frac{\alpha \pm \gamma}{\hbar}\left[\phi_1^{\pm}\left(\frac{\vartheta_1}{1+\vartheta_1^2} \mp \eta_1\delta^2(\Delta^-\mathcal{F})(\Delta^+\mathcal{F})\mathrm{Re}Z_1\right.\right. \\
&\quad + \frac{\eta_1\delta^2}{2}((\mathrm{Im}M_1^+(\Delta^-\mathcal{F})^2 + \mathrm{Im}M_1^-(\Delta^+\mathcal{F})^2)\mathrm{Re}Z_1 \\
&\quad \left.\left. + (\mathrm{Re}M_1^+(\Delta^-\mathcal{F})^2 + \mathrm{Re}M_1^-(\Delta^+\mathcal{F})^2)\mathrm{Im}Z_1)\right) \right. \\
&\quad + \phi_1^{\mp}\frac{\eta_1\delta^2}{2}(\mathrm{Im}M_1^+(\Delta^-\mathcal{F})^2 - \mathrm{Im}M_1^-(\Delta^+\mathcal{F})^2)\mathrm{Re}Z_1 \\
&\quad \left. + (\mathrm{Re}M_1^+(\Delta^-\mathcal{F})^2 - \mathrm{Re}M_1^-(\Delta^+\mathcal{F})^2)\mathrm{Im}Z_1)\right]
\end{aligned}$$

$$
\begin{aligned}
D^{(1)}_{\pm}(n^+,n^-,F) &= \frac{\alpha\pm\gamma}{\hbar}\mathrm{Im}(\psi^0_1\pm\psi^3_1) = \\
&\frac{\alpha\pm\gamma}{\hbar}\left[\mathrm{Re}S^0_1\,\mathrm{Im}A^{\pm}_1+\mathrm{Im}S^0_1\,\mathrm{Re}A^{\pm}_1\pm\mathrm{Re}S^3_1\,\mathrm{Im}C^{\pm}_1\pm\mathrm{Im}S^3_1\,\mathrm{Re}C^{\pm}_1\right.\\
&\left.+\eta_1\delta(\mathrm{Re}Z_1\,\mathrm{Im}B^{\pm}_1+\mathrm{Re}Z_1\,\vartheta_1\,\mathrm{Re}B^{\pm}_1+\mathrm{Im}Z_1\,\mathrm{Re}B^{\pm}_1-\mathrm{Im}Z_1\,\vartheta_1\,\mathrm{Im}B^{\pm}_1)\right]
\end{aligned}
$$

The functionals $S_1(n^+,n^-,F)$, $A^{\pm}_1(F)$, $B^{\pm}_1(F)$ and $C^{\pm}_1(F)$ are as follows:

$$
\begin{aligned}
\mathrm{Re}A^{\pm}_1 &= \frac{1}{1+\vartheta^2_1}-\eta_1\delta^2\Delta^-\mathcal{F}\,(\mathrm{Re}Z_1\,\mathrm{Re}M^+_1\Delta^-\mathcal{F}-\mathrm{Im}Z_1(\Delta^-\mathcal{F}\,\mathrm{Im}M^+_1\mp\Delta^+\mathcal{F})),\\
\mathrm{Im}A^{\pm}_1 &= \frac{-\vartheta_1}{1+\vartheta^2_1}-\eta_1\delta^2\Delta^-\mathcal{F}(\mathrm{Re}Z_1(\Delta^-\mathcal{F}\,\mathrm{Im}M^+_1\mp\Delta^+\mathcal{F})+\mathrm{Im}Z_1\,\Delta^-\mathcal{F}\,\mathrm{Re}M^+_1),\\
\mathrm{Re}B^{\pm}_1 &= \mathrm{Re}S^1_1(-\Delta^-\mathcal{F}\mathrm{Im}M^+_1\pm\Delta^+\mathcal{F})-\mathrm{Im}S^1_1\,\Delta^-\mathcal{F}\,\mathrm{Re}M^+_1\mp\mathrm{Re}S^2_1\,\Delta^+\mathcal{F}\,\mathrm{Re}M^-_1\\
&\quad -\mathrm{Im}S^2_1(\Delta^-\mathcal{F}\mp\Delta^+\mathcal{F}\,\mathrm{Im}M^-_1),\\
\mathrm{Im}B^{\pm}_1 &= \mathrm{Re}S^1_1\,\Delta^-\mathcal{F}\,\mathrm{Re}M^+_1+\mathrm{Im}S^1_1(\pm\Delta^+\mathcal{F}-\Delta^-\mathcal{F}\mathrm{Im}M^+_1),\\
&\quad +\mathrm{Re}S^2_1(\Delta^-\mathcal{F}\mp\Delta^+\mathcal{F}\mathrm{Im}M^-_1)\mp\mathrm{Im}S^2_1\,\Delta^+\mathcal{F}\,\mathrm{Re}M^-_1\\
\mathrm{Re}C^{\pm}_1 &= \frac{1}{1+\vartheta^2_1}-\eta_1\delta^2\Delta^+\mathcal{F}(\mathrm{Re}Z_1\,\Delta^+\mathcal{F}\,\mathrm{Re}M^-_1-\mathrm{Im}Z_1(\Delta^+\mathcal{F}\,\mathrm{Im}M^-_1\mp\Delta^-\mathcal{F})),\\
\mathrm{Im}C^{\pm}_1 &= \frac{-\vartheta_1}{1+\vartheta^2_1}-\eta_1\delta^2\Delta^+\mathcal{F}(\mathrm{Re}Z_1(\Delta^+\mathcal{F}\mathrm{Im}M^-_1\mp\Delta^-\mathcal{F})+\mathrm{Im}Z_1\,\Delta^+\mathcal{F}\,\mathrm{Re}M^-_1)\\
\mathrm{Re}S^0_1 &= -\tau\left.\frac{\partial\mathrm{Re}\varphi^0_1}{\partial t}\right|_0-\frac{\alpha\tau}{2\hbar}\Delta^-\mathrm{Im}\varphi^0_2-\frac{\gamma\tau}{2\hbar}\Delta^-\mathrm{Im}\varphi^3_2\\
\mathrm{Im}S^0_1 &= -\tau\left.\frac{\partial\mathrm{Im}\varphi^0_1}{\partial t}\right|_0+\frac{\alpha\tau}{2\hbar}\Delta^-(\mathrm{Re}\varphi^0_2-\varphi^0_0)+\frac{\gamma\tau}{2\hbar}\Delta^-(\mathrm{Re}\varphi^3_2-\varphi^3_0)\\
\mathrm{Re}S^1_1 &= -\tau\left.\frac{\partial\mathrm{Re}\varphi^1_1}{\partial t}\right|_0-\eta_2\mathrm{Re}\varphi^1_1-\frac{\alpha\tau}{2\hbar}\Delta^-\mathrm{Im}\varphi^1_2-\frac{2\gamma\tau}{\hbar}\mathrm{Re}\varphi^2_1+\frac{\gamma\tau}{2\hbar}\Delta^+(\mathrm{Re}\varphi^2_2+\varphi^2_0)\\
\mathrm{Im}S^1_1 &= -\tau\left.\frac{\partial\mathrm{Re}\varphi^1_1}{\partial t}\right|_0-\eta_2\mathrm{Im}\varphi^1_1+\frac{\alpha\tau}{2\hbar}\Delta^-(\mathrm{Re}\varphi^1_2-\varphi^1_0)-\frac{2\gamma\tau}{\hbar}\mathrm{Im}\varphi^2_1+\frac{\gamma\tau}{2\hbar}\Delta^+\mathrm{Im}\varphi^2_2\\
\mathrm{Re}S^2_1 &= -\tau\left.\frac{\partial\mathrm{Re}\varphi^2_1}{\partial t}\right|_0-\eta_2\mathrm{Re}\varphi^2_1-\frac{\alpha\tau}{2\hbar}\Delta^-\mathrm{Im}\varphi^2_2+\frac{2\gamma\tau}{\hbar}\mathrm{Re}\varphi^1_1-\frac{\gamma\tau}{2\hbar}\Delta^+(\mathrm{Re}\varphi^1_2+\varphi^1_0)\\
\mathrm{Im}S^2_1 &= -\tau\left.\frac{\partial\mathrm{Re}\varphi^2_1}{\partial t}\right|_0-\eta_2\mathrm{Im}\varphi^2_1+\frac{\alpha\tau}{2\hbar}\Delta^-(\mathrm{Re}\varphi^2_2-\varphi^2_0)+\frac{2\gamma\tau}{\hbar}\mathrm{Im}\varphi^1_1-\frac{\gamma\tau}{2\hbar}\Delta^+\mathrm{Im}\varphi^1_2\\
\mathrm{Re}S^3_1 &= -\tau\left.\frac{\partial\mathrm{Re}\varphi^3_1}{\partial t}\right|_0-\eta_2(\mathrm{Re}\varphi^3_1+\mathrm{Re}\varphi^0_1)-\frac{\alpha\tau}{2\hbar}\Delta^-\mathrm{Im}\varphi^3_2-\frac{\gamma\tau}{2\hbar}\Delta^-\mathrm{Im}\varphi^0_2\\
\mathrm{Im}S^3_1 &= -\tau\left.\frac{\partial\mathrm{Im}\varphi^3_1}{\partial t}\right|_0-\eta_2(\mathrm{Im}\varphi^3_1+\mathrm{Im}\varphi^0_1)+\frac{\alpha\tau}{2\hbar}\Delta^-(\mathrm{Re}\varphi^3_2-\varphi^3_0)+\frac{\gamma\tau}{2\hbar}\Delta^-(\mathrm{Re}\varphi^0_2-\varphi^0_0)
\end{aligned}
$$

Where the real and imaginary parts of φ_j are:

$$
\begin{aligned}
\mathrm{Re}\varphi_j^0 &= \frac{\phi_j^+ + \phi_j^-}{2}\left[\frac{1}{1+\vartheta_j^2} - \eta_1\delta^2(\Delta_j^-\mathcal{F})^2(\mathrm{Re}M_j^+\mathrm{Re}Z_j - \mathrm{Im}M_j^+\mathrm{Im}Z_j)\right] - \\
&\quad \frac{\eta_1\delta^2}{2}(\phi_j^+ - \phi_j^-)\Delta_j^+\mathcal{F}\Delta_j^-\mathcal{F}\mathrm{Im}Z_j \\
\mathrm{Im}\varphi_j^0 &= \frac{\phi_j^+ + \phi_j^-}{2}\left[\frac{-\vartheta_j}{1+\vartheta_j^2} - \eta_1\delta^2(\Delta_j^-\mathcal{F})^2(\mathrm{Re}M_j^+\mathrm{Im}Z_j + \mathrm{Im}M_j^+\mathrm{Re}Z_j)\right] + \\
&\quad \frac{\eta_1\delta^2}{2}(\phi_j^+ - \phi_j^-)\Delta_j^+\mathcal{F}\Delta_j^-\mathcal{F}\mathrm{Re}Z_j \\
\mathrm{Re}\varphi_j^1 &= \frac{\eta_1\delta}{2}\left[-(\phi_j^+ + \phi_j^-)\Delta_j^-\mathcal{F}(\mathrm{Im}M_j^+(\mathrm{Re}Z_j - \vartheta_j\mathrm{Im}Z_j) + \right. \\
&\quad \left.\mathrm{Re}M_j^+(\mathrm{Im}Z_j + \vartheta_j\mathrm{Re}Z_j)) + (\phi_j^+ - \phi_j^-)\Delta_j^+\mathcal{F}(\mathrm{Re}Z_j - \vartheta_j\mathrm{Im}Z_j)\right] \\
\mathrm{Im}\varphi_j^1 &= \frac{\eta_1\delta}{2}\left[(\phi_j^+ + \phi_j^-)\Delta_j^-\mathcal{F}(\mathrm{Re}M_j^+(\mathrm{Re}Z_j - \vartheta_j\mathrm{Im}Z_j) - \right. \\
&\quad \left.\mathrm{Im}M_j^+(\mathrm{Im}Z_j + \vartheta_j\mathrm{Re}Z_j)) + (\phi_j^+ - \phi_j^-)\Delta_j^+\mathcal{F}(\mathrm{Im}Z_j + \vartheta_j\mathrm{Re}Z_j)\right] \\
\mathrm{Re}\varphi_j^2 &= \frac{\eta_1\delta}{2}\left[(\phi_j^+ + \phi_j^-)\Delta_j^-\mathcal{F}(\mathrm{Im}Z_j + \vartheta_j\mathrm{Re}Z_j) + \right. \\
&\quad \left.(\phi_j^+ - \phi_j^-)\Delta_j^+\mathcal{F}(\mathrm{Re}M_j^-(\mathrm{Re}Z_j - \vartheta_j\mathrm{Im}Z_j) - \mathrm{Im}M_j^-(\mathrm{Im}Z_j + \vartheta_j\mathrm{Re}Z_j))\right] \\
\mathrm{Im}\varphi_j^2 &= \frac{\eta_1\delta}{2}\left[(\phi_j^+ + \phi_j^-)\Delta_j^-\mathcal{F}(-\mathrm{Re}Z_j + \vartheta_j\mathrm{Im}Z_j) + \right. \\
&\quad \left.(\phi_j^+ - \phi_j^-)\Delta_j^+\mathcal{F}(\mathrm{Re}M_j^-(\mathrm{Im}Z_j + \vartheta_j\mathrm{Re}Z_j) + \mathrm{Im}M_j^-(\mathrm{Re}Z_j - \vartheta_j\mathrm{Im}Z_j))\right] \\
\mathrm{Re}\varphi_j^3 &= \frac{\phi_j^+ - \phi_j^-}{2}\left[\frac{1}{1+\vartheta_j^2} - \eta_1\delta^2(\Delta_j^+\mathcal{F})^2(\mathrm{Re}M_j^-\mathrm{Re}Z_j - \mathrm{Im}M_j^-\mathrm{Im}Z_j)\right] - \\
&\quad \frac{\eta_1\delta^2}{2}(\phi_j^+ + \phi_j^-)\Delta_j^+\mathcal{F}\Delta_j^-\mathcal{F}\mathrm{Im}Z_j \\
\mathrm{Im}\varphi_j^3 &= \frac{\phi_j^+ - \phi_j^-}{2}\left[\frac{-\vartheta_j}{1+\vartheta_j^2} - \eta_1\delta^2(\Delta_j^+\mathcal{F})^2(\mathrm{Re}M_j^-\mathrm{Im}Z_j + \mathrm{Im}M_j^-\mathrm{Re}Z_j)\right] + \\
&\quad \frac{\eta_1\delta^2}{2}(\phi_j^+ + \phi_j^-)\Delta_j^+\mathcal{F}\Delta_j^-\mathcal{F}\mathrm{Re}Z_j
\end{aligned}
$$

Now we can obtain the expressions for $\left.\frac{\partial \varphi_j}{\partial t}\right|_0$:

$$
\begin{aligned}
\left.\frac{\partial \mathrm{Re}\varphi_1^0}{\partial t}\right|_0 &= \frac{1}{2}\left((\phi_1^+)'\left.\frac{\partial n^+}{\partial t}\right|_0 + (\phi_1^-)'\left.\frac{\partial n^-}{\partial t}\right|_0\right)\times \\
&\left[\frac{1}{1+\vartheta_1^2} - \eta_1\delta^2(\Delta^-\mathcal{F})^2\left(\mathrm{Re}M_1^+\mathrm{Re}Z_1 - \mathrm{Im}M_1^+\mathrm{Im}Z_1\right)\right] + \\
&\frac{1}{2}(\phi_1^+ + \phi_1^-)\left[\frac{-2\vartheta_1}{(1+\vartheta_1^2)^2}\left.\frac{\partial \vartheta_1}{\partial t}\right|_0 - \right. \\
&2\eta_1\delta^2\Delta^-\mathcal{F}\Delta^-\left.\frac{\partial \mathcal{F}}{\partial t}\right|_0\left(\mathrm{Re}M_1^+\mathrm{Re}Z_1 - \mathrm{Im}M_1^+\mathrm{Im}Z_1\right) - \\
&\eta_1\delta^2(\Delta^-\mathcal{F})^2\left(\left.\frac{\partial \mathrm{Re}M_1^+}{\partial t}\right|_0\mathrm{Re}Z_1 + \mathrm{Re}M_1^+\left.\frac{\partial \mathrm{Re}Z_1}{\partial t}\right|_0 - \mathrm{Im}Z_1\left.\frac{\partial \mathrm{Im}M_1^+}{\partial t}\right|_0 - \right. \\
&\left.\left.\mathrm{Im}M_1^+\left.\frac{\partial \mathrm{Im}Z_1}{\partial t}\right|_0\right)\right] - \frac{\eta_1\delta^2}{2}\left(\left((\phi_1^+)'\left.\frac{\partial n^+}{\partial t}\right|_0 - (\phi_1^-)'\left.\frac{\partial n^-}{\partial t}\right|_0\right)\Delta^+\mathcal{F}\Delta^-\mathcal{F}\mathrm{Im}Z_1 - \right. \\
&(\phi_1^+ - \phi_1^-)\left(\Delta^+\left.\frac{\partial \mathcal{F}}{\partial t}\right|_0\Delta^-\mathcal{F}\mathrm{Im}Z_1 + \Delta^-\left.\frac{\partial \mathcal{F}}{\partial t}\right|_0\Delta^+\mathcal{F}\mathrm{Im}Z_1 + \right. \\
&\left.\left.\left.\frac{\partial \mathrm{Im}Z_1}{\partial t}\right|_0\Delta^+\mathcal{F}\Delta^-\mathcal{F}\right)\right) \\
\left.\frac{\partial \mathrm{Im}\varphi_1^0}{\partial t}\right|_0 &= \frac{1}{2}\left((\phi_1^+)'\left.\frac{\partial n^+}{\partial t}\right|_0 + (\phi_1^-)'\left.\frac{\partial n^-}{\partial t}\right|_0\right)\times \\
&\left[\frac{-\vartheta_1}{1+\vartheta_1^2} - \eta_1\delta^2(\Delta^-\mathcal{F})^2\left(\mathrm{Re}M_1^+\mathrm{Im}Z_1 + \mathrm{Im}M_1^+\mathrm{Re}Z_1\right)\right] + \\
&\frac{1}{2}(\phi_1^+ + \phi_1^-)\left[\frac{\vartheta_1^2-1}{(1+\vartheta_1^2)^2}\left.\frac{\partial \vartheta_1}{\partial t}\right|_0 - \right. \\
&2\eta_1\delta^2\Delta^-\mathcal{F}\Delta^-\left.\frac{\partial \mathcal{F}}{\partial t}\right|_0\left(\mathrm{Re}M_1^+\mathrm{Im}Z_1 + \mathrm{Im}M_1^+\mathrm{Re}Z_1\right) - \\
&\eta_1\delta^2(\Delta^-\mathcal{F})^2\left(\left.\frac{\partial \mathrm{Re}M_1^+}{\partial t}\right|_0\mathrm{Im}Z_1 + \mathrm{Re}M_1^+\left.\frac{\partial \mathrm{Im}Z_1}{\partial t}\right|_0 + \mathrm{Re}Z_1\left.\frac{\partial \mathrm{Im}M_1^+}{\partial t}\right|_0 - \right. \\
&\left.\left.\mathrm{Im}M_1^+\left.\frac{\partial \mathrm{Re}Z_1}{\partial t}\right|_0\right)\right] + \frac{\eta_1\delta^2}{2}\left(\left((\phi_1^+)'\left.\frac{\partial n^+}{\partial t}\right|_0 - (\phi_1^-)'\left.\frac{\partial n^-}{\partial t}\right|_0\right)\Delta^+\mathcal{F}\Delta^-\mathcal{F}\mathrm{Re}Z_1 + \right. \\
&(\phi_1^+ - \phi_1^-)\left(\Delta^+\left.\frac{\partial \mathcal{F}}{\partial t}\right|_0\Delta^-\mathcal{F}\mathrm{Re}Z_1 + \Delta^-\left.\frac{\partial \mathcal{F}}{\partial t}\right|_0\Delta^+\mathcal{F}\mathrm{Re}Z_1 + \right. \\
&\left.\left.\left.\frac{\partial \mathrm{Re}Z_1}{\partial t}\right|_0\Delta^+\mathcal{F}\Delta^-\mathcal{F}\right)\right)
\end{aligned}
$$

$$
\begin{aligned}
\left.\frac{\partial \mathrm{Re}\varphi_1^1}{\partial t}\right|_0 &= \frac{\eta_1\delta}{2}\left[-\left((\phi_1^+)'\left.\frac{\partial n^+}{\partial t}\right|_0+(\phi_1^-)'\left.\frac{\partial n^-}{\partial t}\right|_0\right)\Delta^-\mathcal{F}(\mathrm{Im}M_1^+(\mathrm{Re}Z_1-\vartheta_1\mathrm{Im}Z_1)+\right.\\
&\mathrm{Re}M_1^+(\mathrm{Im}Z_1+\vartheta_1\mathrm{Re}Z_1))-(\phi_1^++\phi_1^-)\Delta^-\left.\frac{\partial\mathcal{F}}{\partial t}\right|_0\times\\
&(\mathrm{Im}M_1^+(\mathrm{Re}Z_1-\vartheta_1\mathrm{Im}Z_1)+\mathrm{Re}M_1^+(\mathrm{Im}Z_1+\vartheta_1\mathrm{Re}Z_1))-\\
&(\phi_1^++\phi_1^-)\Delta^-\mathcal{F}\left(\left.\frac{\partial \mathrm{Im}M_1^+}{\partial t}\right|_0(\mathrm{Re}Z_1-\vartheta_1\mathrm{Im}Z_1)+\right.\\
&\mathrm{Im}M_1^+\left(\left.\frac{\partial\mathrm{Re}Z_1}{\partial t}\right|_0-\left.\frac{\partial\vartheta_1}{\partial t}\right|_0\mathrm{Im}Z_1-\vartheta_1\left.\frac{\partial\mathrm{Im}Z_1}{\partial t}\right|_0\right)+\\
&\left.\frac{\partial\mathrm{Re}M_1^+}{\partial t}\right|_0(\mathrm{Im}Z_1+\vartheta_1\mathrm{Re}Z_1)+\mathrm{Re}M_1^+\left(\left.\frac{\partial\mathrm{Im}Z_1}{\partial t}\right|_0+\left.\frac{\partial\vartheta_1}{\partial t}\right|_0\mathrm{Re}Z_1+\right.\\
&\left.\left.\vartheta_1\left.\frac{\partial\mathrm{Re}Z_1}{\partial t}\right|_0\right)\right)+\left((\phi_1^+)'\left.\frac{\partial n^+}{\partial t}\right|_0-(\phi_1^-)'\left.\frac{\partial n^-}{\partial t}\right|_0\right)\Delta^+\mathcal{F}(\mathrm{Re}Z_1-\vartheta_1\mathrm{Im}Z_1)+\\
&(\phi_1^+-\phi_1^-)\left(\Delta^+\left.\frac{\partial\mathcal{F}}{\partial t}\right|_0(\mathrm{Re}Z_1-\vartheta_1\mathrm{Im}Z_1)+\right.\\
&\left.\left.\Delta^+\mathcal{F}\left(\left.\frac{\partial\mathrm{Re}Z_1}{\partial t}\right|_0-\left.\frac{\partial\vartheta_1}{\partial t}\right|_0\mathrm{Im}Z_1-\vartheta_1\left.\frac{\partial\mathrm{Im}Z_1}{\partial t}\right|_0\right)\right)\right]\\
\left.\frac{\partial \mathrm{Im}\varphi_1^1}{\partial t}\right|_0 &= \frac{\eta_1\delta}{2}\left[\left((\phi_1^+)'\left.\frac{\partial n^+}{\partial t}\right|_0+(\phi_1^-)'\left.\frac{\partial n^-}{\partial t}\right|_0\right)\Delta^-\mathcal{F}(\mathrm{Re}M_1^+(\mathrm{Re}Z_1-\vartheta_1\mathrm{Im}Z_1)-\right.\\
&\mathrm{Im}M_1^+(\mathrm{Im}Z_1+\vartheta_1\mathrm{Re}Z_1))+(\phi_1^++\phi_1^-)\Delta^-\left.\frac{\partial\mathcal{F}}{\partial t}\right|_0\times\\
&(\mathrm{Re}M_1^+(\mathrm{Re}Z_1-\vartheta_1\mathrm{Im}Z_1)-\mathrm{Im}M_1^+(\mathrm{Im}Z_1+\vartheta_1\mathrm{Re}Z_1))-\\
&(\phi_1^++\phi_1^-)\Delta^-\mathcal{F}\left(\left.\frac{\partial \mathrm{Re}M_1^+}{\partial t}\right|_0(\mathrm{Re}Z_1-\vartheta_1\mathrm{Im}Z_1)+\right.\\
&\mathrm{Re}M_1^+\left(\left.\frac{\partial\mathrm{Re}Z_1}{\partial t}\right|_0-\left.\frac{\partial\vartheta_1}{\partial t}\right|_0\mathrm{Im}Z_1-\vartheta_1\left.\frac{\partial\mathrm{Im}Z_1}{\partial t}\right|_0\right)-\\
&\left.\frac{\partial\mathrm{Im}M_1^+}{\partial t}\right|_0(\mathrm{Im}Z_1+\vartheta_1\mathrm{Re}Z_1)-\mathrm{Im}M_1^+\left(\left.\frac{\partial\mathrm{Im}Z_1}{\partial t}\right|_0+\left.\frac{\partial\vartheta_1}{\partial t}\right|_0\mathrm{Re}Z_1+\right.\\
&\left.\left.\vartheta_1\left.\frac{\partial\mathrm{Re}Z_1}{\partial t}\right|_0\right)\right)+\left((\phi_1^+)'\left.\frac{\partial n^+}{\partial t}\right|_0-(\phi_1^-)'\left.\frac{\partial n^-}{\partial t}\right|_0\right)\Delta^+\mathcal{F}(\vartheta_1\mathrm{Re}Z_1+\mathrm{Im}Z_1)+\\
&(\phi_1^+-\phi_1^-)\left(\Delta^+\left.\frac{\partial\mathcal{F}}{\partial t}\right|_0(\vartheta_1\mathrm{Re}Z_1+\mathrm{Im}Z_1)+\right.\\
&\left.\left.\Delta^+\mathcal{F}\left(\vartheta_1\left.\frac{\partial\mathrm{Re}Z_1}{\partial t}\right|_0+\left.\frac{\partial\vartheta_1}{\partial t}\right|_0\mathrm{Re}Z_1+\left.\frac{\partial\mathrm{Im}Z_1}{\partial t}\right|_0\right)\right)\right]
\end{aligned}
$$

$$
\begin{aligned}
\left.\frac{\partial \mathrm{Re}\varphi_1^2}{\partial t}\right|_0 &= \frac{\eta_1\delta}{2}\left[\left(\left((\phi_1^+)'\left.\frac{\partial n^+}{\partial t}\right|_0+(\phi_1^-)'\left.\frac{\partial n^-}{\partial t}\right|_0\right)\Delta^-\mathcal{F}+(\phi_1^++\phi_1^-)\Delta^-\left.\frac{\partial\mathcal{F}}{\partial t}\right|_0\right)\times\right.\\
&(\mathrm{Im}Z_1+\vartheta_1\mathrm{Re}Z_1)+(\phi_1^++\phi_1^-)\Delta^-\mathcal{F}\left(\left.\frac{\partial \mathrm{Im}Z_1}{\partial t}\right|_0+\left.\frac{\partial\vartheta_1}{\partial t}\right|_0\mathrm{Re}Z_1+\vartheta_1\left.\frac{\partial\mathrm{Re}Z_1}{\partial t}\right|_0\right)+\\
&\left(\left((\phi_1^+)'\left.\frac{\partial n^+}{\partial t}\right|_0-(\phi_1^-)'\left.\frac{\partial n^-}{\partial t}\right|_0\right)\Delta^+\mathcal{F}+(\phi_1^+-\phi_1^-)\Delta^+\left.\frac{\partial\mathcal{F}}{\partial t}\right|_0\right)\times\\
&(\mathrm{Re}M_1^-(\mathrm{Re}Z_1-\vartheta_1\mathrm{Im}Z_1)-\mathrm{Im}M_1^-(\mathrm{Im}Z_1+\vartheta_1\mathrm{Re}Z_1))+\\
&(\phi_1^+-\phi_1^-)\Delta^+\mathcal{F}\left(\left.\frac{\partial\mathrm{Re}M_1^-}{\partial t}\right|_0(\mathrm{Re}Z_1-\vartheta_1\mathrm{Im}Z_1)+\mathrm{Re}M_1^-\left(\left.\frac{\partial\mathrm{Re}Z_1}{\partial t}\right|_0-\right.\right.\\
&\left.\left.\left.\frac{\partial\vartheta_1}{\partial t}\right|_0\mathrm{Im}Z_1-\vartheta_1\left.\frac{\partial\mathrm{Im}Z_1}{\partial t}\right|_0\right)-\left.\frac{\partial\mathrm{Im}M_1^-}{\partial t}\right|_0(\mathrm{Im}Z_1+\vartheta_1\mathrm{Re}Z_1)-\right.\\
&\left.\mathrm{Im}M_1^-\left(\left.\frac{\partial\mathrm{Im}Z_1}{\partial t}\right|_0+\left.\frac{\partial\vartheta_1}{\partial t}\right|_0\mathrm{Re}Z_1+\vartheta_1\left.\frac{\partial\mathrm{Re}Z_1}{\partial t}\right|_0\right)\right)\Bigg]\\
\left.\frac{\partial \mathrm{Im}\varphi_1^2}{\partial t}\right|_0 &= \frac{\eta_1\delta}{2}\left[\left(\left((\phi_1^+)'\left.\frac{\partial n^+}{\partial t}\right|_0+(\phi_1^-)'\left.\frac{\partial n^-}{\partial t}\right|_0\right)\Delta^-\mathcal{F}+(\phi_1^++\phi_1^-)\Delta^-\left.\frac{\partial\mathcal{F}}{\partial t}\right|_0\right)\times\right.\\
&(-\mathrm{Re}Z_1+\vartheta_1\mathrm{Im}Z_1)+(\phi_1^++\phi_1^-)\Delta^-\mathcal{F}\left(-\left.\frac{\partial \mathrm{Re}Z_1}{\partial t}\right|_0+\left.\frac{\partial\vartheta_1}{\partial t}\right|_0\mathrm{Im}Z_1+\vartheta_1\left.\frac{\partial\mathrm{Im}Z_1}{\partial t}\right|_0\right)+\\
&\left(\left((\phi_1^+)'\left.\frac{\partial n^+}{\partial t}\right|_0-(\phi_1^-)'\left.\frac{\partial n^-}{\partial t}\right|_0\right)\Delta^+\mathcal{F}+(\phi_1^+-\phi_1^-)\Delta^+\left.\frac{\partial\mathcal{F}}{\partial t}\right|_0\right)\times\\
&(\mathrm{Re}M_1^-(\mathrm{Im}Z_1+\vartheta_1\mathrm{Re}Z_1)+\mathrm{Im}M_1^-(\mathrm{Re}Z_1-\vartheta_1\mathrm{Im}Z_1))+\\
&(\phi_1^+-\phi_1^-)\Delta^+\mathcal{F}\left(\left.\frac{\partial\mathrm{Re}M_1^-}{\partial t}\right|_0(\mathrm{Im}Z_1+\vartheta_1\mathrm{Re}Z_1)+\mathrm{Re}M_1^-\left(\left.\frac{\partial\mathrm{Im}Z_1}{\partial t}\right|_0+\right.\right.\\
&\left.\left.\left.\frac{\partial\vartheta_1}{\partial t}\right|_0\mathrm{Re}Z_1+\vartheta_1\left.\frac{\partial\mathrm{Re}Z_1}{\partial t}\right|_0\right)+\left.\frac{\partial\mathrm{Im}M_1^-}{\partial t}\right|_0(\mathrm{Re}Z_1-\vartheta_1\mathrm{Im}Z_1)+\right.\\
&\left.\mathrm{Im}M_1^-\left(\left.\frac{\partial\mathrm{Re}Z_1}{\partial t}\right|_0-\left.\frac{\partial\vartheta_1}{\partial t}\right|_0\mathrm{Im}Z_1-\vartheta_1\left.\frac{\partial\mathrm{Im}Z_1}{\partial t}\right|_0\right)\right)\Bigg]
\end{aligned}
$$

$$
\begin{aligned}
\left.\frac{\partial \mathrm{Re}\varphi_1^3}{\partial t}\right|_0 &= \frac{1}{2}\left((\phi_1^+)'\left.\frac{\partial n^+}{\partial t}\right|_0 - (\phi_1^-)'\left.\frac{\partial n^-}{\partial t}\right|_0\right)\times \\
&\left[\frac{1}{1+\vartheta_1^2} - \eta_1\delta^2(\Delta^+\mathcal{F})^2\left(\mathrm{Re}M_1^-\mathrm{Re}Z_1 - \mathrm{Im}M_1^-\mathrm{Im}Z_1\right)\right] + \\
&\frac{1}{2}(\phi_1^+ - \phi_1^-)\left[\frac{-2\vartheta_1}{(1+\vartheta_1^2)^2}\left.\frac{\partial\vartheta_1}{\partial t}\right|_0 - \right. \\
&2\eta_1\delta^2\Delta^+\mathcal{F}\Delta^+\left.\frac{\partial\mathcal{F}}{\partial t}\right|_0\left(\mathrm{Re}M_1^-\mathrm{Re}Z_1 - \mathrm{Im}M_1^-\mathrm{Im}Z_1\right) - \\
&\eta_1\delta^2(\Delta^+\mathcal{F})^2\left(\left.\frac{\partial \mathrm{Re}M_1^-}{\partial t}\right|_0\mathrm{Re}Z_1 - \mathrm{Re}M_1^-\left.\frac{\partial \mathrm{Re}Z_1}{\partial t}\right|_0 - \mathrm{Im}Z_1\left.\frac{\partial \mathrm{Im}M_1^-}{\partial t}\right|_0 - \right. \\
&\left.\left.\mathrm{Im}M_1^-\left.\frac{\partial \mathrm{Im}Z_1}{\partial t}\right|_0\right)\right] - \\
&\frac{\eta_1\delta^2}{2}\left(\left((\phi_1^+)'\left.\frac{\partial n^+}{\partial t}\right|_0 + (\phi_1^-)'\left.\frac{\partial n^-}{\partial t}\right|_0\right)\Delta^+\mathcal{F}\Delta^-\mathcal{F}\mathrm{Im}Z_1 + \right. \\
&(\phi_1^+ + \phi_1^-)\left(\Delta^+\left.\frac{\partial\mathcal{F}}{\partial t}\right|_0\Delta^-\mathcal{F}\mathrm{Im}Z_1 + \Delta^-\left.\frac{\partial\mathcal{F}}{\partial t}\right|_0\Delta^+\mathcal{F}\mathrm{Im}Z_1 + \right. \\
&\left.\left.\left.\frac{\partial \mathrm{Im}Z_1}{\partial t}\right|_0\Delta^+\mathcal{F}\Delta^-\mathcal{F}\right)\right) \\
\left.\frac{\partial \mathrm{Im}\varphi_1^3}{\partial t}\right|_0 &= \frac{1}{2}\left((\phi_1^+)'\left.\frac{\partial n^+}{\partial t}\right|_0 + (\phi_1^-)'\left.\frac{\partial n^-}{\partial t}\right|_0\right)\times \\
&\left[\frac{-\vartheta_1}{1+\vartheta_1^2} - \eta_1\delta^2(\Delta^+\mathcal{F})^2\left(\mathrm{Re}M_1^-\mathrm{Im}Z_1 + \mathrm{Im}M_1^-\mathrm{Re}Z_1\right)\right] + \\
&\frac{1}{2}(\phi_1^+ - \phi_1^-)\left[\frac{\vartheta_1^2-1}{(1+\vartheta_1^2)^2}\left.\frac{\partial\vartheta_1}{\partial t}\right|_0 - \right. \\
&2\eta_1\delta^2\Delta^+\mathcal{F}\Delta^+\left.\frac{\partial\mathcal{F}}{\partial t}\right|_0\left(\mathrm{Re}M_1^-\mathrm{Im}Z_1 + \mathrm{Im}M_1^-\mathrm{Re}Z_1\right) - \\
&\eta_1\delta^2(\Delta^+\mathcal{F})^2\left(\left.\frac{\partial \mathrm{Re}M_1^-}{\partial t}\right|_0\mathrm{Im}Z_1 + \mathrm{Re}M_1^-\left.\frac{\partial \mathrm{Im}Z_1}{\partial t}\right|_0 + \mathrm{Re}Z_1\left.\frac{\partial \mathrm{Im}M_1^-}{\partial t}\right|_0 + \right. \\
&\left.\left.\mathrm{Im}M_1^-\left.\frac{\partial \mathrm{Re}Z_1}{\partial t}\right|_0\right)\right] + \\
&\frac{\eta_1\delta^2}{2}\left(\left((\phi_1^+)'\left.\frac{\partial n^+}{\partial t}\right|_0 + (\phi_1^-)'\left.\frac{\partial n^-}{\partial t}\right|_0\right)\Delta^+\mathcal{F}\Delta^-\mathcal{F}\mathrm{Re}Z_1 + \right. \\
&(\phi_1^+ + \phi_1^-)\left(\Delta^+\left.\frac{\partial\mathcal{F}}{\partial t}\right|_0\Delta^-\mathcal{F}\mathrm{Re}Z_1 + \Delta^-\left.\frac{\partial\mathcal{F}}{\partial t}\right|_0\Delta^+\mathcal{F}\mathrm{Re}Z_1 + \right. \\
&\left.\left.\left.\frac{\partial \mathrm{Re}Z_1}{\partial t}\right|_0\Delta^+\mathcal{F}\Delta^-\mathcal{F}\right)\right)
\end{aligned}
$$

In the above expressions we have used $(\phi_1^{\pm})' = \partial\phi_1^{\pm}/\partial n^{\pm}$ and $\partial\vartheta_1/\partial t|_0 = \langle \partial\mathcal{F}/\partial t|_0 \rangle_1$. We also need to calculate Z_j, $M_j^{\pm}$, $\partial Z_1/\partial t|_0$ and $\partial M_1^{\pm}/\partial t\Big|_0$:

$$\begin{aligned} \mathrm{Re}Z_j &= \frac{Z_{j1}}{Z_{j1}^2 + Z_{j2}^2} \\ \mathrm{Im}Z_j &= \frac{Z_{j2}}{Z_{j1}^2 + Z_{j2}^2} \end{aligned}$$

Where the functionals $Z_{j1}(F)$ and $Z_{j2}(F)$ are as follows:

$$\begin{aligned} Z_{j1} &= 1 - 6\vartheta_j^2 + \vartheta_j^4 + (1-\vartheta_j^2)\left(\eta_1^2 + \delta^2\left((\Delta_j^-\mathcal{F})^2 + (\Delta_j^+\mathcal{F})^2\right)\right) + \delta^4\left(\Delta_j^-\mathcal{F}\,\Delta_j^+\mathcal{F}\right)^2 \\ Z_{j2} &= -2\vartheta_j\left(2 + \eta_1^2 + \delta^2\left((\Delta_j^-\mathcal{F})^2 + (\Delta_j^+\mathcal{F})^2\right) - 2\vartheta_j^2\right) \end{aligned}$$

Therefore, the time derivative $\left.\dfrac{\partial Z_1}{\partial t}\right|_0$ is as follows:

$$\begin{aligned} \left.\frac{\partial \mathrm{Re}Z_1}{\partial t}\right|_0 &= \frac{(Z_{12}^2 - Z_{11}^2)\left.\dfrac{\partial Z_{11}}{\partial t}\right|_0 - 2Z_{11}Z_{12}\left.\dfrac{\partial Z_{12}}{\partial t}\right|_0}{(Z_{11}^2 + Z_{12}^2)^2} \\ \left.\frac{\partial \mathrm{Im}Z_1}{\partial t}\right|_0 &= \frac{(Z_{11}^2 - Z_{12}^2)\left.\dfrac{\partial Z_{12}}{\partial t}\right|_0 - 2Z_{11}Z_{12}\left.\dfrac{\partial Z_{11}}{\partial t}\right|_0}{(Z_{11}^2 + Z_{12}^2)^2} \end{aligned}$$

Where the time derivatives $\left.\dfrac{\partial Z_{11}}{\partial t}\right|_0$ and $\left.\dfrac{\partial Z_{12}}{\partial t}\right|_0$ are as follows:

$$\begin{aligned} \left.\frac{\partial Z_{11}}{\partial t}\right|_0 &= 4(\vartheta_1^3 - 3\vartheta_1)\left.\frac{\partial\vartheta_1}{\partial t}\right|_0 + 2(1-\vartheta_1^2)\left(\delta^2\left(\Delta^+\mathcal{F}\Delta^+\left.\frac{\partial\mathcal{F}}{\partial t}\right|_0 + \Delta^-\mathcal{F}\Delta^-\left.\frac{\partial\mathcal{F}}{\partial t}\right|_0\right) - \right. \\ &\quad \left. \vartheta_1\left.\frac{\partial\vartheta_1}{\partial t}\right|_0 (\eta_1^2 + \delta^2((\Delta^-\mathcal{F})^2 + (\Delta^+\mathcal{F})^2)\right) + \\ &\quad 2\delta^4\Delta^+\mathcal{F}\Delta^-\mathcal{F}\left(\Delta^+\mathcal{F}\,\Delta^-\left.\frac{\partial\mathcal{F}}{\partial t}\right|_0 + \Delta^-\mathcal{F}\,\Delta^+\left.\frac{\partial\mathcal{F}}{\partial t}\right|_0\right) \\ \left.\frac{\partial Z_{12}}{\partial t}\right|_0 &= -2\left[\left.\frac{\partial\vartheta_1}{\partial t}\right|_0 (2 + \eta_1^2 + \delta^2\left((\Delta^-\mathcal{F})^2 + (\Delta^+\mathcal{F})^2\right) - 2\vartheta_1^2) + \right. \\ &\quad \left. 2\vartheta_1\left(\delta^2\left(\Delta^+\mathcal{F}\,\Delta^-\left.\frac{\partial\mathcal{F}}{\partial t}\right|_0 + \Delta^-\mathcal{F}\,\Delta^+\left.\frac{\partial\mathcal{F}}{\partial t}\right|_0\right) - 2\vartheta_1\left.\frac{\partial\vartheta_1}{\partial t}\right|_0\right)\right] \end{aligned}$$

The functionals $M_j^{\pm}(F)$ are as follows:

$$\begin{aligned}
\mathrm{Re}M_j^{\pm} &= \frac{1}{\eta_1}\left[1+\frac{\delta^2(\Delta_j^{\pm}\mathcal{F})^2}{1+\vartheta_j^2}\right] \\
\mathrm{Im}M_j^{\pm} &= \frac{1}{\eta_1}\left[\vartheta_j-\frac{\delta^2\vartheta_j(\Delta_j^{\pm}\mathcal{F})^2}{1+\vartheta_j^2}\right]
\end{aligned}$$

Finally, we need to calculate the time derivative $\left.\frac{\partial M_1^{\pm}}{\partial t}\right|_0$:

$$\begin{aligned}
\left.\frac{\partial \mathrm{Re}M_1^{\pm}}{\partial t}\right|_0 &= \frac{2\delta^2\Delta^{\pm}\mathcal{F}}{\eta_1(1+\vartheta_1^2)}\left(\Delta^{\pm}\left.\frac{\partial\mathcal{F}}{\partial t}\right|_0-\frac{\vartheta_1\Delta^{\pm}\mathcal{F}}{1+\vartheta_1^2}\left.\frac{\partial\vartheta_1}{\partial t}\right|_0\right) \\
\left.\frac{\partial \mathrm{Im}M_1^{\pm}}{\partial t}\right|_0 &= \frac{1}{\eta_1}\left[\left.\frac{\partial\vartheta_1}{\partial t}\right|_0-\frac{\delta^2\Delta^{\pm}\mathcal{F}}{(1+\vartheta_1^2)^2}\left((1-\vartheta_1^2)\Delta^{\pm}\mathcal{F}\left.\frac{\partial\vartheta_1}{\partial t}\right|_0+2\vartheta_1(1+\vartheta_1^2)\Delta^{\pm}\left.\frac{\partial\mathcal{F}}{\partial t}\right|_0\right)\right]
\end{aligned}$$

Appendix E

Numerical method for the hydrodynamic equations describing spatially confined Bloch oscillations

E.1 Nondimensional equations

In order to solve numerically equation (4.66) we will first write it, after replacing n by $1 + \frac{\partial F}{\partial x}$, in the following way:

$$\frac{\partial F}{\partial t} + \mathcal{A}\,\frac{\partial F}{\partial x} + \mathcal{B}\,\frac{\partial^2 F}{\partial x^2} + \mathcal{C}\,J = \mathcal{D}, \tag{E.1}$$

where coefficients $\mathcal{A}$, $\mathcal{B}$, $\mathcal{C}$ and $\mathcal{D}$ are:

$$\begin{aligned}
\mathcal{A} &= \frac{\delta\gamma_e E_0 F}{F^2 + \delta^2\gamma_j\gamma_e} \\
\mathcal{B} &= -\frac{\delta^2\gamma_e}{2(F^2 + \delta^2\gamma_j\gamma_e)} \\
\mathcal{C} &= -1 + \frac{\delta^3\gamma_e E_0}{(F^2 + \delta^2\gamma_j\gamma_e)^3}\left[2\gamma_j F^2 + \gamma_e(F^2 - \delta^2\gamma_j\gamma_e)\right]\left(1 + \frac{\partial F}{\partial x}\right) \\
\mathcal{D} &= -\frac{\delta}{F^2 + \delta^2\gamma_j\gamma_e}\left[\gamma_e E_0 F + \frac{F}{2}\frac{\partial}{\partial x}\mathrm{Im}\left(\frac{f_{2,0}^{B(0)}}{1+2iF}\right) + \frac{\delta\gamma_e}{2}\frac{\partial}{\partial x}\mathrm{Re}\left(\frac{f_{2,0}^{B(0)}}{1+2iF}\right)\right]
\end{aligned} \tag{E.2}$$

Equation (E.1) must be solved together with the following equation for the complex amplitude A:

$$\frac{\partial A}{\partial t} = -\frac{\gamma_e + \gamma_j}{2} A + \frac{1}{2i}\frac{\partial}{\partial x}\left(\frac{f_{2,-1}^{B(0)}}{1+iF}\right), \tag{E.3}$$

with the following boundary conditions at the cathode ($x = 0$):

$$\begin{aligned} \frac{\partial F}{\partial t} + \sigma_0 F &= J, \\ \frac{\partial A}{\partial x} &= 0, \end{aligned} \tag{E.4}$$

and at the anode ($x = L$):

$$\frac{\partial F}{\partial t} + \sigma_L n F = J, \tag{E.5}$$

together with the voltage bias integral constraint:

$$\frac{1}{L}\int_0^L F(x,t)\, dx = \phi, \tag{E.6}$$

The contact conductivity σ_0 must be selected so that $\sigma_0 F$ intersects the second branch of the drift velocity function $J(F)$, which can be obtained from equation (E.1) at the spatially homogeneous steady state limit (i.e. $\partial/\partial t = \partial/\partial x = 0$):

$$J\left(1 - \frac{\delta^3 \gamma_e E_0}{(F^2 + \delta^2 \gamma_j \gamma_e)^3}\left[2\gamma_j F^2 + \gamma_e (F^2 - \delta^2 \gamma_j \gamma_e)\right]\right) = \frac{\delta \gamma_e E_0 F}{F^2 + \delta^2 \gamma_j \gamma_e} \tag{E.7}$$

For calculating the Fourier coefficients $f_{2,0}^{B(0)}$ and $f_{2,-1}^{B(0)}$,:

$$f_{2,0}^{B(0)} = \frac{1}{(2\pi)^2}\int_{-\pi}^{\pi}\int_{-\pi}^{\pi} f^{B(0)}(k; n, f_1)\, e^{-2ik} dk\, d\theta, \tag{E.8}$$

$$f_{2,-1}^{B(0)} = \frac{1}{(2\pi)^2}\int_{-\pi}^{\pi}\int_{-\pi}^{\pi} f^{B(0)}(k; n, f_1)\, e^{-2ik+i\theta} dk\, d\theta, \tag{E.9}$$

we must first calculate the nondimensional multipliers $\tilde{\beta}(n, A, \theta)$ and $\tilde{u}(n, A, \theta)$, which depend on f_1, and can be obtained by solving the following equation:

$$G(\tilde{u}, \tilde{\beta}) = \frac{A(x,t)e^{-i\theta}}{n(x,t)}, \tag{E.10}$$

where

$$G(\tilde{u},\tilde{\beta}) = \frac{\int_0^\pi e^{\tilde{\beta}\cos K}\cosh(\tilde{u}K)cos(K)\,dK - i\int_0^\pi e^{\tilde{\beta}\cos K}\sinh(\tilde{u}K)sin(K)\,dK}{\int_0^\pi e^{\tilde{\beta}\cos K}\cosh(\tilde{u}K)\,dK}. \tag{E.11}$$

Once we have calculated $\tilde{\beta}$ and $\tilde{u}$ from (E.10), we can get $f_2^{B(0)}$:

$$f_2^{B(0)}(n,A,\theta) = \frac{1}{2\pi}\int_{-\pi}^{\pi} f^{B(0)}\,e^{-2ik}dk = \frac{n}{\tilde{\beta}}\left(\tilde{\beta} - \frac{2ie^{-\tilde{\beta}}\sinh(\pi\tilde{u})}{\int_0^\pi e^{\tilde{\beta}\cos K}\cosh(\tilde{u}K)\,dK} - 2(1+i\tilde{u})\,A\,e^{-i\theta}\right). \tag{E.12}$$

Therefore, coefficients $f_{2,0}^{B(0)}$ and $f_{2,-1}^{B(0)}$ will be:

$$\begin{aligned} f_{2,0}^{B(0)}(n,A) &= n\left(1 - \frac{i}{\pi}\int_{-\pi}^{\pi}\frac{e^{-\tilde{\beta}}\sinh(\pi\tilde{u})}{\tilde{\beta}\int_0^\pi e^{\tilde{\beta}\cos K}\cosh(\tilde{u}K)\,dK}\,d\theta\right) - \frac{A}{\pi}\int_{-\pi}^{\pi}\frac{(1+i\tilde{u})e^{-i\theta}}{\tilde{\beta}}\,d\theta, \\ f_{2,-1}^{B(0)}(n,A) &= -\frac{in}{\pi}\int_{-\pi}^{\pi}\frac{e^{-\tilde{\beta}}\sinh(\pi\tilde{u})}{\tilde{\beta}\int_0^\pi e^{\tilde{\beta}\cos K}\cosh(\tilde{u}K)\,dK}\,e^{i\theta}d\theta - \frac{A}{\pi}\int_{-\pi}^{\pi}\frac{(1+i\tilde{u})}{\tilde{\beta}}\,d\theta, \end{aligned} \tag{E.13}$$

E.2 Numerical scheme

Since equation (E.1) has an integral constraint as boundary condition (E.6), we will use an implicit numerical scheme similar to the one described and proved to converge in [26] for partial differential equations with an integral constraint. Since the electric field waves propagate from the cathode to the anode, we use backward differences for approximating spatial first derivatives, avoiding numerical instabilities, and the resulting differential equation is integrated in time by a first order implicit Euler method. This procedure leads to a system of $Nr+2$ linear equations for the $Nr+1$ values of the electric field (F_0 to F_{Nr}) plus the current density J at time t^{n+1}. In order to save computational effort we will set up the finite differences system of equations with a bidiagonal coefficients matrix, instead of tridiagonal, in the following way:

$$a_i F_{i-1}^{n+1} + b_i F_i^{n+1} + c_i J^{n+1} = g_i, \quad i = 1,\ldots,Nr-1 \tag{E.14}$$

where $r = l/h$. This means that we will move the diffusion term $\mathcal{B}\frac{\partial^2 F}{\partial x^2}$ to the RHS, and therefore the coefficients of (E.14) are:

$$\begin{aligned} a_i &= -k\,\mathcal{A}_i^n \\ b_i &= h + k\,\mathcal{A}_i^n \\ c_i &= hk\,\mathcal{C}_i^n \\ g_i &= h\,F_i^n + hk\,\mathcal{D}_i^n - k\,\mathcal{B}_i^n(F_{i+1}^n - 2F_i^n + F_{i-1}^n)/h, \end{aligned}$$

where $h = \Delta x$, $k = \Delta t$ and all the coefficients $\mathcal{A}$, $\mathcal{B}$, $\mathcal{C}$ and $\mathcal{D}$ of (E.1) are evaluated at time t^n.
The voltage bias integral constraint is solved by the Simpson's rule:

$$F_0^{n+1} + 4F_1^{n+1} + 2F_2^{n+1} + ... + 2F_{Nr-2}^{n+1} + 4F_{Nr-1}^{n+1} + F_{Nr}^{n+1} = 3V/h. \quad \text{(E.15)}$$

The boundary condition at the injector contact is:

$$(1 + \sigma_0\,k)F_0^{n+1} - k\,J^{n+1} = F_0^n, \quad \text{(E.16)}$$

and at the collector contact:

$$(-k\sigma_L F_{Nr}^n)F_{Nr-1}^{n+1} + (h + \sigma_L k(h + F_{Nr}^n))F_{Nr}^{n+1} - khJ^{n+1} = hF_{Nr}^n, \quad \text{(E.17)}$$

This system of $Nr + 2$ linear equations can be reduced to a simpler and smaller system, with the objective of finding a bidiagonal matrix, in the following way:

- The current density can be calculated directly from the boundary condition at the injector contact:

$$J^{n+1} = (\sigma_0 + \tfrac{1}{k})F_0^{n+1} - \tfrac{1}{k}F_0^n. \quad \text{(E.18)}$$

- The field at the anode can also be expressed in terms of F_0^{n+1} and F_{Nr-1}^{n+1}:

$$F_{Nr}^{n+1} = \frac{h(F_{Nr}^n - F_0^n) + h(1 + \sigma_0 k)F_0^{n+1} + (\sigma_L k F_{Nr}^n)F_{Nr-1}^{n+1})}{h + \sigma_L k(h + F_{Nr}^n)}. \quad \text{(E.19)}$$

- We can make the following factorization of the system of linear equations:

$$\mathbf{v}\,F_0^{n+1} + \mathbf{T}\cdot\mathbf{F} = \mathbf{g} \quad \text{(E.20)}$$

$$F_0^{n+1}(1 + \kappa_1) + \mathbf{u}\cdot\mathbf{F} = 3V/h - \kappa_2, \quad \text{(E.21)}$$

where coefficients κ_1 and κ_2 are:

$$\kappa_1 = \frac{h(1+\sigma_0 k)}{h+\sigma_L k(h+F^n_{Nr})},$$
$$\kappa_2 = \frac{h(F^n_{Nr}-F^n_0)}{h+\sigma_L k(h+F^n_{Nr})},$$

and $\mathbf{T}$ is the bidiagonal matrix:

$$\mathbf{T} = \begin{pmatrix} b_1 & \cdots & \cdots & \cdots & 0 \\ a_2 & b_2 & \cdots & \cdots & 0 \\ \cdots & \cdots & \cdots & \cdots & \cdots \\ 0 & \cdots & \cdots & a_{Nr-1} & b_{Nr-1} \end{pmatrix}$$

and vectors $\mathbf{F}$, $\mathbf{v}$, $\mathbf{g}$ and $\mathbf{u}$ are:

$$\mathbf{F} = \begin{pmatrix} F^{n+1}_1 \\ F^{n+1}_2 \\ \cdots \\ F^{n+1}_{Nr-1} \end{pmatrix}, \quad \mathbf{v} = \begin{pmatrix} c_1(\sigma_0+\frac{1}{k})+a_1 \\ c_2(\sigma_0+\frac{1}{k}) \\ \cdots\cdots\cdots\cdots \\ c_{Nr-1}(\sigma_0+\frac{1}{k}) \end{pmatrix},$$

$$\mathbf{g} = \begin{pmatrix} g_1+\frac{1}{k}F^n_0 c_1 \\ g_2+\frac{1}{k}F^n_0 c_2 \\ \cdots\cdots \\ g_{Nr-1}+\frac{1}{k}F^n_0 c_{Nr-1} \end{pmatrix}, \quad \mathbf{u} = \left(4, \quad 2, \ldots 2, \quad 4+\frac{\sigma_L k F^n_{Nr}}{h+\sigma_L k(h+F^n_{Nr})}\right).$$

System (E.20)-(E.21) can be efficiently solved by means of the following system with the same bidiagonal matrix $\mathbf{T}$:

$$\mathbf{T}\cdot\mathbf{y} = \mathbf{g} \tag{E.22}$$
$$\mathbf{T}\cdot\mathbf{z} = \mathbf{v} \tag{E.23}$$

After calculating $\mathbf{y}$ and $\mathbf{z}$, we can obtain F^{n+1}_0, $\mathbf{F}$ and J^{n+1}:

$$F^{n+1}_0 = \frac{\mathbf{u}\cdot\mathbf{y} - 3V/h + \kappa_2}{\mathbf{u}\cdot\mathbf{z} - 1 - \kappa_1} \tag{E.24}$$
$$\mathbf{F} = \mathbf{y} - F^{n+1}_0\mathbf{z} \tag{E.25}$$
$$J^{n+1} = (\sigma_0+\frac{1}{k})F^{n+1}_0 - \frac{1}{k}F^n_0. \tag{E.26}$$

It is straightforward to obtain $\mathbf{y}$ and $\mathbf{z}$ from (E.22) and (E.23):

$$\mathbf{y}_1 = \frac{\mathbf{g}_1}{b_1} \tag{E.27}$$

$$\mathbf{y}_j = \frac{\mathbf{g}_j - a_j \mathbf{y}_{j-1}}{b_j}, \qquad j = 2, \dots Nr-1 \tag{E.28}$$

$$\mathbf{z}_1 = \frac{\mathbf{v}_1}{b_1} \tag{E.29}$$

$$\mathbf{z}_j = \frac{\mathbf{v}_j - a_j \mathbf{z}_{j-1}}{b_j}, \qquad j = 2, \dots Nr-1 \tag{E.30}$$

and then (E.24)-(E.26) yield F_0^{n+1}, $\mathbf{F}$ and J^{n+1}.

For calculating the complex amplitude envelope A we use the following explicit scheme:

$$A_i^{n+1} = A_i^n \left(1 - \frac{k}{2}(\gamma_e + \gamma_j)\right) + \frac{k}{2i}\frac{\partial}{\partial x}\left(\frac{\left(f_{2,-1}^{B(0)}\right)_i^n}{1 + iF_i^n}\right), \qquad i = 1, \dots, Nr-1 \tag{E.31}$$

with the following boundary condition at the injector contact:

$$A_0^{n+1} = A_1^{n+1} \tag{E.32}$$

or alternatively $A_0^{n+1} = 0$ also works.
The nondimensional multipliers $\tilde{\beta}_i^{n,\theta}$ and $\tilde{u}_i^{n,\theta}$ are obtained, for $\theta = -\pi \dots \pi$, from equation (E.11) by the Newton-Raphson method, and the Boltzmann distribution function Fourier coefficients $\left(f_{2,0}^{B(0)}\right)_i^n$ and $\left(f_{2,-1}^{B(0)}\right)_i^n$ are calculated from (E.13) using the Simpson's rule for all the integrals over K and over θ.

The summary of the algorithm is the following:

1. For each time step t^n do:
   (a) For each point $i = 1 \dots Nr-1$:
      i. For each $\theta = -\pi \dots \pi$: calculate $G(\tilde{u}, \tilde{\beta})$ from (E.11) using Simpson's rule for integrals, and then obtain $\tilde{\beta}_i^{n,\theta}$ and $\tilde{u}_i^{n,\theta}$ by the Newton-Raphson method from (E.10).

ii. Calculate $\left(f_{2,0}^{B(0)}\right)_i^n$ and $\left(f_{2,-1}^{B(0)}\right)_i^n$ from (E.13), by the Simpson's rule, with the previous values obtained of $\tilde{\beta}_i^{n,\theta}$ and $\tilde{u}_i^{n,\theta}$, and reusing the integrals over K calculated in the previous step.

iii. Calculate coefficients $\mathcal{A}_i^n$, $\mathcal{B}_i^n$, $\mathcal{C}_i^n$ and $\mathcal{D}_i^n$ from (E.2).

iv. Calculate coefficients a_i, b_i, c_i and g_i.

2. Obtain F_i^{n+1} and J^{n+1} from (E.24)-(E.26), and the complex amplitude A_i^{n+1} from (E.31).

3. Go to step 1.

Appendix F

Numerical method for quantum drift diffusion equations for a lateral superlattice with Rashba spin-orbit interaction

F.1 Nondimensional equations

For solving numerically equations (5.68)-(5.71), we will first obtain the dimensionless form considering the hyperbolic scaling, i.e. the collision terms and term proportional to the electric field dominate all others in the kinetic equation.
Let $[x]$, $[F]$, $[t]$, $[v]$ be length, field, time and velocity scales typical for the phenomena described by the quantum drift diffusion equations. The Poisson equation provides that the electron density of the minibands $n^{\pm}$ is of the order of N_D, and that:

$$[x] = \frac{\varepsilon l[F]}{eN_D}$$

From equations (5.15) and (5.29) we obtain also that the scale for the Wigner functions f and for the local equilibrium distribution $\phi^{\pm}$ is N_D. The balance between the field dependent term and the collision term gives:

$$[F] = \frac{\hbar}{el\tau}$$

The characteristic time for the electron to move between minibands is:

$$[t] = \frac{\hbar}{\alpha}$$

$n^{\pm}$, $\phi^{\pm}$	F	x	t	J	$\mathcal{E}$, E, μ, Γ	λ	η
N_D	$\frac{\hbar}{el\tau}$	$\frac{\varepsilon\hbar}{e^2N_D\tau}$	$\frac{\hbar}{\alpha}$	$\frac{\alpha eN_D}{2\hbar}$	K_BT	$\frac{\alpha\tau}{\hbar}$	$\frac{\tau}{\tau_{sc}}$

Table F.1: Hyperbolic scaling and nondimensionalization

If the collision and the field dependent terms dominate the other terms, then the characteristic time $[t]$ is much larger than the inverse of the collision frequency $\tau << [t]$, and the the dimensionless parameter

$$\lambda = \frac{\alpha\tau}{\hbar} \tag{F.1}$$

is very small. On the other hand, the scattering time τ_{sc} is much longer than the collision time, and we will consider:

$$\eta = \frac{\tau}{\tau_{sc}} << 1$$

We now nondimensionalize the quantum drift diffusion system of equations (5.68) and (5.69) by defining $\hat{F} = F/[F]$, $\hat{n}^{\pm} = n^{\pm}/N_D$, $\hat{x} = x/[x]$,..., where $[F]$, $[x]$, etc. are the scales defined above and specified in Table F.1. Omitting hats over the variables, the nondimensional quantum drift diffusion system of equations becomes:

$$\frac{\partial n^{\pm}}{\partial t} + \Delta^{-}\mathcal{D}_{\pm}(n^{+}, n^{-}, F) = \mp\mathcal{R}(n^{+}, n^{-}, F), \tag{F.2}$$

$$\frac{2}{l}\frac{\partial F}{\partial t} + 2\langle\mathcal{D}_{+} + \mathcal{D}_{-}\rangle_1 = J, \tag{F.3}$$

$$\tag{F.4}$$

where

$$\mathcal{R} = \frac{\eta}{\lambda}(n^+ - n^-\,\theta(\mu^- - \mathcal{E}^+_{\min})), \tag{F.5}$$

$$\begin{aligned}\mathcal{D}_\pm = {} & \frac{(\vartheta_1 \pm \beta/\alpha)\phi_1^\pm}{(1+\vartheta_1^2)} \mp \frac{\eta\,(\phi_1^+ - \phi_1^-)\,[2\vartheta_1 \pm \beta/\alpha(1-\vartheta_1^2)]}{2(1+\vartheta_1^2)^2} \\ & + \lambda \frac{[2\vartheta_1 \pm \beta/\alpha(1-\vartheta_1^2)]}{(1+\vartheta_1^2)^2} \frac{\partial \phi_1^\pm}{\partial n^\pm} \left[\Delta^- \left(\frac{\vartheta_1 \pm \beta/\alpha}{(1+\vartheta_1^2)}\phi_1^\pm\right) \pm \frac{\eta}{\lambda}(n^+ - n^-)\right] \\ & + \frac{l\,\lambda}{2} \frac{(3\vartheta_1^2 - 1) \pm (\beta/\alpha)\vartheta_1(3-\vartheta_1^2)}{(1+\vartheta_1^2)^3}\,\phi_1^\pm \left[J - 2\left\langle\left\langle \frac{(\phi_1^+ + \phi_1^-)\vartheta_1}{(1+\vartheta_1^2)}\right\rangle_1\right\rangle_1\right. \\ & \left. -2\frac{\beta}{\alpha}\left\langle\left\langle \frac{(\phi_1^+ - \phi_1^-)}{(1+\vartheta_1^2)}\right\rangle_1\right\rangle_1\right] - \lambda \frac{(1+(\beta/\alpha)^2)}{2(1+\vartheta_1^2)}\,\Delta^- n^\pm \\ & + \frac{\lambda}{2(1+\vartheta_1^2)}\left[(1-(\beta/\alpha)^2 \mp 2(\beta/\alpha)\vartheta_1)\,\Delta^-\left(\frac{\phi_2^\pm}{1+\vartheta_2^2}\right)\right. \\ & \left. + [((\beta/\alpha)^2 - 1)\vartheta_1 \mp 2\beta/\alpha]\,\Delta^-\left(\frac{\vartheta_2\phi_2^\pm}{1+\vartheta_2^2}\right)\right].\end{aligned} \tag{F.6}$$

These equations must be solved together with the Poisson equation:

$$\frac{\partial F}{\partial x} = n^+ + n^- - 1 \tag{F.7}$$

And the voltage bias boundary condition, which in dimensionless form can be written:

$$\int_0^{Nl} F(x,t)\,dx = \Phi Nl = V, \tag{F.8}$$

With respect to the boundary conditions at the contacts it has to be taken into account that the triple spatial averages that appear in (5.71) make necessary to consider the interval $(-2l, 0)$ for the injecting contact and $(Nl, Nl + 2l)$ for the receiving contact. Al all points $(-2l, 0)$ of the ohmic injecting contact we adopt (in dimensionless form):

$$\frac{2}{l}\frac{\partial F}{\partial t} + \sigma F = J \tag{F.9}$$

$$n^\pm = \frac{1}{2}, \tag{F.10}$$

And at the receiving contact $(Nl, Nl + 2l)$:

$$\frac{\partial F}{\partial x} = \frac{\partial n^\pm}{\partial x} = 0 \tag{F.11}$$

The contact conductivity σ must be selected so that σF intersects the second branch of the function $J(F) = 2\langle \mathcal{D}_+ + \mathcal{D}_- \rangle_1$ at the steady state limit, which can be obtained from the following equation (subscript s means steady state limit):

$$
\begin{aligned}
& \frac{F}{1+F^2}\left(\phi_{1s}^+ + \phi_{1s}^-\right) + \frac{\beta/\alpha}{1+F^2}\left(\phi_{1s}^+ - \phi_{1s}^-\right) \\
& \frac{l\lambda}{2(1+F^2)^3}\left[(3F^2-1)(\phi_{1s}^+ + \phi_{1s}^-) + \beta/\alpha F(3-F^2)(\phi_{1s}^+ - \phi_{1s}^-)\right] J_{\mathrm{s}} \\
& -\frac{l\lambda}{(1+F^2)^4}\left[F(\phi_{1s}^+ + \phi_{1s}^-) + \beta/\alpha(\phi_{1s}^+ - \phi_{1s}^-)\right] \\
\times \quad & \left[(3F^2-1)(\phi_{1s}^+ + \phi_{1s}^-) + \beta/\alpha F(3-F^2)(\phi_{1s}^+ - \phi_{1s}^-)\right] \\
& -\frac{\eta\beta\,(1-F^2)}{\alpha\,(1+F^2)^2}\left(\phi_{1s}^+ - \phi_{1s}^- + \left.\frac{\partial\phi_1^+}{\partial n^+}\right|_s + \left.\frac{\partial\phi_1^-}{\partial n^-}\right|_s\right) \\
& +\frac{2\eta F}{(1+F^2)^2}\left(-\left.\frac{\partial\phi_1^+}{\partial n^+}\right|_s + \left.\frac{\partial\phi_1^-}{\partial n^-}\right|_s\right) = \frac{1}{2}J_{\mathrm{s}}. \qquad \text{(F.12)}
\end{aligned}
$$

The above equation can be obtained taking into account that, at the steady state limit, $\frac{\partial u}{\partial x} = \frac{\partial u}{\partial t} = 0$, so $\Delta^- u = 0$ and $\langle u \rangle_1 = u$. The value of $\phi_{1s}^\pm$ can be obtained from:

$$
\begin{aligned}
& \phi_{1s}^\pm = \frac{1}{2\pi}\int_{-\pi}^{\pi} \phi_s^\pm(\mu_s^\pm, K)\, cosK\, dK \qquad \text{(F.13)} \\
& \phi_s^\pm(\mu_s^\pm, k) = \frac{\sqrt{m^* K_B T}}{4\pi\hbar L_z N_D}\int_{-\infty}^{\infty} \frac{\mathcal{D}_\Gamma(E - \mathcal{E}^\pm - E_1)}{1 + e^{E-\mu_s^\pm}} dE \\
\mathcal{D}_\Gamma(E) \quad = \quad & \frac{\sqrt{\sqrt{E^2+\sqrt{2}\Gamma E+\Gamma^2} + E + \frac{\Gamma}{\sqrt{2}}} - \sqrt{\sqrt{E^2+\sqrt{2}\Gamma E+\Gamma^2} - E - \frac{\Gamma}{\sqrt{2}}}}{\sqrt{E^2+\sqrt{2}\Gamma E+\Gamma^2}} \\
+ \quad & \frac{\sqrt{\sqrt{E^2-\sqrt{2}\Gamma E+\Gamma^2} + E - \frac{\Gamma}{\sqrt{2}}} + \sqrt{\sqrt{E^2-\sqrt{2}\Gamma E+\Gamma^2} - E + \frac{\Gamma}{\sqrt{2}}}}{\sqrt{E^2-\sqrt{2}\Gamma E+\Gamma^2}}.
\end{aligned}
$$

Before solving numerically the system of 4 equations (F.2)-(F.7) with unknowns F, $n^\pm$ and J, we can eliminate the population of one miniband from the Poisson equation (F.7). Since we expect the lower miniband to be more populated, we express:

$$
n^- = 1 + \frac{\partial F}{\partial x} - n^+ \qquad \text{(F.14)}
$$

We can transform the operator $\Delta^- u(x,t) = u(x+l/2,t) - u(x-l/2,t)$ in a differential operator in the following way:

$$\Delta^- u(x,t) = l \left\langle \frac{\partial u}{\partial x} \right\rangle_1 \tag{F.15}$$

Now we should express $\phi_j^\pm$ and $\frac{\partial \phi_j^\pm}{\partial n^\pm}$ as functions of $n^\pm$. In the low temperature limit, the local equilibrium distribution function ϕ becomes the Boltzmann distribution, whose Fourier coefficients are proportional to the electron population $n^\pm$. Therefore, we will write the coefficients $\phi_j^\pm$ in the same way:

$$\phi_j^\pm = \frac{\int_{-\pi}^{\pi} \phi^\pm(\mu^\pm, K)\, cos(jK)\, dK}{\int_{-\pi}^{\pi} \phi^\pm(\mu^\pm, K)\, dK}\, n^\pm = \mathcal{I}_{\mathrm{j0}}^\pm(\mu^\pm)\, n^\pm, \tag{F.16}$$

And the dependency of $\mathcal{I}_{j0}^\pm$ with respect to $n^\pm$ is small. The expression for $\frac{\partial \phi_j^\pm}{\partial n^\pm}$ is

$$\begin{aligned} \frac{\partial \phi_j^\pm}{\partial n^\pm} &= \frac{\int_{-\pi}^{\pi} \frac{\partial \phi^\pm}{\partial \mu^\pm}\, cos(jK)\, dK}{\int_{-\pi}^{\pi} \frac{\partial \phi^\pm}{\partial \mu^\pm} dK} = \mathcal{I}_{\mathrm{j1}}^\pm(\mu^\pm) \\ \frac{\partial \phi^\pm}{\partial \mu^\pm} &= \frac{\sqrt{m^* K_B T}}{4\pi\hbar L_z N_D} \int_{-\infty}^{\infty} \frac{e^{E-\mu^\pm}}{(1+e^{E-\mu^\pm})^2} \mathcal{D}_\Gamma(E - \mathcal{E}^\pm - E_1)\, dE \end{aligned} \tag{F.17}$$

The leading order term in (F.6) is the first term of the RHS, therefore, we can write $\mathcal{D}_\pm$ in the following way:

$$\mathcal{D}_\pm = \mathcal{D}_\pm^{(0)} + \lambda\, \mathcal{D}_\pm^{(1)}, \tag{F.18}$$

where the leading order term is:

$$\mathcal{D}_\pm^{(0)} = \frac{\vartheta_1 \pm \beta/\alpha}{1+\vartheta_1^2}\, \phi_1^\pm, \tag{F.19}$$

and the first correction is:

$$\mathcal{D}_{\pm}^{(1)} = \mp \frac{\eta\,(\phi_1^+ - \phi_1^-)\,[2\vartheta_1 \pm \beta/\alpha(1-\vartheta_1^2)]}{2\lambda(1+\vartheta_1^2)^2} \tag{F.20}$$
$$+ \frac{[2\vartheta_1 \pm \beta/\alpha(1-\vartheta_1^2)]}{(1+\vartheta_1^2)^2} \frac{\partial \phi_1^{\pm}}{\partial n^{\pm}} \left[\Delta^- \left(\frac{\vartheta_1 \pm \beta/\alpha}{(1+\vartheta_1^2)} \phi_1^{\pm} \right) \pm \frac{\eta}{\lambda}(n^+ - n^-) \right]$$
$$+ \frac{l}{2} \frac{(3\vartheta_1^2 - 1) \pm (\beta/\alpha)\vartheta_1(3-\vartheta_1^2)}{(1+\vartheta_1^2)^3} \phi_1^{\pm} \left[J - 2 \left\langle \left\langle \frac{(\phi_1^+ + \phi_1^-)\vartheta_1}{(1+\vartheta_1^2)} \right\rangle_1 \right\rangle_1 \right.$$
$$\left. -2\frac{\beta}{\alpha} \left\langle \left\langle \frac{(\phi_1^+ - \phi_1^-)}{(1+\vartheta_1^2)} \right\rangle_1 \right\rangle_1 \right] - \frac{(1+(\beta/\alpha)^2)}{2(1+\vartheta_1^2)} \Delta^- n^{\pm}$$
$$+ \frac{1}{2(1+\vartheta_1^2)} \left[(1 - (\beta/\alpha)^2 \mp 2(\beta/\alpha)\vartheta_1)\, \Delta^- \left(\frac{\phi_2^{\pm}}{1+\vartheta_2^2} \right) \right.$$
$$\left. + [((\beta/\alpha)^2 - 1)\vartheta_1 \mp 2\beta/\alpha]\, \Delta^- \left(\frac{\vartheta_2 \phi_2^{\pm}}{1+\vartheta_2^2} \right) \right].$$

In this way, after substituting (F.14)-(F.16) and (F.17) in (F.2) and (F.3), we can obtain the following system of quantum drift diffusion equations:

$$\frac{\partial F}{\partial t} + \left\langle \mathcal{A}_1 \frac{\partial F}{\partial x} \right\rangle_1 + \mathcal{B}_1\, J = \mathcal{C}_1, \tag{F.21}$$
$$\frac{\partial n^+}{\partial t} + \left\langle \mathcal{A}_2 \frac{\partial n^+}{\partial x} \right\rangle_1 = \mathcal{C}_2, \tag{F.22}$$

The contribution to the drift coefficients $\mathcal{A}_1$ and $\mathcal{A}_2$ of (F.21) and (F.22) will come from the corresponding terms of the leading order $\mathcal{D}_{\pm}^{(0)}$ of (F.19), and the RHS coefficients $\mathcal{C}_1$ and $\mathcal{C}_2$ will include the rest of the terms (including

the diffusion terms). The coefficients $\mathcal{A}_i$, $\mathcal{B}_i$ and $\mathcal{C}_i$ are:

$$
\begin{aligned}
\mathcal{A}_1 &= \frac{\vartheta_1 - \beta/\alpha}{1+\vartheta_1^2}\, l\, \mathcal{I}_{10}^- \\
\mathcal{A}_2 &= \frac{\vartheta_1 + \beta/\alpha}{1+\vartheta_1^2}\, l\, \mathcal{I}_{10}^+ \\
\mathcal{B}_1 &= \frac{-l}{2} \\
\mathcal{C}_1 &= \left\langle \frac{-2}{1+\vartheta_1^2} \left[\left(\vartheta_1 (\mathcal{I}_{10}^+ - \mathcal{I}_{10}^-) + \frac{\beta}{\alpha} \left(\mathcal{I}_{10}^- + \mathcal{I}_{10}^+ \right) \right) n^+ + \left(\vartheta_1 - \frac{\beta}{\alpha} \right) \mathcal{I}_{10}^- \right] \right\rangle_1 \\
&\quad + \lambda \left\langle \frac{-2\eta\,(\beta/\alpha)(\vartheta_1^2 - 1)}{\lambda\,(1+\vartheta_1^2)^2} \left[(\mathcal{I}_{10}^+ + \mathcal{I}_{10}^-)\, n^+ - \mathcal{I}_{10}^- \left(1 + \frac{\partial F}{\partial x} \right) \right] \right. \\
&\quad - \frac{2l}{(1+\vartheta_1^2)^2} \left[(2\vartheta_1 + (\beta/\alpha)(1-\vartheta_1^2))\, \mathcal{I}_{11}^+ \frac{\partial}{\partial x} \left\langle \frac{\vartheta_1 + \beta/\alpha}{1+\vartheta_1^2}\, \mathcal{I}_{10}^+ n^+ \right\rangle_1 \right. \\
&\quad \left. + (2\vartheta_1 - (\beta/\alpha)(1-\vartheta_1^2))\, \mathcal{I}_{11}^- \frac{\partial}{\partial x} \left\langle \frac{\vartheta_1 - \beta/\alpha}{1+\vartheta_1^2}\, \mathcal{I}_{10}^- \left(1 + \frac{\partial F}{\partial x} - n^+ \right) \right\rangle_1 \right] \\
&\quad - \frac{2\eta \left(2n^+ - 1 - \frac{\partial F}{\partial x} \right)}{\lambda (1+\vartheta_1^2)^2} \left[2\vartheta_1 (\mathcal{I}_{11}^+ - \mathcal{I}_{11}^-) + \frac{\beta}{\alpha} (1-\vartheta_1^2)(\mathcal{I}_{11}^+ + \mathcal{I}_{11}^-) \right] \\
&\quad - \frac{l}{(1+\vartheta_1^2)^3} \left[J - 2 \left\langle \left\langle \frac{1}{1+\vartheta_1^2} \left(n^+ \left(\vartheta_1 (\mathcal{I}_{10}^+ - \mathcal{I}_{10}^-) + \frac{\beta}{\alpha} (\mathcal{I}_{10}^+ + \mathcal{I}_{10}^-) \right) \right) \right. \right. \right. \\
&\quad \left. \left. \left. + \left(1 + \frac{\partial F}{\partial x} \right) \mathcal{I}_{10}^- (\vartheta_1 - \beta/\alpha) \right) \right\rangle_1 \right\rangle_1 \left[n^+ \left((3\vartheta_1^2 - 1)(\mathcal{I}_{10}^+ - \mathcal{I}_{10}^-) + \frac{\beta}{\alpha} \vartheta_1 (3 - \vartheta_1^2)(\mathcal{I}_{10}^+ + \mathcal{I}_{10}^-) \right) \right. \\
&\quad \left. + \left(1 + \frac{\partial F}{\partial x} \right) \mathcal{I}_{10}^- \left(3\vartheta_1^2 - 1 - \frac{\beta}{\alpha} \vartheta_1 (3 - \vartheta_1^2) \right) \right] + \frac{l(1 + (\beta/\alpha)^2)}{1+\vartheta_1^2} \left\langle \frac{\partial^2 F}{\partial x^2} \right\rangle_1 \\
&\quad - \frac{l}{1+\vartheta_1^2} \left[(1 - (\beta/\alpha)^2) \left[\frac{\partial}{\partial x} \left\langle \frac{n^+ (\mathcal{I}_{20}^+ - \mathcal{I}_{20}^-) + \mathcal{I}_{20}^- (1 + \frac{\partial F}{\partial x})}{1+\vartheta_2^2} \right\rangle_1 \right. \right. \\
&\quad \left. - \vartheta_1 \frac{\partial}{\partial x} \left\langle \frac{\vartheta_2}{1+\vartheta_2^2} \left[n^+ (\mathcal{I}_{20}^+ - \mathcal{I}_{20}^-) + \mathcal{I}_{20}^- \left(1 + \frac{\partial F}{\partial x} \right) \right] \right\rangle_1 \right] \\
&\quad + 2(\beta/\alpha) \left[\vartheta_1 \frac{\partial}{\partial x} \left\langle \frac{-n^+ (\mathcal{I}_{20}^+ + \mathcal{I}_{20}^-) + \mathcal{I}_{20}^- \left(1 + \frac{\partial F}{\partial x} \right)}{1+\vartheta_2^2} \right\rangle_1 \right. \\
&\quad \left. \left. + \frac{\partial}{\partial x} \left\langle \frac{\vartheta_2}{1+\vartheta_2^2} \left[-n^+ (\mathcal{I}_{20}^+ + \mathcal{I}_{20}^-) + \mathcal{I}_{20}^- \left(1 + \frac{\partial F}{\partial x} \right) \right] \right\rangle_1 \right] \right\rangle_1
\end{aligned}
$$

$$
\begin{aligned}
\mathcal{C}_2 = & \frac{-\eta}{l}\left(n^+\left(1+\theta(\mu^- - \mathcal{E}^+_{\min})\right) - \left(1+\frac{\partial F}{\partial x}\right)\theta(\mu^- - \mathcal{E}^+_{\min})\right) \\
& -l\left\langle n^+ \frac{\partial}{\partial x}\left(\frac{\vartheta_1 + \beta/\alpha}{1+\vartheta_1^2}\,\mathcal{I}^+_{10}\right)\right\rangle_1 \\
& -\lambda\, l^2 \frac{\partial}{\partial x}\left\langle \frac{-\eta\left(\mathcal{I}^+_{10} n^+ - \mathcal{I}^-_{10}(1+\frac{\partial F}{\partial x} - n^+)\right)\left[2\vartheta_1 + \beta/\alpha(1-\vartheta_1^2)\right]}{2\lambda l(1+\vartheta_1^2)^2}\right. \\
& + \frac{[2\vartheta_1 + \beta/\alpha(1-\vartheta_1^2)]}{(1+\vartheta_1^2)^2}\mathcal{I}^+_{11}\left[\frac{\partial}{\partial x}\left\langle \frac{\vartheta_1 \pm \beta/\alpha}{(1+\vartheta_1^2)}\phi_1^{\pm}\right\rangle_1 + \frac{\eta}{\lambda l}\left(2n^+ - 1 - \frac{\partial F}{\partial x}\right)\right] \\
& + \frac{(3\vartheta_1^2 - 1) + (\beta/\alpha)\vartheta_1(3-\vartheta_1^2)}{2(1+\vartheta_1^2)^3}\,\mathcal{I}^+_{10}\, n^+\left[J - 2\left\langle\left\langle \frac{\vartheta_1}{1+\vartheta_1^2}\left(\mathcal{I}^+_{10}\, n^+\right.\right.\right. \\
& \left.\left.\left. + \mathcal{I}^-_{10}\left(1 + \frac{\partial F}{\partial x} - n^+\right)\right)\right\rangle_1\right\rangle_1 - 2\frac{\beta}{\alpha}\left\langle\left\langle \frac{\mathcal{I}^+_{10}\, n^+ - \mathcal{I}^-_{10}(1+\frac{\partial F}{\partial x} - n^+)}{1+\vartheta_1^2}\right\rangle_1\right\rangle_1\Bigg] \\
& - \frac{(1+(\beta/\alpha)^2)}{2(1+\vartheta_1^2)}\left\langle \frac{\partial n^+}{\partial x}\right\rangle_1 + \frac{1}{2(1+\vartheta_1^2)}\left[(1-(\beta/\alpha)^2 - 2(\beta/\alpha)\vartheta_1)\,\frac{\partial}{\partial x}\left\langle \frac{\mathcal{I}^+_{20}\, n^+}{1+\vartheta_2^2}\right\rangle_1\right. \\
& \left.\left. + \left[((\beta/\alpha)^2 - 1)\vartheta_1 - 2\beta/\alpha\right]\frac{\partial}{\partial x}\left\langle \frac{\vartheta_2\, \mathcal{I}^+_{20}\, n^+}{1+\vartheta_2^2}\right\rangle_1\right]\right\rangle_1
\end{aligned}
$$

F.2 Numerical scheme

The spatial averages in (F.21) and (F.22) lead to a type of equations for which little seems to be known, specially from the numerical point of view. The numerical scheme we have used is based on an implicit scheme for both partial differential equations (F.21) and (F.22) which employs a fixed point iteration method to find the numerical solution of F, n^+ and J at each time step. On the other hand, for equation (F.21) we use a similar scheme to the one described and proved to converge in [26] for partial differential equations with an integral constraint. Since the electric field $-F$ waves propagate from the cathode to the anode, we use backward differences for approximating spatial first derivatives, avoiding numerical instabilities, and the resulting differential equation is integrated in time by a first order implicit Euler method. This procedure leads to a system of $(N+4)r+2$ linear equations for the $(N+4)r+1$ values of the electric field (F_{-2r} to F_{Nr+2r}) plus the current density J at time t^{n+1}:

$$
a_i F_{i-1}^{n+1} + b_i F_i^{n+1} + c_i J^{n+1} = g_i, \quad i = 1, \ldots, Nr-1 \qquad \text{(F.23)}
$$

where $r = l/h$.
The discretization of the spatial averages is based on the Simpson's rule:

$$\langle u_i^n \rangle_j = \frac{1}{3jr}(u_{i-jr/2}^n + \cdots + s_{i-1}u_{i-1}^n + s_i u_i^n + s_{i+1}u_{i+1}^n + \cdots + u_{i+jr/2}^n),$$

where s_i, s_{i-1} and s_{i+1} are:

$$s_i = \begin{cases} 4, & jr = 2(1+2m) \\ 2, & jr = 4(1+m) \end{cases} \qquad s_{i-1} = s_{i+1} = \begin{cases} 1, & jr = 2 \\ 2, & jr = 2(1+2m) \\ 4, & jr = 4(1+m), \end{cases}$$

where $m = 0, 1, 2, \ldots$. In this way, we can split $\left\langle (F_x)_i^{n+1} \right\rangle_1$ in three terms:

$$\begin{aligned} \left\langle (F_x)_i^{n+1} \right\rangle_1 &= \frac{1}{3r}\left[(F_x)_{i-r/2}^{n+1} + \cdots + (F_x)_{i+r/2}^{n+1} \right] = \\ &= \left(\frac{s_{i-1} - s_i}{3rh} \right) F_{i-1}^{n+1} + \left(\frac{s_i - s_{i+1}}{3rh} \right) F_i^{n+1} + \left\langle (F_x)_i^{n+1} \right\rangle_1^*, \end{aligned} \quad \text{(F.24)}$$

the first two terms in (F.24) will contribute to the a_i and b_i coefficients and the third term will contribute to the g_i coefficient of (F.23).

Therefore, the coefficients of the finite differences system of equations (F.23) will be:

$$\begin{aligned} a_i &= \frac{k\, s_{i-1}}{3r}(\mathcal{A}_1)_{i-1}^{n+1} - \frac{k\, s_i}{3r}(\mathcal{A}_1)_i^{n+1} \\ b_i &= h + \frac{k\, s_i}{3r}(\mathcal{A}_1)_i^{n+1} - \frac{k\, s_{i+1}}{3r}(\mathcal{A}_1)_{i+1}^{n+1} \\ c_i &= hk(\mathcal{B}_1)_i^{n+1} \\ g_i &= h\, F_i^n + hk\, (\mathcal{C}_1)_i^{n+1} - \left\langle (\mathcal{A}_1 F_x)_i^{n+1} \right\rangle_1^*, \end{aligned}$$

where $h = \Delta x$, $k = \Delta t$ and all the coefficients $\mathcal{A}_1$, $\mathcal{B}_1$ and $\mathcal{C}_1$ of (F.21) are evaluated at time t^{n+1}.
The voltage bias integral constraint is solved by the Simpson's rule:

$$F_0^{n+1} + 4F_1^{n+1} + 2F_2^{n+1} + ... + 2F_{Nr-2}^{n+1} + 4F_{Nr-1}^{n+1} + F_{Nr}^{n+1} = 3V/h. \quad \text{(F.25)}$$

The boundary condition at the injector contact is:

$$(2 + \sigma\, lk)F_i^{n+1} - l\, k\, J^{n+1} = 2F_i^n, \quad i = -2r, \ldots, 0, \qquad \text{(F.26)}$$

and at the collector contact:

$$F_i^{n+1} = F_{Nr-1}^{n+1}, \quad i = Nr, \ldots, (N+2)r \tag{F.27}$$

If we use second order backward difference for approximating the first derivative ($\frac{\partial F}{\partial x} \approx \frac{3F_i - 4F_{i-1} + F_{i-2}}{2h}$), equations (F.23) would be:

$$a_i F_{i-2}^{n+1} + b_i F_{i-1}^{n+1} + c_i F_i^{n+1} + d_i F_{i+1}^{n+1} + e_i J^{n+1} = g_i,$$

but in this case the coefficient matrix would not be bidiagonal, and equation (F.27) would become:

$$F_i^{n+1} = \tfrac{4}{3} F_{Nr-1}^{n+1} - \tfrac{1}{3} F_{Nr-2}^{n+1}, \quad i = Nr, \ldots, (N+2)r - 1$$

This system of $(N+4)r + 2$ linear equations can be reduced to a simpler and smaller system, with the objective of finding a bidiagonal matrix, in the following way:

- First of all, the value of the field at all the points of each ohmic contact is the same, so we only need to calculate F_0 and F_{Nr}.

- The current density can be calculated directly from the boundary condition at the injector contact:

$$J^{n+1} = (\sigma + \tfrac{2}{lk}) F_0^{n+1} - \tfrac{2}{lk} F_0^n, \tag{F.28}$$

- The field at the collector contact points can be obtained from the previous point:

$$F_{Nr}^{n+1} = F_{Nr-1}^{n+1}, \tag{F.29}$$

  or alternatively, if we use second order backward difference for approximating the first derivative:

$$F_{Nr}^{n+1} = \tfrac{4}{3} F_{Nr-1}^{n+1} - \tfrac{1}{3} F_{Nr-2}^{n+1}.$$

- We can make the following factorization of the system of linear equations:

$$\mathbf{v}\, F_0^{n+1} + \mathbf{T} \cdot \mathbf{F} = \mathbf{g} \tag{F.30}$$

$$F_0^{n+1} + \mathbf{u} \cdot \mathbf{F} = 3V/h \tag{F.31}$$

where $\mathbf{T}$ is the bidiagonal matrix:

$$\mathbf{T} = \begin{pmatrix} b_1 & \cdots & \cdots & \cdots & 0 \\ a_2 & b_2 & \cdots & \cdots & 0 \\ \cdots & \cdots & \cdots & \cdots & \cdots \\ 0 & \cdots & \cdots & a_{Nr-1} & b_{Nr-1} \end{pmatrix}$$

and vectors $\mathbf{F}$, $\mathbf{v}$, $\mathbf{g}$ and $\mathbf{u}$ are:

$$\mathbf{F} = \begin{pmatrix} F_1^{n+1} \\ F_2^{n+1} \\ \cdots \\ F_{Nr-1}^{n+1} \end{pmatrix}, \quad \mathbf{v} = \begin{pmatrix} c_1(\sigma + \frac{2}{lk}) + a_1 \\ c_2(\sigma + \frac{2}{lk}) \\ \cdots\cdots\cdots\cdots \\ c_{Nr-1}(\sigma + \frac{2}{lk}) \end{pmatrix},$$

$$\mathbf{g} = \begin{pmatrix} g_1 + \frac{2}{lk} F_0^n c_1 \\ g_2 + \frac{2}{lk} F_0^n c_2 \\ \cdots\cdots \\ g_{Nr-1} + \frac{2}{lk} F_0^n c_{Nr-1} \end{pmatrix}, \quad \mathbf{u} = (4 \quad 2 \quad \ldots \quad 2 \quad 4)$$

System (F.30)-(F.31) can be efficiently solved by means of the following system with the same bidiagonal matrix $\mathbf{T}$:

$$\mathbf{T} \cdot \mathbf{y} = \mathbf{g} \tag{F.32}$$

$$\mathbf{T} \cdot \mathbf{z} = \mathbf{v} \tag{F.33}$$

After calculating $\mathbf{y}$ and $\mathbf{z}$, we can obtain F_0^{n+1}, $\mathbf{F}$ and J^{n+1}:

$$F_0^{n+1} = \frac{\mathbf{u} \cdot \mathbf{y} - 3V/h}{\mathbf{u} \cdot \mathbf{z} - 1} \tag{F.34}$$

$$\mathbf{F} = \mathbf{y} - F_0^{n+1}\mathbf{z} \tag{F.35}$$

$$J^{n+1} = (\sigma + \frac{2}{lk})F_0^{n+1} - \frac{2}{lk}F_0^n. \tag{F.36}$$

It is straightforward to obtain $\mathbf{y}$ and $\mathbf{z}$ from (F.32) and (F.33):

$$\mathbf{y}_1 = \frac{\mathbf{g}_1}{b_1} \tag{F.37}$$

$$\mathbf{y}_j = \frac{\mathbf{g}_j - a_j\mathbf{y}_{j-1}}{b_j}, \qquad j = 2, \ldots Nr-1 \tag{F.38}$$

$$\mathbf{z}_1 = \frac{\mathbf{v}_1}{b_1} \tag{F.39}$$

$$\mathbf{z}_j = \frac{\mathbf{v}_j - a_j\mathbf{z}_{j-1}}{b_j}, \qquad j = 2, \ldots Nr-1 \tag{F.40}$$

and then (F.34)-(F.36) yield F_0^{n+1}, $\mathbf{F}$ and J^{n+1}.

The coefficients $\mathcal{I}_{j0}^{\pm}$ and $\mathcal{I}_{j1}^{\pm}$ can be obtained from (F.16) and (F.17) by using the Newton-Raphson metohd.

For calculating n^+ we use the following explicit scheme:

$$(n^+)_i^{n+1} = (n^+)_i^n + k\,\left(-\left\langle(\mathcal{A}_2\, n^+)_i^{n+1}\right\rangle_1 + (\mathcal{C}_2)_i^{n+1}\right), \qquad i = 1, \ldots, Nr-1 \tag{F.41}$$

At the cathode, the miniband populations $n^{\pm}$ are:

$$(n^{\pm})_i^{n+1} = \frac{1}{2}, \qquad i = -2r, \ldots, 0 \tag{F.42}$$

and at the anode:

$$(n^{\pm})_i^{n+1} = (n^{\pm})_{Nr-1}^{n+1}, \qquad i = Nr, \ldots, (N+2)r \tag{F.43}$$

Finally, the Poisson equation yields n^-:

$$(n^-)_i^{n+1} = 1 + (F_x)_i^{n+1} - (n^+)_i^{n+1}, \qquad i = 1, \ldots, Nr-1 \tag{F.44}$$

The summary of the algorithm is as follows:

1. For each time step t^n do:
2. While the fixed point iteration does not converge:
3. Calculate averages $\vartheta_j = j\,\langle F\rangle_j$, and coefficients $\mathcal{I}_{j0}^{\pm}$ and $\mathcal{I}_{j1}^{\pm}$ for $n^{\pm}$ for each point $i = 0 \ldots (N+2)r$ at time t^{n+1}.
4. Calculate coefficients $\mathcal{A}_i$, $\mathcal{B}_i$ and $\mathcal{C}_i$.
5. Calculate coefficients a_i, b_i, c_i and g_i
6. Obtain F_i^{n+1} and J^{n+1} from (F.34)-(F.36), and $(n^{\pm})_i^{n+1}$ from (F.41)-(F.44).
7. If the fixed point iteration converges then go to step 1, else go to step 2.

Appendix G

Numerical method for quantum drift diffusion equations for a two miniband superlattice

G.1 Nondimensional equations

In this model we must first consider that the pseudo-differential operators $\Delta_j^{\pm} F(x,t) = F(x + jl/2) \pm F(x - jl/2)$ can be transformed in derivatives of the spatial averages functions. We have already seen that the operator $\Delta_j^{-} F$ can be easily transformed in a first derivative spatial average:

$$\Delta_j^{-} F(x,t) = jl \frac{\partial}{\partial x} < F(x,t) >_j, \tag{G.1}$$

and it is easy to prove that operator $\Delta_j^{+} F$ can be expressed in terms of the second derivative:

$$\Delta_j^{+} F(x,t) = 2F(x,t) + \frac{j^2 l^2}{4} \frac{\partial^2}{\partial x^2} \left\langle \langle F(x,t) \rangle_{j/2} \right\rangle_{j/2}. \tag{G.2}$$

Since we can express $F(x + l)$ in the following way:

$$F(x + l) = \frac{1}{2} \left(\Delta_2^{-} F(x) + \Delta_2^{+} F(x) \right), \tag{G.3}$$

it is easy to obtain the following formula for $F(x + l)$ in terms of $F(x)$ and its first two derivatives:

$$F(x + l) = F(x) + l \frac{\partial}{\partial x} \langle F(x) \rangle_2 + \frac{l^2}{2} \frac{\partial^2}{\partial x^2} \langle \langle F(x) \rangle_1 \rangle_1 \tag{G.4}$$

$n^{\pm}$, $\phi^{\pm}$	F	x	t	J	$\mathcal{E}$, E, μ, Γ	λ	η_2	η_1
N_D	$\frac{\hbar}{el\tau}$	$\frac{\varepsilon\hbar}{e^2N_D\tau}$	$\frac{\hbar}{\alpha}$	$\frac{\alpha eN_D}{\hbar}$	K_BT	$\frac{\alpha\tau}{\hbar}$	$\frac{\tau}{\tau_{sc}}$	$\frac{2g\tau}{\hbar}$

Table G.1: Hyperbolic scaling and nondimensionalization

For solving numerically equations (6.62)-(6.65), we will first obtain the dimensionless form considering the hyperbolic scaling in the same way it was done in appendix F

By defining $\hat{F} = F/[F]$, $\hat{n}^{\pm} = n^{\pm}/N_D$, $\hat{x} = x/[x]$,..., where $[F]$, $[x]$, etc. are the scales specified in Table G.1 and then omitting hats over the variables, the nondimensional quantum drift diffusion system of equations becomes:

$$\frac{\partial n^{\pm}}{\partial t} + \Delta^{-}\mathcal{D}_{\pm} = \mp\mathcal{R}, \tag{G.5}$$

$$\frac{1}{l}\frac{\partial F}{\partial t} + \langle \mathcal{D}_{+} + \mathcal{D}_{-} \rangle_1 = J, \tag{G.6}$$

These equations must be solved together with the Poisson equation:

$$\frac{\partial F}{\partial x} = n^{+} + n^{-} - 1 \tag{G.7}$$

And the voltage bias boundary condition, which in dimensionless form can be written:

$$\int_0^{Nl} F(x,t)\,dx = \Phi Nl = V, \tag{G.8}$$

With respect to the boundary conditions at the contacts it has to be taken into account that the triple spatial averages that appear in (5.71) make necessary to consider the interval $(-2l, 0)$ for the injecting contact and $(Nl, Nl + 2l)$ for the receiving contact. Al all points $(-2l, 0)$ of the ohmic injecting contact we adopt (in dimensionless form):

$$\frac{1}{l}\frac{\partial F}{\partial t} + \sigma_0 F = J \tag{G.9}$$

$$n^{\pm} = n^{\pm}_{st} = \frac{1}{2} \mp \frac{\eta_2(1 + \eta_1^2 + 4\delta^2F^2)}{8\delta^2F^2 + 2\eta_2(1 + \eta_1^2 + 4\delta^2F^2)}. \tag{G.10}$$

The boundary conditions in the anode region ($Nl \leq x \leq Nl + 2l$), in dimensionless form, are:

$$\frac{1}{l}\frac{\partial F}{\partial t} + \sigma_L \left(n^+ + n^-\right) F = J, \tag{G.11}$$

$$n^+ = 0, \tag{G.12}$$

where σ_0 and σ_L are the cathode and anode conductivities respectively. The lower miniband electron density n^- in the anode region is obtained from the Poisson equation (G.7). The contact conductivity σ_0 must be selected so that $\sigma_0 F$ intersects the second branch of the function $J(F) = 2\langle \mathcal{D}_+ + \mathcal{D}_- \rangle_1$ at the steady state limit, which can be obtained from (G.5) and (G.6) taking into account that, at the steady state limit, $\frac{\partial u}{\partial x} = \frac{\partial u}{\partial t} = 0$, so $\Delta^- u = 0$ and $\langle u \rangle_j = u$ and $\Delta^+ u = 2u$.

Before solving numerically the system of 4 equations (G.5)-(G.7) with unknowns F, $n^\pm$ and J, we can eliminate the population of one miniband from the Poisson equation (G.7). Since we expect the lower miniband to be more populated, we express:

$$n^- = 1 + \frac{\partial F}{\partial x} - n^+ \tag{G.13}$$

Now, we should express $\phi_j^\pm$ and $\frac{\partial \phi_j^\pm}{\partial n^\pm}$ as functions of $n^\pm$. In the low temperature limit, the local equilibrium distribution function ϕ becomes the Boltzmann distribution, whose Fourier coefficients are proportional to the electron population $n^\pm$. Therefore, we will write the coefficients $\phi_j^\pm$ in the same way:

$$\phi_j^\pm = \frac{\int_{-\pi}^{\pi} \phi^\pm(\mu^\pm, K)\, cos(jK)\, dK}{\int_{-\pi}^{\pi} \phi^\pm(\mu^\pm, K)\, dK}\, n^\pm = \mathcal{I}_{\mathrm{j0}}^\pm(\mu^\pm)\, n^\pm, \tag{G.14}$$

And the dependency of $\mathcal{I}_{j0}^\pm$ with respect to $n^\pm$ is small. The expression for $\frac{\partial \phi_j^\pm}{\partial n^\pm}$ is

$$\frac{\partial \phi_j^\pm}{\partial n^\pm} = \frac{\int_{-\pi}^{\pi} \frac{\partial \phi^\pm}{\partial \mu^\pm}\, cos(jK)\, dK}{\int_{-\pi}^{\pi} \frac{\partial \phi^\pm}{\partial \mu^\pm} dK} = \mathcal{I}_{\mathrm{j1}}^\pm(\mu^\pm) \tag{G.15}$$

$$\frac{\partial \phi^\pm}{\partial \mu^\pm} = \frac{\sqrt{2} m^* k_B T}{\pi^2 \hbar^2 N_D} \int_{-\infty}^{\infty} \frac{\Gamma^3 e^{\mu^\pm - E}}{(\Gamma^4 + [E - \mathcal{E}^\pm(k)]^4)(1 + e^{\mu^\pm - E})}\, dE, \tag{G.16}$$

In order to transform equations (G.5) and (G.6) in the following set of quantum drift diffusion equations

$$\frac{\partial F}{\partial t} + \left\langle \mathcal{A}_1 \frac{\partial F}{\partial x} \right\rangle_1 + \mathcal{B}_1 \, J = \mathcal{C}_1, \tag{G.17}$$

$$\frac{\partial n^+}{\partial t} + \left\langle \mathcal{A}_2 \frac{\partial n^+}{\partial x} \right\rangle_1 = \mathcal{C}_2, \tag{G.18}$$

and then apply the numerical scheme, we can write $\mathcal{D}_\pm$ as the sum of the leading order term $\mathcal{D}_\pm^{(0)}$ plus the first correction $\mathcal{D}_\pm^{(1)}$. We will keep the leading order contribution to the drift terms in the LHS coefficients $\mathcal{A}_1$ and $\mathcal{A}_2$, and the RHS coefficients $\mathcal{C}_1$ and $\mathcal{C}_2$ will include the rest of the terms (including the diffusion terms). After inserting G.14 in the leading order $\mathcal{D}_\pm^{(0)}$, it can be expressed as:

$$\mathcal{D}_\pm^{(0)} = \mathcal{D}_1^\pm n^\pm + \mathcal{D}_2^\pm n^\mp \tag{G.19}$$

where

$$\begin{aligned}
\mathcal{D}_1^\pm = -(1 \pm \frac{\gamma}{\alpha}) \Big[& \mathcal{I}_{10}^\pm \left(\frac{\vartheta_1}{1+\vartheta_1^2} \mp \eta_1 \delta^2 (\Delta^- \mathcal{F})(\Delta^+ \mathcal{F}) \mathrm{Re} Z_1 \right. \\
& + \frac{\eta_1 \delta^2}{2} ((\mathrm{Im} M_1^+ (\Delta^- F)^2 + \mathrm{Im} M_1^- (\Delta^+ F)^2) \mathrm{Re} Z_1 \\
& \left. + (\mathrm{Re} M_1^+ (\Delta^- F)^2 + \mathrm{Re} M_1^- (\Delta^+ F)^2) \mathrm{Im} Z_1) \right) \\
\mathcal{D}_2^\pm = & \mathcal{I}_{10}^\mp \frac{\eta_1 \delta^2}{2} (\mathrm{Im} M_1^+ (\Delta^- F)^2 - \mathrm{Im} M_1^- (\Delta^+ F)^2) \mathrm{Re} Z_1 \\
& (\mathrm{Re} M_1^+ (\Delta^- F)^2 - \mathrm{Re} M_1^- (\Delta^+ F)^2) \mathrm{Im} Z_1) \Big]
\end{aligned}$$

Inserting (G.13) and (G.19) in (G.5) and (G.6), we can obtain the coefficients $\mathcal{A}_i$, $\mathcal{B}_i$ and $\mathcal{C}_i$:

$$\begin{aligned}
& \mathcal{A}_1 = l(\mathcal{D}_1^- + \mathcal{D}_2^+) \\
& \mathcal{A}_2 = l(\mathcal{D}_1^+ - \mathcal{D}_2^+) \\
& \mathcal{B}_1 = -l \\
& \mathcal{C}_1 = -l \left[(\mathcal{D}_1^+ - \mathcal{D}_1^- + \mathcal{D}_2^- - \mathcal{D}_2^+) n^+ - \mathcal{D}_1^- - \mathcal{D}_2^+ - \left\langle \mathcal{D}_+^{(1)} + D_-^{(1)} \right\rangle_1 \right] \\
& \mathcal{C}_2 = -\mathcal{R} - l \frac{\partial}{\partial x} \left\langle \mathcal{D}_2^+ \left(1 + \frac{\partial F}{\partial x} \right) + D_+^{(1)} \right\rangle_1
\end{aligned}$$

G.2 Numerical scheme

The main difference between this numerical scheme and the scheme used for the Spintronics model (Appendix F) is the boundary condition at the anode, therefore equations (F.23)-(F.25) are valid here, and equations (F.27) must be replaced by:

$$(-kl\sigma_L F_i^{n+1})F_{i-1}^{n+1} + (h + \sigma_L kl(h + F_i^{n+1}))F_i^{n+1} - khlJ^{n+1} = hF_i^{n+1}, \tag{G.20}$$

which is valid for all points of the anode ($i = Nr, \ldots, (N+2)r$). Therefore, equation (F.29) must be replaced by:

$$F_{Nr}^{n+1} = \frac{h(F_{Nr}^n - F_0^n) + h(1 + \sigma_0 lk)F_0^{n+1} + (\sigma_L klF_{Nr}^{n+1})F_{Nr-1}^{n+1})}{h + \sigma_L kl(h + F_{Nr}^{n+1})}. \tag{G.21}$$

The factorization equation (F.30) is still valid here:

$$\mathbf{v}\, F_0^{n+1} + \mathbf{T} \cdot \mathbf{F} = \mathbf{g}, \tag{G.22}$$

and after inserting G.21 in the voltage bias integral constraint (F.25), then (F.31) must be replaced by:

$$F_0^{n+1}(1 + \kappa_1) + \mathbf{u} \cdot \mathbf{F} = 3V/h - \kappa_2, \tag{G.23}$$

where coefficients κ_1 and κ_2 are:

$$\kappa_1 = \frac{h(1 + \sigma_0 lk)}{h + \sigma_L kl(h + F_{Nr}^{n+1})},$$
$$\kappa_2 = \frac{h(F_{Nr}^n - F_0^n)}{h + \sigma_L kl(h + F_{Nr}^{n+1})},$$

and $\mathbf{T}$ is the bidiagonal matrix:

$$\mathbf{T} = \begin{pmatrix} b_1 & \cdots & \cdots & \cdots & 0 \\ a_2 & b_2 & \cdots & \cdots & 0 \\ \cdots & \cdots & \cdots & \cdots & \cdots \\ 0 & \cdots & \cdots & a_{Nr-1} & b_{Nr-1} \end{pmatrix}$$

and vectors $\mathbf{F}$, $\mathbf{v}$, $\mathbf{g}$ and $\mathbf{u}$ are:

$$\mathbf{F} = \begin{pmatrix} F_1^{n+1} \\ F_2^{n+1} \\ \cdots \\ F_{Nr-1}^{n+1} \end{pmatrix}, \quad \mathbf{v} = \begin{pmatrix} c_1(\sigma_0 + \frac{1}{lk}) + a_1 \\ c_2(\sigma_0 + \frac{1}{lk}) \\ \cdots\cdots\cdots\cdots \\ c_{Nr-1}(\sigma_0 + \frac{1}{lk}) \end{pmatrix},$$

$$\mathbf{g} = \begin{pmatrix} g_1 + \frac{1}{lk} F_0^n \, c_1 \\ g_2 + \frac{1}{lk} F_0^n \, c_2 \\ \cdots\cdots \\ g_{Nr-1} + \frac{1}{lk} F_0^n \, c_{Nr-1} \end{pmatrix}, \quad \mathbf{u} = \left(4, \quad 2, \ldots 2, \quad 4 + \frac{\sigma_L kl F_{Nr}^{n+1}}{h + \sigma_L kl (h + F_{Nr}^{n+1})} \right).$$

System (G.22)-(G.23) can be efficiently solved by means of the following system with the same bidiagonal matrix $\mathbf{T}$:

$$\mathbf{T} \cdot \mathbf{y} = \mathbf{g} \tag{G.24}$$

$$\mathbf{T} \cdot \mathbf{z} = \mathbf{v} \tag{G.25}$$

After calculating $\mathbf{y}$ and $\mathbf{z}$, we can obtain F_0^{n+1}, $\mathbf{F}$ and J^{n+1}:

$$F_0^{n+1} = \frac{\mathbf{u} \cdot \mathbf{y} - 3V/h + \kappa_2}{\mathbf{u} \cdot \mathbf{z} - 1 - \kappa_1} \tag{G.26}$$

$$\mathbf{F} = \mathbf{y} - F_0^{n+1} \mathbf{z} \tag{G.27}$$

$$J^{n+1} = (\sigma_0 + \frac{1}{lk}) F_0^{n+1} - \frac{1}{lk} F_0^n. \tag{G.28}$$

It is straightforward to obtain $\mathbf{y}$ and $\mathbf{z}$ from (G.24) and (G.25):

$$\mathbf{y}_1 = \frac{\mathbf{g}_1}{b_1} \tag{G.29}$$

$$\mathbf{y}_j = \frac{\mathbf{g}_j - a_j \mathbf{y}_{j-1}}{b_j}, \qquad j = 2, \ldots Nr - 1 \tag{G.30}$$

$$\mathbf{z}_1 = \frac{\mathbf{v}_1}{b_1} \tag{G.31}$$

$$\mathbf{z}_j = \frac{\mathbf{v}_j - a_j \mathbf{z}_{j-1}}{b_j}, \qquad j = 2, \ldots Nr - 1 \tag{G.32}$$

and then (G.26)-(G.28) yield F_0^{n+1}, $\mathbf{F}$ and J^{n+1}.

The coefficients $\mathcal{I}_{j0}^{\pm}$ and $\mathcal{I}_{j1}^{\pm}$ can be obtained from (G.14) and (G.15) by using the Newton-Raphson metohd.

For calculating n^+ we use the following explicit scheme:

$$(n^+)_i^{n+1} = (n^+)_i^n + k \left(- \left\langle (\mathcal{A}_2 \, n^+)_i^{n+1} \right\rangle_1 + (\mathcal{C}_2)_i^{n+1} \right), \qquad i = 1, \ldots, Nr - 1 \tag{G.33}$$

At the cathode, the miniband populations $n^{\pm}$ are:

$$(n^{\pm})_i^{n+1} = \frac{1}{2} \mp \frac{\eta_2(1+\eta_1^2+4\delta^2(F_i^{n+1})^2)}{8\delta^2(F_i^{n+1})^2+2\eta_2(1+\eta_1^2+4\delta^2(F_i^{n+1})^2)}, \qquad i=-2r,\ldots,0 \tag{G.34}$$

and at the anode:

$$(n^{+})_i^{n+1} = 0, \qquad i=Nr,\ldots,(N+2)r \tag{G.35}$$

$$(n^{-})_i^{n+1} = 1+(F_x)_i^{n+1}-(n^{+})_i^{n+1}, \qquad i=Nr,\ldots,(N+2)r \tag{G.36}$$

Finally, the Poisson equation yields n^{-}:

$$(n^{-})_i^{n+1} = 1+(F_x)_i^{n+1}-(n^{+})_i^{n+1}, \qquad i=1,\ldots,Nr-1 \tag{G.37}$$

The summary of the algorithm is as follows:

1. For each time step t^n do:
2. While the fixed point iteration does not converge:
3. Calculate averages $\vartheta_j = j\ \langle F\rangle_j$, operators $\Delta^- F = l\frac{\partial}{\partial x}\langle F\rangle_1$ and $\Delta^+ F = 2F+\frac{l^2}{4}\frac{\partial^2}{\partial x^2}\left\langle \langle F\rangle_{1/2}\right\rangle_{1/2}$, and coefficients $\mathcal{I}_{j0}^{\pm}$ and $\mathcal{I}_{j1}^{\pm}$ for $n^{\pm}$ for each point $i=0\ldots(N+2)r$ at time t^{n+1}.
4. Calculate coefficients $\mathcal{A}_i$, $\mathcal{B}_i$ and $\mathcal{C}_i$.
5. Calculate coefficients a_i, b_i, c_i and g_i
6. Obtain F_i^{n+1} and J^{n+1} from (G.26)-(G.28), and $(n^{\pm})_i^{n+1}$ from (G.33) and (G.37).
7. If the fixed point iteration converges then go to step 1, else go to step 2.

Bibliography

[1] K. N. Alekseev, M. V. Gorkunov, N. V. Demarina, T. Hyart, N. V. Alexeeva and A. V. Shorokhov, "Suppressed absolute negative conductance and generation of high-frequency radiation in semiconductor superlattices". Europhys. Lett. **73**, 934-940 (2006).

[2] M. Álvaro and L. L. Bonilla, "Nonequilibrium free energy, H theorem and self-sustained oscillations for Boltzmann-BGK descriptions of semiconductor superlattices". J. Stat. Mech. P01018 (15 pp) (2011).

[3] M. Álvaro and L. L. Bonilla, "Two miniband model for self-sustained oscillations of the current through resonant-tunneling semiconductor superlattices". Phys. Rev. B. **82**, 035305 (8 pp) (2010).

[4] K. Aoki, P. Markowich and S. Takata, "Kinetic Relaxation Models for Energy Transport". J. Stat. Phys. **127**, 287-312 (2007).

[5] Ashcroft N W and Mermin N D, "Solid State Physics", Fort Worth: Harcourt Brace College Publishers (1976).

[6] Bastard G "Wave Mechanics Applied to Semiconductor Heterostructures". Halsted, New York 1988.

[7] Bechouche P., Mauser N.J. and Poupaud F, "Semiclassical limit for the Schrödinger-Poisson equation in a crystal". Commun. Pure Appl. Math. **54** 851 (2001).

[8] P. L. Bhatnagar, E. P. Gross, and M. Krook, "A Model for Collision Processes in Gases. I. Small Amplitude Processes in Charged and Neutral One-Component Systems". Phys. Rev. **94** 511-525 (1954).

[9] L. L. Bonilla, L. Barletti, R. Escobedo and M. Alvaro, "Nonlinear electronic transport in semiconductor superlattices", in *Applied and Industrial Mathematics in Italy II. Selected contributions from the 8th SIMAI*

Conference, V. Cutello, G. Fotia and L. Puccio, eds. Series on Advances in Mathematics for Applied Sciences **75**, pp. 184-195. World Sci., Singapore 2007.

[10] L.L. Bonilla, L. Barletti and M. Álvaro, "Nonlinear electron and spin transport in semiconductor superlattices". SIAM J. Appl. Math. **69**, 494-513 (2008).

[11] L. L. Bonilla and M. Carretero, "Nonlinear electron transport in nanostructures". Numerical Analysis and Applied Mathematics. T.E. Simos, G. Psihoyios and Ch. Tsitouras, eds. Pp. 9-12. American Institute of Physics Proceedings **1048**, Melville, N.Y., (2008).

[12] L.L. Bonilla, R. Escobedo and A. Perales, "Generalized drift-diffusion model for miniband superlattices". Phys. Rev. B **68**, 241304(R) (4 pp) (2003).

[13] L.L. Bonilla and R. Escobedo, "Wigner-Poisson and nonlocal drift-diffusion model equations for semiconductor superlattices", Math. Mod. Meth. Appl. Sci. **15**(8), 1253-1272 (2005).

[14] L. L. Bonilla and H. T. Grahn, "Nonlinear dynamics of semiconductor superlattices". Rep. Prog. Phys. **68**, 577-683 (2005).

[15] L. L. Bonilla and F. J. Higuera, "The onset and end of the Gunn effect in extrinsic semiconductors". SIAM J. Appl. Math. **55** 16251649 (1995).

[16] Bonilla L L, Platero G and Sánchez D, "Microscopic derivation of transport coefficients and boundary conditions in discrete drift-diffusion models of weakly coupled superlattices", Phys. Rev. B **62**, 2786 (2000).

[17] L. L. Bonilla and S. W. Teitsworth, "Nonlinear wave methods for charge transport". Wiley-VCH, Weinheim, 2010.

[18] L.L. Bonilla, R. Escobedo, M. Carretero and G. Platero, "Multiquantum well spin oscillator", Appl. Phys. Lett. **91** (2007), 092102 (3 pp).

[19] J. J. Brey, F. Moreno, and J. W. Dufty, "Model kinetic equation for low-density granular flow". Phys. Rev. E **54**, 445-456 (1996).

[20] Bryksin V V and Kleinert P. "An analytic approach to the real-space transfer in semiconductor superlattices with highly doped barriers". J. Phys.: Condens. Matter **9** 7403 (1997).

[21] Bryksin V V and Kleinert P. "Theory of quantum diffusion in biased semiconductors" J. Phys.: Condens. Matter **15** 1415 (2003).

[22] P. N. Butcher, "The Gunn effect". Rep. Prog. Phys. **30**, 97-148 (1967).

[23] M. Büttiker and H. Thomas, "Current instability and domain propagation due to Bragg scattering". Phys. Rev. Lett. **38**, 78-80 (1977).

[24] J. C. Cao and X.L. Lei, "Synchronization and chaos in miniband semiconductor superlattices". Phys. Rev. B **60**, 1871-1878 (1999).

[25] Capasso F, Mohammed K and Cho A Y, "Sequential resonant tunneling through a multiquantum well superlattice" Appl. Phys. Lett. **48** 478 (1986).

[26] A. Carpio, P. Hernando, and M. Kindelan, "Numerical Study of Hyperbolic Equations with Integral Constraints Arising in Semiconductor Theory". SIAM J. Numer. Anal. **39** 168-191 (2001).

[27] E. Cebrián, L.L. Bonilla and A. Carpio, "Self-sustained current oscillations in the kinetic theory of semiconductor superlattices". J. Comput. Phys. **228**, 7689-7705 (2009).

[28] C. Cercignani, I. M. Gamba and C. D. Levermore. "A drift-collision balance for a Boltzmann-Poisson system in bounded domains", SIAM J. Appl. Math. **61** 1932-1958 (2001).

[29] C. Cercignani, R. Illner and M. Pulvirenti, "The mathematical theory of dilute gases". Springer, New York, 1994. Chapter 8.

[30] S. Chapman and T. G. Cowling, The mathematical theory of non-uniform gases. 3rd ed. Cambridge U. P., Cambridge 1970.

[31] P. Degond and C. Ringhofer. "Quantum moment hydrodynamics and the entropy principle", J. Stat. Phys. **112** 587-628 (2003).

[32] L. Demeio, L. Barletti, A. Bertoni, P. Bordone, C. Jacoboni. "Wigner-function approach to multiband transport in semiconductors". Physica B **314** 104-107 (2002).

[33] L. Esaki and R. Tsu, "Superlattice and negative differential conductivity in semiconductors". IBM J. Res. Develop. **14** 61-65 (1970).

[34] R. Escobedo and L. L. Bonilla, "Numerical methods for a quantum drift-diffusion equation in semiconductor physics". J. Math. Chem. **40** 3-13 (2006).

[35] J. Feldmann, K. Leo, J. Shah, D. A. B. Miller, J. E. Cunnigham, T. Meier, G. von Plessen, A. Schulze, P. Thomas, and S. Schmitt-Rink, "Optical investigation of Bloch oscillations in a semiconductor superlattice". Phys. Rev. B **46** 7252-7255 (1992).

[36] M. V. Fischetti, "Theory of electron transport in small semiconductor devices using the Pauli master equation" J. Appl. Phys. **83**, 270 (1998).

[37] Gerhardts R R "Effect of elastic scattering on miniband transport in semiconductor superlattices" Phys. Rev. B **48** 9178 (1993).

[38] H. Haug and A.-P. Jauho, "Quantum Kinetics in Transport and Optics of Semiconductors". 2nd ed Springer, Berlin 2008.

[39] K. Hofbeck, J. Grenzer, E. Schomburg, A. A. Ignatov, K. F. Renk, D. G. Pavel'ev, Yu. Koschurinov, B. Melzer, S. Ivanov, S. Schaposchnikov and P. S. Kop'ev, "High-frequency self-sustained current oscillation in an Esaki-Tsu superlattice monitored via microwave emission". Phys. Lett. A **218**, 349-353 (1996).

[40] T. Hyart, A. V. Shorokhov, and K. N. Alekseev, "Theory of Parametric Amplification in Superlattices". Phys. Rev. Lett. **98**, 220404 (4 pp) (2007).

[41] T. Hyart, N. V. Alexeeva, J. Mattas and K.N. Alekseev, "Terahertz Bloch oscillator with a modulated bias". Phys. Rev. Lett. **102**, 140405 (4 pp) (2009).

[42] Ignatov A A, Dodin E P and Shashkin V I. "Transient response theory of semiconductor superlattices: connection with Bloch oscillations" Mod. Phys. Lett. B **5** 1087 (1991).

[43] A. A. Ignatov and V.I. Shashkin, "Bloch oscillations of electrons and instability of space-charge waves in semiconductor superlattices". Sov. Phys. JETP **66**, 526-530 (1987).

[44] A. A. Ignatov and Yu.A. Romanov, "Nonlinear electromagnetic properties of semiconductors with a superlattice", Phys. stat. sol. (b) **73**, 327-333 (1976).

[45] H. Jiang and W. Cai, J. Comput. Phys. **229**, 4461 (2010).

[46] L. P. Kadanoff and G. Baym, "Quantum Statistical Mechanics", W. A. Benjamin Inc., New York, 1962.

[47] Kadanoff L P and Baym G "Quantum Statistical Mechanics: Greens Function Methods in Equilibrium and Nonequilibrium Problems". Redwood City: Addison-Wesley 1989.

[48] E. O. Kane, "The $k \cdot p$ method", in R. Willardson and A. Beer (Eds.), *Physics of III-V Compounds, Semiconductors and Semimetals*, Vol. 1, Chapt. 3, pp. 75100, Academic Press, New York, 1966.

[49] J. Kastrup, R. Hey, K. Ploog, H.T. Grahn, L. L. Bonilla, M. Kindelan, M. Moscoso, A. Wacker and J. Galán, "Electrically tunable GHz oscillations in doped GaAsAlAs superlattices" Phys. Rev. B **55**, 2476 (1997).

[50] P. Kleinert, V. V. Bryksin and O. Bleibaum, "Spin accumulation in lateral semiconductor superlattices induced by a constant electric field". Phys. Rev. B **72** 195311 (6 pp) (2005).

[51] H. Kroemer, "Gunn effect — bulk instabilities". Chapter 2 of *Topics in Solid State and Quantum Electronics*, edited by W. D. Hershberger. Pages 20-98. John Wiley, N. Y. 1972.

[52] H. Kroemer, "On the nature of the negative-conductivity resonance in a superlattice Bloch oscillator". cond-mat/0007482 (unpublished).

[53] H. Kroemer, "Large-amplitude oscillation dynamics and domain suppression in a superlattice Bloch oscillator". cond-mat/0009311 (unpublished).

[54] S.A. Ktitorov, G.S. Simin and V.Ya. Sindalovskii, "Bragg reflections and the high-frequency conductivity of an electronic solid-state plasma". Sov. Phys. Solid State **13**, 1872-1874 (1972) [Fiz. Tverd. Tela **13**, 2230-2233 (1971)].

[55] B. Laikhtman and D. Miller, "Theory of current-voltage instabilities in superlattices". Phys. Rev. B **48**, 5395-5412 (1993).

[56] X. L. Lei, "Balance equations for hot-electron transport in a general energy band in crossed magnetic and electric fields", Phys. Rev. B **51** 5184-5191 (1995).

[57] X. L. Lei, "Distribution function and balance equations of drifting Bloch electrons in an electric field", Phys. Rev. B **51** 5526-5530 (1995).

[58] X. L. Lei, N.J.M. Horing and H.L. Cui, "Convective instability of a biased semiconductor superlattice". J. Phys. Cond. Mat. **7**, 9811-9817 (1995).

[59] L. Lei and C. S. Ting, "Theory of nonlinear electron transport for solids in a strong electric field", Phys. Rev. B **30** 4809-4812 (1984).

[60] K. Leo, "High-field transport in semiconductor superlattices". Springer Tracts in Modern Physics **187**. Springer, Berlin 2003.

[61] O. Morandi, "Multiband Wigner-function formalism applied to the Zener band transition in a semiconductor". Phys. Rev. B **80** 024301 (2009).

[62] O. Morandi and L. Demeio, "A Wigner-Function Approach to Interband Transitions Based on the Multiband-Envelope-Function Model" Transport Theor. Stat. Phys. **37** 437 (2008).

[63] O. Morandi and M. Modugno, "Multiband envelope function model for quantum transport in a tunneling diode". Phys. Rev. B **71** 235331 (2005).

[64] G. Platero and R. Aguado, "Photon-assisted transport in semiconductor nanostructures", Phys. Rep. **395** , pp. 1-157 (2004)

[65] F. Poupaud, "On a System of Nonlinear Boltzmann Equations of Semiconductor Physics". SIAM J. Appl. Math. **50**, 1593-1606 (1990).

[66] E. I. Rashba, "Properties of semiconductors with an extremum loop. 1. Cyclotron and combinational resonance in a magnetic field perpendicular to the plane of the loop", Sov. Phys. Solid State **2**, 1224-1238 (1960).

[67] Rossi F, Di Carlo A and Lugli P. "Microscopic theory of quantum-transport phenomena in mesoscopic systems: a Monte Carlo approach" Phys. Rev. Lett. **80**, 3348 (1998).

[68] S. Rott, Theory of electronic transport in semiconductor superlattices. Ph.D. Thesis, Friedrich-Alexander-Universität, Erlangen-Nürnberg, 1999.

[69] D. Sánchez, A.H. MacDonald and G. Platero. "Field-domain spintronics in magnetic semiconductor multiple quantum wells". Phys. Rev. B **65**, 035301 (10 pp) (2002).

[70] R. Scheuerer, K. F. Renk, E. Schomburg, W. Wegscheider and M. Bichler, "Nonlinear superlattice transport limited by Joule heating". J. Appl. Phys. **92**, 6043-6046 (2002).

[71] E. Schomburg, T. Blomeier, K. Hofbeck, J. Grenzer, S. Brandl, A. A. Ignatov, K. F. Renk, D.G. Pavel'ev, Yu. Koschurinov, B. Ya. Melzer, V. Ustinov, S. Ivanov, A. Zukhov and P.S. Kop'ev. "Current oscillation in superlattices with different miniband widths". Phys. Rev. B **58**, 4035-4038 (1998).

[72] J. Shah, "Hot Carriers in Semiconductor Nanostructures: Physics and Applications", pp. 279, Academic Press, Boston 1992.

[73] A. Sibille, "Semiconductor superlattices: growth and electronic properties", ed. by H.T. Grahn. Page 29 World Sci., Singapore, 1995.

[74] R. Terazzi, T. Gresch, M. Giovanni, N. Hoyler, N. Sekine and J. Faist, "Bloch gain in quantum cascade lasers". Nat. Phys. **3**, 329-332 (2007).

[75] M.B. Unlu, B. Rosen, H.L. Cui and P. Zhao, "Multi-band Wigner function formulation of quantum transport", Phys. Lett. A **327**, 240 (2004).

[76] A. Wacker, "Semiconductor superlattices: A model system for nonlinear transport", Phys. Rep. **357**, pp. 1-111 (2002).

[77] W. T. Wenckebach, "Essential of Semiconductor Physics", J. Wiley & Sons, Chichester, 1999.

[78] C. Zener, "A theory of the electrical breakdown of solid dielectrics". Proc. R. Soc. London, Ser. A **145**, 523-529 (1934).

[79] R. Zwanzig, "Nonequilibrium Statistical Mechanics". Oxford U.P., New York, 2001.